

**BIOCHEMICAL AND VIROLOGIC ANALYSIS OF THE  
HUMAN CYTOMEGALOVIRUS ENCODED UL97**

CLAIRE SHANNON-LOWE BSc. (Hons), MSc

Thesis submitted for the degree of Doctor of Philosophy,  
Faculty of Medicine, University College London

November 2002

Department of Virology,  
Royal Free and University College Medical School,  
Royal Free Campus  
University College London

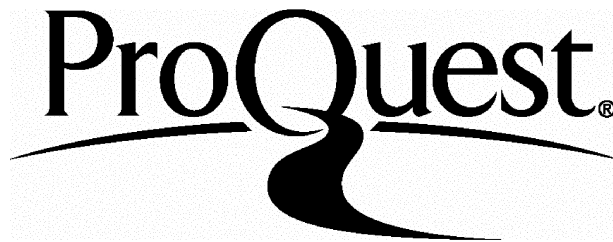
ProQuest Number: U642103

All rights reserved

INFORMATION TO ALL USERS

The quality of this reproduction is dependent upon the quality of the copy submitted.

In the unlikely event that the author did not send a complete manuscript and there are missing pages, these will be noted. Also, if material had to be removed, a note will indicate the deletion.



ProQuest U642103

Published by ProQuest LLC(2015). Copyright of the Dissertation is held by the Author.

All rights reserved.

This work is protected against unauthorized copying under Title 17, United States Code.  
Microform Edition © ProQuest LLC.

ProQuest LLC  
789 East Eisenhower Parkway  
P.O. Box 1346  
Ann Arbor, MI 48106-1346

## **Abstract**

Human cytomegalovirus (HCMV) remains a significant cause of morbidity and mortality in immunocompromised patients. It is one of the most important opportunistic agents in the pathology of HIV, where it frequently causes sight-threatening retinitis. Currently approved antiviral drugs include ganciclovir, cidofovir and foscarnet. The HCMV UL97 gene encodes a phosphotransferase that has been shown to catalyse the initial phosphorylation of ganciclovir (GCV) to its monophosphate form, whereafter it is converted to the active triphosphate by cellular kinases. HCMV disease often necessitated long-term antiviral therapy, which in turn led to the emergence of ganciclovir resistant strains of HCMV. Mutations in the UL97 gene have been shown to impair GCV phosphorylation, thus conferring GCV resistance to HCMV and have been associated with disease progression.

HCMV has been observed in almost every organ system in the body, but little information is available on the extent of UL97 mutations in the organs of chronically treated AIDS patients. A point mutation assay was employed to determine the prevalence of UL97 mutations in post mortem organs of patients who died with AIDS. The results showed that quantitative differences in resistant genotypes between organs of the same individual and between individuals occurs which has relevance to the management of patients on long term therapy for HCMV.

In order to investigate functional effects of UL97 drug resistance mutations, wild type and mutant UL97 proteins were produced using a recombinant baculovirus expression system. Autophosphorylation properties of wild type and mutant UL97 were similar, while the mutations reduced ganciclovir phosphorylation to below 20% of the wild type UL97.

The novel antiviral benzimidavir, inhibited autophosphorylation of wild type and mutant UL97 proteins. Enzyme kinetic analysis demonstrated benzimidavir acts by competitive inhibition of ATP binding to UL97. The mutation at codon 397, which confers resistance to benzimidavir, reduced autophosphorylation by 90%. These observations have implications for combination therapy with benzimidavir and ganciclovir.

**BIOCHEMICAL AND VIROLOGIC ANALYSIS OF THE  
HUMAN CYTOMEGALOVIRUS ENCODED UL97**

CLAIRE SHANNON-LOWE BSc. (Hons), MSc

Thesis submitted for the degree of Doctor of Philosophy,  
Faculty of Medicine, University College London

November 2002

Department of Virology,  
Royal Free and University College Medical School,  
Royal Free Campus  
University College London



## **Acknowledgements**

Many people have helped for the duration of my PhD project, both professionally by patient guidance and support, and by inspiration and encouragement. There are too many to thank individually.

I would particularly like to thank Vince and Paul for giving me the opportunity of carrying out this PhD project. In addition, I would like to thank Vince for believing in me and for his encouragement and critical analysis of my work.

I would especially like to thank Matt for his continuous support, objectivity when mine was lacking, help and friendship. I thank Azeem for inspiring me in this work and for showing me all the heavenly glory. I thank Keirissa and Esteban for their help, friendship and for coping admirably with my stress, particularly during the latter stages of my thesis. I would like to thank Duncan and Aycan for their advice and imparting me with their knowledge. I would also like to thank Gill for her support in my defection.

Finally, I would like to thank Mike for all the many wonderful ways in which he has encouraged and supported me throughout the period of my thesis and for being my rock.

# TABLE OF CONTENTS

<b>ABSTRACT</b> .....	<b>2</b>
<b>ACKNOWLEDGEMENTS</b> .....	<b>3</b>
<b>TABLE OF CONTENTS</b> .....	<b>4</b>
<b>LIST OF FIGURES</b> .....	<b>10</b>
<b>LIST OF TABLES</b> .....	<b>14</b>
<b>LIST OF ABBREVIATIONS</b> .....	<b>15</b>
<b>CHAPTER 1</b> .....	<b>5</b>
<b>General Introduction</b> .....	<b>5</b>
1.1. HERPESVIRUSES.....	6
1.1.1. <i>The Herpesviridae</i> .....	6
1.1.2. <i>Classification of Herpesviruses</i> .....	9
1.1.3. <i>Human Herpesviruses</i> .....	12
1.2. HUMAN CYTOMEGALOVIRUS.....	16
1.2.1. <i>Epidemiology</i> .....	16
1.2.2. <i>HCMV pathogenesis in the immunocompromised host</i> .....	17
1.2.3. <i>HCMV and Renal Transplant Recipients</i> .....	23
1.2.4. <i>HCMV and Liver Transplant Recipients</i> .....	24
1.2.5. <i>HCMV and Bone Marrow Transplant Recipients</i> .....	25
1.2.6. <i>HCMV and Acquired Immunodeficiency Syndrome</i> .....	26
1.3 REPLICATION OF HUMAN CYTOMEGALOVIRUS.....	35
1.3.1. <i>Viral attachment and penetration</i> .....	35
1.3.2. <i>Immediate Early Events</i> .....	36
1.3.3. <i>DNA Replication</i> .....	38
1.3.4. <i>Latency</i> .....	42
1.4. IMMUNOLOGY .....	43
1.4.1. <i>Immune Response to HCMV</i> .....	43
1.4.2. <i>Immune Modulation Strategies</i> .....	46
1.5. ANTIVIRAL CHEMOTHERAPY .....	51

1.5.1. Nucleoside analogues .....	51
1.5.2. Foscarnet .....	55
1.5.3. Cidofovir .....	56
1.5.4. Non-Nucleoside HCMV Inhibitors.....	56
1.5.5. Fomiversen.....	60
1.6. ANTIVIRAL RESISTANCE .....	62
1.6.1. Antiviral resistance and UL97.....	62
1.6.2. Antiviral resistance and UL54.....	65
1.6.3. Antiviral resistance associated with both UL97 and UL54.....	70
1.7. THE HCMV ENCODED PHOSPHOTRANSFERASE UL97 .....	72
1.8. PROTEIN KINASES.....	75
1.9. BACULOVIRUS EXPRESSION SYSTEMS .....	78
AIMS OF THE THESIS.....	82
<b>CHAPTER 2.....</b>	<b>8</b>
<b>MATERIALS AND METHODS.....</b>	<b>8</b>
2.1. GENERATION OF A RECOMBINANT BACULOVIRUS.....	9
2.1.1. Polymerase Chain Reaction of HCMV UL97.....	9
2.1.2. UL97 polymerase chain reaction.....	9
2.1.3. Purification of the PCR product.....	10
2.1.4. Cloning UL97 into pGEM-T Easy.....	10
2.1.5. Transformations using the ligation reactions.....	11
2.1.6. Plasmid purification and analysis .....	11
2.1.7. Restriction Endonuclease Digestion.....	13
2.1.8. DNA Sequence analysis .....	13
2.1.9. Cloning of UL97 into the Baculovirus Transfer Vector pBlueBacHis2 C and pMelBac C.....	14
2.1.10. Co-transfection of the recombinant transfer vectors with the Baculovirus DNA	15
2.1.11. Plaque Assay.....	15
2.1.12. Plaque purification .....	16
2.1.13. PCR analysis of plaque purified recombinant baculovirus.....	17
2.1.14. Generation of a high titre baculovirus stock.....	17

2.2. CELL CULTURE.....	18
2.2.1. Freezing cultured cells.....	18
2.2.2. Initiating culture from frozen cells .....	18
2.2.3. Maintenance of adherent cells and suspension cultures .....	18
2.3. MOLECULAR BIOLOGY TECHNIQUES .....	19
2.3.1. Site Directed Mutagenesis .....	19
2.3.2. Quantitative competitive polymerase chain reaction .....	20
2.3.3. UL97 polymerase chain reaction.....	22
2.3.4. Microtitre point mutation assay.....	23
2.4. PROTEIN DETECTION AND PURIFICATION METHODS .....	25
2.4.1. Preparation of a Crude Cell Lysate.....	25
2.4.2. Ammonium Sulphate Precipitation .....	25
2.4.3. Ion Exchange Chromatography.....	26
2.4.4. Immunoaffinity chromatography .....	27
2.4.5. Sodium dodecyl sulphate polyacrylamide gel electrophoresis (SDS-PAGE)	28
2.4.6. Coomassie brilliant blue staining.....	28
2.4.7. Western blotting.....	28
2.5. ENZYME ANALYSIS .....	31
2.5.1. Protein Kinase Assays .....	31
2.5.2. GCV Kinase Assay (in vitro).....	31
2.5.3. GCV kinase assay (in vitro / in vivo) .....	32
2.5.4. Plaque Reduction Assay.....	32
CHAPTER 3 .....	125
Tissue Distribution of Drug Resistant UL97 Mutants of HCMV.....	125
3.1. Introduction.....	126
3.2. Results.....	127
3.2.1. HCMV gB quantitative competitive polymerase chain reaction .....	127
3.2.2. Analysis of the distribution of mutant to wild type alleles of HCMV UL97	129
.....	129
3.3. Discussion.....	139

CHAPTER 4 .....	9
Construction of a Recombinant Baculovirus Expressing the HCMV UL97	
Phosphotransferase .....	9
4.1. Introduction .....	9
4.2 Results .....	10
4.2.1. PCR amplification of the HCMV UL97 ORF .....	10
4.2.2. Cloning of the UL97 into pGEM-T Easy .....	10
4.2.3. Restriction enzyme analysis of the putative recombinant clones .....	11
4.2.4. Sequencing of the UL97 ORF .....	11
4.2.5. Restriction enzyme digestion of pGem-T-UL97, pBlueBacHis and pMelBac 14	
4.2.6. Subcloning of the UL97 into the baculovirus transfer vectors pBlueBacHis and pMelBac .....	14
4.2.7. Co-transfection of BBH-WT, MB-WT and Bac-N-Blue linearized DNA to produce recombinant baculoviruses .....	15
4.2.8. Analysis of protein expression of BVBBH-WT and BVMB-WT .....	19
4.3. Discussion.....	25
<b>CHAPTER 5 .....</b>	<b>162</b>
<b>Expression, purification and biochemical analysis of the.....</b>	<b>162</b>
<b>HCMV UL97.....</b>	<b>162</b>
5.1. Introduction.....	163
5.2. Results.....	164
5.2.1. Preparation of soluble protein extracts from insect cells .....	164
5.2.2. Protein kinase assay of the soluble crude lysate of Baculovirus infected cells	164
5.2.3. Secretion of UL97 from infected insect cells.....	165
5.2.4. Optimisation of secretion of UL97 from infected insect cells .....	165
5.2.5. Optimisation of the ammonium sulphate precipitation.....	170
5.2.6. Optimisation of the solubility of UL97 .....	170
5.2.7. Anion exchange chromatography.....	176
5.2.8. Immunoprecipitation of UL97.....	176
5.2.9. Purification of the recombinant wild type and mutant UL97 proteins.....	177
5.2.10. Analysis of UL97 autophosphorylation. ....	182

5.2.11. Enzyme kinetic analysis of autophosphorylation. ....	30
5.2.12. Analysis of mutant UL97 autophosphorylation .....	31
5.2.13. Enzyme kinetic analysis of mutant UL97 autophosphorylation.....	32
5.3. Discussion.....	36
CHAPTER 6.....	192
Analysis of UL97 function using the antivirals GCV and 1263W94 .....	192
6.1 Introduction.....	193
6.2. Results.....	194
6.2.1. Cytotoxicity of GCV for Sf21 insect cells .....	194
6.2.2. Plaque reduction assay of the wild type and mutant UL97-expressing baculoviruses .....	194
6.2.3. Plaque reduction assay of the baculoviruses expressing structural mutations in the UL97 gene .....	196
6.2.4. GCV phosphorylation by recombinant UL97 .....	196
6.2.5. Phosphorylation of recombinant UL97 in the presence of 1263W94.....	199
6.2.6. Comparison of the wild type and mutant UL97 autophosphorylation in the presence of 1263W94 .....	199
6.2.7. Titration of 1263W94 against the wild type and mutant UL97 .....	202
6.2.8. Determination of the IC <sub>50</sub> of 1263W94 against the wild type and mutant UL97 species .....	202
6.2.9. IC <sub>50</sub> of 1263W94 against the UL97 encoding the M460I mutation.....	202
6.2.10. Inhibition of UL97 autophosphorylation by 1263W94.....	202
6.2.11. Analysis of 1263W94 inhibition of UL97 autophosphorylation.....	207
6.2.12. Lineweaver Burke analysis of 1263W94 mediated phosphorylation inhibition .....	207
6.2.13. Inhibition of phosphorylation by 1263W94.....	214
6.3. Discussion.....	214
CHAPTER 7.....	223
General Discussion.....	223
References.....	233

## List of Figures

<b>Figure</b>	<b>Title</b>	<b>Page</b>
1.1	Electron micrograph of a herpesvirus	23
1.2	Schematic diagram of the sequence arrangements in the six classes of genomes of the viruses comprising the family Herpesviridae	24
1.3	Schematic representation of the four isomers of the HCMV genome illustrating the major immediate early genes	26
1.4	Model of HCMV DNA replication	55
1.5	Immune evasion mechanisms of HCMV	64
1.6	Structures of the Anti-Herpetic Compounds	69
1.7	Structures of BAY 38-4766 and chlorophenylmethyl BDT	73
1.8	Structure of Maribavir (1263W94/ benzimidavir)	76
1.9	Conserved regions in the HCMV UL97	81
1.10	Conserved regions in the HCMV DNA polymerase (UL54)	85
1.11	Molecular structure of protein kinases	93
2.1	Oligonucleotide probes for the point mutation assay	115
2.2	Illustration of the western blot set up	120
3.1	Principle of the Microtitre Point Mutation Assay	127
3.2	Quantitative Competitive Polymerase Chain Reaction	129
3.3	Analysis of the Median HCMV Loads in Multiple Post Mortem Tissues	130
3.4	Distribution of Wild Type and Mutant UL97 Genotypes in Multiple Post Mortem Organs of AIDS Patient 1	131
3.5	Distribution of Wild Type and Mutant UL97 Genotypes in Multiple Post Mortem Organs of AIDS Patient 2	132
3.6	Distribution of Wild Type and Mutant UL97 Genotypes in Multiple Post Mortem Organs of AIDS Patient 3	133
3.7	Distribution of Wild Type and Mutant UL97 Genotypes in Multiple Post Mortem Organs of Patient 4	134

<b>3.8</b>	Distribution of Wild Type and Mutant UL97 Genotypes in Multiple Post Mortem Organs of AIDS Patient 5	<b>135</b>
<b>3.9</b>	Correlation between Presence of UL97 Mutations and Viral Load	<b>136</b>
<b>3.10</b>	Correlation between the Number of UL97 Mutations and Viral Load	<b>147</b>
<b>4.1</b>	Polymerase Chain Reaction Amplification of the UL97 ORF	<b>144</b>
<b>4.2</b>	Purification of the PCR-Amplified UL97	<b>145</b>
<b>4.3</b>	Restriction Enzyme Digestion of pGEM-UL97	<b>146</b>
<b>4.4</b>	Polymerase Chain Reaction Analysis of pGEM-UL97	<b>148</b>
<b>4.5</b>	Baculovirus Transfer Vector pBlueBacHis C (Invitrogen)	<b>149</b>
<b>4.6</b>	Baculovirus Transfer Vector pMelBac C (Invitrogen)	<b>150</b>
<b>4.7</b>	Purification of the Digested UL97	<b>151</b>
<b>4.8</b>	Restriction Enzyme Digestion of pBlueBacHis-UL97 and pMelBac-UL97	<b>153</b>
<b>4.9</b>	PCR analysis of the pBlueBacHis-UL97 and the pMelBac-UL97	<b>154</b>
<b>4.10</b>	Plaque Purification of the Putative Recombinant Baculoviruses BVBBH-UL97 and BVMB-UL97	<b>155</b>
<b>4.11</b>	PCR Analysis of Plaque Purified Recombinant Baculoviruses	<b>156</b>
<b>4.12</b>	Time Course of UL97 Expression in BVMB-UL97 and BVBBH-UL97 Infected Insect Cells	<b>157</b>
<b>5.1</b>	Phosphorylation of Baculovirus expressed UL97	<b>165</b>
<b>5.2</b>	Time Course of Expression of UL97 in Recombinant Baculovirus Infected Serum Free Insect Cells	<b>166</b>
<b>5.3</b>	Time Course of UL97 Expression and Secretion from Sf9 Serum Free Insect Cells	<b>167</b>
<b>5.4</b>	Expression and Secretion of Recombinant UL97 from Serum Free Insect Cells Following Protein Concentration	<b>168</b>
<b>5.5</b>	Western Blot of MOI Optimisation for UL97 Expression and Secretion	<b>170</b>
<b>5.6</b>	Western Blot of concentrated secreted proteins from BVMB-UL97 infected insect cells	<b>171</b>



<b>5.7</b>	<b>Optimisation of Secretion of UL97 from BVMB-UL97 Infected Insect Cells</b>	<b>172</b>
<b>5.8</b>	<b>Optimisation of the Ammonium Sulphate Precipitation</b>	<b>173</b>
<b>5.9</b>	<b>Ammonium Sulphate Precipitation</b>	<b>174</b>
<b>5.10</b>	<b>Ammonium Sulphate Precipitation of UL97</b>	<b>176</b>
<b>5.11</b>	<b>Optimisation of Anion Exchange Chromatography</b>	<b>177</b>
<b>5.12 a</b>	<b>Purification of the Wild Type and Mutant UL97 proteins</b>	<b>178</b>
<b>5.12 b</b>	<b>Purification of the Wild Type and Mutant UL97 proteins</b>	<b>179</b>
<b>5.13</b>	<b>Immunoprecipitation of UL97</b>	<b>180</b>
<b>5.14</b>	<b>Analysis of UL97 Autophosphorylation</b>	<b>182</b>
<b>5.15</b>	<b>Lineweaver Burke Analysis of UL97 Autophosphorylation</b>	<b>184</b>
<b>5.16</b>	<b>Autophosphorylation of the Recombinant Mutant and Wild Type UL97</b>	<b>185</b>
<b>5.17</b>	<b>Lineweaver Burke Analysis of UL97 Autophosphorylation of the Mutant UL97 Species</b>	<b>186</b>
<b>6.1</b>	<b>Cytotoxicity of Ganciclovir for Sf21 insect cells</b>	<b>194</b>
<b>6.2</b>	<b>Graphical Representation of the Plaque Reduction Assays of the Drug Resistant Baculoviruses</b>	<b>196</b>
<b>6.3</b>	<b>Graphical Representation of the Plaque Assays of the Structurally Mutated UL97-Expressing Baculoviruses</b>	<b>197</b>
<b>6.4</b>	<b>Ganciclovir phosphorylation by recombinant UL97</b>	<b>199</b>
<b>6.5</b>	<b>Autoradiographs of the Protein Kinase Assays of UL97 in the presence of 1263W94</b>	<b>200</b>
<b>6.6</b>	<b>Graphical Representation of the Autophosphorylation of UL97 in the presence of 1263W94</b>	<b>202</b>
<b>6.7</b>	<b>1263W94 Titration against UL97</b>	<b>203</b>
<b>6.8</b>	<b>IC<sub>50</sub> of 1263W94 for the Wild Type and Mutant UL97 Protein Species</b>	<b>204</b>
<b>6.9</b>	<b>IC<sub>50</sub> of 1263W94 for the M460I Encoded UL97</b>	<b>205</b>
<b>6.10</b>	<b>Inhibition of UL97 Autophosphorylation by 1263W94</b>	<b>208</b>
<b>6.11</b>	<b>Analysis of 1263W94 Inhibition of UL97 Autophosphorylation</b>	<b>209</b>
<b>6.12</b>	<b>Lineweaver Burke Analysis of 1263W94 Mediated Phosphorylation</b>	<b>210</b>

**inhibition**

<b>6.13</b>	<b>Analysis of the Lineweaver Burke Plots of 1263W94 Mediated UL97 Autophosphorylation Inhibition</b>	<b>211</b>
<b>6.14</b>	<b>1263W94 mediated inhibition of GCV phosphorylation</b>	<b>212</b>

## List of Tables

<b>Table</b>	<b>Title</b>	<b>Page</b>
<b>1.1</b>	Classification of the Human Herpesviruses	<b>27</b>
<b>1.2</b>	HCMV diseases in the immunocompromised	<b>33</b>
<b>1.3</b>	Definitions of Cytomegalovirus end organ disease	<b>34</b>
<b>1.4</b>	Interaction between Human Cytomegalovirus and HIV in vitro	<b>43</b>
<b>1.5</b>	Regimens used in the Treatment of Patients with HCMV Retinitis	<b>46</b>
<b>1.6</b>	Comparison of studies of maintenance therapy for HCMV retinitis	<b>47</b>
<b>1.7</b>	Characteristics of patients included in studies on the decline in incidence of HCMV retinitis in the era of HAART	<b>49</b>
<b>1.8</b>	Reported UL97 mutations conferring GCV resistance identified from clinical isolates	<b>82</b>
<b>1.9</b>	Antiviral susceptibilities of clinical isolates containing mutations in the DNA polymerase UL54	<b>87</b>
<b>2.1</b>	Primer sequences for the GeneEditor™ in vitro Site Directed Mutagenesis System	<b>112</b>
<b>2.2</b>	Solutions for preparing resolving and stacking gels for Tris-glycine SDS-PAGE	<b>121</b>
<b>6.1</b>	Analysis of 1263W94 inhibition of UL97 autophosphorylation	<b>207</b>

## List of Abbreviations

A	alanine
AIDS	acquired immunodeficiency syndrome
AcMNPV	<i>autographa californica</i> multiple nuclear polyhedrosis virus
ACV	aciclovir
cAMP	cyclic adenosine monophosphate
APS	ammonium persulphate
ATP	adenosine triphosphate
BAL	bronchial alveolar lavage
bp	base pairs
BSA	bovine serum albumin
B cell	bursa of Fabricius
CAT	chloramphenicol acetyl transferase
Cdk2	cyclin dependant kinase-2
CD	cell differentiation antigen
CDV	cidofovir
Ci	Curies
cm	centimetres
CNBr	cyanogen bromide
CNS	central nervous system
CPE	cytopathic effect
cpm	counts per minute
CREB	cAMP response element binding protein
CRS	cis-repression signal
CSF	cerebral spinal fluid
CTL	cytotoxic T lymphocytes
d	days
D	aspartic acid
DNA	deoxyribonucleic acid
DNase	deoxyribonuclease
DR	direct repeat

ddATP	dideoxyadenosine triphosphate
ddCTP	dideoxycytosine triphosphate
ddGTP	dideoxyguanosine triphosphate
ddTTP	dideoxythymidine triphosphate
DTT	dithiothreitol
EBNA	Epstein-Barr nuclear antigen
EBV	Epstein-Barr virus
<i>E.coli</i>	<i>Escherichia coli</i>
EDTA	ethylenediaminetetraacetic acid
EK	enterokinase
e.g.	exempli gratia
Erk	extracellular signal-related kinase
<i>et al.</i>	<i>et alii</i>
EHV	equine herpesvirus
ERK2	extracellular signal-regulated kinase 2
ES	exanthem subitum
F	phenylalanine
FBS	fetal bovine serum
FITC	fluorescein isothiocyanate
g	relative gravitational force
G	glycine
18-G	18 guage needle
GTP	Guanosine triphosphate
GCV	ganciclovir
GCV-MP	ganciclovir monophosphate
GCV-TP	ganciclovir triphosphate
gp	glycoprotein
GST	glutathione-s-transferase
GVHD	graft versus host disease
h	hours
H	histidine

HCMV	human cytomegalovirus
HHV-6	human herpesvirus 6
HHV-7	human herpesvirus 7
HHV-8	human herpesvirus 8
HIV	human immunodeficiency virus
HLA	human leukocyte antigen
HSV-1	herpes simplex virus 1
HSV-2	herpes simplex virus 2
HVS	herpesvirus saimiri
I	isoleucine
IC <sub>50</sub>	concentration required to inhibit viral replication by 50%
ICP	infected cell protein
IE	immediate early
IFN	interferon
Ig	immunoglobulin
IL	interleukin
IMCAC	immobilised metal chelate affinity chromatography
IRS	internal repeat sequence
IU	international units
K	lysine
kDa	kilodalton
kbp	kilobase pairs
K <sub>i</sub>	inhibition constant
K <sub>m</sub>	Michaelis constant
KS	Kaposi's sarcoma
KSHV	Kaposi's sarcoma-associated herpesvirus
L	leucine
LB	Luria Bertani broth
LTR	long terminal repeat
M	methionine
MAP	mitogen-activated protein

MCMV	murine cytomegalovirus
MCP-3	macrophage chemotactic protein 3
MCS	multiple cloning site
MEM	minimal essential medium
mg	milligram
MIE	major immediate early
min	minutes
MIP-1 $\alpha$	macrophage inflammatory protein 1 $\alpha$
mM	millimolar
mm	millimeter
MOI	multiplicity of infection
mRNA	messenger ribonucleic acid
MS	multiple sclerosis
N	asparagine
NF	nuclear transcription factor
NLS	nuclear localisation signal
ng	nanograms
nm	nanometers
NK	natural killer
NKC	natural killer gene complex
NTA	nitrilo-tri-acetic acid
OD	optical density
o/n	overnight
ORF	open reading frame
ori-lyt	origin of lytic replication
P	proline
p	protein
PAGE	polyacrylamide gel electrophoresis
PBMC	peripheral blood mononuclear cells
PBS	phosphate-buffered saline
PCR	polymerase chain reaction

PCV	penciclovir
pfu	plaque forming units
pmol	picomoles
pp	phosphoprotein
PKA	protein kinase-A
Q	glutamine
R	arginine
RBS	ribosome binding site
RE	restriction endonuclease
RFLP	restriction fragment length polymorphism
RNA	ribonucleic acid
RNase	ribonuclease
s	seconds
SCID	severe combined immunodeficiency
SDS	sodium dodecyl sulphate
sdw	sterile distilled water
<i>Sf</i>	<i>spodoptera frugiperda</i>
T	threonine
T7	phage T7
<i>Taq</i>	thermus aquaticus DNA polymerase
tat	transactivating factor
TBE	90 mM Tris-borate, 2 mM EDTA
T cell	thymus cell
TE	10 mM Tris/ 1 mM EDTA buffer
TEMED	N, N, N', N'-tetramethylethylenediamine
TK	thymidine kinase
TM	TM buffer
TNF	tumor necrosis factor
TRS	terminal repeat sequence
U	unique
UL	unique long region



US	unique short region
UV	ultraviolet light
V	valine
v	volts
VACV	valaciclovir
$V_{\max}$	maximum velocity
v/v	volume-to-volume ratio
VZV	varicella-zoster virus
w/v	weight-to-volume ratio
wt	wild type
$\mu\text{g}$	micrograms
$\mu\text{l}$	microlitres
$\mu\text{m}$	micrometre
Y	tyrosine

**CHAPTER 1**  
**General Introduction**

## **1.1. Herpesviruses**

### **1.1.1. The Herpesviridae**

The family Herpesviridae are highly disseminated throughout nature and consists of approximately 100 herpesviruses infecting most animal species. Membership of the family is based upon the structure and morphology of the virion as observed by electron microscopy (figure 1.1). Typically the herpesvirus consists of a core, which contains the linear double-stranded DNA and a 100-110 nm icosadeltahedral capsid containing 162 capsomeres, 12 pentameric at the vertices and 150 hexameric. Surrounding the capsid is an amorphous, sometimes asymmetrical material termed the tegument, which may vary in thickness, depending on the location of the virion within the cell. The outer covering, the lipid envelope surrounds the tegument and has a typical trilaminar appearance, suggestive of it being derived from patches of altered cellular membranes. The envelope contains numerous proteinaceous spikes consisting of glycoproteins. The overall size of the herpesvirions varies from 120-300 nm depending upon the thickness of the tegument and the condition of the envelope (Roizman., 1996).

The DNA sequence arrangement of the herpesviruses can be divided into six groups according to the presence and location of terminal repeat sequences (figure 1.2). Group A exhibits a unique sequence flanked by a large direct sequence repeat at each terminus, whereas group B has the terminal sequence repeated multiple times at both termini. Group C consists of two regions of unique sequences enclosed by the terminal repeat sequences. These are smaller in number and include other unrelated sequences, which are directly repeated. The terminal sequences of group D are repeated internally in an inverted orientation. This means that the stretch of unique sequences flanked by the inverted repeats (Small, or S) can invert such that infected cells potentially comprise of two populations differing with respect to the orientation of the S component relative to the large (L) component. In group E, the sequences from both termini are repeated in an inverted orientation and juxtaposed internally, dividing the genome into two components, each of which consists of unique sequences flanked by inverted repeats. The termini in group F are not identical and are not repeated or inverted.

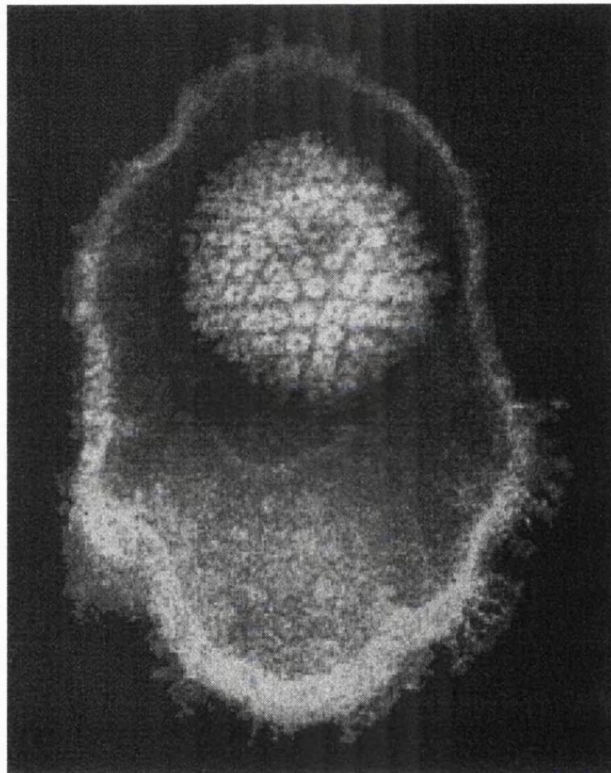


**Figure 1.1. Electron Micrograph of a Herpesvirus**

Taken from The Big Picture Book of Viruses at [www.tulane.edu/~dmsander/Big\\_Virology/BVHomePage.html](http://www.tulane.edu/~dmsander/Big_Virology/BVHomePage.html). Electronmicrograph by Linda Stannard.

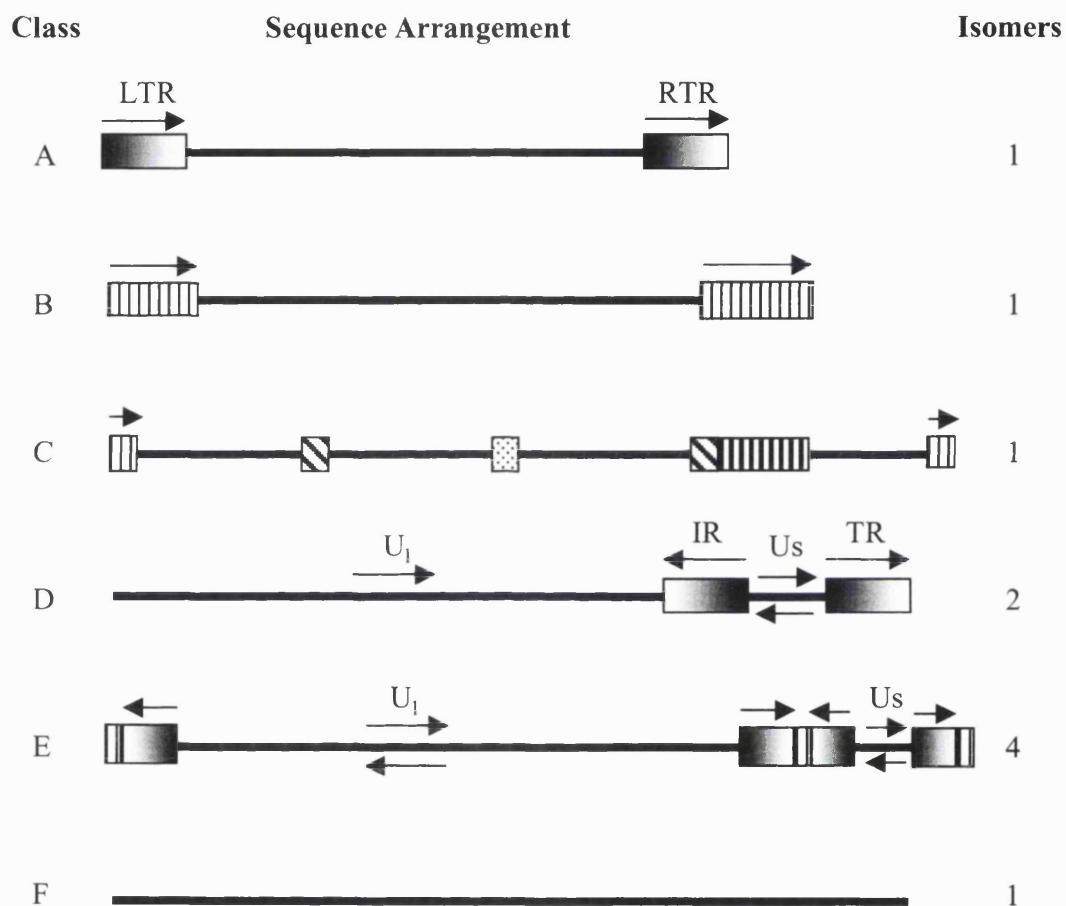


**Figure 1.2. Schematic diagram of the sequence arrangements in the six classes of genomes of the viruses comprising the family *Herpesviridae*.**

The human herpesviruses are classified into each class as follows; A:-Human herpesvirus 6 and 7; C:-Epstein Barr virus; D:-Varicella zoster virus; E:-Herpes simplex virus 1 and 2, human cytomegalovirus. The arrows depict the possible isomers of each class and the boxed regions correspond to the repeat elements.

The herpesviruses share many significant biological properties in addition to the morphological properties described so far. All the herpesviruses encode a large number of enzymes, which are involved in nucleic acid (metabolism thymidine kinase, thymidylate synthetase, dUTPase and ribonucleotide reductase) and DNA synthesis (DNA polymerase, helicase and primase). The viral DNA replication and assembly of capsids occurs in the nucleus and the release of progeny virus invariably results in the destruction of the host cell. A major biological property of the herpesviruses is the ability of the virus to remain a latent infection within the natural host with only a subset of viral genes being expressed.

### 1.1.2. Classification of Herpesviruses

The classification of the herpesviruses is multifactorial and was predominantly based upon their highly variable biological properties, including host range and cell tropism, rate of replication, destruction of cells in culture and cellular sites of latency. However, although highly diverse, the genomes of the human herpesviruses which have been sequenced are now used for classification of the viruses based on the criteria of gene content and sequence similarities. The herpesvirus genomes range in size from 125 to 230 kbp, encoding 70 to 200 genes and as indicated in figure 1.3, have varied patterns of repeated sequences. The International Committee on the Taxonomy of Viruses (ICTV) has classified the herpesviruses into three subfamilies, the *alphaherpesvirinae*, *betaherpesvirinae* and *gammaherpesvirinae*. Table 1.1. shows the classification of the human herpesviruses. The herpesviruses from all three subfamilies have been shown to contain approximately 40 genes, which are common to all the viruses in terms of genomic position and amino acid sequences, indicating a common evolutionary heritage.

#### *Alphaherpesvirinae*

The *Alphaherpesvirinae* are characterised by their broad host range, relatively short replication cycle, rapid spread in culture, efficient destruction of infected cells and the capacity of the virus to establish a latent infection, primarily in the sensory ganglia.

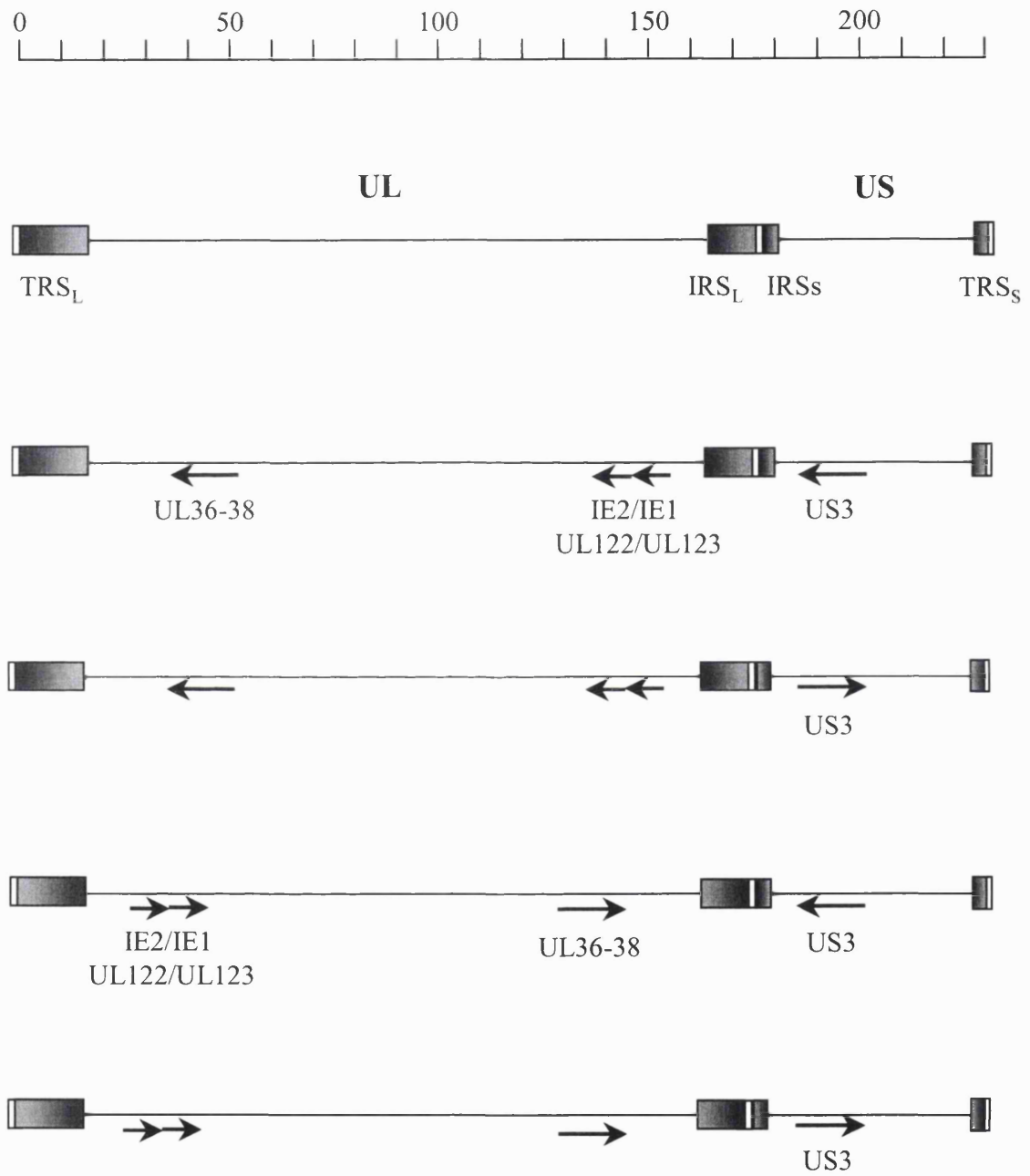


Figure 1.3. Schematic representation of the four isomers of the HCMV genome illustrating the major immediate early genes.

**Table 1.1. Classification of the Human Herpesviruses**

<b>Human Herpesvirus</b>	<b>Abbreviation</b>	<b>Classification</b>
Herpes simplex virus 1	HSV-1	alpha ( $\alpha$ )
Herpes simplex virus 2	HSV-2	alpha ( $\alpha$ )
Varicella zoster virus	VZV	alpha ( $\alpha$ )
Epstein barr virus	EBV	gamma ( $\gamma$ )
Cytomegalovirus	CMV	beta ( $\beta$ )
Human herpesvirus 6	HHV-6	beta ( $\beta$ )
Human herpesvirus 7	HHV-7	beta ( $\beta$ )
Human Herpesvirus 8 (Kaposi's sarcoma-associated virus)	HHV-8	gamma ( $\gamma$ )



***Betaherpesvirinae***

The *Betaherpesvirinae* are characterised by a more restricted host range, a long replication cycle and slow infection in culture. The infected cells frequently become enlarged (cytomegalia) and carrier cultures are frequently established. Latent infection is established and primarily maintained in secretory glands, lymphoreticular cells, kidneys.

***Gammaherpesvirinae***

The *Gammaherpesvirinae* are characterised by a limited host range. All the members of this subfamily replicate in lymphoblastoid cells, although some can cause lytic infection in epithelioid and fibroblastic cells. The gammaherpesvirus subfamily comprises of the *lymphocryptovirus* and *rhadinovirus* genera. These viruses are principally lymphotropic, infecting either B-lymphocytes ( $\gamma 1$  viruses) or T lymphocytes ( $\gamma 2$  viruses) and infection is primarily latent. Lytic replication infrequently occurs following primary infection and is generally limited to a small subset of spontaneously replicating cells.

**1.1.3. Human Herpesviruses**

Eight human herpesviruses have been identified to date and with the advances in detection of new viruses, more are likely to be found.

***Herpes simplex virus types 1 and 2 (HSV-1 and HSV-2)***

HSV consists of two antigenic types, HSV-1 and HSV-2 which are highly related, showing 70 – 80% genetic identity and are classified as alphaherpesvirinae of genome structure E (figure 1.2). The virus infects and replicates in the mucocutaneous cells, whereupon it is transported via retrograde axonal transport to the cell bodies of neurons in sensory ganglions, the trigeminal ganglion if the initial infection was oral or the dorsal root ganglion if the initial infection was genital. The virus persists in these cells in a latent state and can persist for the lifetime of the infected individual. Latent virus can either reactivate spontaneously, or can be induced to reactivate upon a variety of stimuli. During reactivation the virus is transported via the nerve cell axons to the point of original infection where it replicates. HSV replication can manifest as a variety of clinical conditions, most common of which are oral-facial and genital

infections. Gingivostomatitis and pharyngitis are the most frequent clinical manifestations of primary HSV-1 infection and herpes labialis (cold sores) in reactivated HSV-1 infection. Both HSV-1 and HSV-2 produce primary genital infection although most cases are due to HSV-2. Infection may often be asymptomatic or subclinical, suggesting that the incidence of genital herpesvirus infections may be under diagnosed. Neonatal HSV infection is primarily due to HSV-2 where transmission from mother to newborn occurs during the birthing process. The greatest risk factor for the newborn is primary infection of the mother as the baby is exposed to significantly more virus than those with reactivated infection. Three categories of neonatal disease can develop; (1) disease localised to skin, eye or mouth, (2) encephalitis with or without skin, eye or mouth involvement, (3) disseminated infection involving multiple organs including CNS, lung, liver, adrenal glands, skin, eye and or mouth. Encephalitis is the most common infection of the central nervous system, accounting for 10 to 20% of all cases. Most cases have demonstrable clinical and serological evidence of infection prior to encephalitis. Other problematic HSV infections include herpetic eye infection and herpetic skin infection.

### ***Varicella zoster virus (VZV)***

Varicella zoster virus is also classified as an alphaherpesvirus with the type D genome structure. It is the etiologic agent of both varicella (chicken pox) and zoster (shingles). Primary VZV infection causes varicella in susceptible individuals, usually during childhood, and causes an uncomplicated disease. Following primary infection, VZV establishes latent infection in the neural ganglia and reactivates as herpes zoster, particularly in the elderly population. Severe neuralgia is often associated with zoster, which can often persist upon resolution of clinical symptoms. Transmission occurs primarily via aerosolised respiratory secretions from individuals with varicella.

### ***Epstein-Barr virus (EBV)***

Epstein-Barr virus is classified as a gammaherpesvirus (genus *lymphocryptovirus*), has a type C genome structure and can be divided into two types, A and B based upon the DNA sequence divergence in EBV nuclear antigens (EBNAs), 2, 3, 4 and 6, with EBNA-2 being the most divergent. Primary EBV infection usually occurs in childhood when infection is usually asymptomatic. Initial events following transmission of the virus are poorly understood, but one school of thought suggests the virus may infect

and replicate in oropharyngeal epithelial cells, although this issue is still contentious. B lymphoid cells are the primary target of EBV, they are infected before the onset of clinical symptoms and EBV can spontaneously transform these cells into immortal lymphoblastoid cell lines. Primary EBV infection in adolescence or adulthood usually results in infectious mononucleosis (IM, glandular fever). Since the discovery of EBV it has been associated with human malignant tumours of either hematopoietic or epithelial cell origin, including Burkitts lymphoma, nasopharyngeal carcinoma, Hodgkins lymphoma and post transplant lymphoproliferative disease.

***Human herpesvirus 6 (HHV-6)***

Human herpesvirus 6 is classified as a betaherpesvirus with a group B genome structure and has been classified as such due to its DNA sequence homology to HCMV (66%), the prototype member of the betaherpesvirinae. HHV-6 exists as two variants, A and B based upon antigenic specificity, genetic polymorphism and in vitro growth. HHV-6 is ubiquitous in the human population, with 90% seropositivity demonstrable within the first two years of life. Primary infection with HHV-6 B has been associated with exanthem subitum in infants (Pruksanandonda et al., 1992, Leach et al., 2000), but no clinical syndromes have yet been linked with HHV-6 A. In the immunocompetent host, HHV-6 infections have been associated with encephalitis (Asano et al., 1992), hepatitis (Asano et al., 1990) and more controversially, with multiple sclerosis (Soldan et al., 1997). In immunocompromised individuals, either transplant patients or AIDS patients, HHV-6 infection has been shown to give rise to bone marrow suppression (Drobyski et al., 1993, Carrigan and Knox., 1994), pneumonitis (Buchbinder et al., 2000), graft versus host disease (Takemoto et al., 2000) and encephalitis in bone marrow patients (Singh and Paterson, 2000, Singh and Carrigan, 1996, Imbert-Marcille et al., 2000) and acute rejection in liver transplant patients (Humar et al., 2002). In individuals infected with HIV, HHV-6 has been implicated as a cofactor for AIDS pathogenesis and progression, primarily because HHV-6 has a cellular tropism for CD4+ T-lymphocytes, similar to that of HIV (Lusso et al., 1993).

***Human herpesvirus 7 (HHV-7)***

Human herpesvirus 7 has been classified as a betaherpesvirus with a type B genome structure. The complete sequence of HHV-7 shows it is most closely related to HHV-6, and related to HCMV to a lesser extent (Berneman et al., 1992). Association of

primary HHV-7 infection with disease is not certain, although HHV-7 may be associated with some cases of exanthem subitum, but this may be due to its potential to reactivate HHV-6 (Tanaka-Taya et al., 2000). In the immunocompromised host, HHV-7 has been implicated in increasing the relative risk of developing HCMV disease if both HHV-7 and HCMV are detected in the blood (Kidd et al., 2000).

### ***Human herpesvirus 8 (HHV-8)***

Human herpesvirus 8 or Kaposi's sarcoma-associated herpesvirus (KSHV) is the most recently discovered member of the human herpesviruses (Chang et al., 1994). Initially, HHV-8 was identified by representational difference analysis of non-diseased tissues and KS tissue of the same patient as herpesvirus-like DNA sequences. Now HHV-8 has been identified in all the forms of KS as well as AIDS-related primary effusion lymphomas (Cesarman et al., 1995) and multicentric Castleman's disease (Soulier et al., 1995), implying this virus is the etiological agent of KS. The sequences were homologous to, but distinct from, capsid and tegument protein genes of the gammaherpesviruses HVS and EBV, thus, together with the sequencing of the HHV-8 genome to date, has been classified as a gammaherpesvirus, of the genus *Rhadinovirus*.

## **1.2. Human Cytomegalovirus**

### **1.2.1. Epidemiology**

The natural transmission of HCMV occurs by both direct and indirect person to person contact during primary infection, reinfection or reactivation. HCMV is an extremely labile virus requiring intimate contact for its spread. Horizontal transmission may occur from birth, either during delivery when the baby is exposed to maternal genital secretions or from breast milk (Stagno et al., 1983), and virus excretion persists for years following congenitally, perinatally or early postnatally acquired infections. In the United States, HCMV is the most common cause of congenital infection, affecting between 0.2% to >3% of all live births (Alford et al., 1990). The majority of infection is acquired during young childhood (8 – 60% ≤ 6 months) as a result of infection acquired during birth or following breast feeding. Transmission among young children attending play groups and day care centres may occur in up to 80% of children, compared to 20% of children cared for at home (Pass et al., 1986). Infection steadily increases after infancy with a short but rapid increase at school entry so that by

adolescence 40% to 80% of children are infected which increases by approximately 1% per annum thereafter (Griffiths and Baboonian, 1984). This figure reaches 90% to 100% in low socio-economic areas of the world. Children in day care centres with sub-clinical infection are the major source of HCMV transmission to their parents, which is of particular importance if the mother is pregnant. In different populations, 0.7% to 4% of seronegative pregnant women experience primary infection, and such women have a 20-fold increased risk of infection if they care for children in day care centres (Pass et al., 1986, 1987).

Transmission in the adult population occurs primarily via a sexual route, where HCMV is shed from both the male and female genital tracts. This is shown by the correlation between seropositivity and (1) seropositivity of partner in marriage (or seronegativity in both partners), (2) number of sexual partners, (3) number of STD's, (4) non-use of barrier contraception, (5) young age of first sex.

An increased rate of productive HCMV infection is observed in the immunocompromised patient group, such as transplant and AIDS patients. These patients either reactivate their own virus due to their state of immunosuppression, or experience primary infection by direct exposure of a seronegative individual to an organ from a seropositive donor (D+/R-). During the period of immunosuppression, nearly 100% of seropositive patients, seropositive allograft recipients and AIDS patients with a CD4 count of  $<50/\text{mm}^2$  excrete HCMV (Weir et al., 1988, Dummer, 1990, Meyers et al., 1986, Gallant et al., 1992).

### **1.2.2. HCMV pathogenesis in the immunocompromised host**

This section will highlight the impact of HCMV on the immunocompromised, including the recipients of solid organs and bone marrow as well as the acquired immunodeficiency disease (AIDS) patients. HCMV causes a range of diseases and complications in the immunocompromised host (table 1.2) and for this reason a definition for HCMV end organ disease has been internationally agreed (table 1.3). The disease manifestations vary between the immunocompromised patient groups, such that pneumonitis is the most prevalent manifestation of HCMV disease in the bone marrow recipients, whereas hepatitis is the most frequent in liver transplant patients and retinitis in the AIDS patients. Severe disseminated HCMV disease can spread to and

Table 1.2. HCMV diseases in the immunocompromised (Griffiths et al., 2000)

Symptoms	Solid organ transplant	Bone marrow transplant	AIDS
Fever/hepatitis	++	+	+
Gastrointestinal	+	+	+
Retinitis	+	+	++
Pneumonitis	+	++	
Myelosuppression		++	
Encephalopathy			+
Polyradiculopathy			+
Addisonian state			+
Immunosuppression	+		
Rejection/GVHD	+	?	

+, Diseases that occur in the designated patient population

++, Diseases that were the most common

?, Suggested, but not proven association

**Table 1.3. Definitions of Cytomegalovirus end organ disease.  
(Ljungman et al., 2002)**

<b>Disease</b>	<b>Definition</b>
Pneumonia (transplant recipients)	Radiographic changes and/or hypoxia CMV detected in BAL or lung biopsy
Pneumonia (HIV infected individuals)	Symptoms of pneumonia with hypoxaemia CMV detected in the lung Absence of other pathogens
Gastrointestinal Hepatitis	Gastrointestinal symptoms with CMV detected by histology Abnormal liver function tests, histological changes and CMV detection in liver biopsy
Neurological	Symptoms of encephalitis, transverse myelitis or other CNS symptoms, plus CMV in CSF
Retinitis	Typical ophthalmological lesions without virological proof

be detected in every organ system in the body, however some systems are more common than others. Investigations over the years have shown that HCMV detection and viral load are the critical factors in pathogenesis of the immunocompromised (Einsele et al., 1991, Kidd et al., 1993, Pillay et al., 1992, 1993, Fox et al., 1995). Among recipients of solid organ transplants, risk factors have been identified for the potential development of HCMV (end organ) disease. These include donor/recipient (D/R) serostatus giving rise to primary infection, re-infection or reactivation, viraemia (Pillay et al., 1993) and peak viral load following transplant (Cope et al., 1997a, 1997b, Gor et al., 1998). The most significant of these is the peak viral load following transplantation, from which the 'threshold concept of HCMV disease' was determined. Molecular techniques such as quantitative competitive PCR have been employed to perform longitudinal studies upon different patient groups at risk of HCMV disease. These studies have not only highlighted the risk factors for development of HCMV disease, but have demonstrated the importance of routinely monitoring and quantifying the HCMV DNAemia in patients at most risk of developing disease. This is of particular importance when considering pre-emptive therapy with antivirals such as ganciclovir (GCV). If viral loads exceed the threshold level in the post transplant period, antiviral therapy can be initiated to prevent disease by lowering the viral load to below threshold levels, which is a more realistic goal than complete eradication of the virus. Viral load probability of disease curves constructed for each of the transplant groups (Emery, 2000A) demonstrated that disease probability remains low until a specific viral load (threshold level) is reached, then accelerates rapidly for a relatively small increase in viral load. This study demonstrated HCMV disease occurred at a median of 5.7 log<sub>10</sub> genomes/ml blood in liver transplant recipients, 4.9 log<sub>10</sub> in bone marrow recipients, 6.48 log<sub>10</sub> genomes/ml urine or 5.6 log<sub>10</sub> genomes/ml blood (Hassan Walker et al., 1999) in renal transplant recipients and 4.9 log<sub>10</sub> genomes/ml blood in AIDS retinitis patients.

Criteria for the treatment of HCMV infection and disease have mainly evolved from the transplant setting for two major reasons. (1) Transplant patients have a clearly defined risk of infection. (2) Transplant recipients are most intensely immunosuppressed early in the post transplantation period and become less immunosuppressed as immunosuppressive therapy is gradually withdrawn, thus the risk of disease development occurs over a defined period of time, usually the first 3 months following



transplant. In general, the degree of immunosuppression in the recipient can be correlated with increased risk of HCMV infection. The patients at highest risk of HCMV disease are in the D+/R- group, where disease is often more severe than in the D+/R+ group, suggesting that pre-existing immunity may modulate HCMV infection. However as the level of immunosuppression increases, the contribution of this immunity to HCMV disease decreases. The strategies used in the transplant setting aim to reduce and maintain the viral load below the threshold level, above which disease may occur rapidly. Two major strategies are employed in the transplant patient groups, prophylaxis and pre-emptive therapy.

Prophylaxis is given to all patients at risk of developing HCMV infection/ disease in the post transplant period, before HCMV infection is detected. Prophylaxis for a defined period of time has been extremely successful at controlling viral replication (Gane et al., 1997, Lowance et al., 1999). The period of prophylaxis generally occurs when the patient is most intensely immunosuppressed, which is usually the first 3 months post transplant. A meta-analysis based upon 13 prospective, randomised studies comparing anti-HCMV prophylaxis using either aciclovir (ACV) or GCV versus placebo or no treatment demonstrated a significant decrease in the incidence of HCMV infection and disease (Couchoud et al., 1998). A randomised trial involving the universal prophylactic administration of i.v. GCV to patients for 100 days following liver transplantation was associated with an HCMV disease rate of 1% among all patients and 10% among the D+/R- group (Winston et al., 1995). This compared with a similar trial involving universal prophylactic administration of oral GCV for 100 days post liver transplant, which reduced the HCMV rate to 5% among all patients and to 15% among the D+/R- group (Gane et al., 1997). However, it has become increasingly evident that approximately 25-30 days following the period of prophylaxis, late HCMV disease has become a problem (Limaye et al., 2000). This is exacerbated by the delay in intervention with antiviral drugs due to infrequent outpatient visits, resulting in replication of the virus to levels exceeding that of the threshold level, so significantly increasing the risk of disease (Emery et al., 1999A). Furthermore, these patients will require an extended period of i.v. GCV therapy to control viral replication and for undetectable levels of virus to be achieved. Another important consideration for prophylactic therapy concerns the development of resistance of HCMV to the antiviral drugs. Reports of increased risk of resistance following prophylaxis in the literature

(Alain et al., 1997, Rosen et al., 1997, Baldanti et al., 1998a, Mendez et al., 1999, Kruger et al., 1999) are conflicting with reports which show no association (Gane et al., 1997, Boivin et al., 1993). A recent report examined the antiviral susceptibility of isolates from 240 recipients of solid organ transplants, 68% of whom were D+/R- (Limaye et al., 2000). This study demonstrated 10.4% of the patients developed HCMV disease within the year following transplantation. GCV resistance, as defined by IC<sub>50</sub> and UL97 mutations, occurred in 7% of the D+/R- group. The majority of the isolates were also cross resistant to cidofovir and sensitive to foscarnet, but significantly all the patients were treated prophylactically with GCV and all disease was late onset (>10 months post transplantation).

Pre-emptive therapy is given to high-risk patients with evidence, such as detection of HCMV by PCR in the blood, of HCMV infection in an attempt to prevent progression of asymptomatic infection into HCMV disease (Emery, 2001). Since as few as 30% of patients at risk will develop HCMV disease, over-treatment in patients receiving antiviral therapy could reach approximately 70%. Thus, pre-emptive therapy reduces the number of patients exposed to the potentially toxic antiviral drug, but can only be successful if regular monitoring of the patient for HCMV occurs using sensitive detection methods and treatment is implemented upon detection. This is of greatest value to HCMV naïve patients (D+R-) as the antigen exposure, which occurs with the initial HCMV replication, should result in priming of the immune system to HCMV. A number of studies involving the pre-emptive treatment of high risk transplant patients have demonstrated a reduction in the rate of HCMV disease comparable to that of universal prophylaxis. The rate of HCMV disease was reduced to 0% - 6% (Boeckh et al., 1996, 1998, Kusne et al., 1999, Egan et al., 1998, Singh et al., 2000A).

The efficacies of various antiviral drugs have been examined for each of the prophylactic and pre-emptive arms of therapy. The majority of studies described so far have used either oral or i.v. GCV, but due to various factors including renal toxicity, indirect effects of therapy, potential resistance and attempts to improve antiviral efficacy, further antivirals have been evaluated. Several studies comparing high dose ACV either alone or in combination with GCV have shown no advantage of GCV alone. One study in liver transplant patients (D+/R-) treated with ACV prophylaxis demonstrated HCMV disease occurred in 58%, and a combination of ACV and GCV

(D+/R-) demonstrated HCMV disease occurred in 25% (Badley et al., 1997). This is in contrast to patients treated with GCV prophylaxis where HCMV disease occurred in up to 15% of patients. ACV prophylaxis 5 days pre-transplant followed by delayed GCV also shows no advantage (Paya et al., 1993, Duncan et al., 1994). Oral valganciclovir (VACV) has been used successfully as prophylactic treatment for HCMV, whereby the incidence of HCMV disease 90 days post transplant in the D+/R- group was reduced from 45% (placebo) to 3% (VACV). At six months post transplant, the incidence of disease was the same in the placebo group, but had increased to 16% in the VACV group (Lowance et al., 1999). So although VACV decreased the incidence of viraemia, viruria and graft rejection as well as herpes simplex virus infection, it resulted in delayed onset of disease as observed for with GCV prophylaxis. A major advantage, however, is that VACV is considerably better tolerated than GCV, with minor CNS events such as hallucinations and confusion being the only significant side effects occurring in up to 10% of patients. Two small studies examined foscarnet prophylaxis in bone marrow patients and found the risk of HCMV disease was 9%, comparable with GCV prophylaxis, however nearly half the patients experienced severe side effects including renal toxicity, leading to discontinuation of therapy. All renal toxicity was reversible upon discontinuation of therapy. Cidofovir has been used successfully in the primary treatment of HCMV pneumonia (56%), as secondary pre-emptive therapy following either relapse (83%) or failure of primary GCV therapy (55%) and as primary pre-emptive therapy (58%) (Ljungman et al., 2001). The dosage of cidofovir balanced with efficacy must be fully examined as renal toxicity occurred in a high proportion of patients, up to 35% in some patients. A distinct advantage however was as secondary pre-emptive therapy following failure of primary GCV therapy. The study did not examine why primary GCV therapy failed, or indeed if this was as a result of GCV resistance, but when considering cidofovir as secondary therapy, cross resistance may be a potential problem.

### **1.2.3. HCMV and Renal Transplant Recipients**

Renal dysfunction rarely occurs as a result of HCMV infection, but in the renal transplant patient, HCMV has been proposed to play a direct role in renal dysfunction and graft rejection (Kidd et al., 2000, Lowance et al., 1999). In renal transplant recipients, a distinct glomerulopathy characterised by enlargement of endothelial cells, and fibrillar materials in glomerular capillaries have been associated with HCMV

viraemia (Richardson et al., 1981). Between 15% to 50% of renal transplant recipients excrete HCMV following transplantation, 30% to 40% of whom develop HCMV disease (Balfour et al., 1989). HCMV seronegative patients acquiring primary infection from the seropositive kidney donor are at greater risk of developing disease than those with re-infection (donor virus infecting an immune individual), who in turn are at greater risk than those with reactivation of latent virus (Grundy et al., 1988, Ranjan et al., 1991). Also, therapies which increase the degree of immunosuppression, such as antithymocyte globulin (ATG) which are directed at eliminating T-lymphocytes are associated with more frequent and severe HCMV infections in the post transplant period (Rubin et al., 1981). Longitudinal PCR analysis to detect HCMV DNA (Fox et al., 1992), in the urine of 196 patients following renal transplantation identified 35 patients who developed CMV viraemia (Cope et al., 1997B). Twelve of these patients developed CMV disease as defined in table 1.3, all of whom were symptomatic during their periods of highest viral load. The relationship between maximum viral load, DNAemia and donor/recipient serostatus was determined using univariate and multivariate analysis. The univariate analysis showed that every 0.25 log<sub>10</sub> increase in viral load resulted in a 79% increase in risk of HCMV disease. The multivariate analysis showed that peak viral load was a significant risk factor for HCMV disease in both urine and blood. This was mirrored in a similar study by Hassan-Walker et al., (1999) in a study of 87 renal transplant patients, who also received antithymocyte globulin (ATG) to treat graft rejection. Univariate analysis showed ATG was a significant risk factor for the development of disease.

#### **1.2.4. HCMV and Liver Transplant Recipients**

HCMV is the most common infection following liver transplantation, being detected in 20% to 60% of patients, 50% of whom develop HCMV disease (Paya et al., 1989). Following liver transplantation, a distinct syndrome of bile duct sclerosis, the vanishing bile duct syndrome, has been associated with HCMV infection. The cause of the syndrome is unknown but it has been suggested that HCMV infection leads to increased expression of MHC antigens in the graft, predisposing the graft to rejection. Another suggestion involves the mimicry of MHC antigens by HCMV proteins leading to host-mediated graft dysfunction. The risk factors for HCMV disease include large doses of immunosuppressive drugs, seropositive organ donor and the appearance of viraemia (Sutherland et al., 1992, Portela et al., 1995, Badley et al., 1996). Cope et al.,

(1997B) performed a similar study to that determined in renal transplant patients, whereby PCR analysis was performed upon the blood of 162 patients, 51 of whom developed viraemia and of the 47 analysed in detail, 20 developed HCMV disease. Univariate analysis identified the viral load, donor seropositivity and total methyl prednisolone as significant risk factors for HCMV disease. Multivariate analysis identified maximum viral load and total methyl prednisolone as independent risk factors for the development of HCMV disease. This independence implies that (1) large quantities of methyl prednisolone for rejection episodes predispose the patient to HCMV disease at lower viral loads, and (2) higher viral loads are needed to produce HCMV disease in patients who experience few rejection episodes so receiving lower levels of augmented methyl prednisolone. Studies using PCR to detect virus in peripheral blood is the best predictor of HCMV disease (Patel et al., 1995) but assumes that detection will mirror the events occurring in the body as a whole. This is not always the case and attempts to circumvent HCMV disease by pre-emptive therapy could be further refined to avoid treatment of patients with two consecutive positive PCR results, not destined to develop disease, with potentially toxic antiviral drugs. A new assay for the detection of HCMV-specific IgM to a cocktail of purified recombinant protein antigens derived from UL32 (pp150), UL44 (pp52), UL83 (pp65), and pUL80a (pp38) was retrospectively employed to determine the best patients to receive pre-emptive therapy. IgM was detected in 29 patients out of 47 with DNAemia from the study by Cope et al., [(1997B), Emery et al., 2000B]. These patients would have received pre-emptive therapy, including the 18 who went on to develop HCMV disease. This is in comparison with the 36 patients who would have received pre-emptive therapy on the basis of two consecutive PCR-positive results, 19 of whom went on to develop disease. IgM was not detected in one patient who developed disease, but in whom two consecutive PCR-positive results were obtained. IgM detection by this assay could theoretically enable the initiation of pre-emptive therapy at an early stage, before the development of clinically overt disease, in fewer patients. This assay was more sensitive than the crude viral antigen microtitre ELISA (Maine et al., 2000) and detected HCMV-specific IgM before the detection of viral proteins by the pp65 antigenaemia assay. IgM was also demonstrated in patients receiving large doses of methyl prednisolone, although the maximum titre of IgM was lower, presumably reflecting the lower virus load required to produce HCMV disease.

### **1.2.5. HCMV and Bone Marrow Transplant Recipients**

Of all the transplant groups, bone marrow allograft recipients have the highest HCMV related mortality and a complex association between HCMV and graft versus host disease (GVHD). The incidence of HCMV infection following allogenic BMT ranges from 40 to 50%, regardless of the serostatus of the donor and recipient. The most significant HCMV associated disease in this transplant group is HCMV pneumonia, which occurs in 10% to 15% of patients. With the advent of GCV treatment, the rate of HCMV pneumonia-related mortality from nearly 80% to between 10% and 20%. The disease is usually diagnosed by clinical evidence and the detection of HCMV in bronchoalveolar lavage (BAL). The proposed mechanism of pathogenesis of disease concerns host-directed, immunologic destruction of the lung associated with GVHD.

The risk factors for HCMV in the bone marrow transplant recipients include the receipt of marrow from a seropositive allogenic donor, reactivation of the recipient HCMV and acute GVHD. A longitudinal analysis involving 110 patients following bone marrow transplantation identified 49 patients with HCMV viraemia, 15 of whom developed HCMV disease (Gor et al., 1998). As expected, HCMV disease occurred more frequently in allogenic bone marrow recipients than in autologous transplant recipients. This study importantly showed that peak viral load precedes the onset of pneumonitis, the most common manifestation of HCMV disease in this population, consistent with the immunopathologic nature of HCMV pneumonitis. Symptomatic patients experienced significantly elevated viral load, including those patients experiencing reactivation of their own virus. Univariate analysis showed both elevated viral load and reactivation of recipient virus was associated with increased risk for development of HCMV disease, however multivariate analysis showed only elevated viral load was a significant risk factor.

### **1.2.6. HCMV and Acquired Immunodeficiency Syndrome**

HCMV has long been considered a cofactor in the pathogenesis of HIV, possibly by influencing the induction or progression of the disease (Griffiths, 1992, 1998). Although direct evidence for this relationship has not been substantiated, epidemiological studies (Webster et al., 1989, Sabin et al., 1995) implicate HCMV in HIV progression. HCMV and HIV proviral DNA have been identified in the same post mortem organs from patients who died with AIDS (Nelson et al., 1988, Webster et al.,

1995). The median viral loads of HCMV and HIV were determined for multiple post mortem organs, but the viral load between organs were similar irrespective of the presence of HIV suggesting there is not an *in vivo* relationship between the viruses (Emery et al., 1999B). Several mechanisms have been proposed by which HCMV interacts with HIV (table 1.4.) where *in vitro* studies have shown HCMV can upregulate HIV activation or alter HIV tropism.

HCMV remains one of the most important opportunistic pathogens in the pathology of HIV. Over 90% of patients with HIV are also HCMV seropositive. HCMV is maintained in a latent state in the healthy body by cell mediated immunity, but in HIV patients the majority of HCMV disease is caused by the reactivation of this latent virus due to a decrease in CD4 and CD8 HCMV-specific cytotoxic T cell numbers. Prospective studies suggested that following an AIDS diagnosis, the probability of developing invasive HCMV disease within 2 years was approximately 24%, and a CD4 count of  $< 50/\text{mm}^3$  is an important risk factor. HCMV was the commonest opportunistic viral infection in patients with AIDS and retinitis, colitis and encephalitis were the most frequently observed end organ diseases, although HCMV disease has been observed in almost every organ system. This universal infection of the body and by implication, multiple cell types suggests a generation of multiple viral variants with extended cellular tropism. HCMV retinitis was the most common manifestation of HCMV disease, occurring in up to 30% of AIDS patients. Of the patients who develop HCMV disease, up to 85% of these will develop HCMV retinitis. The natural history of a case of untreated HCMV retinitis described how a patch of white granular necrosis was initially observed on the retina of one eye, spread to the other eye within 1 month and by 5 months post diagnosis, the patient was blind and experiencing hypoadrenalism (Bowen et al., 1995). The patient died within 8 months of initial diagnosis highlighting the severity of the disease without antiviral intervention. A study of 45 AIDS patients with HCMV retinitis treated with GCV identified the importance of HCMV load in the pathogenesis of HCMV retinitis (Bowen et al., 1996). A trend was identified for high HCMV load in blood to be associated with a shorter time to retinitis progression, however a significant relationship was identified for high viral load in blood and a shorter time to death. Following 21 days induction therapy with GCV, 33/39 patients

**Table 1.4. Interaction between Human Cytomegalovirus and HIV *in vitro***

<b>Effect of interaction</b>	<b>Proximity of HIV/herpesvirus</b>	<b>Mechanism of interaction</b>
Activate HIV proviral DNA	Same cells	Transactivation
	Neighbouring cells	Cytokine release
		Antigen presentation
Alter HIV tropism	Same cells	Pseudotype formation
	Neighbouring cells	Induce HIV receptor/coreceptor
		Induce alternative HIV receptor



with a median viral load of 4.95 log<sub>10</sub> genomes/ml (85%) became PCR negative. These patients had a median time to disease progression of 78 days compared with 40 days for the remaining patients with a median viral load of >4.95 log<sub>10</sub> genomes/ml. The difference in median survival time between the 2 groups was 3.9 months and the risk of death was increased by 88% for each log increase in blood viral load. Somewhat surprisingly, between 15% and 20% of patients with HCMV retinitis were HCMV PCR negative, suggesting HCMV infection and peak in viral load occurred prior to retinitis onset. This poses the problem of monitoring the antiviral response during therapy, especially with retinitis progression with undetectable blood PCR. Before the advent of highly active antiretroviral therapy (HAART), the prognosis for patients in whom HCMV disease had been diagnosed was poor.

One of the most important risk factors for the development of HCMV disease was the CD4 count, where patients with a CD4 count of <50 cells/μl had a 21.4% risk of disease (Gallant et al., 1992). Once HCMV disease was established, treatment strategies involved a combination of induction and maintenance therapy, which temporally inhibited disease progression, but relapse was inevitable and invariably treatment was continued indefinitely. The most important consideration was to identify patients at highest risk of developing HCMV disease, as with the transplant group, by HCMV PCR. Several studies have been employed to determine if HCMV reactivation, as detected by PCR, is a predictive factor of HCMV disease. A prospective study of 97 patients examined whole blood for HCMV DNA by PCR monthly over a 15 months (Bowen et al., 1997). The results showed that HCMV detection at baseline was significantly associated with the development of HCMV disease, and was of greater significance than the CD4 count. Two further studies in the same year confirmed these results (Dodt et al., 1997, Shinkai et al., 1997) and indicated that PCR was superior to antigenaemia and cell culture in the prediction of HCMV disease. HCMV PCR became positive at a median of 46 days prior to HCMV disease compared with 34 days for antigenaemia and 1 day for cell culture (Dodt et al., 1997). These studies also used viral load to predict disease development, such that median viral load was significantly higher in patients who went on to develop disease (4.77 log<sub>10</sub> vs 4.0 log<sub>10</sub>) and that for every 0.25 log<sub>10</sub> increase in viral load, a 37% increase in the probability of HCMV disease occurred (Bowen et al., 1997).

This section will discuss the treatment strategies available for these patients and how the disease course has changed with the advent of HAART. Newly diagnosed HCMV retinitis is treated with a 14 to 21 day induction course of high dose i.v. GCV (5mg/kg twice daily) or foscarnet (90 mg/kg twice daily (Jacobson., 1997a & b). Table 1.5. gives the induction and maintenance drug regimens as well as the intraocular implants and injections. Therapy initially halts the retinal cell destruction and reduces the virus in blood and urine to undetectable levels by PCR. Induction therapy was generally followed by maintenance therapy, which continued long term. If therapy was stopped following induction therapy, progression of HCMV retinitis recurred within two to six weeks. Eventually, despite long term therapy, HCMV retinitis reactivated and retinal damage continued.

Re-induction therapy with the same or alternative drug only temporarily controlled further viral replication, but the time to total visual loss was prolonged. Table 1.6 gives a comparison of trials comparing GCV therapy either administered orally or intravenously, showing mean time to disease progression. The median time to progression of HCMV disease in the trials examined was 57 days (range 54 to 86 days) for oral GCV and 64 days (range 62 to 109 days) for iv. GCV. A direct comparison of foscarnet and GCV induction therapy for 21 days showed 86% of patients treated with GCV had a complete response at 3 weeks compared to 68% of patients treated with foscarnet (Moyle et al., 1992). This is similar to independent studies of GCV and foscarnet induction therapy, where 83% of patients treated with GCV showed a complete response (Buhles et al., 1988) and 73% of patients treated with foscarnet (Gerna et al., 1994).

The introduction of HAART has had a considerable impact on the occurrence of opportunistic infections in HIV patients, including HCMV disease, and a reduction in the death rate from AIDS (Palella et al., 1998; Mocroft et al., 1998). HAART is generally accepted as a potent combination of antiretroviral drugs, including at least one protease inhibitor or a non-nucleoside reverse transcriptase inhibitor, plus at least two nucleoside reverse transcriptase inhibitors. A dramatic decrease in HCMV retinitis has been observed in various studies on the decline in incidence of HCMV retinitis in the era of HAART (outlined in table 1.7.).

**Table 1.5. Regimens used in the Treatment of Patients with HCMV Retinitis**

<b>Drug</b>	<b>Induction regimen</b>	<b>Maintenance regimen</b>
<b>GCV</b>		
Intravenous		
Standard dose	5 mg/kg/ every 12 hrs	5 mg/kg/day
High dose	5-7.5 mg/kg every 12 hrs	10 mg/kg/day
Oral	NA	1 g 3 times/day
Implant	Surgical placement	Replacement 6 months
Intraocular injections	400 µg twice/wk	400 µg twice/wk
<b>Foscarnet</b>		
Standard dose	90 mg/kg every 12 hrs	90 mg/kg/day
High dose	90 mg/kg every 12 hrs	120 mg/kg/day
Intraocular injections	2400 µg twice/wk	2400 µg/wk
<b>GCV and Foscarnet</b>	90 mg of foscarnet/kg every 12 hr plus 5 mg GCV/kg/day for 14 days  or 5mg GCV/kg/12 hr plus 90mg of foscarnet/kg/day for 14 days	5 mg GCV/kg/day plus 90 mg of foscarnet/kg/day
<b>Cidofovir</b>	5 mg/kg/wk for 2 wks	5 mg/kg every 2 wks

Adapted from Jacobson., 1997

**Table 1.6. Comparison of studies of maintenance therapy for HCMV retinitis**

<b>Study</b>	<b>Patient no.</b>	<b>Drug regimen</b>	<b>% progression</b>	<b>Mean time to progression (Days)</b>	<b>Endpoint (fundus enlargement)</b>
Spector et al., 1996	725	oral GCV Placebo	14% 26%		Progression
Hardens et al., 1996	159	oral GCV i.v. GCV	72% 76%		Progression
Squires et al., 1996	1653	oral GCV i.v. GCV	12.4% 14.1%	57 days 62 days	Progression
	1774	oral GCV i.v. GCV	15.8% 20.9%	54 days 66 days	Progression
Danner & Matheron., 1996	159	oral GCV i.v.GCV	57% 32%	86 days 109 days	Progression
Drew et al., 1995	115	oral GCV i.v. GCV	67% 54%	57 days 62 days	Progression

Prior to HAART, HCMV disease progression was well documented, as discussed earlier, and there were no cases reported of resolution of HCMV viraemia without the use of specific antiviral intervention. The detection of HCMV viraemia was both predictive of the development of HCMV disease and higher levels of asymptomatic viraemia were associated with an increased risk of death. Upon the introduction of HAART, the natural history of HCMV disease was profoundly altered, with a decline in the number of newly diagnosed cases of HCMV disease and a halt in the progression of previously diagnosed HCMV disease including retinitis. There were reports however, describing new cases of HCMV retinitis occurring at unusually high CD4+ counts following HAART (Gilquin et al., 1997; Mallolas et al., 1997). These were the minority or cases.

A study of 16 HIV-positive patients was designed to determine the effect of HAART on the outcome of asymptomatic HCMV viraemia (Deayton et al., 1999). The introduction of HAART reduced the risk of HCMV disease due to the prompt reduction in HCMV load to undetectable levels. This was all the more encouraging when considering the median HCMV load in these patients was equivalent to previously observed levels at time of diagnosis of HCMV retinitis. This effect is consistent with the reduction in viral load observed in immunocompromised transplant patients upon reduction of immunosuppressive therapy, whereupon a recovery of immune function is observed. Indeed, patients with quiescent HCMV-associated end organ disease showed a sustained increase in the CD4+ cell count and have a strong CMV-specific CD4+ lymphocyte response (Komanduri et al., 1998; Autran et al., 1997). Further studies of patients with a positive HCMV PCR at commencement of HAART suggested that detection of HCMV was associated with an increased risk of HCMV disease development, but not death (Casado et al., 1999). The authors suggest such patients should receive pre-emptive therapy before the initiation of HAART (Casado et al., 1999; Spector et al., 1999).

From the increasing data showing control of HCMV viraemia by restoration of cellular immunity, it was reasonable to assume that individuals with quiescent HCMV disease taking HAART may no longer need to continue taking life-long maintenance therapy for HCMV. Several studies have supported this assumption, where patients did not experience

**Table 1.7. Characteristics of patients included in studies on the decline in incidence of HCMV retinitis in the era of HAART.**

No. Patients	CD4+ count, cells/ $\mu$ l	Duration of HAART at inclusion, median months	Duration of follow up, median months	No. relapses	Reference
14	105	Not reported	16.4	0	Whitcup et al., 1999
22	>150	Not reported	19.5	3	MacDonald et al., 2000
48	>75	18.0	24.0	2	Jouan et al., 2001
36	>100	17.5	20.7	1	Berenguer et al., 2002
16	<100	0	21	2	Deayton et al., 1999
7	230	3	9	0	Tural et al., 1998
11	183	9	5.2	0	Macdonald et al., 1998
5	179	18	12	0	Kirk et al., 1999
8	105	3.1	22.5	0	Di Perri et al., 1999
5	>100	3	19	0	Soriano et al., 2000
103	<100	3.5	8.2	0*	Deayton et al., 2000

\* HAART for 6 months

recrudescence of existing HCMV retinitis following discontinuation of maintenance therapy, detailed in table 1.7., (Tural et al., 1998, Macdonald et al., 1998, 2000, Kirk et al., 1999, Di Perri et al., 1999, Whitcup et al., 1999, Jouan et al., 2001, Soriano et al., 2000, Berenguer et al., 2002).

Declining levels of the previously recovered lymphoproliferative response to HCMV have been observed after long term HAART, where the CD4+ T-cell count falls to below 75cells/ $\mu$ l, indicative of HAART failure (Torriani et al., 2000, Gerna et al., 2001). One study identified patients who did not respond to HCMV even following long term HAART in the presence of fairly high levels of CD4+ T-cells. An explanation given for this phenomenon was exhaustion of the memory CD4+ T-cell clonotypes (Gerna et al., 2001). This study also identified almost a third of patients showed declining levels of previously reacquired responsiveness to HCMV, even among those who discontinued their anti-HCMV maintenance therapy. This risk of recurrence of HCMV disease during long term HAART suggests the continued need to monitor the levels of HCMV viraemia and more importantly, the resumption of HCMV maintenance therapy. This has implications for the risk of recrudescence of HCMV disease, and indeed the risk of development of drug resistant virus. This highlights the need to identify new antivirals with activity against drug-resistant HCMV, when the options for control and/or treatment of disease are running out.

### 1.3 Replication of Human Cytomegalovirus

#### 1.3.1. Viral attachment and penetration

HCMV has a wide range of permissivity *in vivo*, as exemplified by detection of the virus in almost every organ system of the body in AIDS patients. The best documented cell types include epithelial and endothelial cells and fibroblasts. Peripheral blood leukocytes (Hassan-Walker et al., 1998), specialised parenchymal cells such as neurons in the brain and retina, smooth muscle cells and hepatocytes can also be infected with the virus (Sinzger and Jahn., 1996). When cells are grown in culture however, the host range is greatly restricted, with primary fibroblasts producing the greatest yield of virus.

Entry of HCMV into most cell types occurs efficiently. The initial interaction of HCMV with the host cell comprises of an initial adsorption, fusion of the viral envelope with the host cell membrane and penetration of the virus. Sequence analysis has predicted that HCMV encodes at least 65 glycoproteins, of which 8 major glycoprotein species are present in the greatest proportion in the HCMV envelope. Glycoprotein B (gB) is a type 1 transmembrane protein encoded by the UL55 gene and is one of only five glycoproteins conserved throughout the herpesvirus family. The gB protein is the major structural protein of the viral envelope, is present on the surface of infected cells and is involved in all stages of HCMV entry. The other conserved proteins are homologues of the HSV glycoproteins gH, gL, gM and gN. Initial cellular attachment has been shown to be mediated by cell surface heparin sulphate proteoglycans. The surface glycoprotein complex C-II (gC-II), comprising of the integral membrane protein complex gM (UL100) and gN (UL73), together with gB (UL55), were demonstrated by heparin affinity chromatography, to be the heparin-binding components of the viral envelope (Compton et al., 1993; Kari and Gehrz., 1992). A more stable binding state may then be achieved by the interaction of the virion with a second cellular receptor, as demonstrated by the enzymatic removal of heparin sulphate from the surface of CHO and fibroblast cells (Boyle and Compton., 1998). A reduction in the binding of soluble gB to the cell surface of 40% was observed, but a significant proportion of the soluble gB was still able to associate with the cell surface. Initially this receptor was thought to be host cellular annexin II on endothelial cells, which showed a direct interaction with gB (Pietropaolo and Compton., 1997), and was also found to be associated with HCMV virions by immunocytochemical studies (Wright et al., 1995). However, pre-treatment of virions and cells with anti-annexin II antibodies did not affect the entry of HCMV into fibroblasts, HCMV was able to penetrate annexin II-deficient 293 cells and cell-to-cell spread remained unaffected in the presence of anti-annexin antibodies or exogenous protein (Pietropaolo and Compton., 1999). To date the second receptor has not been determined.

Following binding, HCMV can fuse directly with the plasma membrane in a pH-independent manner (Compton et al., 1993). This is accomplished by gB and a three surface glycoprotein complex gCIII consisting of gH (UL75), gL (UL115) and gO (UL74) (Cranage et al., 1988; Gretch et al., 1988; Milne et al., 1998; Li et al., 1997;



Huber and Compton., 1997, 1998, 1999). Neutralising anti-gB monoclonal antibodies significantly blocked viral fusion events, including penetration and cell-to-cell spread, while viral attachment remained unaffected (Navarro et al., 1993). Similarly, an anti-gH antibody can prevent cell-to-cell transmission of the virus (Rasmussen et al., 1984) and antibodies that mimic the gH/gL complex block virus penetration of cells (Keay et al., 1989; Keay and Baldwin., 1992). This is consistent with all three components of the gCIII complex and gB being essential for viral entry. Finally, the gCII complex is made up of gM (UL100) and gN (UL73). This is also known as the integral membrane complex, purely by analogy to the complexes seen in EBV and the alphaherpesviruses. The function in HCMV is unknown, but both gM and gN are known to be dispensable for growth in cell culture in other herpesviruses (Kari et al., 1994; Mocarski., 2001)

### 1.3.2. Immediate Early Events

The HCMV replicative gene expression evolves via a temporal cascade, which typifies the herpesvirus family as originally observed by Honess, 1974. This cascade proceeds from the initial transcription of the immediate early or alpha genes (IE, $\alpha$ ) without the need for *de novo* protein synthesis, followed by the early or beta genes (E,  $\beta$ ) and finally the late or gamma genes (L,  $\gamma$ ). Thus the viral functions expressed during the earliest phases of the replication cycle play regulatory roles in the timing of the cascade (Leatham et al., 1991). The immediate early ( $\alpha$ ) gene expression is essential for the switch from  $\alpha$  to  $\beta$  and partly  $\gamma$  gene expression and thus for the progression of the replication cycle.

The binding and fusion of the virus with the host cell membrane triggers a cascade of physiological responses, which begin with the heparin sulphate-dependent association with the virions. This association promotes a rapid induction of the cellular transcription factors, FOS, JUN and MYC. Several other signalling pathways are stimulated via the action of G-protein coupled receptors, such as the mitogen-activated protein kinase pathway (Monick, 1992). The activation of cellular transcription factors is essential for the initiation of replication of HCMV. Following the interaction of the viral envelope with the cell membrane, the matrix (or tegument) proteins UL69 and UL82 enter the cell and activate the immediate early (IE) promoter. The immediate early (*ie*) gene expression initiates from a small number of *ie* genes, UL36-38; *ie-1/ie-*

2; TRS1-IRS1 and US3, which are controlled by a complex upstream regulatory region consisting of a modulator, a nuclear factor 1 binding (NF-1) domain, an enhancer and a promoter. The enhancer exhibits extremely strong activity and is the regulatory region for RNA polymerase II directed transcription. The enhancer contains arrays of 18-, 19- and 21-bp repeated elements encoding consensus binding sites for NF- $\kappa$ B/rel, cyclic adenosine monophosphate response element binding protein (ATF or CREB) and Sp1 and YY1 respectively. The binding of these factors to one or more of the cognate sites stimulates transcription (Meier and Stinski., 1996). The UL69 co-operatively interacts with IRS1 and TRS1 to activate the IRS1/TRS1 promoter and enhance transcription directed by the major IE promoter (Romanowski et al., 1997).

The majority of IE transcription is derived from the *ie1* and *ie-2* genes which encode the nuclear phosphoproteins IE-1 (UL123/IE72) and IE-2 (UL122/IE86). These make up the major immediate early (MIE) locus. IE72 and IE86 have been shown to exhibit transactivation properties (Everett and Dunlop., 1984) and as such are essential for HCMV replication. Deletion mutants lacking the *ie-1* or *ie-2* genes are severely impaired in ability to replicate (Marchini et al., 2001, Greaves and Mocarski, 1998, Mocarski et al., 1996). The generation of an IE1 72 null mutant, (Greaves and Mocarski., 1998) led to the identification of at least two functions of the IE1 72 protein, (1) activation of *ie1/ie2* promoter expression and (2) efficient expression of viral  $\beta$ - and  $\gamma$ -genes via transactivation of UL44, which is responsible for establishing viral replication. In addition, the transactivation capabilities of IE2 86 alone or in combination with pTRS1/pIRS1 are positively influenced by the presence of IE1 72 (Iskenderian et al., 1996). IE-2-p86 also plays a major role in triggering the lytic replicative cycle of HCMV. IE-2 86 has two main functions, (1) Repression of transcription from the MIE enhancer-promoter by direct DNA contact of IE-2 with a sequence element located between the TATAA box and the transcriptional start site of the enhancer-promoter at the CRS element. This blocks the association of RNA polymerase II with the pre-initiation complex. (2) IE-2 is a strong transactivator of viral early promoters and is thought to be required for progression of the replicative cycle from the IE to the early phase.

Transient expression assays have shown that the IRS1 and TRS1 gene products are required for complementation of the HCMV origin of lytic replication-dependent (*oriLyt*) DNA replication (Pari and Anders., 1993; Pari et al., 1993). It has been hypothesised that the products of the IRS1/TRS1 locus and the IE1/IE2 loci act cooperatively to activate the early gene promoters required for DNA replication. This activity is significantly augmented by the UL69 and UL82 gene products (Romanowski et al., 1997).

### 1.3.3. DNA Replication

The DNA replication in HCMV is prolonged with 2 distinct peaks of viral DNA synthesis observed at 18-24 hours and 60-80 hours post infection. Mature virus particles are released from the cell over a 24-48 hour period (Penfold and Mocarski., 1997). As with many herpesviruses, the HCMV genome circularises in the nucleus of permissive cells by 4 hours post infection and is followed by the production of concatameric DNA formed by the directional rolling circle mode of replication, illustrated in figure 1.4. (LaFemina and Hayward., 1983; McVoy and Adler., 1994). These 'endless' concatamers are subsequently cleaved and packaged during virion assembly. The HCMV contains one origin of lytic phase-dependent DNA replication (*oriLyt*) which directs the initiation of DNA synthesis. Eleven loci have been identified as essential for *oriLyt*-dependent DNA replication (Pari and Anders., 1993), including six herpesvirus-conserved replication-fork proteins. These include the DNA polymerase, encoded by UL54, and its associated processivity factor (UL44), a single stranded DNA-binding protein (ppUL57) and a three subunit helicase-primase complex (pUL70, pUL102, pUL105). Further loci identified included UL36-38, UL112-113, IE1/IE2, IRS1/TRS1 and UL84. This region was largely characterised by virtue of the homology and/or function existing between the HCMV replication fork proteins and their counterparts in HSV and EBV, which were well characterised. The activity of the DNA polymerase (pUL54) is dependent upon the association of the polymerase processivity factor (ppUL44) (Ertl and Powell., 1992, Cihlar et al., 1997), which binds to the double stranded DNA and prevents dissociation of the polymerase from the DNA template. The single stranded DNA binding protein (ppUL57) is predicted to prevent the re-annealing of DNA strands following unwinding by the putative HCMV helicase-primase complex (pUL70-pUL102-pUL105).

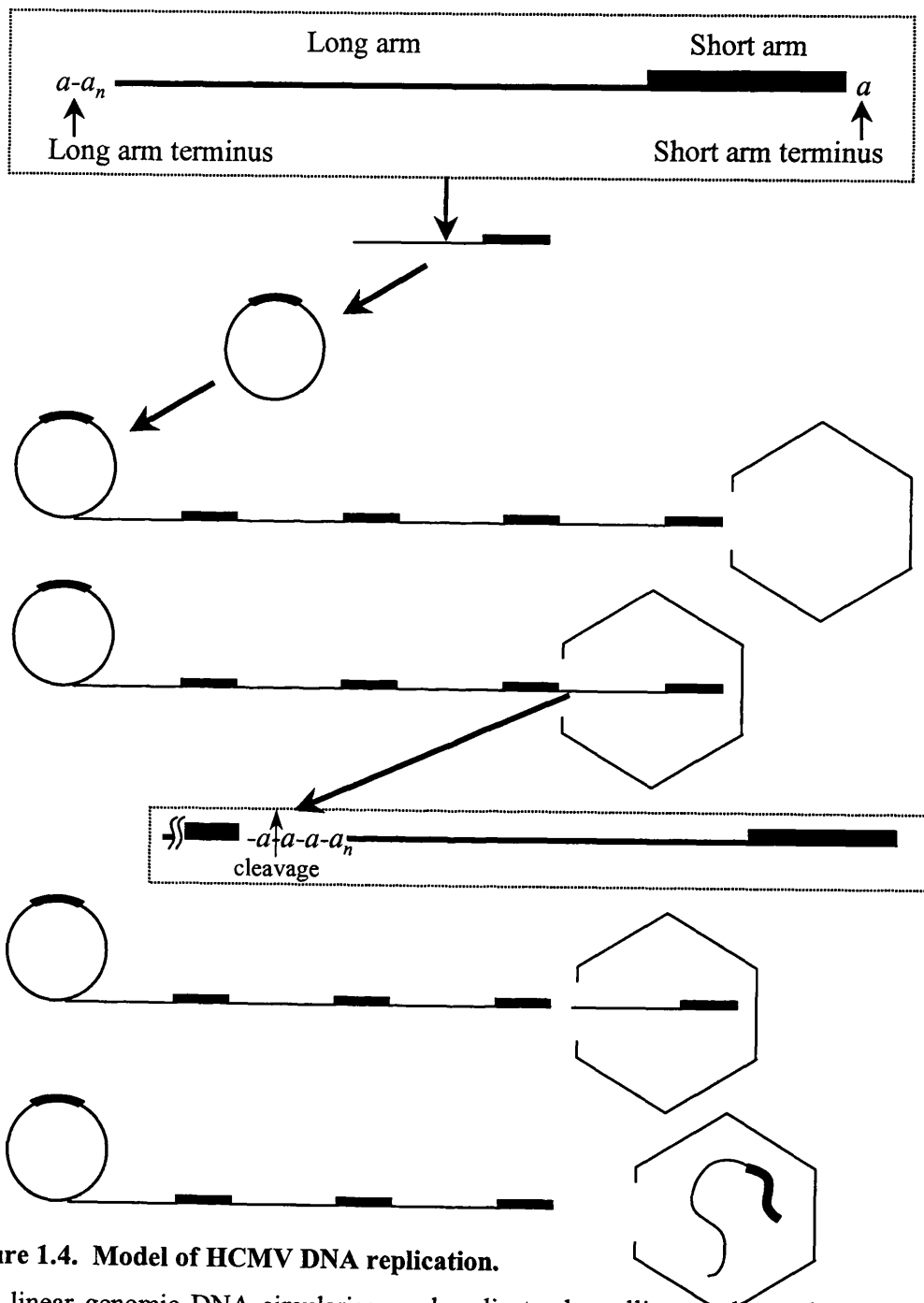


**Figure 1.4. Model of HCMV DNA replication.**

Unit linear genomic DNA circularises and replicates by rolling circle mechanism to form a long linear concatamer. Short arm termini are preferably fed into empty capsids and DNA is fed until a complete genome has entered and the capsid is full. Cleavage occurs between the final  $a$  sequences located between genomes of the concatamer. (Taken from McVoy and Adler., 1994)

The functions of these proteins have not been well studied, thus their functions are derived by analogy to their HSV counterparts. The TRS1/IRS1 and *ie1/ie2* genes are thought to activate gene expression, the UL36 and UL37 are thought to prevent apoptosis and the proteins encoded by the UL112-113 region are thought to orchestrate recruitment of the replication fork proteins to the nuclear sites associated with viral transcription and DNA synthesis (Ahn et al., 1999).

Following DNA replication, the concatameric DNA needs to be cleaved into unit genome length, a process known as maturation. Maturation occurs in the nucleus, where the newly replicated DNA matures into virions. The concatameric viral DNA is known to be packaged into preformed B capsids composed of MCP, mCP, mC-BP and SCP together with the AP precursor (Beudet-Miller., 1996). The cleavage and packaging of DNA into unit genome lengths is directed by two highly conserved short sequence elements, denoted *pac1* and *pac2*. These enable the recognition of DNA bearing an *a* sequence to be correctly cleaved and packaged (McVoy et al., 1998). The HCMV genomic DNA *a* sequences are found at the L-S junctions in varying numbers and within a 220bp region carrying both the *pac1* and *pac2* sequences, so generating the cleavage/packaging sites (Mocarski et al., 1987). An enzyme complex is thought to perform this function by analogy to the terminase complex, which performs the cleavage of concatameric DNA in HSV. The terminase complex performs specific functions including DNA binding, prohead (capsid) binding, ATPase activity and endonucleolytic cleavage of the precursor viral DNA. Six HCMV ORF's are thought to be involved in this process; UL104, UL89, UL77, UL56, UL52, although by analogy to HSV, UL51, UL47 and UL48 are also proposed to have some role in the process.

The HCMV UL89 gene appears to encode an endonucleolytic subunit of the putative HCMV DNA terminase, identified by virtue of the presence of an ATP binding P-loop motif, AYDYFGKT (Underwood et al., 1998). The UL56 codes for a packaging motif (*pac*) binding protein with DNA sequence-specific binding capability and specific nuclease activity, apparently binding to the *pac* sequences (cleavage recognition sites) and endonucleolytically cleaving the viral DNA (Bogner et al., 1998; Krosky et al., 1998). The roles of each of these proteins has been clarified by purifying the terminase subunits pUL56 and pUL89 (Scheffczik et al., 2002). Using circular plasmid DNA containing a single *a* sequence as the substrate, purified HCMV pUL89 exhibited

enzymatic activity, converting sc plasmid DNA into oc and linear molecules. The enzymatic activity of pUL89 can be enhanced by the addition of pUL56, demonstrating positive cooperativity between the two proteins. Both proteins however, demonstrated comparable and random enzymatic activity in their ability to cleave DNA without packaging signals. Electron microscopy revealed pUL56 is necessary for the DNA binding, whereas the pUL89 mediated cleavage of linearized DNA. Further, pUL56 can bind to mature and immature capsids and was found to be associated on one side of the capsid shell, strongly suggesting that pUL56 may function as a portal protein or contains a portal protein-binding site. From these results, Scheffczik and colleagues postulate the initiation of DNA packaging takes place in discrete stages: Stage 1: attachment of pUL56 to pac sites of concatameric DNA; Stage 2: specific cleavage by the concerted action of pUL56 and pUL89; Stage 3: attachment of DNA-protein complexes to the procapsid. The pUL56 contains the ATPase function, so providing the energy for the translocation of concatameric DNA to the procapsids and for the attachment of the DNA-protein complexes to the procapsid. Like the HSV homologues, the function of the remaining proteins proposed to be involved in the function of the terminase remain to be elucidated. Their functions could be compared to those of bacteriophages, by which the mechanism of DNA packaging into capsids and indeed the terminase complex was first identified.

The function of the terminase complex has recently become of interest, due to the action of various new antivirals designed not to utilise either the UL97 or the DNA polymerase. These have been described in section 1.5.4. Also of particular interest in the design of new antivirals, comparative to those which are particularly effective in the elimination of HIV as part of the HAART regimen, is the HCMV protease. The protease is highly conserved among all human herpesviruses and functions both as a virion structural component and for processing the capsid assembly protein. The herpesvirus proteases are synthesised as a fusion with capsid assembly protein processing two specific proteolytic cleavage sites. One takes place at the maturation site (M-site, Ala 643-Ser 644) near the C-terminus of the assembly protein, while the others occur at the release site (R-site, Ala 256-Ser 257) separating the amino-terminal protease from the assembly protein domain (Newcomb et al., 1996; Stevens et al., 1994). The HCMV protease contains an internal site (I-site) which is located within the protease domain (Holwerda et al., 1994). In addition, the HCMV protease contains an

unusual protein fold for serine proteases and a unique catalytic triad; Ser, His, His (Shieh et al., 1996; Batra et al., 2001; Qiu et al., 1996). The crystal structure revealed a homodimeric enzyme with two well separated active sites on opposite faces of the dimer (Tong et al., 1996). The capsid AP undergoes proteolytic cleavage, catalysed by the protease (Welch et al., 1991), which can be abolished by the addition of an 'external guide sequence oligonucleotide', which consists of a sequence complementary to the protease mRNA to recruit intracellular RNase P for specific degradation of the target RNA (Dunn et al., 2001). Using this methodology, inhibition of the protease blocks the step of packaging of the viral genome into the preformed capsids, as has been observed with the HSV-1 protease (Gao et al., 1994). This was further shown by the majority of capsids found in the nucleus being B capsid like, indicating viral DNA was not efficiently packaged and capsid maturation was blocked.

### **1.3.4 Latency**

Epstein Barr virus is the most extensively studied human herpesvirus in terms of latency, with the genome maintained as a covalently closed episome within the nucleus of B-cells and the types of latency clearly defined by the latency transcripts produced. The HCMV genome is also maintained as a covalently closed circular molecule within the nucleus of CD14+ peripheral blood mononuclear cells, as demonstrated by the migration of a closed circular plasmid in native gel electrophoresis and PCR (Bolovan-Fritts et al., 1999). Modern techniques have however identified further cells in which HCMV remains latent. These include lineage-committed myeloid cells which generate granulocytes, macrophages and dendritic cells (Hahn et al., 1998, Sinclair and Sissons., 1996, Soderberg-Naucler and Nelson., 1999) as well as mononuclear cells derived from peripheral blood or bone marrow (Slobedman et al., 1999, Taylor-Wiedeman et al., 1991).

HCMV latency transcripts are generated from the *ie1/ie2* region and give rise to four transcripts, ORF55, ORF42, ORF45 and ORF94 from the sense DNA strand and three transcripts, ORF59, ORF154 and ORF152/UL124 from the antisense strand (Kondo et al., 1996). The function of these transcripts during latency remains unclear as mutational analysis has not revealed if the products are required for establishment or maintenance of latency. It is known however that the pattern of latent gene expression

changes as the progenitor cells mature into monocytes or dendritic cells (Hahn et al., 1998).

## **1.4. Immunology**

### **1.4.1. Immune Response to HCMV**

Upon infection, the virus first encounters the cells of the innate immune system, including macrophages, natural killer (NK) cells, natural killer T (NKT) cells and peripheral blood mononuclear (PBMC) cells. Almost every cell type can produce type I and II interferons and TNF- $\alpha$  cytokines, which are synthesised immediately upon infection, mobilising macrophage and NK cytotoxic activity. NK cells are an important part of the innate cellular immune system, particularly during the early immune responses. The NK cells can lyse virally infected cells without prior sensitisation and are triggered immediately without the need for clonal expansion. The NK cells respond to aberrant expression of cell surface molecules, in particular the reduction or lack of MHC class I expression on target cells, also known as the 'missing self' hypothesis. This induces the non-specific lysis of infected cells by via FasL-mediated pathways or perforin. MHC class I molecules act as inhibitory receptors for NK cells, which is of major importance for herpesvirus immunity, since down-regulation of cellular MHC class I has been demonstrated in cells infected by herpesviruses (Hengel et al., 1998). This down-regulation could effectively render the herpesvirus-infected cells more susceptible to NK-mediated lysis and will be elaborated in the following section on immune evasion strategies of HCMV. The importance of NK cells for protection against herpesvirus infections has been clearly demonstrated in patients with NK cell defects, where these patients frequently suffer from severe HCMV, HSV and EBV infections (Biron et al., 1989, Bonavida et al., 1986).

The majority of work performed to elucidate the protective effect of NK cells against herpesviruses has come from studies of murine cytomegalovirus (MCMV). Some of the earliest work demonstrated a correlation between genetic abnormalities, such as severe combined immunodeficiency (SCID), leading to enhanced morbidity and mortality following MCMV challenge (Bancroft et al., 1981, Welsh et al., 1991, Welsh et al., 1994). Analysis of mice which are susceptible and non-susceptible to MCMV infection has led to the identification of the murine cytomegalovirus 1 (Cmv 1) locus,



which maps to the NK-gene complex (NKC) on mouse chromosome 6. This complex contains an array of NK-cell regulatory genes which control NK-mediated lysis of target cells and cytokine release via multiple stimulatory and inhibitory signals (Scalzo et al., 1992, Raulet., 1992).

Naive T cells become activated following the presentation of peptide antigens on MHC molecules by professional and non-professional antigen presenting cells, such as dendritic cells. Both CD4 and CD8 T cell populations contribute towards the control of viral infections. Naive CD8 T cells proliferate and differentiate into effector cells upon recognition of MHC class 1-antigen complexes displayed on infected cells or antigen presenting cells. Once activated, these cells can perform cell killing by perforin and the FasL pathways, like the NK cells.

Until recently, the *in vitro* enumeration of antigen-specific CD8 T cells was determined by limiting dilution analysis, which tended to underestimate the number of antigen-specific cells due to the apoptotic nature of these activated cells. The study of the antigen specificity of CD8 cells and analysis of cytokine production at the single cell level have been revolutionised by the development of tetrameric MHC/peptide reagents and ELISPOT technology. CD8 cytotoxic T lymphocytes (CTL) can be detected directly using HLA class I molecules refolded with the appropriate HLA-restricted peptide and transformed into a tetrameric complex using biotin and streptavidin, together with a fluorochrome for detection. These tetramers can bind to the T cell receptor (TCR) on the CD8 CTLs to determine the frequency of these cells *in vivo* without prior need for expansion of the CTLs. Tetramers can also determine the precise peptides to which the majority of the CTLs are directed against.

The tetramer technology has revealed an enormous CD8 T cell proliferation occurs during primary infection, the majority of which are antigen specific and secrete cytokines concurrently with their activation, as shown by ELISPOT assay. The majority of the CD8 CTL response in the healthy HCMV seropositive individuals are directed against very few immunodominant epitopes, predominantly pp65, IE1-Exon4, gB, pp150 and pp28, 92% of which is against pp65 and 76% against IE1-exon4 (Gyulai et al., 2000). Following the initial immune response, the majority of the activated

effector T cells die off and the remaining cells, which do not die, persist as memory cells.

A study of healthy HCMV seropositive donors demonstrated HCMV-specific CD8 T cell frequencies of between 0.75 and 1.85% for HLA\*A0201- and HLA\*B702-restricted peptides (Gillespie et al., 2000). This is surprising since it is among the highest recorded frequencies in chronic viral infections. In immunosuppressed (renal transplant) individuals with reactivated HCMV as detected by PCR, the CTL frequencies against pp65 using HLA A\*0201 dramatically increased to up to 15% (Engstrand et al., 2000). This is in contrast to a matched HCMV seropositive renal transplant group with no evidence of HCMV disease, where a CD8 CTL frequency of 0.2% to 9% was observed. In individuals who had liver transplants >3 years previously, the CD8 CTL frequencies against pp65 using the HLA B\*0702 tetramers did not significantly differ from immunocompetent individuals, with frequencies of 1.2% (range 0.3 – 5.8%) and 1.1% (range 0.1 – 5%) respectively (Singhal et al., 2000).

#### **1.4.2. Immune Modulation Strategies**

HCMV primary infection is usually efficiently controlled by the immune system and does not generally cause major illness. However, immune control does not completely eradicate the virus, which continues to persist in the host in a state of latency, and recurrent infections may occur when the host becomes immunocompromised. To achieve this persistence, especially when confronted by a fully primed immune system, CMVs have developed various means of modulating the host immune system. (1) HCMV can establish a latent state of infection where it does not adversely affect the host cell but restricts the number of viral genes expressed so minimising exposure to the immune system. (2) HCMV can replicate in specific ('privileged') tissues, which have a less stringent immune surveillance, such as the epithelial cells of the salivary glands. These cells do not express sufficient MHC class 1 molecules to mediate viral clearance by CD8 cells. This potentially allows the virus to be shed into body fluids, which are transmitted between individuals. (3) HCMV can compromise the antiviral host defence mechanisms by expressing distinct factors designed to evade the hosts immune responses, thereby lengthening the time available for the virus to multiply. The next section will concentrate on the means by which the HCMV can subvert and

evade the hosts immune system. Figure 1.5 illustrates the various mechanisms by which HCMV evades the immune system.

Cellular MHC class I molecules are expressed on the surface of almost all nucleated cells and play a pivotal role in regulating the immune response to infection by virtue of their ability to present peptides to cytotoxic CD8 T lymphocytes. In order to understand how HCMV can interfere with this process, it is important to understand how the MHC molecules are assembled and transported to the cell surface. Briefly, the nascent MHC class I is translocated to the ER lumen via the sec61 protein complex and binds the  $\beta_2m$ . This complex is folded and modified whereupon the heterodimer associates with TAP to form the peptide loading complex. Ubiquitinated proteins are cleaved in the proteasome, bind to TAP and are translocated to the ER lumen in an ATP-dependent manner. The peptide binds to the MHC class I HC/ $\beta_2m$  heterodimer and the whole complex is released from TAP and traffics through the ER and golgi compartments to the cell membrane (Heemels and Ploegh., 1995).

Human (Beersma et al., 1993; Warren et al., 1994) and murine (Del Val et al., 1989) cytomegaloviruses induce a MHC class I down-regulation by causing the retention of class I molecules in the endoplasmic reticulum. Initially a dramatic decrease in cell surface levels of MHC class I molecules in infected cells was observed (Barnes and Grundy., 1992). Since then several HCMV genes have been shown to be responsible for this phenomenon. HCMV deletion mutants revealed a 7kb region of approx 10 genes were required for class I down regulation in HCMV infected cells (Hengel, 1996; Jones, 1995). US2, 3, 6 and 11 were able to decrease the class I expression at the cell surface when expressed individually (Ahn et al, 1996; Jones et al, 1996; Wertz et al, 1996a). The US2 and US11 gene products cause reverse translocation the nascent class I heavy chains from the ER through the sec61 complex back to the cytosol where they are deglycosylated by host *N*-glycanase and are rapidly degraded by proteasomes (Wiertz et al, 1996a, Weirtz et al., 1996b). The endoplasmic reticulum-resident glycoprotein US3 destabilises the maturation and transport to the cell surface of the class I heavy chains. US3 does this by complexing with the  $\beta_2$  microglobulin-associated class I heavy chain, which accumulates in the ER (Ahn et al, 1996; Jones et al, 1996) and is not recycled back through the golgi (Lee et al., 2000), thus class I

molecules are retained but not degraded during the IE period of infection. The mechanism of class I down-regulation used by the US6 gene product is to bind directly to the TAP complex, thereby inhibiting peptide translocation from the cytosol to the ER lumen, since only peptide-loaded class I molecules can leave the ER for transport to the cell surface (Hengel et al, 1997; Lehner et al, 1997). US6 binds to TAP in a manner, which does not affect the peptide binding properties of TAP (Ahn et al.,1997), therefore inhibition is by a unique mechanism of action. Translocation of the peptides from the cytosol to the ER lumen via TAP requires ATP hydrolysis to provide energy for the process. US6 inhibits the binding of ATP by TAP1 and also prevents the conformational rearrangement of TAP induced by peptide binding (Hewitt et al., 2001). Thus by preventing TAP from utilising its energy source, ATP, US6 inhibits peptide translocation.

The expression of MHC class II proteins is restricted to antigen presenting cells, B cells, macrophages and dendritic cells, which take up and present exogenous antigens to CD4 T cells. The MHC class II molecules are assembled in the ER by combination of three class II - $\alpha$  and - $\beta$  dimers with a homotrimeric invariant chain (Ii) that precludes loading of peptides. The  $\alpha/\beta/Ii$  complexes are then transported through the golgi, where the targeting signals in the cytoplasmic domain of the Ii direct the complex to the endosomal-lysosomal compartments. Proteolysis of the Ii chain produces the class II-associated Ii-chain peptide (CLIP) which traffics to the MHC class II compartment where HLA-DM facilitates the displacement of CLIP molecules with lysosomal peptides in the peptide-binding groove of class II molecules. These move to the cell surface where they present antigen to CD4 T lymphocytes (Cresswell, P., 1996). Tomazin et al., (1999) showed that the HCMV encoded US2 causes the degradation of two essential proteins involved in the MHC class II antigen presentation pathway. HLA-DM binds to the class II- $\alpha/\beta$  complex, stabilises the class II and catalyses the loading of peptides. In US2 stably transfected cells, DM- $\alpha$  was rapidly degraded, plus class II DR- $\alpha$  and the class I HC. This is important due to the ability of HCMV to replicate in the endothelial cells, glial cells or macrophages, so allowing the virus to remain undetectable by both CD4 and CD8 T cells, especially after reactivation of the virus.

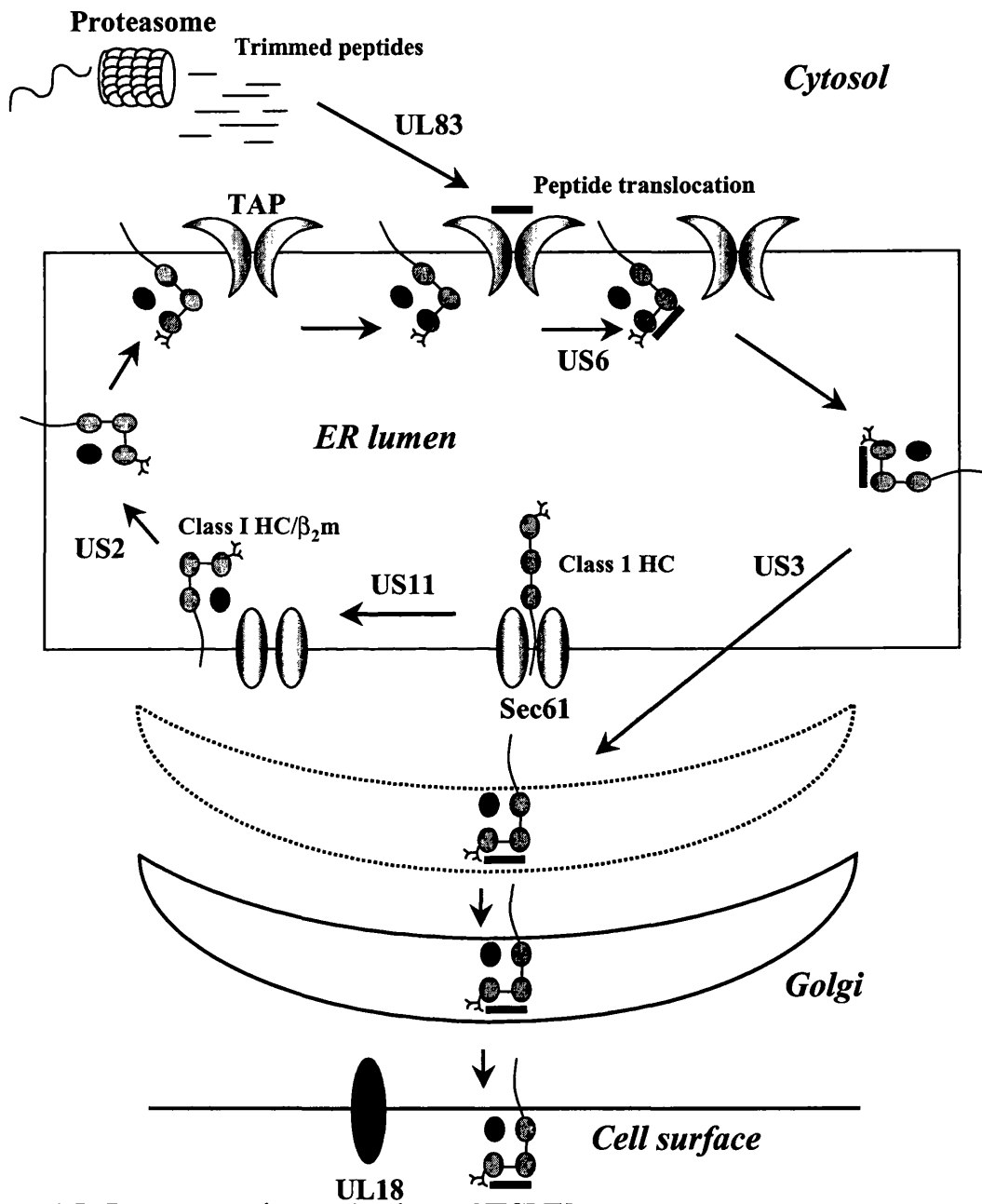


**Figure 1.5. Immune evasion mechanisms of HCMV**

Steps in the MHC class I presentation pathway is shown with the points at which the pathway is subverted by HCMV. US2 and US11 cause translocation of MHC class I back through the sec61 into the cytosol to be degraded by the proteasome. US3 complexes with β<sub>2</sub>m, causing accumulation of MHC class I in the ER. US6 binds to TAP and inhibits peptide translocation from the cytosol to the ER. UL83 (pp65) blocks presentation of HCMV proteins at immediate early times post infection.

The observation that even though the 72 kD IE protein from CMV is abundantly expressed in the IE phase of infection, it is relatively poorly recognised by CMV-specific T-cells, led to the identification of another mechanism of evasion of T-cell responses, as demonstrated in the vaccinia expression system. Recognition of the 72kd IE protein was selectively abrogated by co-expression of pp65, a protein which possesses an associated kinase activity (Gilbert et al, 1996). The interpretation of this finding was that the phosphorylation of the 72kd substrate by pp65 would limit the access of the 72kd protein to the class I processing machinery.

Although interference with the class I surface expression would seem a simple way for the virus to escape the immune surveillance, the down-regulation of the class I could potentially lead to improved recognition by the NK cells (Karre et al, 2002). An increasing amount of evidence suggests that NK cells recognise and destroy cells that no longer express MHC class I molecules on their cell surface, the 'missing self hypothesis' (Ljunggren and Karre, 1990) therefore any virus-infected cell that has decreased or lost MHC class I expression in order to avoid CTL attack could be susceptible to attack by NK cells. HCMV seems to have evolved a strategy to avoid being recognised by the host immune system. The HCMV UL18 gene encodes a protein with homology to the class I heavy chain (Beck and Barrell, 1988; Browne et al, 1992) which can complex with the  $\beta_2M$  and is also able to bind a profile of peptides similar to that of MHC class I. In one study, human cells lacking endogenous class I MHC transfected with the UL18 resulted not only in an increase of cell surface  $\beta_2m$ , but also became resistant to NK cell lysis (Reyburn et al, 1997). However this finding was disputed (Leong et al, 1998) and more recent work using a UL18 $\Delta$  HCMV strain showed infected macrophages and endothelial cells exhibited decreased susceptibility to NK lysis (Odeberg et al., 2002). Thus, the function of UL18 awaits further classification. NK cells express an inhibitory receptor CD94/NKG2A, which is present on the majority of NK cells in the peripheral blood (Valiante et al., 1997). The only known ligand for this receptor, which is expressed on virtually all cells, is HLA-E. The interaction between the two entities requires the binding of a TAP-dependent ligand representing the amino acids 3-11 of leader sequences of HLA class I H chains to HLA-E (Braud et al., 1998a & b, Lee et al., 1998). The N-terminal part (aa 15-23) of the HCMV encoded UL40 is identical to the HLA-E ligand in the signal sequence

(aa 3-11) of most HLA-C alleles. Ulbrecht et al., (2000) demonstrated UL40 is a TAP-independent HLA-E ligand which allows expression of HLA-E on HCMV-infected cells when the delivery of viral peptides to the ER is shut down, thereby allowing an HLA-E-mediated inhibition of CD94/NKG2A-positive NK cells.

HCMV has been shown to encode four chemokine receptor homologues, UL33, US28, US27 and UL78 (Chee et al., 1990), of which US28 and US27 appear to be functional (Billstrom et al., 1998, Bodaghi et al., 1998). US28 has a wide range of chemokine ligands including primarily RANTES and also MCP-3 and MIP-1 $\alpha$  (Billstrom et al., 1998) and as such has been characterised as a CC chemokine receptor (CCR1) (Neote et al., 1993). The affinity of US28 for its chemokine ligands is much higher than most chemokine receptors for the same ligands. Billstrom et al., (1998) demonstrated the CC chemokine RANTES bound to HCMV-infected endothelial cells via the CC chemokine receptor US28 in the absence of the other CC chemokine receptors (CCR1, CCR2a or CCR2b, CCR3, CCR4 and CCR5) on the surface of the primary endothelial cells. Following this, US28 coupled to G $\alpha_{16}$  and G $\alpha_i$  proteins activating intracellular calcium flux and stimulating the MAP kinase-signalling pathway through ERK2 MAP kinase. This has potential implications with respect to HCMV infection of hematopoietic cells such as monocytes, where exogenous cytokines may promote monocyte proliferation and may lead to HCMV persistence and latency. The function of the US27, UL33 and UL78 have not yet been elucidated.

UL144, UL146 and UL147 were identified in a region of the HCMV genome encoding 19 ORF which are only present in low passage, virulent strains of HCMV (Cha et al., 1996). UL144 was identified as a structural homologue of herpesvirus entry mediator (HVEM) of the TNF superfamily by virtue of its homology to HveA, which mediates entry of HSV-1 (Benedict et al., 1999). The UL144 does not however bind to any of the known TNF ligands and cannot be detected on the surface of infected cells suggesting its action is intracellular. UL146 and 147 exhibit weak amino acid homology to CXC chemokines, with UL146 encoding an IL-8 like chemokine, denoted vCXC-1 (Penfold et al., 1999). The UL146 was found in the medium of infected cells and induced chemotaxis of neutrophils, thus possibly aiding the dissemination of the virus. The function of UL147 has not yet been determined. The reason why HCMV might have to have had to acquire these complementary strategies in order to avoid

immune recognition might be because of its prolonged replication period, which means that the virus has an extended exposure to immune recognition and attack.

## **1.5. Antiviral Chemotherapy**

### **1.5.1. Nucleoside analogues**

The majority of the antiviral compounds currently used for the treatment of herpesvirus infections are nucleoside analogues. The best studied and the drug most closely considered as the perfect antiviral agent is aciclovir (ACV) [9-(2-hydroxyethoxymethyl)-guanine]. The structure of ACV (figure 1.6) is based upon the nucleoside guanosine, which consists of the purine base guanine, covalently linked to the 1' –carbon on the sugar molecule ribose. The ACV differs from the ribose ring in that the 2'- and 3'- carbons are missing, thus ACV is acyclic. DNA replication consists of a condensation reaction, which occurs between the DNA chain 3'-hydroxyl group and the 5'-phosphate of the next nucleoside triphosphate to be incorporated, resulting in a phosphate ester linkage and elongation of the DNA chain by one base. ACV is an obligate DNA chain terminator, as it does not possess a 3'-hydroxyl onto which successive nucleoside triphosphates are added, thus addition of ACV to replicating DNA results in the premature termination of DNA replication. For the drug to be active however, it must be initially phosphorylated at the 5'-hydroxyl position in order to incorporate the analogue into the DNA chain. In herpes simplex virus infected cells the drug diffuses across the plasma membrane and the initial phosphorylation of ACV is performed by the virally encoded thymidine kinase (TK). The monophosphorylated ACV is recognised by the host cell phosphotransferases which subsequently fully activate the drug to the triphosphate form, whereupon it can act as an obligate chain terminator and simultaneously inhibit the virally encoded DNA polymerase, thus inhibiting viral replication (Cheng et al., 1983, McGuirt et al., 1982). ACV is such a good substrate for the virally encoded TK, but not the cellular TK that it remains in an unphosphorylated inactive form in uninfected cells, which effectively minimises the toxic side effects of the drug.

ACV has been shown to be most effective against HSV-1 and VZV (Wagstaff et al., 1994) but less effective against HCMV infection, and this was initially thought to be due primarily to the absence of an HCMV encoded TK homologue. However, a direct



role for the HCMV encoded UL97 has been demonstrated in the phosphorylation of ACV using a recombinant GST-UL97 fusion protein expressed from baculovirus, although ACV was phosphorylated less efficiently than GCV (Talarico et al., 1999). This observation may be accounted for by a greater affinity (3- to 5-fold) of GCV-monophosphate for the cellular GMP kinase, which performs the second phosphorylation event. Importantly, ACV-triphosphate (TP) is a more potent alternative substrate inhibitor of the HCMV DNA polymerase than GCV-TP (5- to 10-fold) (Stanat et al., 1991) and ACV, but not GCV is an obligate chain terminator. ACV is administered either topically, orally or intravenously and is neither bone marrow toxic nor immunosuppressive (Steele et al., 1980, McGuffin et al., 1980). Peak concentrations (10µg/ml) of ACV in plasma are achieved following a 5mg/kg i.v. dose as opposed to an oral dose of 200mg which results in peak concentrations of only 0.6µg/ml, thus an oral bioavailability of 15-30%. Although ACV has little efficacy in the treatment of HCMV infections, it has shown some benefit in the prophylaxis of HCMV reactivation following bone marrow and solid organ transplantation (Balfour et al., 1989, Meyers et al., 1996, Barkholt et al., 1999). Prophylactic ACV therapy in these patients has been shown to delay HCMV infections and prevent cases of HCMV disease. In an attempt to increase the oral bioavailability of ACV, valaciclovir, the valine ester of ACV was developed. The valine increases the oral bioavailability of ACV, so that upon cleavage of the valine from the ACV by valine esterase, plasma levels of ACV reach up to 54%.

GCV [9-(1,3-dihydroxy-2-propoxymethyl)-guanine], like ACV is an analogue of guanosine and virtually identical in structure to ACV, with the addition of a 3'-hydroxyl group (figure 1.6). This confers a marked improvement in antiviral activity against HCMV but results in GCV not being an obligate chain terminator. GCV is effective against several of the human herpesviruses, including HSV-1 and 2 (Cheng et al., 1983, DeClerq et al., 1993), VZV, and HHV-6 (Ansari and Emery, 1999), but limited activity against EBV (Littler et al., 1988, Tung et al., 1994) and HHV-8 (Cannon et al., 1999). Like ACV, GCV is dependent upon metabolic activation by phosphorylation to the triphosphate form. The initial phosphorylation in HCMV infected cells is performed by the HCMV encoded UL97 gene product (Littler et al., 1992, Sullivan et al., 1992), and subsequent phosphorylation steps are performed by cellular enzymes, as with ACV.

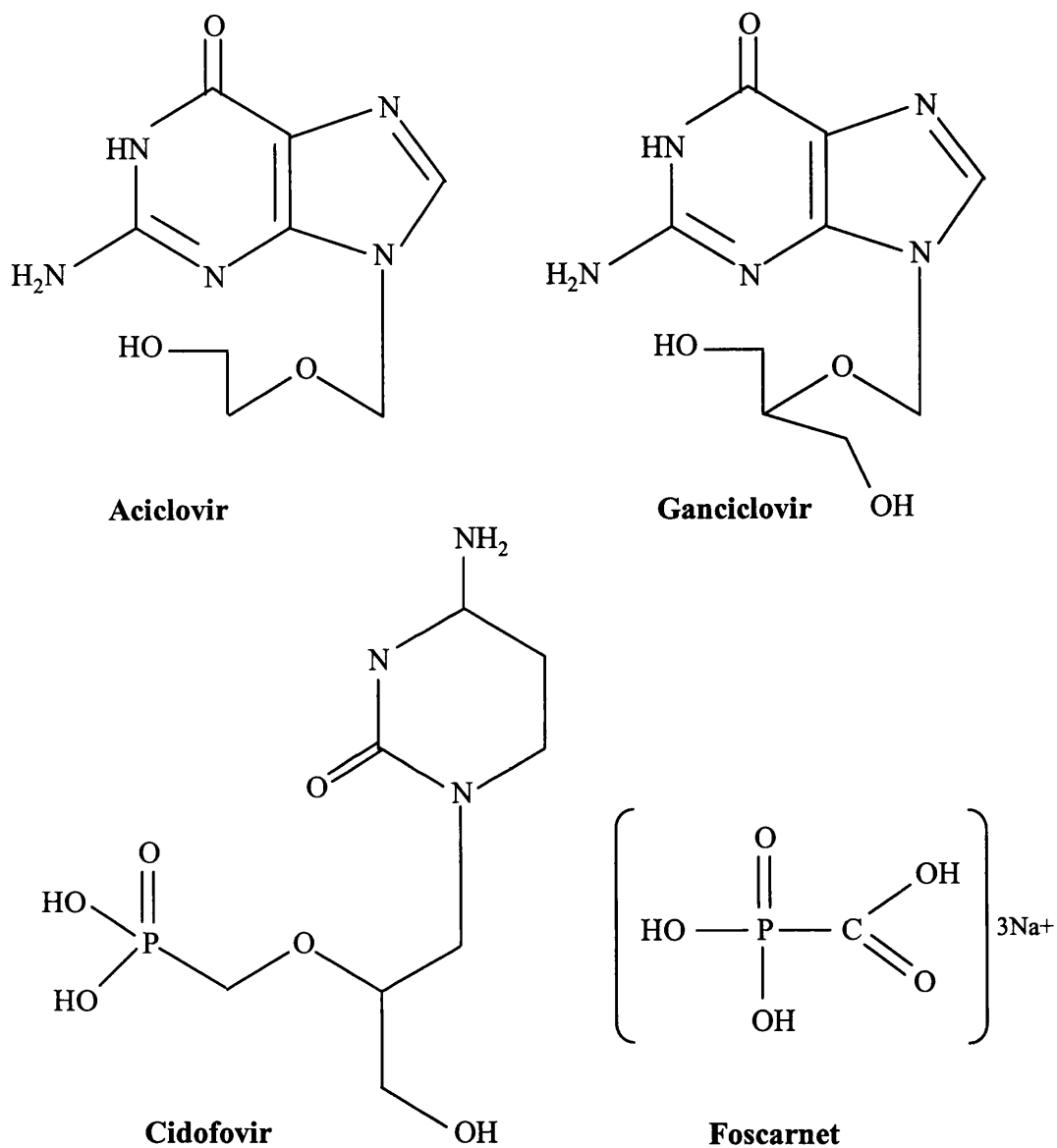


**Figure 1.6. Structures of the anti-herpetic compounds.**

The molecular structures of aciclovir [9-(2-hydroxyethoxymethyl)guanine]; GCV [9-(1,3-dihydroxy-2-propoxymethyl)guanine]; cidofovir [(S)-1-(3-hydroxy-2-phosphonyl-methoxypropyl)cytosine] and foscarnet (trisodium phosphonoformate hexahydrate).

The fully activated GCV triphosphate competes with dGTP for the viral DNA polymerase (HCMV UL54) during viral DNA replication and has been shown to slow down the velocity of polymerisation following incorporation into the growing DNA chain. The fact that GCV is not an obligate chain terminator and is incorporated into the growing DNA chain serves to increase its cytotoxicity, presumably because it can be incorporated into nascent cellular DNA. GCV can be administered orally, intravenously or as an intraocular implant for the treatment of HCMV retinitis. Oral bioavailability of GCV is poor (5-9%) and peak plasma concentrations of only 8µg/ml are achieved following a 5mg/kg i.v. injection. The improvement in oral bioavailability of valganciclovir led to the development of valganciclovir (VGCV), and indeed the oral bioavailability was greatly improved, achieving approximately 60% in HIV-infected patients (Gane et al., 1997). More importantly, HIV-infected and liver transplant patients receiving 900mg of VGCV once a day achieved a similar plasma concentration to that of i.v. GCV at 5mg/kg/day (Gane et al., 1997, Pescovitz et al., 2000). Also an oral dose of 450mg VGCV provided an exposure equivalent to that of 1000mg GCV three times daily, thus limiting the exposure to the drug and potential toxic effects.

The major dose limiting side effect of GCV is severe neutropenia, but the drug is also mutagenic, carcinogenic and inhibits the growth of bone marrow progenitor cells. This means treatment of severely immunocompromised patients such as bone marrow recipients must be carefully controlled. Anaemia and thrombocytopenia have also been observed with both i.v. and oral formulations.

### **1.5.2. Foscarnet**

Foscarnet (phosphono formic acid; PFA) is a pyrophosphate analogue (figure 1.6), which directly binds to and blocks the pyrophosphate-binding site of the viral DNA polymerase in a non-competitive manner resulting in the inhibition of DNA polymerisation. Foscarnet is generally considered second line therapy for most forms of serious HCMV infection, however it is the drug of choice in patients who develop dose-limiting neutropenia while on GCV, and more especially in those patients who fail to respond to GCV therapy, usually due to resistance. A combination of foscarnet with GCV have been successfully used as maintenance therapy in AIDS patients (Dieterich et al., 1993, Jacobson et al., 1994) and transplant patients (Bacigalupo et al., 1994) to

reduce the toxicity profile of foscarnet. Foscarnet has been shown to have activity against several of the human herpesviruses, including HSV-1 and -2, VZV, EBV and HHV-6. The in vitro activity of foscarnet is subject to considerable variability due to the inefficiency of transport of this highly charged molecule across the cell membrane. The bioavailability of foscarnet is poor whereby a peak plasma concentration of 509 $\mu$ M is achieved following an i.v. dose of 60mg/kg (Wagstaff et al., 1994) and oral bioavailability is only 10-20% of this. The major toxicity of foscarnet is renal impairment mainly due to nephrotoxicity associated with raised creatinine in the urine, which is usually reversible upon discontinuation of the drug.

### **1.5.3. Cidofovir**

Cidofovir (HPMPC, (S)-1-(3-hydroxy-2-phosphonylmethoxypropyl)-cytosine) is an acyclic nucleotide phosphonate (figure 1.6), an analogue of cytosine monophosphate and therefore is not dependent upon an initial phosphorylation by a virally encoded TK or UL97. Cidofovir is di- and tri-phosphorylated by the cellular enzymes pyrimidine nucleoside monophosphate kinase and pyruvate kinase respectively (Cihlar and Chen., 1996). Cidofovir is incorporated with the correct complementation to dGMP in the template DNA and is not excised by the 3' to 5' exonuclease activity of the HCMV DNA polymerase. This incorporation into the DNA causes a decrease in the rate of DNA elongation by 31% for one molecule of CDV and incorporation of two consecutive molecules prohibits the DNA from elongating further (Xiong et al., 1997). Cidofovir is active against a variety of the human herpesviruses including HSV-1 and -2, VZV and EBV (De Clerq et al., 1993), with significant activity against both HSV-1 and HCMV (IC<sub>50</sub> 0.06 – 0.08 $\mu$ g/ml). Cidofovir is mainly used to treat HCMV infections in patients who have acquired resistance to either GCV or foscarnet however, cross-resistance to GCV-resistant mutant strains is relatively common, especially with high-level GCV resistance (Smith et al., 1997). The drug is administered intravenously for HCMV infection or intravitreally for the treatment of retinitis, although bioavailability is poor at only 5%. Dose-dependent nephrotoxicity is the main side effect of cidofovir treatment, which can be accompanied with neutropenia and severe metabolic acidosis.

#### **1.5.4. Non-Nucleoside HCMV Inhibitors**

##### **Benzothiadiazine dioxide dibenzyl (BDT) derivatives**

Benzothiadiazine dioxide dibenzyl (BDT) derivatives are potent non-nucleoside HCMV inhibitors (Martinez et al., 2000A, Martinez et al., 2000B) (figure 1.7). They have a unique structure with respect to the nature of the heterocyclic base and also the lack of the 5'OH mimetic group as is present in GCV and other current anti CMV drugs, which points to a different mechanism of action. At present this mode of action is unknown. The drug activity was measured by CPE reduction in time of addition assays, and when BDT, GCV and cidofovir were added to the assay system 48 and 72 hours post infection, all 3 drugs lost their capacity to inhibit viral DNA synthesis. This confirms that the action of BDT occurs in the early stages of HCMV replication.

Another member of the non-nucleosidic class of anti-HCMV drugs is BAY 38-4766. This drug inhibits HCMV replication by inhibition of the cleavage of high-molecular-weight viral DNA concatamers to monomeric genomic length (McSharry et al., 2001). Kinetic studies revealed the replication cycle of HCMV was inhibited in the late stages, suggesting that the drug inhibits viral maturation. This suggestion was confirmed by the electron microscopic observation that only subviral particles lacking viral DNA bud from the cellular membrane, and the production of viral mRNAs and de novo synthesis of viral DNA was not affected by the presence of the drug. Sequence analysis of BAY 38-4766-resistant HCMV strains mapped resistance to the UL89 terminase and UL104 genes, whose products are involved in the viral DNA concatamer cleavage process.

##### **BDCRB and 1263W94 (Maribavir, formally Benzimidavir)**

The antivirals 2-bromo-5,6-chloro-1-β-D-ribofuranosyl benzimidazole (BDCRB) and its 2-chloro analogue (TCRB) originally demonstrated significant antiviral activity against HCMV at non-cytotoxic concentrations (Townsend et al., 1995). Antiviral activity was demonstrated not to be mediated by inhibition of HCMV RNA, DNA or protein synthesis in HCMV infected cells (Chulay et al., 1999), unlike most of the currently licensed antivirals. The target of antiviral action of BDCRB was determined by passaging the HCMV through increasing concentrations of BDCRB to select a drug resistant isolate.

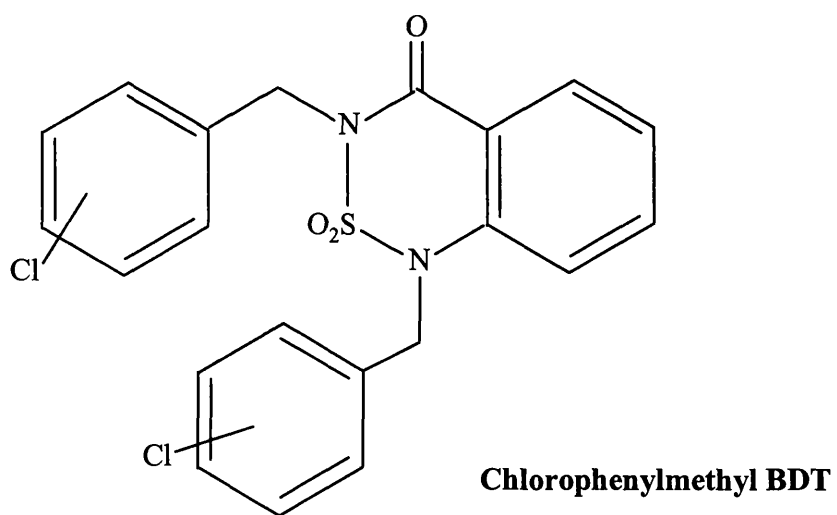
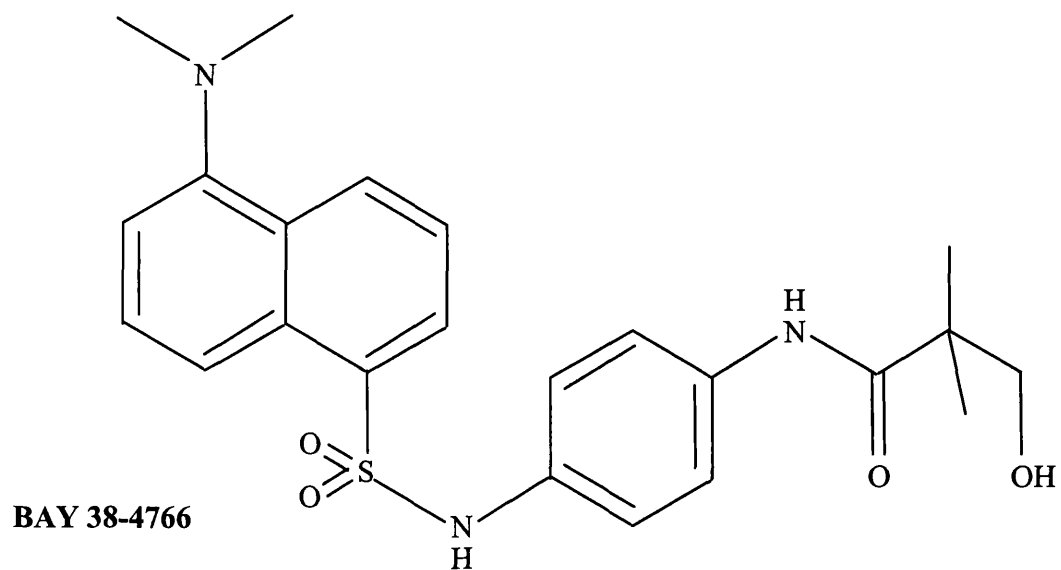


Figure 1.7. Structures of BAY 38-4766 and chlorophenylmethyl BDT

Genetic mapping experiments demonstrated resistance mutations in the UL89 gene (D344E and A355T) (Underwood et al., 1998), which encodes an endonucleolytic subunit of the putative HCMV terminase. BDCRB thus appears to act by blocking the cleavage of concatameric DNA to unit genome length, without inhibition of the synthesis of viral DNA, mRNA or proteins. The concatameric viral DNA is known to be packaged into preformed capsids in unit genome lengths with specific nucleotide sequences at the termini. Six HCMV ORF's are thought to be involved in this process; UL104, UL89, UL77, UL56, UL52 and UL51, due to their homology with the HSV ORFs known to be involved, where the UL89 is highly conserved across the herpesvirus family. This conservation suggested a similar sensitivity of all the human herpesviruses to the BDCRB, however HSV and VZV are not susceptible to the antiviral activity of the compound (Underwood et al., 1998).

The proteins of the terminase complex perform specific functions in the sequence-specific cleavage of the *a* sequence during the maturation of HCMV DNA into unit genome size. These activities include DNA binding, prohead (capsid) binding, ATPase activity and endonucleolytic cleavage of the precursor viral DNA. The HCMV UL89 appears to encode the DNA terminase, identified by virtue of the presence of an ATP binding P-loop motif, AYDYFGKT.

Further sequencing of the HCMV genes postulated to be involved in the DNA cleavage to unit length, identified mutations in the UL56 gene (Krosky et al., 1998). UL56 codes for a packaging motif binding protein with DNA sequence-specific binding capability with specific nuclease activity, apparently binding to *pac* sequences (cleavage recognition sites) and endonucleolytically cleaves the viral DNA (Bogner et al., 1998). Mutations identified in both the UL89 and UL56 genes suggests an interaction between the UL89 and UL56 encoded proteins, consistent with the proposed role of each in viral DNA maturation.

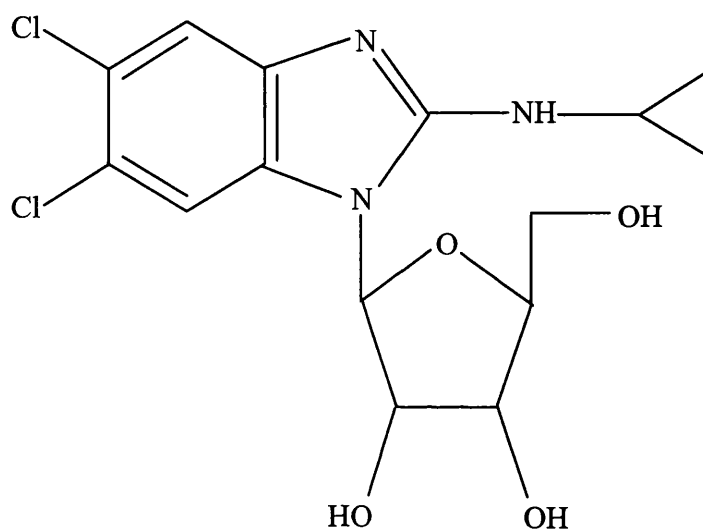
Although BDCRB was highly selective for HCMV and had little cytotoxicity *in vitro*, it was rapidly metabolised to the aglycone (2-bromo-5,6-dichloro benzimidazole) when administered to rats and monkeys (Chan et al., 2000). This metabolite is inactive against HCMV. 1263W94 was identified from a panel of benzimidazole analogues as a potential antiviral against herpesviruses (figure 1.8). 1263W94 is as potent against HCMV *in vitro* as BDCRB and exhibits several major improvements. 1263W94 is

metabolically more stable in rats, monkeys and humans (Chan et al., 2000), has measurable, but limited penetration into the brain and vitreous humor of laboratory animals, shows little cytotoxicity against bone marrow precursor cells *in vitro* and lack of mutagenicity in preclinical assays (Chulay et al., 1999). These features also present as an improvement over the antivirals currently used against HCMV. A major advantage of 1263W94, like BDCRB, is the mechanism of action does not involve the initial phosphorylation of the drug to its active form and the DNA polymerase is not involved, although DNA synthesis is inhibited. The most useful feature to the drug is the sensitivity of GCV-resistant virus to 1263W94. This suggests 1263W94 could be used following the emergence of clinical HCMV resistance in the immunocompromised patient groups, or indeed in combination with GCV for the treatment of HCMV disease. An important consideration for the use of 1263W94 as an antiviral for the treatment of HCMV disease is the penetration of the drug into the vitreous humor to provide good access to the retina. Phase 1 trials performed in normal healthy volunteers showed 1263W94 was rapidly and well absorbed, with plasma total drug concentrations well above the *in vitro* IC<sub>50</sub> and a near linear increase in C<sub>max</sub> with increasing doses of drug (Chulay et al., 1999). Further phase 1 trials in HIV patients mirrored these results, indicating neither HIV infection nor the anti-HIV medications altered the pharmacokinetics of 1263W94, which is essential if the drug is to be used in the treatment of HCMV disease in the HIV population. The disadvantage of 1263W94 is it is extensively bound to plasma proteins. This has effectively limited the penetration of the drug into the vitreous humor of animals. Considering this is the only antiviral effective against GCV-resistant HCMV, only radical implants of the drug into the eye would be effective for treatment of drug-resistant HCMV retinitis.

### 1.5.5. Fomiversen

Fomiversen (ISIS 2922) is a novel 21-base phosphorothioate oligonucleotide, ie DNA molecules in which a single non-bridging oxygen has been replaced by a sulphur, resulting in increased *in vivo* stability. The DNA sequence (5'GCG TTT GCT CTT CTT CTT GCG-3') is complementary to messenger RNA encoding regulatory proteins of immediate early region 2 (IE2) encoding the 55 and 86 kDa polypeptides (IE86 and IE55) of HCMV, which correspond to nucleotide co-ordinates 170120-170140. The mechanism by which fomiversen inhibits HCMV replication is complex as it appears several mechanisms,





**Maribavir (1263W94 / Benzimidavir)**

**Figure 1.8. Structure of 1263W94 (Maribavir / benzimidavir).**

The molecular structure of 1263W94 [5,6-dichloro-2-isopropylamino-1-( $\beta$ -L-ribofuranosyl)-1H-benzimidazole].

including the desired antisense inhibition of target gene expression and non-antisense mechanisms are responsible for the antiviral activity of fomiverson. The antisense mechanism is presumably mediated by RNase H cleavage of target RNA at the site of oligonucleotide hybridisation. Anderson et al., 1996 demonstrated an inhibition of IE55 synthesis, by western blot, in cells transformed with cDNAs expressing IE55 and treated with fomiverson at concentrations as low as 25nM. This correlated with a reduction in IE55-encoding mRNA. Despite this evidence, the progressive introduction of base changes into the nucleotide sequence to disrupt the stability of a base paired oligonucleotide-RNA duplex only resulted in small changes in activity (2.3 fold). This indicates apparent non-antisense activities of the drug, such as interaction with the virus particles to prevent adsorption and specific inhibition of the enzymes involved in viral DNA synthesis.

Fomiverson is the first antisense oligonucleotide drug to be approved for HCMV treatment by the FDA. The major potential therapeutic indication is the treatment of HCMV-induced retinitis in AIDS patients. Fomiverson is administered as an intravitreal injection, which achieves maximal retinal concentrations approximately 2-5 days post administration and an elimination half-life of 78 hours (in monkeys). The most frequent adverse events include intraocular pressure and mild to moderate intraocular inflammation. Marked retinal toxicity has been observed in a recipient of high concentrations of the drug (Piascik, 1999, Leeds et al., 1998).

### **1.6. Antiviral resistance**

#### **1.6.1. Antiviral resistance and UL97**

The evidence that HCMV could become resistant to GCV and other anti-herpesvirus drugs was originally obtained in the laboratory by passaging a susceptible laboratory reference virus (AD169) through cell culture in the presence of increasing concentrations of the drug. The mutant virus obtained, designated B759<sup>f</sup>D100, was resistant to GCV but was found to be susceptible to foscarnet. It was also observed that the mutant induced a decreased phosphorylation of GCV in infected cells compared to the cells infected with the wild type strain (Biron et al., 1986). This suggested that a gene(s) in the HCMV genome had obtained a mutation, which resulted in the reduced the synthesis of an enzyme contributing to the intracellular phosphorylation of GCV.

The mechanism of GCV phosphorylation by an HCMV encoded enzyme was determined by Sullivan et al., (1992) and Littler et al., (1992). Sullivan et al., performed marker transfer experiments using an overlapping set of nine cosmids containing fragments representing the complete sequence of the GCV resistant strain B759<sup>r</sup>D100. It was shown that the recombinant viruses isolated from marker transfer experiments using two plasmids with a 13 kilobase overlap were unable to induce GCV phosphorylation in infected cells. Analysis of the UL97 ORF contained within the overlap revealed a 4 amino acid deletion in codons 638 to 641 which lie in a conserved region among protein kinases implicated in substrate binding. Littler et al., cloned a truncated part of the UL97 ORF (M<sub>r</sub> 39,000) into an expression vector, raised antisera to the protein and identified UL97 in HCMV infected cells and extracts from *E.coli*-expressing UL97. These extracts were able to phosphorylate GCV efficiently, and furthermore, HCMV-seropositive serum was able to neutralise the phosphorylating activity of the UL97. Both sets of results suggested that UL97 was responsible for the initial phosphorylation of GCV.

The initial findings that HCMV could become resistant to GCV prompted the investigation into GCV resistance in the clinical setting. Studies were performed into the efficacy of GCV therapy in immunocompromised patients, where it was demonstrated by Erice et al., (1987) that GCV therapy eliminated viraemia after 4.7 days of therapy. One AIDS patient in their study however had persistent HCMV viraemia despite being treated with multiple courses of GCV. Two further patients were identified (Erice et al., 1989) with persistent viraemia and progressive HCMV disease which was unresponsive to GCV. A series of experiments were performed upon these and further clinical isolates and the resistant laboratory strain 759<sup>r</sup>D100, which indicated that the resistance of clinical HCMV isolates to GCV was due to their reduced ability to phosphorylate GCV in virus infected cells (Stanat et al., 1991). Further, the mechanism did not appear to involve the DNA polymerase, however a decreased susceptibility to cidofovir was observed in the resistant laboratory strain, suggesting the polymerase may also be altered.

Since UL97 has been shown to perform the initial phosphorylation of GCV, many resistant clinical HCMV isolates have been characterised with respect to their UL97 mutations. Table 1.8 summarises the UL97 mutations identified in the literature. The

mutations identified comprise mainly of single point mutations, some double mutations and few small deletions. In most cases the most common mutations detected in resistant isolates have been located at specific codons such as 460 (22%), 594 (21%) and 595 (25%). Marker transfer experiments have demonstrated that the mutations M460V/I, H520Q, A594V, L595S/F, deletion of codon 595 and deletion of codons 591 to 594 confer GCV resistance due to an impaired intracellular phosphorylation of GCV to GCV monophosphate.

Two classes of mutations in the HCMV UL97 phosphotransferase leading to GCV resistance can be discerned. The majority of mutants occurring in clinical isolates map to a section of the protein kinase which recognises peptide and protein substrates, namely subdomains VIII to IX. These include the mutations, which occur at codons 520, 590-598, 600, 603 and 607 outlined in Figure 1.9. The mutations, which have been mapped to codon 460, correspond to a non-conserved residue within the consensus sequence HRDLKXXN of subdomain VI. This motif forms the catalytic loop responsible for the phosphotransfer. This suggests that the first set of mutations affect the phosphorylation of GCV without major effects upon the phosphorylation of the natural substrate. However, mutations at the 460 codon may sterically alter the catalytic loop such that the phosphotransfer is impaired.

The clinical isolates reported to date (table 1.8) have yielded GCV resistant mutants which are either single point mutations, a combination of mutations, 1 to 4 codon deletions and more recently a nine codon deletion, however no nonsense or frameshift mutations have been observed indicating that UL97 is an essential gene in the replication of HCMV. Armed with this knowledge, He et al., (1997) generated a null mutant UL97 by performing site directed mutagenesis upon the invariant lysine at codon 355 in the catalytic domain II of UL97. This resulted in the inhibition of the autophosphorylation activity. The corresponding lysine in cyclic AMP-dependent protein kinase aligns and directly interacts with the  $\alpha$ - and  $\beta$ -phosphates of ATP. Further conserved residues were investigated for their role in the autophosphorylation of UL97 (Michel et al., 1999). The conserved residues were identified by sequence alignment of motifs, which are involved in the protein kinase autophosphorylation, none of which have been found in phenotypically resistant HCMV. The mutations

were generated in catalytic domain I (Y355D and G340V), domain II (V354L and K359Q), domain III (E380V), domain VI (A442V and L446R), domain VII-VIII (F523C and M526I), domain IX (D574A, G579A and L583F) and domain X + XI (Y617stop). The 340 mutation resides in the highly conserved GXGXXG motif, essential for phosphate binding, and completely inhibited autophosphorylation, but the 335 mutation, located 5aa upstream of this crucial position did not alter the phosphorylation. The mutations located in domain VI, next to or within the consensus HRDLKXXN which forms the catalytic loop, completely inhibited autophosphorylation. The mutation giving rise to the stop codon at 617 also resulted in no autophosphorylation. The remaining mutations resulted in little or no reduction in activity. It is interesting however that all point mutations or small deletions found in the UL97 gave rise to proteins which were still able to autophosphorylate, suggesting that the protein should maintain normal function with respect to its natural substrates (viral/cellular proteins). The region of the UL97 responsible for the nuclear localisation has been mapped between aa 48 and 110, suggesting the transport of UL97 into the nucleus is a signal mediated process (Michel et al., 1998). Mutants lacking the first 110 aa of UL97 were not localised within the nucleus of transiently infected cells, although these mutants remained functional for autophosphorylation and GCV phosphorylation. In contrast, mutants lacking the first 48 aa of UL97 were transported to the nucleus.

### **1.6.2. Antiviral resistance and UL54**

The HCMV DNA polymerase (UL54) is the major target of the currently used antiviral agents available for the treatment of HCMV infections. It was therefore reasonable to assume that like UL97, UL54 could develop mutations leading to resistance to these drugs in the clinical setting. Following sequential passage of the susceptible reference strain AD169 in increasing concentrations of GCV, sequence analysis of the UL54 ORF revealed the presence of the point mutations F412V and L501I (Lurain et al., 1992). Antiviral susceptibility of these mutant viruses was determined and revealed resistance to GCV and cidofovir, but susceptibility to foscarnet. It was also demonstrated that these mutant viruses contained point mutations in the UL97 ORF.

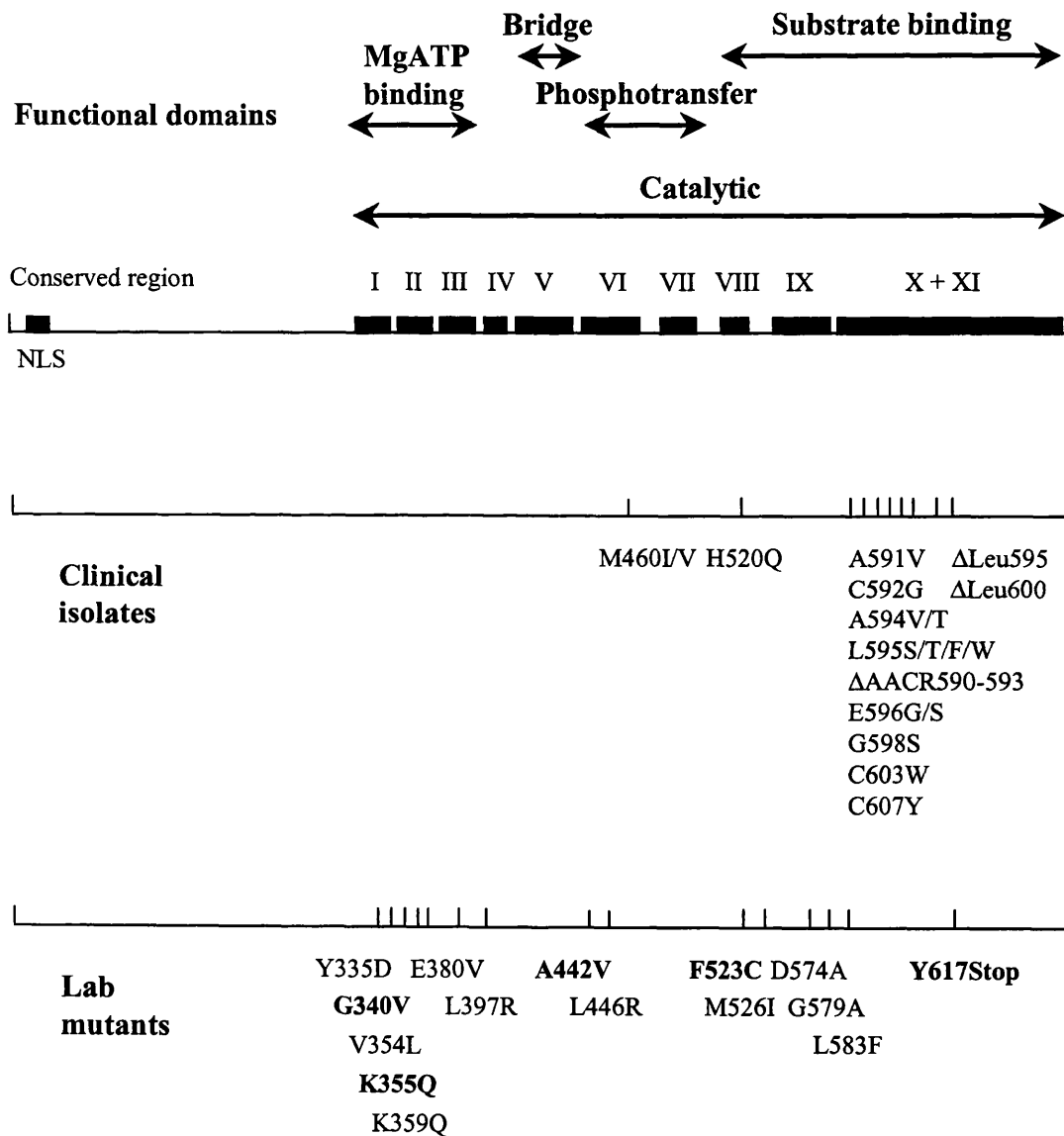


**Figure 1.9. Conserved regions in the HCMV UL97.**

The general locations of the conserved catalytic domains are illustrated with the locations of the drug resistance-associated mutations detected in clinical isolates and laboratory mutants. Further mutants have been made in the laboratory which have been detected in clinical isolates, including M460V, H520Q, A594V and L595S.

Table 1.8. Reported UL97 mutations conferring GCV resistance identified from clinical isolates

UL97 mutations	Catalytic domain	Protein kinase	GCV kinase	References
M460I	VI	nd	-	Lurain et al.,1994; Smith et al.,1997;Chou et al.,1995A;Wolf et al.,1995A and 1995B
M460V	VI	+	-	Chou et al.,1995A and 1995B; Erice et al.,1992; Smith et al.,1997; Wolf et al.,1995A; Alain et al.,1997
H520Q	VIII	+	-	Erice et al.,1992; Chou et al.,1995a; Hanson et al.,1995
A590T	X	nd	-	Wolf et al.,1998A
A591D	X	nd	-	Wolf et al.,1998A
A591V	X	nd	-	Chou et al.,1995A; Smith et al.,1997; Wolf et al.,1995B
C592G	X	nd	-	Erice et al.,1992; Smith et al.,1997; Chou et al.,1995A; Alain et al.,1997
A594V	X	+	-	Chou et al.,1995A and B; Erice et al.,1992; Smith et al.,1997; Alain et al.,1997; Rosen et al.,1997
A594T	X	nd	-	Erice et al.,1997
L595S	X	nd	-	Chou et al.,1995A and B; Erice et al.,1992; Smith et al.,1997; Wolf et al.,1995A; Lurain et al.,1994
L595T	X	nd	-	Smith et al.,1997
L595F	X	nd	-	Smith et al.,1997; Wolf et al.,1995A; Chou et al.,1995B
L595W	X	nd	-	Chou et al.,1995a; Crumpacker et al.,1996
ΔLeu595	X	nd	-	Baldanti et al.,1995A
E596G	X	nd	-	Chou et al.,1995A
E596D	X	nd	-	Wolf et al.,1998A
E596S	X	nd	-	Chou et al.,1995A
N597I	X	nd	-	Wolf et al.,1998A
G598S	X	nd	-	Baldanti et al.,1995A; Wolf et al.,1998A
G598V	X	nd	-	Wolf et al.,1998A
K599M	X	nd	-	Wolf et al.,1998A
C603W	X	nd	-	Smith et al.,1997
C603Y	X	nd	-	Wolf et al.,1998A
A606D	X	nd	-	Wolf et al.,1998A
C607Y	X	nd	-	Baldanti et al.,1998; Smith et al.,1998
V665I	XI	nd	-	Chou et al.,1995A
ΔLeu600	X	nd	-	Crumpacker et al.,1996
Δ595-603	X	nd	nd	Chou and Meichsner., 2000
Δ 590-593	X	+	-	Sullivan et al.,1993; Michel et al.,1998

To determine the direct effect of these mutations upon antiviral susceptibility, recombinant viruses were generated, whereby the UL54 mutations were transferred to AD169 and the IC<sub>50</sub> for each drug, plus the efficiency of GCV phosphorylation were determined (Lurain et al., 1992, Sullivan et al., 1993). These experiments revealed that the recombinant L501I and A987G viruses were resistant to GCV and cidofovir but sensitive to foscarnet. Phosphorylation of GCV in these mutants was equivalent to that of the wild type virus, suggesting drug resistance in these mutants was caused by a decrease in the affinity of the viral polymerase for the antiviral compounds. Like UL97, this evidence prompted the characterisation of UL54 mutations in the clinical setting. The majority of GCV resistant clinical isolates are associated with specific sequence alterations in the UL97 gene alone or in combination with UL54 mutations. Resistant isolates expressing UL54 mutations alone are extremely rare but mutations at N408D and T700A were observed by Erice et al., (1997), and shown to confer high level resistance to GCV and cidofovir. Similarly, the mutations T700A and V715M observed by Baldanti et al., (1996) conferred high level foscarnet resistance.

The investigation into the direct involvement of UL54 in antiviral drug resistance involved the construction and antiviral susceptibility of recombinant viruses containing mutations in UL54 alone (Cihlar et al., 1998a, figure 1.10). The characterised UL54 mutations from clinical isolates are located within UL54 conserved regions designated I to VII and  $\delta$ -region C. Specific amino acid residues located in the regions I, II and III have been shown to directly participate in the binding of deoxynucleoside triphosphates, chelating the Mg<sup>2+</sup> ion and interacting with the primer and template (Ye and Huang., 1993). The domains located within the conserved region IV and the  $\delta$ -region C are postulated to be involved in the 3'-5' exonuclease function of the polymerase (Bernad et al., 1989). Cihlar et al., (1998) constructed 17 recombinant viruses containing single amino acid substitutions in the UL54 gene. Antiviral susceptibility studies demonstrated two major distinct cross-resistance profiles. Most of the mutations conferring the same drug resistance phenotype cluster together in specific conserved regions. The majority of GCV-cidofovir resistance-associated mutations are located in regions IV and  $\delta$ -region C. Mutations associated with foscarnet and adefovir resistance are located in the conserved regions II and VI. The mutations in region III exhibit both a marked hypersensitivity to foscarnet (K805Q) and the highest foscarnet



resistance ever reported (T821I). This is mirrored by mutations in this region in HSV DNA polymerase (Gibbs et al., 1988, Larder et al., 1987). Furthermore, multiple mutations in the UL54 are additive and cause resistance to multiple antiviral drugs. Clinical isolates which are resistant to GCV, cidofovir and foscarnet have been shown to have two or more of the following mutations in UL54: N408D, F412C, L501I, K513E/R, D588E, Y751H, V781I, L802M, K805Q, T821I, S897P and R1052C (Smith et al., 1997). These mutations have not been identified in drug-sensitive HCMV isolates (Chou et al., 1999). Table 1.9 lists the UL54 mutations observed in clinical resistance to GCV and those generated by site directed mutagenesis. The table highlights the degree to which each mutation contributes to GCV resistance. Drug resistance is not the only consequence of mutations in the UL54 gene. Baldanti et al., (1996) reported single amino acid changes in the UL54 conferred a slow growth phenotype. Marker transfer experiments were used to introduce the V715M and T700A mutations to recombinant AD169 viruses, which were shown to be resistant to foscarnet. The slow growth phenotype was demonstrated by the slow replication rate of the recombinant viruses in cell culture as demonstrated by a delay in plaque formation with respect to the parental AD169 from which they were derived.

The analysis of the role of UL54 mutations alone in drug susceptibility provides a valuable insight into the relative importance of finding these mutations in the clinical setting, by giving an indication of the cross resistance potential of each of the mutations. Mutations in the non-catalytic domains of UL54 have been described by Chou et al., (1999), who looked at interstrain variation of UL54 in 40 unrelated subjects and its effect on the genotypic diagnosis of antiviral drug resistance. The study showed >98% interstrain homology at both the nucleotide and amino acid level, with an average of 46 nucleotide changes per strain, >80% of which are silent. The codons with amino acid changes are strongly clustered outside the defined conserved catalytic domains and show no overlap with mutations shown to be related to drug resistance.

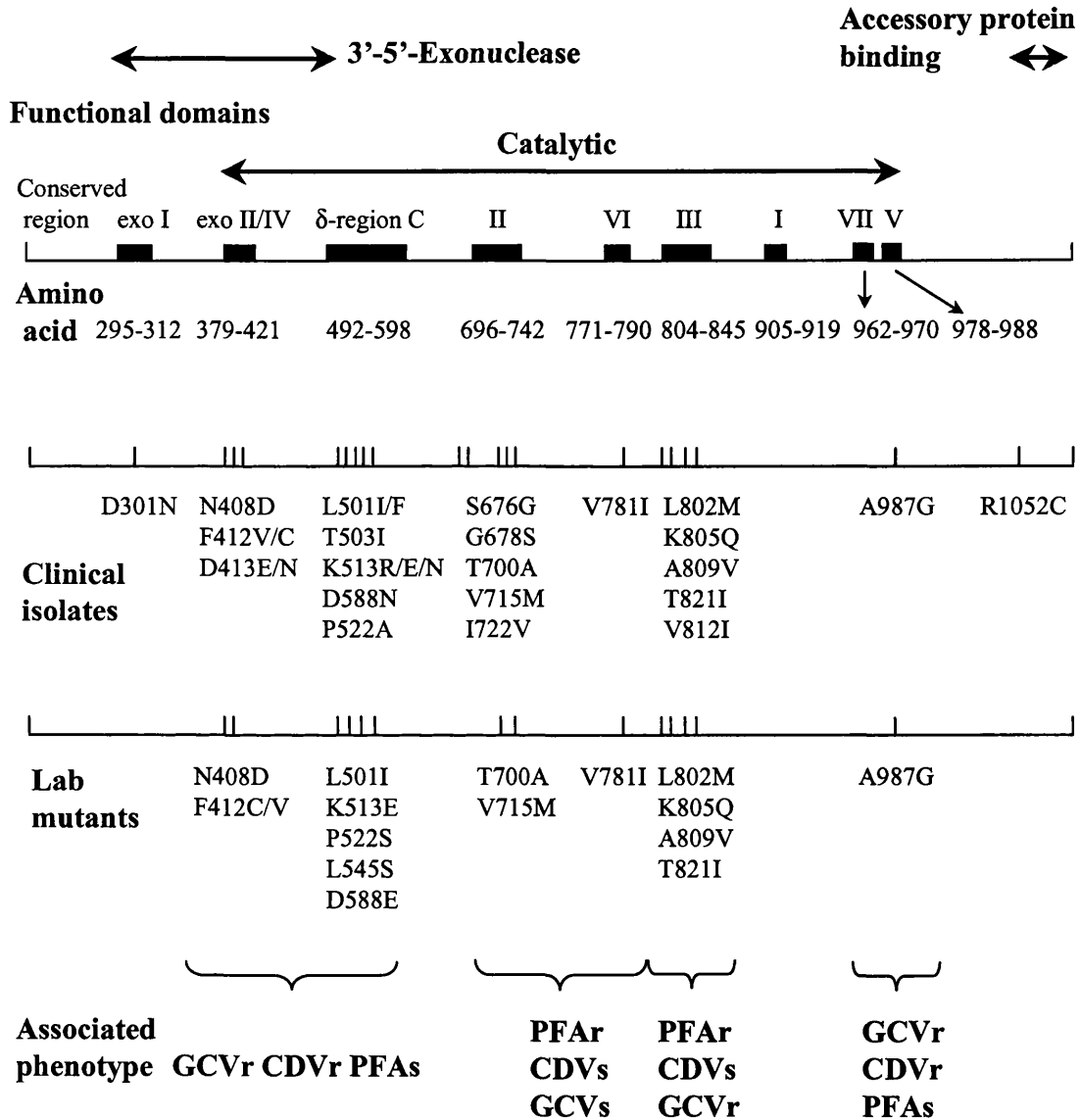


Figure 1.10. Conserved regions in the HCMV DNA polymerase (UL54) and the general locations of the drug resistance-associated mutations observed in clinical isolates and laboratory mutations. The HCMV antiviral drug susceptibility has been described for each of the mutations. Regions of antiviral cross resistance are illustrated. The boundaries of the conserved regions were defined by Biron and Baldanti., 1996.

### **1.6.3. Antiviral resistance associated with both UL97 and UL54**

Clinical isolates containing either UL97 mutations, UL54 mutations or both UL97 and UL54 mutations show different antiviral susceptibility profiles. A study by Smith et al., (1997) looked at the antiviral susceptibility profiles of 28 GCV resistant clinical isolates. The isolates which were low-level resistant to GCV ( $IC_{50}$  of  $\geq 8 \mu M$  and  $\leq 30 \mu M$ ) but susceptible to cidofovir and foscarnet had mutations in the UL97 alone or mutations in the UL97 and the non-catalytic domains of the UL54. Isolates containing mutations in both genes were highly resistant to GCV ( $IC_{50}$  of  $\geq 30 \mu M$ ) and cross resistant to cidofovir ( $IC_{50}$  of  $\geq 2.1 \mu M$ ). This cross resistance is extended to foscarnet ( $IC_{50}$  of  $\geq 324 \mu M$ ) when two or more mutations in the catalytic domains of the UL54 occur. Chou et al., (1997) demonstrated cross resistance between GCV and cidofovir in a patient treated for 9 months with oral GCV and no previous exposure to cidofovir, expressing a UL54 mutation at codon 412 (F412C). Additionally, Baldanti et al., (1996) demonstrated the emergence of GCV and foscarnet resistance in a clinical isolate where the GCV resistance was due to a mutation at codon 460 in UL97 and the foscarnet resistance was due to a mutation at codon 715 in the UL54. These data confirm that the mechanisms of foscarnet resistance in this case were unrelated to those of GCV resistance, probably a result of the sequential addition of the two different mutations, and not due to cross resistance.

Clinically, it has been observed that resistance of HCMV to GCV can develop within 3 to 4 months of GCV therapy (Drew et al., 1991a & b), and that prolonged GCV therapy is associated with high level resistance to GCV. The exception to this however was demonstrated by Wolf et al., (1998) who showed children with primary combined immunodeficiency (CID) and HCMV disease developed mutations in the UL97 within 10 days to 3 weeks of GCV therapy. All the patients with UL97 alterations exhibited mutations at codon 460 (M460L/V). One patient was treated with GCV for 3 days (3 weeks, 2 months previously) contained mixed wild type and mutant UL97 sequences in both the 460 codon and multiple mutations were found between codons 590 to 606 (Thr 590, Asp 591, Ser 595, Asp 596, Ile 597, Val 598, Met 599, Tyr 603 and Asp 606). Smith et al., (1997) showed the mean  $ID_{50}$  of GCV-resistant isolates cultured during the first 9 months of GCV therapy was significantly lower than that of GCV-resistant isolates cultured after  $>9$  months of therapy:  $25 \mu M$  versus  $54 \mu M$ . Additionally, 19% of

**Table 1.9. Antiviral susceptibilities of clinical isolates containing mutations in the DNA polymerase UL54.**

Region	UL54 mutation	Antiviral Susceptibility IC <sub>50</sub> (μM)			References
		GCV	Foscarnet	Cidofovir	
	AD169 susceptible control	3.5	45	0.75	Cihlar et al., 1998*
exo I	D301N	10-20 fold	2-3 fold	5-16 fold	Tatarowicz et al., 1992
	N408D	<b>17.15</b>	58.5	4.2	Erice et al., 1997, Baldanti et al., 1996, Sullivan et al., 1993, Cihlar et al., 1998*
IV	F412V/C	<b>15.05/14.7</b>	49.5/54	<b>11.6/13.5</b>	Chou et al., 1997, Cihlar et al., 1998*
	D413N	<b>&gt;200</b>	<b>201.7</b>	<b>&gt;10</b>	Erice et al., 1997, Baldanti et al., 1996*
	L501I/F	<b>21</b>	63	<b>6.8</b>	Erice et al., 1997, Cihlar et al., 1998*
	T503I	<b>46.3</b>	136	<b>2.1</b>	Smith et al., 1997, Cihlar et al., 1998*
δ-Region	K513R/E/N	<b>17.5</b>	63	<b>6.8</b>	Smith et al., 1997, Cihlar et al., 1998*
	P522A	<b>10.85</b>	49.5	<b>2.7</b>	Erice et al., 1997, Cihlar et al., 1998*
	D588N	4.55	<b>103.5</b>	0.8	Smith et al., 1997, Cihlar et al., 1998*
	S676G	3.85	40.5	0.9	Smith et al., 1997, Cihlar et al., 1998*
II	G678S	nd	nd	3-6 fold	Smith et al., 1998
	T700A	4.2	<b>261</b>	0.97	Baldanti et al., 1996, Cihlar et al., 1998*
	V715M	4.55	<b>427.5</b>	0.8	Baldanti et al., 1996, Cihlar et al., 1998*
	I726V	nd	nd	nd	Smith et al., 1997
VI	V781I	3.5	<b>234</b>	0.9	Smith et al., 1997, Cihlar et al., 1998*
	L802M	3.85	<b>144</b>	0.7	Chou et al., 1997, Cihlar et al., 1998*
	K805Q	3.5	<b>8.0</b>	<b>1.65</b>	Smith et al., 1997, Cihlar et al., 1998*
III	A809V	7.8	<b>410</b>	0.5	Chou et al., 1998*
	V812I	nd	nd	nd	
	T821I	<b>15.75</b>	<b>945</b>	1.4	Cihlar et al., 1998*
	841A	nd	nd	nd	
VII	S897P	nd	nd	nd	
V	A987G	<b>18.5</b>	54	<b>8.5</b>	Chou et al., 2000, Cihlar et al., 1998*
outside	R1052C	1	4 fold	7 fold	Smith et al., 1997
V	Δ 981-982	<b>28</b>	<b>225</b>	<b>3.75</b>	Chou et al., 2000

\* = Paper in which IC<sub>50</sub> was determined for UL54 mutations alone

Bold type face indicates concentrations of antivirals which are >2 fold higher than the susceptible AD169 strain

the GCV-resistant isolates cultured during the first 9 months were high level resistant, versus 64% after >9 months of therapy.

### **1.7. The HCMV encoded phosphotransferase UL97**

The HCMV UL97 encodes a protein kinase which autophosphorylates on serines and threonines (He et al., 1997) and exhibits homology to other protein kinases. It is located within the conserved region of herpesvirus genomes containing capsid morphogenesis and DNA processing functions (Chee et al., 1989). UL97 is present in virions and is probably a constituent of the tegument, since hydropathy analysis of the protein does not reveal any region consistent with transmembrane domains and is not analogous to any herpesvirus capsid proteins (Chee et al., 1990, Cohen et al., 1980). UL97 is responsible for the initial phosphorylation of the antiviral GCV (He et al., 1997) and mutations within this gene confers resistance to GCV, as discussed in section 1.6. However almost nothing is known about the natural functions of the UL97 and the intracellular localisation of the protein. Previous reports demonstrated the nuclear localisation of the VZV-encoded thymidine kinase ([TK], Shiraki et al., 1985), and the cytoplasmic localisation of the HSV-1 TK, which are responsible for the phosphorylation of ACV, penciclovir and GCV (Haar et al., 1997). Considering these proteins have no homology to the UL97, no conclusions could be drawn about either the role or the localisation of the UL97, although it has been shown to accumulate in the nuclei of infected cells by indirect immunofluorescence (Michel et al., 1996). Nuclear uptake of proteins is a highly selective, signal mediated process, thus the identification of two homologous N-terminal sequences comprising RARRRQ at amino acid positions 31-36, and RGGRKRPLRP at positions 190-199 in the N-terminal region confirmed that UL97 was targeted to the nucleus. This correlates with other virally encoded proteins, ie pp65, which have two co-operative sequences for nuclear transport. Additionally, a truncated UL97 lacking the N-terminal NLS was shown to be impaired for nuclear transport. This also adds to the evidence suggesting UL97 is a tegument protein since herpesvirus tegument proteins are acquired in the nucleus (Ward et al., 1996).

Temporal expression studies demonstrated the expression of UL97 begins 5 hours post infection, continues throughout the remainder of the replicative cycle and exhibits a

relatively high steady state level during late times (Van Zeijl et al., 1997). The UL97 was post translationally modified by autophosphorylation within 1 hour of its expression. This is in contrast to the data by Michel et al., 1996, who detected initial UL97 expression 16 hours post infection. Synthesis of UL97 was significantly reduced upon treatment with the DNA replication inhibitors GCV and PAA, thus classifying UL97 as an early-late protein. Results gained from phosphorylation studies of TK deficient cells infected with recombinant vaccinia virus encoding the UL97 suggests that the natural function of the UL97 protein is not directly linked to the phosphorylation of natural nucleosides and the phosphorylation of the GCV is incidental, comparable with the phosphorylation of GCV by the VZV-encoded ORF 46.

Ng et al., (1996) utilised the partial homology of UL97 to its putative analogue in HSV-1, UL13, to construct and characterise a recombinant HSV-1 in which the UL13 was replaced by UL97. The UL13 encodes a protein kinase known to phosphorylate the HSV-1 immediate early protein ICP22. This study demonstrated the UL97 protein could partially substitute the function of the UL13 and perform the phosphorylation of the HSV-1 ICP22 in the absence of UL13. The nature and number of amino acid residues of ICP22 phosphorylated by the UL97 may suggest that a similar protein is involved in the natural infection of HCMV which resembles ICP22. However an  $\alpha$ 22/ICP22 related gene/protein has not been identified in HCMV. Additionally, this study also showed the UL97 can confer partial GCV sensitivity upon a UL13-, TK-virus.

To date no UL97 deletion mutants have been identified in nature and indeed recombinant viruses with mutations in the UL97 have been difficult to isolate (Michel et al., 1996). The mutations detected in GCV resistant clinical isolates reside in the region of the UL97 conferring substrate specificity and do not affect the enzymatic activity (Michel et al., 1999). To determine the function of the UL97 in viral replication, Prichard et al., (1999) constructed recombinant viruses in which >70% of the UL97 ORF was deleted and a selectable genetic marker was inserted. The UL97 deletion mutant exhibited a marked decrease in replication efficiency, approximately 100-fold by 72 hours post infection and 10000-fold by 120 hours, which was readily reversible upon infection with the deletion mutant of a cell line expressing the UL97 *in*

*trans*, reversing the replication deficit 100 fold. Also, the appearance of progeny virus was delayed approximately 48 hours, suggesting defective replication. Upon infection of HeLa cells, the recombinant virus expressed comparable levels of the MIE gene products and appeared to enter the early phase of DNA replication, as evidenced by the levels of mRNA transcripts from the UL44. The levels of transcripts were lower however than in infections with the parent virus, suggesting the deletion mutant cannot efficiently synthesise DNA. This gives a clear indication that UL97 is essential for HCMV replication.

The UL97 deletion mutant was further characterised by Wolf et al., (2001) in an attempt to determine the natural function and substrate of UL97. Wolf et al., demonstrated disruption of two distinct phases of replication in the deletion mutant: (1) Early phase as demonstrated by a 4- to 6-fold reduction in DNA accumulation. No difference was observed in the accumulation of the IE1<sub>491aa</sub> and IE2<sub>579aa</sub>  $\alpha$  proteins, but there was a slight reduction in the accumulation of the proteins ppUL44 and pp65, both early-late proteins, compared to wild type. These differences could not account for the poor replication of the deletion mutant. (2) Late phase as demonstrated by a 100- to 1000-fold reduction in replication. BDCRB was used to inhibit the cleavage of concatameric viral DNA and packaging of progeny DNA into nucleocapsids. The DNA accumulation and cleavage of the WT and mutant viruses were comparable in the BDCRB block, but upon release, the yield of mutant virus was reduced by 1000-fold. A severe encapsidation defect was observed and empty capsids accumulated in the nuclei of infected cells, which contained neither viral DNA nor internal core structures. DNA containing virions were not observed in the cytoplasm of mutant-infected cells.

### 1.8. Protein Kinases

The protein kinases encoded by the herpesvirus families include the HSV-1 UL13 and VZV ORF47 (alphaherpesviruses), the HCMV UL97 and HHV-6 U69 (betaherpesviruses) and the EBV BGLF4 (gammaherpesviruses). All five genes reside at equivalent positions in their respective genomes and all were identified by library searches based on the predicted individual protein kinases and their homologies not

only to other herpesvirus protein kinases but also of cellular kinases, which have distinct patterns of conserved residues as illustrated in figure 1.11.

Hanks et al., (1988) established that all protein kinases are divided into kinase domain motifs consisting of 11 subdomains which are conserved throughout the protein kinase family. These are defined as regions containing patterns of conserved residues, which are never interrupted by large amino acid insertions. The individual subdomains have specific functions, which co-operatively result in successful phosphotransfer by performing the three main roles of protein kinases: (1) binding and orientation of the ATP phosphate donor as a complex with a divalent cation (usually  $Mg^{2+}$  or  $Mn^{2+}$ ); (2) binding and orientation of the protein (or peptide) substrate; and (3) transfer of the  $\gamma$ -phosphate from ATP to the acceptor hydroxyl residue (serine, threonine or tyrosine) of the protein (or peptide) substrate. The functional roles of the individual kinase subdomains, including the precise roles of the highly conserved amino acid residues in each subdomain in the catalytic phosphotransfer have been elucidated (Hardie and Hanks, 1995). The resolution of the crystal structure of the mouse protein kinase A-C $\alpha$  (PKA-C $\alpha$ ) facilitated the designation of the subdomains. It was found that the subdomains of the PKA-C $\alpha$  folded in a two lobed structure. The smaller N-terminus lobe, which includes the subdomains I-IV, is primarily involved in the anchoring and orientating of the nucleotide. The larger C-terminal lobe, which includes the subdomains VI-XI, is largely responsible for the binding of the peptide substrate and initiating the phosphotransfer. The subdomain V residues span the two lobes and the deep cleft between the two lobes is recognised as the site of catalysis (Bossemeyer et al., 1993; Zhang et al., 1993).

As stated previously, the conserved catalytic domains are important either directly as components of the active site or indirectly by imposing constraints on the secondary structure so contributing to the formation of the active site. This section will give an overview of the roles of the individual subdomains and more specifically, the importance of the highly conserved kinase motifs. Subdomain I contains the conserved motif GXGXXGXV, which is predicted to form a fold around the nucleotide. The glycines are in contact with the ribose moiety and the terminal pyrophosphates so functioning to anchor the non-transferable phosphates of the ATP. This motif is also



present in ATP synthetases and many nucleotide binding proteins. An invariant and highly conserved lysine lies in subdomain II and directly interacts with the  $\alpha$ - and  $\beta$ -phosphates so aiding the anchoring and orientating of the ATP. This lysine forms a salt bridge with the carboxyl group of the nearly invariant glutamic acid in subdomain III, so helping to stabilise the interactions between the invariant lysine and the  $\alpha$ - and  $\beta$ -phosphates. Subdomain IV contains no invariant residues so does not appear to be directly involved in the catalysis or the substrate recognition. Subdomain V links the small and large lobes of the catalytic subunit and forms hydrogen bonds with the adenine or ribose ring to help anchor the ATP. Subdomain VI contains the consensus motif HRDLKXXN, of which the aspartic acid and asparagine are invariant. This motif forms the catalytic loop and being an invariant residue, it is postulated that the aspartic acid is the catalytic base responsible for accepting the proton from the attacking substrate hydroxyl group during the phosphotransfer. The lysine in the loop may be responsible for neutralising the negative charge of the  $\gamma$ -phosphate during transfer so facilitating the phosphotransfer. The asparagine helps to stabilise the loop via hydrogen bonding with the aspartic acid and chelates the  $Mg^{2+}$  ion that bridges the  $\alpha$  and  $\gamma$ - phosphates of the ATP. Subdomain VII contains a highly conserved DGF triplet which chelates the primary  $Mg^{2+}$  ion that bridges the  $\beta$ - and  $\gamma$ - phosphates of the ATP thereby orientating the  $\gamma$ - phosphates for transfer. Subdomain VIII contains a highly conserved APE motif, of which the nearly invariant glutamic acid forms an ion bond with an invariant arginine in subdomain XI, so stabilising the large lobe. Subdomains VI and VIII are the major domains involved in substrate specificity, conferring either protein serine/threonine or protein tyrosine kinase activity. The consensus DLKPEN in subdomain VI is a strong indicator of serine/threonine specificity, and the consensus DLRAAN is a strong indicator of tyrosine specificity. Subdomain VIII also contains consensus sequences for substrate specificity, albeit limited among the serine/threonine kinases. The consensus for the tyrosine kinase specificity is P-I/V-K/R-W-T/M-APE, while the serine/threonine kinase consensus is G-T/S-XX-Y/F-XAPE. The nearly invariant aspartic acid in subdomain IX acts to stabilise the catalytic loop by hydrogen bonding to amino acid residues that precede the loop. The function of subdomain X remains unknown. As previously mentioned, subdomain XI contains a nearly invariant arginine which hydrogen bonds with the glutamic acid in subdomain VIII to stabilise the large loop.

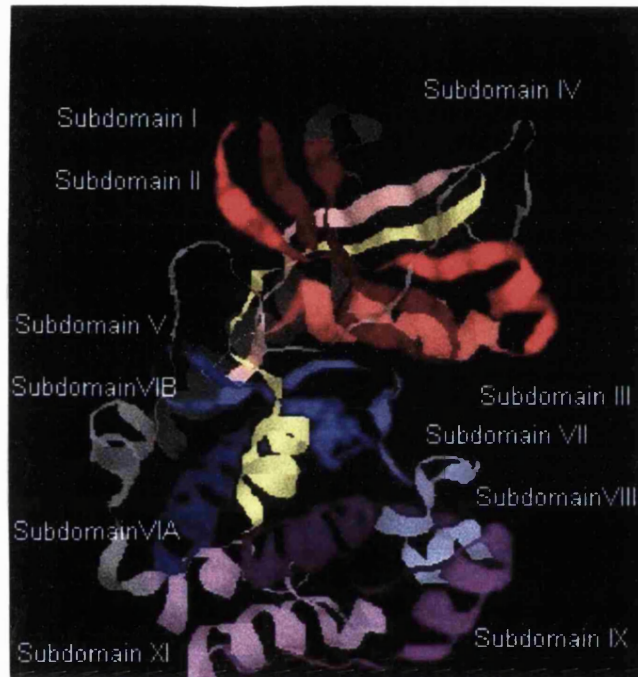


**Figure 1.11. Molecular structure of protein kinases.**

Taken from The Protein Kinase Resource at  
[www.nih.go.jp/mirror/kinases/pk\\_home.html](http://www.nih.go.jp/mirror/kinases/pk_home.html)

## **1.9. Baculovirus Expression Systems**

Various expression systems have been utilised for heterologous protein expression, in order to generate large amounts of foreign protein. Initially, *in vivo* recombination between the gene of choice and bacteriophages, followed by genetic selection to recover the recombinant clones, was employed for studies of individual genes. This was extremely cumbersome and time consuming, so with the advent of recombinant DNA technology, the cloning of foreign genes into vectors and plasmids was hugely simplified. This has led to the large scale synthesis of foreign genes, so enabling the study and characterisation of a large number of diverse proteins. Expression of heterologous genes can be performed in prokaryotic (*E.coli*) and eukaryotic (mammalian and insect) systems, each of which have their own inherent advantages and disadvantages. The overwhelming advantage of the prokaryotic expression system is the ease in which the foreign DNA can be manipulated and heterologous proteins expressed, largely due to the extensive knowledge of *E.coli* genetics. The problems with this system however are largely due to the necessity to study proteins which are correctly post translationally modified and can be purified from the host proteins as soluble, functionally active proteins.

Recombinant baculoviruses have become one of the most versatile and widely used systems for the expression of heterologous genes in cultured insect cells and insect larvae. Heterologous genes expressed in such systems are derived from widely varying sources, such as eukaryotes, fungi, plants, bacteria and viruses and are produced either as fusion or non-fusion proteins at levels ranging from 0.1% to 50% of the total insect cell proteins. Moreover, most of the proteins produced are correctly post translationally processed, modified, appropriately compartmentalised and importantly, are functionally active, so are believed to closely resemble their authentic counterparts.

The baculoviruses (family *Baculoviridae*) are large double stranded DNA viruses, which can infect a diverse range of insect species. Each baculovirus strain however is highly species specific, such as the *autographa californica* multiple nuclear polyhedrosis virus (AcMNPV) which naturally infects the alfalfa looper. During the life cycle of the baculovirus, infectious virus particles enter susceptible insect cells, the viral DNA is uncoated in the nucleus and the DNA replication begins about 6 hours

post infection. This is followed by a division in the replication cycle, whereby extracellular virus particles (ECV) are budded from the membrane of infected cells during the early phase of replication and are detectable 10 hours post infection. Later during the infection cycle, large intranuclear occlusions form in the infected cells, which is characteristic of AcMNPV and other MNPV subgroups. These occlusions are known as polyhedra derived virus (PDV) and consist of virus particles encapsulated by a single protein of molecular weight of approximately 29 kD, known as polyhedrin. These PDV are released when the infected cells are lysed during the last phase of the infection cycle, usually 2 days post infection accumulating up to 6 days post infection. When the infected insect dies, thousands of PDVs are released as the host decomposes. The PDVs are important for the horizontal transmission of the virus, and polyhedrin serves to protect these encapsulated virions from inactivation by heat and desiccation. When insect larvae feed on the contaminated vegetation the PDVs dissolve in the midgut of the insect, releasing the virus so initiating another round of infection. Several factors regarding the polyhedrin protein have enabled the AcMNPV to become an effective tool for the expression of foreign proteins. During the late phases of infection, the polyhedrin protein accumulates to very high levels, accounting for 30 – 50% of the total insect protein, but polyhedrin is not essential for the life cycle of the baculovirus under tissue culture conditions (Smith et al., 1983). Artificial deletion or insertional activation of the polyhedrin gene of AcMNPV results in the production of the occlusion body-negative viruses, which can be exploited by replacement the polyhedrin gene with a foreign gene under the control of the polyhedrin promoter. Proteins under control of the polyhedrin promoter should theoretically be expressed to the same levels as the polyhedrin, however it seems expression levels vary depending on the inherent nature of the foreign protein and the effective translatability of the mRNA encoding the protein.

The steps involved in the generation of a recombinant baculovirus begin with the cloning of the gene of interest into a suitable transfer vector. The available transfer vectors encode the *E.coli* origin of replication and an antibiotic resistance gene to enable the large scale production and selection of the recombinant transfer vector in *E.coli* using standard techniques. A large number of transfer vectors are commercially available to generate either non-fused or fused proteins, summarised by Ansari and Emery, 1999. The proteins can be fused with tags, which facilitate the purification of

the recombinant protein. The hexa-histidine tag enables the purification of the recombinant protein by immobilised metal chelate affinity chromatography, using nickel-agarose column chromatography. The proteins can also be fused to secretory signals, facilitating the easy purification of the recombinant protein away from the culture medium, especially when the insect cells are cultured in serum free medium.

The majority of promoters used to drive the expression of the recombinant protein in baculovirus systems are the very late promoters, usually p10 and polyhedrin (Wang et al., 1991), because the majority of protein synthesis shuts down by 48 hours post infection but the p10 and polyhedrin promoters are still active at these late times. This results in a relative increase in the levels recombinant protein compared to other cellular proteins. Another advantage of using the baculovirus as an expression system is the flexibility of the size of the nucleocapsid, allowing the baculovirus particles to accommodate large amounts of foreign DNA. By using multiple baculovirus promoters, two or more foreign genes can be inserted into the genome and express multiple proteins (Emery et al., 1987; Belyaev and Roy, 1993; Wang et al., 1991; Belyaev et al., 1995). This has great potential for the production of multi-subunit enzymes and complex vaccines and studying protein-protein interactions.

Following confirmation of the cloning of the gene of interest into the transfer vector by restriction digestion and DNA sequencing, the transfer vector is co-transfected with linearised baculovirus DNA into the insect cells. The most efficient method of co-transfection utilises cationic liposomes, which form complexes with the DNA and facilitate the interaction with the negatively charged cell membrane, whereby the complexes are taken up into the cell and transported to the cytoplasm where the recombination occurs. As with the transfer vectors, several linearised DNAs are available for co-transfection, in all of which the polyhedrin gene has been replaced by the Lac Z gene. The recombinant baculoviruses are derived by homologous recombination between the transfer vector and the appropriate baculovirus DNA, resulting in the insertion of the foreign gene into the baculovirus DNA. Selection of the recombinant viruses depend upon which linearised DNA was used, resulting in selection of either clear or blue plaques. Firstly, the bacterial 2-galactosidase gene can be replaced by the foreign gene upon recombination, thus the recombinant viruses appear as clear plaques upon staining with X-gal, non-recombinants appear as blue

(AcRP23.lacZ and AcUW1.lacZ). Secondly, the linearised DNA can contain a lethal deletion in the essential ORF 1629 of wild type AcMNPV. If this DNA is co-transfected with a polyhedrin locus based transfer vector, the lethal deletion is repaired by homologous recombination, so replication competent virus will only be generated by successful recombination (Baculogold™). Thirdly, the DNA containing the lethal mutation has been combined with the mutant 2-galactosidase gene, so recombination results in repair of the lethal deletion and the 2-galactosidase gene enabling selection of blue plaques (Bac-N-Blue™). Following recombination, the plaques are purified and analysed to ensure any illegitimate recombination events have not occurred.

## **AIMS OF THE THESIS**

The objectives of the work performed for this higher degree were:

1. To determine the HCMV load in various post mortem tissues of AIDS patients who died with HCMV disease following long term antiviral therapy.
2. To examine the prevalence of point mutations in the HCMV UL97 open reading frame associated with antiviral resistance.
3. To determine if a relationship exists between viral load and the presence or absence of mutations within the HCMV UL97.
4. To clone the HCMV UL97 open reading frame and overexpress the gene products in a suitable heterologous expression system.
5. To introduce various point mutations associated with GCV resistance into the UL97 open reading frame.
6. To investigate the effect of these mutations upon the function of the UL97 protein kinase.
7. To investigate the effect of these mutations upon the phosphorylation of GCV.
8. To determine the mode of action of the novel antiviral 1263W94 and the effect of the point mutations upon its activity.

**CHAPTER 2**  
**Materials and Methods**



## **2.1. Generation of a recombinant baculovirus**

### **2.1.1. Polymerase Chain Reaction of HCMV UL97**

#### Design of HCMV UL97 primers

The primers for the amplification of the HCMV UL97 gene by polymerase chain reaction (PCR), were designed to contain 2 different restriction endonuclease sites which do not cut within the UL97, and GC clamps at the 5' ends. This enabled the directional cloning of the UL97 PCR product, in the correct reading frame for protein expression, into the baculovirus transfer vector. The GC clamps on the 5' ends of the primers ensure minimal breathing of the primer during the annealing, so increasing the efficiency of the amplification. The primers were also designed to ensure the minimal number of bases were added to the 5' end of the UL97, so when the protein is expressed, the number of additional amino acids at the carboxy terminal of the UL97 gene product did not interfere with the function of the protein. The enzymes designed to cut the 5' and 3' ends of the UL97 were Kpn I and Hind III respectively, as highlighted in the primer sequences below.

Sense            5'-GGG GTA C↓CC ATG TCC TCC GCA CTT CGG TCT CGG-3'

Antisense       5'-CCC A↑AG CTT TTA CTC GGG GAA CAG TTG GCG GCA-3'

### **2.1.2. UL97 polymerase chain reaction**

The UL97 polymerase chain reaction (PCR) was initially performed using a non proof-reading enzyme to ensure the complete UL97 gene could be amplified. Total genomic DNA, extracted from the human embryo lung cells infected with the Towne strain of HCMV, was used as the template DNA for the PCR. The DNA template added varied in concentration from 100ng to 1µg for optimisation. The PCR reaction mix comprised of a 1x buffered solution containing 200µM of each dNTP, (dATP, dGTP, dCTP, dTTP, Promega, UK), 200ng of each primer, 10% v/v Q-solution and 2.5 units of Hot StarTaq (Qiagen) made up to a final volume of 100µl with sterile distilled water (SDW). The thermal cycling conditions comprised of an initial denaturation at 95<sup>0</sup>C for 15 minutes followed by 25 rounds of denaturation at 94<sup>0</sup>C for 1 minute, annealing at 55<sup>0</sup>C for 2 minutes and extension at 72<sup>0</sup>C for 3 minutes. A final extension was performed at 72<sup>0</sup>C for 10 minutes. The thermal cycling was performed using a Hybaid thermal cycler.

The resulting 2160bp PCR product was subsequently analysed on a 1% agarose gel (Gibco BRL) containing 10mg/ml ethidium bromide in 1X TBE buffer and visualised on a UV transilluminator. The size of the PCR product was determined using a 1kb DNA ladder (Promega, UK).

To ensure that no base changes occur during the thermal cycling reaction, a 3'-5' semi proof-reading enzyme was used for amplifying the UL97 gene for the cloning stages. The PCR reaction mix comprised of a 1X buffered solution containing 360µM of each dNTP, 200ng of each primer, 2mM MgCl<sub>2</sub> and 2 units of DyNAzyme EXT DNA polymerase (Flowgen) made up to 100µl with sterile distilled water (SDW). The thermal cycling conditions comprised of an initial denaturation at 94°C for 4 minutes followed by 25 cycles of denaturation at 94°C for 1 min, annealing at 55°C for 1 min and extension at 72°C for 4 mins. The resulting product was analysed as above.

### 2.1.3. Purification of the PCR product

Purification of the amplified UL97 was achieved using the Wizard™ PCR Preps DNA purification system (Promega). The desired DNA band was excised in approximately 300mg of a 1% TAE low melting temperature agarose gel containing 10mg/ml ethidium bromide using a sterile scalpel. The gel slice was melted in a 1.5ml eppendorf tube at 70°C and 1ml of the resin was mixed with the melted agarose then applied to a minicolumn. The resin/DNA was drawn into the minicolumn by vacuum and washed with 80% isopropanol, then the DNA was eluted in 50µl of SDW.

### 2.1.4. Cloning UL97 into pGEM-T Easy

Ligation reactions between the UL97 and the pGEM-T Easy Vector (Promega, UK) were performed using a 1:1 molar ratio of the gene-cleaned UL97 PCR product and the vector, which was determined using the following calculation:-

$$\frac{\text{ng of vector} \times \text{kb size of insert}}{\text{kb size of vector}} \times \text{insert:vector molar ratio} = \text{ng of insert}$$

The ligation reactions were performed using the following conditions:-

2xRapid Ligation Buffer, T4 DNA Ligase	5µl
pGEM-T Easy Vector (50ng)	1µl
UL97 PCR product (35.7ng)	1.3µl
T4 DNA Ligase (3 Weiss units/µl)	1µl
Deionised water to a final volume of	10µl

The ligation reactions were incubated overnight at 4<sup>0</sup>C

### 2.1.5. Transformations using the ligation reactions

Four grams of Luria-Bertani (LB, Sigma) broth base was autoclaved in 200 ml of distilled water into which ampicillin was added for a final concentration of 50µg/ml. LB agar plates were made by autoclaving 3% agar bacteriological (Sigma) with the LB broth plus the same concentration of ampicillin with IPTG (Sigma) and X-gal (Sigma) added for a final concentration of 0.5mM and 40µg/ml respectively.

Two microlitres of the ligation reactions were added to 50µl of just thawed JM109 high efficiency competent cells and the contents were mixed by gently flicking the tubes, which were then placed on ice for 30 minutes. The cells were heat shocked in a water bath at 42<sup>0</sup>C for 90 seconds and immediately returned to the ice for 2 mins. 950µl of LB broth was added and the tubes were incubated at 37<sup>0</sup>C in a shaking incubator for 1 hour. 100µl of each transformation culture was plated onto the amp, IPTG, X-gal plates and were incubated inverted overnight at 37<sup>0</sup>C. Individual white colonies were picked, inoculated into 5ml LB broth containing ampicillin and streaked onto an agar plate to ensure the purity of the picked colony, and incubated at 37<sup>0</sup>C overnight whereupon the plasmid was purified and analysed for the presence of the UL97 insert.

### 2.1.6. Plasmid purification and analysis

#### *Minipreparation of plasmid DNA*

A 5ml culture in LB broth containing Amp was generated from a single white colony from a purity plate and incubated for ~ 8 hours at 37<sup>0</sup>C with vigorous shaking. The bacterial cells were harvested by centrifugation at 10,000 x g for 1-2 mins in a microfuge and a small scale purification of the plasmid was performed using the Wizard<sup>TM</sup> Minipreps DNA purification system (Promega). The protocols are based on

a modified alkaline lysis procedure followed by binding of the DNA to the anion-exchange resin under the appropriate low salt and pH conditions. The bacterial cells were resuspended in the cell resuspension solution (50mM Tris-HCl, pH 7.5, 10mM EDTA) containing 100µg/ml RNase A. The cells were then gently lysed in the cell lysis solution (0.2M NaOH, 1% SDS). The lysate was neutralised by the addition of the neutralisation solution (1.32M potassium acetate, pH 4.8) and the insoluble complexes were removed by centrifugation at 10,000 x g for 5 mins. The cleared lysate was added to the barrel of the minicolumn assembly containing 1ml of the resuspended resin and a vacuum applied to pull the resin/lysate mix into the minicolumn. This was washed with 2ml of column wash (80mM potassium acetate, 8.3mM Tris-HCl, pH 7.5, 40µM EDTA and 55% ethanol) then dried under vacuum for 30 secs. The plasmid was then eluted into 50µl sterile water. The concentration of plasmid DNA was measured at 260nm using the spectrophotometer.

### *Maxipreparation of plasmid DNA*

One ml of a culture generated from a single white colony was used to inoculate 100ml LB broth and grown as before for 12-16 hours. The bacterial cells were harvested by centrifugation at 6000 x g for 15 mins at 4<sup>o</sup>C and the plasmid was purified using the Qiagen Plasmid Purification Protocol according to the manufacturers instructions. The protocols are based on a modified alkaline lysis procedure followed by binding of the DNA to the anion-exchange resin under the appropriate low salt and pH conditions. The bacterial cells were resuspended in buffer P1 (50mM Tris.HCl, pH 8.0; 10mM EDTA) containing 100µg RNase A, then gently lysed with buffer P2 (200mM NaOH, 1% SDS). The lysate was neutralised by the addition of acidic buffer P3 (3.0M potassium acetate, pH5.5) and was pushed through the QIAfilter cartridge to remove the insoluble complexes containing chromosomal DNA, salt, detergent and proteins which form during the neutralisation step. The lysate was incubated with an endotoxin removal buffer on ice for 30 mins. The cleared lysate was loaded onto a pre-equilibrated QIAGEN-tip by gravity flow for the plasmid DNA to binds to the QIAGEN resin. Contaminants such as degraded RNA, cellular proteins and metabolites are not retained in the resin. The tip was washed with a medium salt buffer QC (1.0 mM NaCl; 50 mM MOPS, pH 7.0; 15% isopropanol) to remove any remaining contaminants of the plasmid preparation such as RNA and protein. The plasmid DNA

was eluted from the resin with a high salt buffer QN (1.6M NaCl; 50mM MOPS, pH 7.0; 15% isopropanol), desalted and concentrated by isopropanol precipitation, then washed with 70% ethanol to remove residual salt and to replace the isopropanol with ethanol. The purified plasmid DNA was briefly air dried and resuspended in 100µl TE buffer (10mM Tris-HCl, pH 8.0; 1mM EDTA). The concentration of DNA was measured at 260nm using the spectrophotometer.

### 2.1.7. Restriction Endonuclease Digestion

Restriction endonuclease digestion was performed on plasmid DNA obtained from both the mini- and maxi-preps to ensure the presence of the UL97 gene. 500ng of the plasmid DNA was digested with 2 units of *EcoRI* for 1 hour at 37°C. The undigested and digested DNA was run on a 1% agarose gel containing ethidium bromide and visualised under UV light. Clones were selected for further use if the UL97 had been cleaved from of the plasmid following digestion. *EcoRI* was selected for the digestion because UL97 does not contain an *EcoRI* RE sites and there are 2 sites in the pGEM either side of the UL97, enabling a clean drop out of the UL97.

### 2.1.8. DNA Sequence analysis

Ten micrograms of plasmid DNA was added to 5µl of a denaturation solution (1M NaOH, 1mM EDTA) and incubated at room temperature for a minimum of 5 mins. During this incubation, a spin dialysis column was prepared in a 0.5 ml eppendorf tube. The tube was pierced with an 18-G syringe needle and the hole plugged with 20µl glass beads. Five hundred microlitres of a mixture of 2 parts Sepharose CL-6B (Sigma) and 1 part TE buffer (10mM Tris-HCL, pH 8.0, 0.1mM EDTA) was added to the glass beads. The 0.5ml eppendorf was placed inside a second 1.5 ml pierced eppendorf and both were placed inside a 15ml falcon tube and centrifuged at 1500rpm for 4 mins to compact the sepharose, following which the 1.5ml eppendorf was replaced with a second 1.5ml eppendorf and the denatured DNA added to the sepharose. The spin column was centrifuged as above and 8µl of the eluted DNA was annealed to an appropriate oligonucleotide primer by the addition of 5µg of the primer and 1µl of 10 X TM buffer (100mM-Tris HCl, pH 8.0, 100mM MgCl<sub>2</sub>). This was incubated at 37°C for 15 mins and slowly cooled to room temperature, whereupon a sequencing/labelling mix was added comprising of 1µl DTT (0.1M), 2µl of the dGTP labelling mix (prediluted to

1/5 in SDW), 0.5µl (5µCi) [ $\alpha$ -<sup>35</sup>S] dATP, and 2µl (3.25U) of a 1/8 dilution of T7 sequenase polymerase. This was incubated at room temp for 3 mins then placed on ice. Termination of the reactions was performed by adding 3.5µl of the sequencing/DNA mix to 2.5µl of each of the 4 termination dideoxynucleotides (ddGTP, ddATP, ddTTP, ddCTP) and incubating the mix at 37<sup>0</sup>C for 5 mins. The reaction was stopped by adding 4µl of stop solution. The samples were subsequently incubated at 94<sup>0</sup>C for 4 mins and analysed by denaturing polyacrylamide gel electrophoresis or were frozen at -20<sup>0</sup>C until needed.

### **2.1.9. Cloning of UL97 into the Baculovirus Transfer Vector pBlueBacHis2 C and pMelBac C**

The pBlueBacHis2 A, B and C are baculovirus transfer vectors which contain an N-terminal hexahistidine tag for expression and purification of recombinant fusion proteins. The pMelBac A, B and C are transfer vectors designed to direct the expression of the recombinant proteins through the secretory pathway to the extracellular medium by utilising the signal sequence for the highly expressed and efficiently secreted honeybee melittin. They are supplied in three different versions for cloning of the gene in-frame with the histidine tag and the melittin respectively. The pBlueBacHis2 C and pMelBac C were selected to ensure UL97 was cloned the correct reading frame following digestion of the vectors and the UL97 with Kpn I and Hind III.

Following the transformation, maxiprep and digestion of the transfer vectors with Kpn I and Hind III, ligation reactions were performed at a 1:1, 2:1 and 5:1 molar ratio between the UL97 and 100ng of the vectors using the formula described in section 2.1.4.

The ligation reactions were performed using the following conditions:-

	<b>1:1</b>	<b>2:1</b>	<b>5:1</b>
pMelBac C or pBlueBacHis C	100ng	100ng	100ng
UL97	43.5ng	86.9ng	217.4ng
T4 DNA ligase	2µl	2µl	2µl
10X ligation buffer	1µl	1µl	1µl
Deionised water to a final volume of	10µl	10µl	10µl

The ligation reactions were incubated overnight at 16<sup>0</sup>C and transformed into JM109 cells as described in section 2.1.5. Single white colonies were picked and a maxiprep was performed as described in section 2.1.6. One hundred nanograms of the harvested plasmid

DNA was digested with the restriction endonucleases *XhoI* and *Sall* to drop out the UL97. The UL97 does not contain RE sites for either of these two enzymes, so ensuring the ligation of UL97 into the transfer vectors.

### **2.1.10. Co-transfection of the recombinant transfer vectors with the Baculovirus DNA**

The Baculovirus transfer vectors were co-transfected with Bac-N-Blu linearized AcMNPV DNA (Invitrogen) by the technique of cationic liposome mediated transfection whereby the linearized DNA and the transfer vectors are mixed with the InsectinPlus<sup>TM</sup> liposomes in serum free medium. For each co-transfection a 35mm culture dish was seeded with 2X10<sup>6</sup> Sf21 cells in complete TC100 medium and incubated at room temperature for 1hr by which time the cells were fully attached to the bottom of the culture dish. The transfection mixture was prepared using 4µg of recombinant transfer plasmid, 0.5µg of Bac-N-Blu DNA and 20µl of InsectinPlus<sup>TM</sup> liposomes in 1ml of serum free TC100 medium. The mixture was vortexed vigorously for 10 seconds and incubated at room temperature for 15 mins. During this incubation, the medium of the Sf21 cells was removed and the cell sheet was washed twice with 2ml of TC100 without FCS following which the transfection mixture was added to the cells dropwise. The cells were incubated at room temperature for 4 hours with gentle rocking to ensure an even distribution of the transfection mixture over all the cells. Following this incubation period, 2ml of complete TC100 was added to the cells and the dishes were placed in a humidified chamber and incubated at 28<sup>0</sup>C for 72hr or until a cytopathic effect was observed. At this time the transfection supernatant was harvested and used to identify and plaque purify recombinant virus by plaque assay.

### **2.1.11. Plaque Assay**

SF21 cells were seeded at a density of 1.5x10<sup>6</sup> cells in 35mm tissue culture dishes and incubated at room temperature for 1 hour for the cells to attach to the dishes. Serial log dilutions of the virus to be titred were prepared in TC100 medium and infection was

performed in duplicate for each dilution. Following the hour incubation, the cells were infected by the dropwise application of 100µl of the virus dilutions to their respectively labelled cell monolayers. The monolayers were incubated at RT for 1 hour with gentle agitation every 15 mins to ensure all the cells were in continuous contact with the inoculum and to prevent the cells from drying. Mock infections were performed where the virus inoculum was substituted for TC100. The agarose overlay containing 3g of type VII agarose (Sigma) in 100ml SDW was autoclaved for 15 mins and placed in a waterbath at 55<sup>0</sup>C to ensure the agarose was at 55<sup>0</sup>C immediately prior to use. Following the 1hr incubation, the virus inoculum was removed from the cells and was replaced by 2ml of a 1:2 dilution of the agarose solution with room temperature complete TC100 media. The agarose was allowed to set and 1ml of complete TC100 media was added to each dish. The plaque assays were incubated at 28<sup>0</sup>C for 3-4 days or until a fully confluent monolayer was formed in the mock infections.

The plaques were visualised by the addition of 1ml of fresh medium containing 15µl of a 2% X-gal solution to each dish followed by a 4hr incubation at 28<sup>0</sup>C. 1ml of a 0.025% solution of neutral red was then added to the dishes and incubated for 2hrs following which the stains were removed and the dishes inverted and incubated overnight at 28<sup>0</sup>C. The final incubation was performed in the dark for the blue stain to fully develop and the neutral red to fully destain. All the plaques which stained blue were counted and the virus titre was determined as plaque forming units per ml (PFU/ml).

### **2.1.12. Plaque purification**

Serial log dilutions were made of the cotransfection supernatant from section 2.1.20 between 10<sup>-1</sup> – 10<sup>-4</sup> and were subjected to a plaque assay. The recombinant baculovirus was identified by the blue staining and an agarose plug was removed using a sterile pasteur pipette into 0.5 ml of complete TC100 media. The eppendorf was vigorously vortexed to release the virus particles which were immediately used for a further plaque purification. The resulting plaque purified virus was subsequently analysed by PCR to ensure the presence of the desired gene and stored at 4<sup>0</sup>C.



### **2.1.13. PCR analysis of plaque purified recombinant baculovirus**

The plaque purified virus stocks (P0) were used to infect 35mm tissue culture dishes which were seeded at a density of  $1.5 \times 10^6$  SF21 cells. Following the 1hr incubation at room temperature, the inoculum was removed and replaced with 2ml complete TC100 medium and incubated for 3 days. The cells were harvested into the culture media and pelleted by centrifugation for 10 mins at 1500rpm. The cells were washed twice with sterile PBS and the DNA was extracted from the cells using the Promega Wizard tissue extraction kit. The OD of the extracted DNA was measured at 260nm and 1 $\mu$ g total cellular DNA was used in a PCR reaction comprising of a 1 x buffered solution of 200 $\mu$ M each dNTP, 200ng each primer, 10% v/v Q-solution and 2.5U HotStarTaq (Qiagen) made up to a final volume of 100 $\mu$ l with sterile distilled water. The primers used were as follows:-

F 5' – TTT ACT GTT TTC GTA ACA GTT TTG – 3' (Bac-1)

R 5' – CAA CAA CGC ACA GAA TCT AGC – 3' (Bac-2)

A PCR reaction using the original UL97 cloning primers was also performed using the same conditions as the universal baculovirus primers, with the same thermal cycling conditions as originally used.

### **2.1.14. Generation of a high titre baculovirus stock**

The plaque purified and PCR verified recombinant baculovirus stocks were used to generate high titre stocks to be used for the protein expression studies. A 35mm tissue culture dish was seeded with SF21 cells at a density of  $1.5 \times 10^6$  and infected with 100 $\mu$ l of the P0 stock. Following the 1hr incubation, the virus inoculum was removed and replaced with 2ml of complete TC100 media and incubated for 5 days. The media was harvested and the cellular debris was removed by centrifugation. This was termed the P1 stock. 1ml of the P1 stock was used to infect a 25cm<sup>2</sup> tissue culture flask seeded with SF21 cells at a density of  $2.5 \times 10^6$ . The inoculum was removed following the 1hr incubation and replaced by 5ml complete TC100 medium and cultured for approximately 5 days. The media was harvested and centrifuged to remove the cellular debris then titrated by plaque assay. This P2 stock was used to infect SF21 cells seeded in a 75cm<sup>2</sup> tissue culture flask at a density of  $5 \times 10^6$  cells at an MOI of 0.1. The

virus innoculum was replaced by 10ml complete TC100 media. The culture medium was harvested as described above and titrated by plaque assay. This P3 stock was subsequently used for protein expression studies.

## **2.2. CELL CULTURE**

### **2.2.1. Freezing cultured cells**

The Sf21 and Sf9 cells were snap frozen in liquid nitrogen in complete TC100 or Sf900II containing 10% DMSO respectively, at a cell density of  $1-2 \times 10^7$ /ml/vial. The vials were stored in liquid nitrogen until use.

### **2.2.2. Initiating culture from frozen cells**

The vials of Sf21 cells were removed from liquid nitrogen and placed in a water bath at  $37^{\circ}\text{C}$  with gentle agitation to rapidly thaw the cells. The vial was decontaminated by treating with 70% ethanol and placed on ice. Ten millilitres of complete TC100 medium (10% FCS; Penicillin & streptomycin) was placed in a  $75\text{cm}^2$  tissue culture flask and the 1ml cell suspension was added directly to the medium. The flask was incubated at  $28^{\circ}\text{C}$  for 1 hour to allow the cells to attach, following which the medium was gently removed and replaced with 10ml fresh complete TC100 medium to remove the DMSO and the cellular debris/unhealthy cells which do not adhere. The medium was changed again after 24 hours by which time the cells should have reached 70% confluency. The vials of SF9 cells were removed from liquid nitrogen and thawed the same as the Sf21 cells. The cells were raised directly into a 20ml shake giving a cell density of  $0.5-1.0 \times 10^6$  assuming a viability of 50%. The cells were also raised into a 20ml mixture of 50/50 new and conditioned medium. The conditioned medium was medium that previous cells were growing in which was harvested at the time of passage, then filter sterilised.

### **2.2.3. Maintenance of adherent cells and suspension cultures**

The cells were passaged every 3 days or at confluency by gently scraping the cells from the bottom of the flask using a cell scraper (Sigma) and resuspending the cells in 10ml of fresh complete TC100. Log phase growth was maintained by splitting the cells 1:3 and a record kept of the passage number. Suspension cultures were passaged every 5 days by harvesting the cells into a 50ml falcon tube, centrifugation at 1500rpm for 10

minutes and the supernatant discarded. The cells were resuspended in 50ml fresh Sf900 serum free medium (sfm) and split at 1:5 into 40ml SF900 sfm in a sterile 250ml Erlenmeyer flask. The suspensions were maintained at 28°C in a shaking incubator rotating at 90rpm.

### 2.3. MOLECULAR BIOLOGY TECHNIQUES

#### 2.3.1. Site Directed Mutagenesis

Site directed mutagenesis was performed on the UL97-pMelBac transfer vector using the GeneEditor™ *in vitro* Site Directed Mutagenesis System (Promega). The GeneEditor is a high-efficiency system for the generation and selection of oligonucleotide-directed mutations. Selection oligonucleotides provide encoded mutations that alter the ampicillin resistance gene, creating a new additional resistance to the GeneEditor™ antibiotic selection mix and facilitating the selection of the desired mutation generated by the mutagenic oligonucleotide.

An initial alkaline denaturation was performed on 2µg of UL97-pMelBac DNA in 5µl of a 2M NaOH, 1mM EDTA solution. The denatured DNA was added to a column containing 20µl of glass beads (Sigma) and 500µl of Sepharose CL6B (Sigma) equilibrated in TE buffer, pH8.0 in a 2:1 ratio. The column was spun at 1400rpm for 5 mins to elute the purified DNA. Two microlitres of the denatured DNA was analysed on a 1% agarose gel to verify the denaturation and ensure no significant losses occurred.

One hundred nanograms of the template denatured DNA was added to an annealing solution containing 0.25pmol of the appropriate phosphorylated selection oligonucleotide (top strand); 1.25pmol of the phosphorylated mutagenic oligonucleotide and 10XTM buffer (100mM Tris/100mM MgCl<sub>2</sub>) made up to a final volume of 20µl in SDW. The annealing reactions were performed at 37°C in a thermal cycler for 15 mins then chilled slowly to room temp and placed on ice. Mutant strand synthesis and ligation were performed by the serial addition of 5µl SDW; 3µl synthesis 10X buffer (100mM Tris-HCl, pH7.5, 5mM dNTP's, 10mM ATP and 20mM DTT); 1µl T4 DNA polymerase (5-10 units) and 1µl T4 DNA ligase (1-3 units). The reaction

was incubated at 37<sup>0</sup>C for 90mins for the mutant strand synthesis and ligations to occur.

The mutagenic primers used for the site directed mutagenesis were designed to generate point mutations in the functionally important putative catalytic domains of the UL97 protein kinase. The primers used and the catalytic domains in which the point mutations occur are listed in table 2.1.

Following the mutant strand synthesis and the ligation reactions, 1.5µl of each mutagenesis reaction or control reaction (~10ng of template DNA) was transformed into 100µl BMH 71-18 *mutS* (a repair minus (*mutS*) strain of E.coli) competent cells as described in section X. A 900µl culture of LB without antibiotics was incubated for 60 mins at 37<sup>0</sup>C with shaking (~225rpm), then made up to a 5ml culture in LB containing 100µl Antibiotic Selection Mix and incubated for 18 hours in a shaking 37<sup>0</sup>C incubator. The plasmid was harvested as described in section 2.1.6. A second transformation into E.coli JM109 cells was performed to ensure the proper segregation of the mutant and wild type plasmids, so resulting in a high proportion of mutants. A 900µl culture in SOC medium (without antibiotics) containing the transformants was incubated at 37<sup>0</sup>C for 60 mins following which 100µl of the culture was plated onto 2 LB plates containing 125µg/ml ampicillin; 100µl of the Antibiotic Selection Mix; 0.5mM IPTG and 80µg/ml X-Gal. The plates were incubated overnight at 37<sup>0</sup>C. Single white colonies were picked and used to generate 5ml overnight cultures and purity plates for each mutant. The plasmid DNA was harvested and analysed for the presence of the desired mutation.

### **2.3.2. Quantitative competitive polymerase chain reaction**

The DNA from each patient sample has three single round PCR reactions performed upon it, which are co-amplified with a specific copy number of control plasmid. The control plasmid (pUC18) contains the region of gB (UL55) amplified by the gB-specific primers as below (Darlington et al., 1991, Fox et al., 1992).

gB1 5' G A G G A C A A C G A A A T C C T G T T G G G C A

gB2 5' G T C G A C G G T G G A G A T A C T G C T G A G G

**Table 2.1. Primer sequences for the GeneEditor™ *in vitro* Site Directed Mutagenesis System.**

Primer sequence (5'-3')		Mutation	Catalytic domain
CGC GTG GTC <b>GAG</b> GTG GCG CG	(A)	K355Q	II
CGC GGT CTG <b>CGC</b> ACG GCC AC	(T)	L397R	V
TGC CAC TTT <b>GCC</b> ATT ACA CCC	(A)	D456A	VI
C ATT ACA CCC ATT <b>AAC</b> GTG C	(G)	M460I	VI
ACA CCC ATG AAA <b>GTG</b> CTC ATC	(C)	N461G	VI
GAA TGT TAC CAG <b>CCT</b> GCT TTC C	(C)	H520Q	VIII
C TGC CGC <b>ACG</b> TTG GAG AAC GG	(G)	A594T	X
C TGC CGC GCG TTT <b>GAG</b> AAC GG	(G)	L595F	X
ACC ATG CTG CTC GAA TAC GTC	(A)	H662L	XI
CAC GAA TAC ATC AGA AAG AAC G	(G)	V665I	XI

Site directed mutagenesis was performed upon the UL97 cloned into the baculovirus transfer vector pMelBac. The mutagenic primers used are given in table 2.1 together with the codon, the resulting amino acid change and the catalytic domain in which the codons reside within the protein kinase. The mutagenic base change is highlighted in **bold** and the wild type base is highlighted in (*italics*) after the primer sequence.

The control sequence gB has been engineered to contain a restriction site for *Hpa* I for the distinction between the amplified wild type and control sequence DNA, while being amplified with the same kinetics as the wild type DNA. The PCR reaction mix comprised of a 1 x buffered solution containing 2mM MgCl<sub>2</sub>, 200µM dNTP's, 100ng of each primer (gB1 and gB2) and 5 units of Amplitaq gold made up to 93µl with SDW. One microgram of DNA extracted from patient tissue was added to each reaction with 2µl of a specified copy number of control sequence DNA. The thermal cycling conditions comprised of an initial denaturation for 12 minutes at 95°C followed by 39 rounds of a denaturation at 94°C, annealing at 60°C and elongation at 72°C each for 30 seconds and a final elongation at 72°C for 10 minutes. Ten microlitres of the PCR amplicons were digested by 3 units of *Hpa* 1 in a 1x buffered solution at 37°C for 2 hours. The digested amplicons were separated by 12% acrylamide gel electrophoresis at 40 mA until 15 minutes after the loading dye has run off the bottom of the gel. The DNA was stained with ethidium bromide (1.5µl of a 10 mg/ml stock in 100ml of TBE), examined and photographed by UV transillumination. The photographs were analysed by using the NIH image software (available by anonymous FTP from [zippy.nimh.nih.gov](http://zippy.nimh.nih.gov)[128.231.98.32]), which allows the densitometric analysis of electronically scanned images of ethidium bromide stained gels. The viral load was determined by applying the following equation:-

$$(\% \text{ wild type area} / \% \text{ control area}) \times \text{control plasmid copy number}$$

This gives viral load per µg total DNA.

### **2.3.3. UL97 polymerase chain reaction**

A nested UL97 PCR was performed on 1µg of all the HCMV positive (gB PCR) tissue DNA. Each PCR reaction comprised of a 1 X buffered solution containing 100ng of each primer (outer below), 2mM MgCl<sub>2</sub>, 200µM each dNTP and 1 unit of Amplitaq gold polymerase (Perkin Elmer, UK) for both rounds of amplification.

UL97 A 5' C A A C G T C A C G G T A C A T C G A C G T T T

UL97 B 5' G C C A T G C T C G C C C A G G A G A C A G G

The thermal cycling conditions comprised of an initial denaturation at 95°C for 12 minutes followed by 29 cycles of denaturation at 94°C for 1 minute, annealing at 60°C for 1 minute and extension at 72°C for 2 minutes, followed by a final extension at 72°C for 10 minutes. One microlitre of the outer PCR amplicon was used as the template in a nested PCR using the following primer set:-

UL97 C 5' C A T C G A C A G C T A C C G A C G T G C

UL97 D 5' G T A G C T C A T T T G C G C C G C C A G

Two nested PCR reactions were performed for each DNA sample, such that either one of the nested primers was 5' biotinylated to enable one DNA strand to adhere to the wells of a streptavidin coated microtitre plate. Each nested PCR reaction contained 100ng of each primer including 50ng of biotinylated primer C or D. The denaturation, annealing and extension times were reduced to 45 seconds each. The resulting 568bp amplicon was detected by 1.5% agarose gel electrophoresis.

#### **2.3.4. Microtitre point mutation assay**

Ten microlitres of each DNA amplicon was added to four wells (G, A, T, C) of the microtitre plate containing 1x TTA buffer (100mM Tris HCl, pH 7.8, 0.5% Tween 20, 1.0% Na azide) and incubated at 37°C for 1 hour to allow the binding of the biotin labelled DNA to the streptavidin coated wells. The wells were washed three times with 1x TTA buffer by a vacuum aspirator and 0.15M NaOH was added to each well at room temperature for 5 minutes to denature the DNA. The plate was washed 4 times with 1x TTA and 25µl of an anneal mix ([PMA diluent:- 40mM Tris HCl, pH 7.8, 20mM MgCl<sub>2</sub>, 50mM NaCl], 25µl of 66µg/ml probe 1 – 6, [figure 2.1]) was added to each well, the plates sealed and incubated at 37°C for 30 minutes to allow the probe to anneal to the bound denatured DNA. The probes terminate one base prior to the point mutation to be detected. Labelling mix (2.5 units klenow polymerase, 0.1M DTT, 24µl of 1/10 dilution of either [<sup>35</sup>S] dGTP, dATP, dTTP or dCTP [ NEN Dupont 1000-1500 Ci/mmol]) was added to each well and incubated at room temperature for 3 minutes. The klenow polymerase adds one [<sup>35</sup>S]-labelled base, mutant or wild type, to the 3' end of each probe. Following this incubation, the radiolabelled probe was denatured with





0.15M NaOH and the labelled probe transferred to a liquid scintillation cocktail (Sigmafluor™). The radioactivity was detected as counts per minutes in an LKB Rackbeta liquid scintillation counter. Figure 2.3 illustrates the oligonucleotide probes used in the point mutation assay.

## **2.4. PROTEIN DETECTION AND PURIFICATION METHODS**

### **2.4.1. Preparation of a Crude Cell Lysate**

Six million cells were harvested following infection and 72 hours incubation by removing the cells from the monolayer into suspension and centrifuging at 1500rpm for 10 mins. The pelleted cells were washed three times in Dulbecco's PBS and resuspended in 500µl of ice cold sonication buffer (50mM Tris-HCl, pH7.6, 100mM NaCl, 0.1% Nonidet P-40, 10% glycerol, 10µg/ml Aprotinin and Leupeptin and 1mM Pefabloc). The cells were sonicated three times for 10 secs at 5 microns with 30 secs incubation on ice between each sonication. The disrupted cells were centrifuged for 10 mins at 4°C at 12000rpm, the supernatant removed and the pellet discarded.

### **2.4.2. Ammonium Sulphate Precipitation**

A 50ml aliquot of the sonicated crude cell lysate was prechilled to 4°C and ammonium sulphate, calculated to give a 10%-60% saturation for optimisation purposes, was slowly added with stirring. The calculation used to determine the number of grams of ammonium sulphate to add to 1 litre at 4°C to give the desired percentage saturation was as follows:-

$$g = \frac{533 (S_2 - S_1)}{100 - 0.3 S_2}$$

S<sub>1</sub> was the starting concentration and S<sub>2</sub> was the final concentration. The equation allows for the increase in total volume following the addition of the ammonium sulphate. The solution was equilibrated for 1hr at 4°C following each cut and centrifuged at 3000g for 40mins. The supernatant was removed following the first precipitation and ammonium sulphate added to give the next concentration. The protein pellet was kept on ice until the final concentration was reached when the supernatant was discarded and the pellets resuspended in 5ml of 20mM Tris-HCl, pH 8.5. The protein solutions were dialysed in 20mM Tris-HCl, pH 8.5 for 48 hours at 4°C to give a total of a 1/10 000 dilution of the ammonium sulphate. The protein

concentration was determined using the Lowry method and the protein was analysed for the presence of UL97 by SDS PAGE and Western blot. The maximum % saturation which did not precipitate the UL97 and the minimum % saturation which precipitated all of the UL97 was chosen for the ammonium sulphate cut.

### **2.4.3. Ion Exchange Chromatography**

Optimisation of the binding pH and salt concentration for binding and elution was initially performed. The UL97 was dialysed into a series of buffers over a range of pH's from 5.0 to 9.0.

		Optimal buffering capacity
1.	20mM piperazine	5.0 – 6.0
2.		
3.		
4.	20mM bis-Tris propane	6.4 – 7.3
5.		
6.	20mM Tris HCl	7.6 – 8.5
7.		
8.		
9.	20mM ethanolamine	9.0 – 9.5

Two millilitres of a 50% slurry of DEAE cellulose was centrifuged for 1 minute at 5000 x g, the supernatant removed and the DEAE was equilibrated by four washes in 5 ml of each of the buffers. The supernatant was removed following the final wash and the DEAE was resuspended to give a 1:1 slurry. Five hundred micrograms of protein was added to the equilibrated DEAE and incubated at 4°C on a rotary platform to allow the UL97 to bind the DEAE. The DEAE was allowed to settle and the supernatant assayed for protein to determine the binding efficiency by dividing the amount of protein present ( $A_{280}$ ) before binding by the amount present following binding. The DEAE-protein was washed four times in each respective buffer containing 50mM NaCl and the protein was eluted in each respective buffer containing 1M NaCl.

Following optimisation of the buffer and pH for binding, the same series of experiments was performed using the optimal buffer over a range of NaCl

concentrations from 0.05M in 0.5M increments to 0.5M. This identified the maximum NaCl concentration at which UL97 bound to the DEAE with minimal binding of contaminating proteins and the minimum NaCl concentration at which the UL97 was eluted.

### **2.4.4. Immunoaffinity chromatography**

The UL97 monoclonal antibody was dialysed against 0.1M NaHCO<sub>3</sub>/0.5M NaCl at 4°C with 3 buffer changes over a period of 24 hours. The antibody was centrifuged for 1 hour at 100 000 x g at 4°C to remove aggregates and the concentration of the antibody was determined (mg/ml Ab = A<sub>280</sub>/1.44). The antibody was diluted to 5 mg/ml in 0.1M NaHCO<sub>3</sub>, pH 8.3, 0.5M NaCl. The UL97 monoclonal antibody was immobilised onto cyanogen bromide (CNBr) activated Sepharose 4B (Pharmacia). The dried Sepharose was rehydrated in ice cold 1mM HCl (150 ml / g Sepharose) for 15 minutes then filtered in a Buchner flask and washed with 2 gel volumes of ice cold HCl. The rehydrated gel was removed from the flask and added to the UL97 mAb in coupling buffer (0.1M NaHCO<sub>3</sub>, pH 8.3, 0.5M NaCl). The antibody and gel were mixed on a rotary platform at 4°C overnight to allow the coupling of the antibody to the gel. Following coupling, the antibody-gel was filtered and the coupling efficiency determined by dividing the amount of protein present (A<sub>280</sub>) before coupling by the amount present following coupling. The gel was washed twice in 5 gel volumes of coupling buffer, added to blocking buffer (0.05M glycine, pH 8.0) to saturate the remaining reactive groups on the Sepharose and allowed to settle for 2 hours. The gel was then resuspended in blocking buffer to give a 1:1 slurry and stored at 4°C.

One hundred microlitres of a 50% slurry of immobilised UL97 monoclonal antibody was added to protein extracts from BVMB-UL97 infected Sf21 cells and allowed to bind at 4°C for a minimum of 1 hour. The sepharose beads were then pelleted by centrifugation for 20 s at 13000 x g, washed in sonication buffer, pH 9.0. Following the washes, the sepharose beads were pelleted and the antibody-antigen complex was dissociated upon addition of the dissociation buffer (50mM glycine, pH 2.5, 0.15M NaCl). The mixture was immediately pulsed to remove the sepharose beads and the eluate was removed and neutralised in 0.2 volumes of Tris HCl, pH 9.0.

#### **2.4.5. Sodium dodecyl sulphate polyacrylamide gel electrophoresis (SDS-PAGE)**

The proteins obtained from the crude cellular lysate were separated by sodium dodecyl sulphate polyacrylamide gel electrophoresis. Six millilitres of an 8% resolving gel was poured between two vertical sealed glass plates (atto minigel) and overlaid with 20 $\mu$ l of water saturated butanol (50:50 v/v) and allowed to set. The butanol was removed by washing with distilled water and a 5% stacking gel was poured over the resolving gel. The components of the gels are given in table 2.2. Equal volumes of the protein samples and 2X sample buffer (125mM Tris-HCl, pH 6.8, 4% SDS, 10% glycerol, 0.02% Bromophenol blue, 200mM DTT) were boiled for 5 mins and 20 $\mu$ l of each sample were electrophoresed in Tris-glycine buffer (250mM Tris-HCl, 192mM glycine, 0.1% SDS).

#### **2.4.6. Coomassie brilliant blue staining**

The SDS-PAGE gels were stained with Coomassie brilliant blue stain (40% methanol, 10% acetic acid, 50% sdw, 0.25% Coomassie brilliant blue R250 (Sigma), v/v/v/w) by soaking the gel in the stain for 1-2 hours. The gel was then destained in 40% methanol, 10% acetic acid, 50% sdw (v/v/v) until the protein bands were visible (approximately 2 hours).

#### **2.4.7. Western blotting**

The SDS-PAGE gels were prepared for Western blotting by sandwiching the gel between layers of thin and thick filter paper soaked in transfer buffer (48mM Tris-HCl, 0.0375% (w/v) SDS, pH 9.6) with methanol-soaked polyvinylidene difluoride membrane (PVDF, Sigma) arranged as illustrated in fig 2.2. The proteins were electrophoretically transferred at 2.5 mA/cm<sup>2</sup> of gel for 1 hour using a semi-dry blotter (Pharmacia Biotech). Following transfer the membrane was incubated for 1 hour at room temp in blocking buffer [3% bovine serum albumin (Sigma) in TBS buffer (10mM Tris-HCl, pH7.5, 150mM NaCl)] followed by washing with 0.05% Tween 20, 0.1% Triton X-100 in TBS buffer. The membrane was then incubated at room temperature for 1 hour with a 1/500 dilution of a mouse anti-UL97 monoclonal antibody. The membrane was washed as before and incubated again at room temperature for 1 hour with an alkaline phosphatase-conjugated goat anti-mouse antibody diluted to 1/6000 with blocking buffer. The membrane was further washed

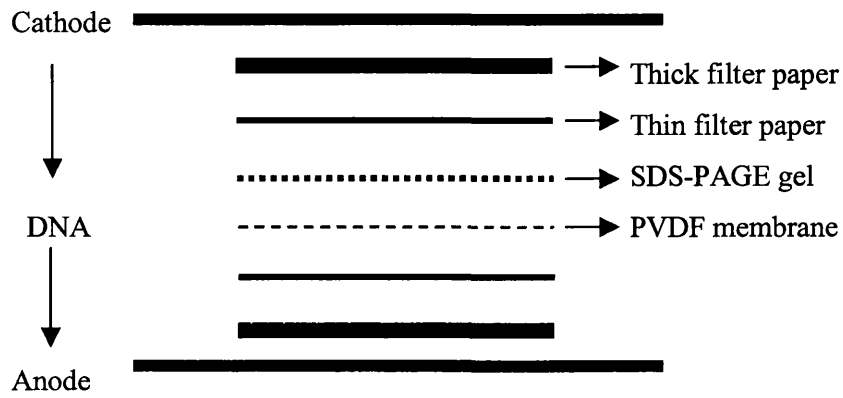


**Figure 2.2. Illustration of the Western blot set up**

Illustration of the arrangement of the SDS-PAGE gel with respect to the PVDF membrane for the electrophoretic transfer of proteins from the SDS-PAGE gel to the PVDF membrane for Western blot.

**Table 2.2** Solutions for preparing resolving and stacking gels for Tris-glycine SDS-PAGE

Component	Resolving gel (15ml)		Stacking gel (5ml)
	Volume (ml) 8% gel	Volume (ml) 12% gel	Volume (ml) 5% gel
SDW	6.9	4.9	6.3
30% acrylamide	4.0	6.0	1
1.5M Tris pH8.8	3.8	3.8	
1.0M Tris pH 6.8			2.5
10% SDS	0.15	0.15	0.1
10% APS	0.15	0.15	0.1
TEMED	0.009	0.006	0.02

with TBS/Tween/Triton and TBS buffer and the immunoreactive bands were visualised by incubation of the membrane with one tablet of 5-bromo-4-chloro-3-indolyl phosphate/nitro blue tetrazolium chloride (Sigma) dissolved in 10 ml distilled water.

## **2.5. Enzyme analysis**

### **2.5.1. Protein Kinase Assays**

Three microlitres of the protein samples (either crude cell lysate or purified) were added to 10 $\mu$ l of 2X kinase buffer (100mM Tris HCl, pH 9.0, 20mM MgCl<sub>2</sub>, 10 $\mu$ M ATP, 4mM DTT, 2M NaCl and 10 $\mu$ Ci of [ $\gamma$ <sup>32</sup>P] ATP at >5000 Ci/mmol, [Amersham]), and made up to 20 $\mu$ l with SDW to give a 1X concentration of the kinase buffer. The reactions were incubated for 30 mins at 37°C and terminated with the addition of 2X SDS sample buffer followed by boiling for 3 mins. The reactions were subjected to SDS-PAGE (8%), the gels equilibrated in a gel drying solution (30% methanol, 5% glycerol) on an orbital shaker for 30 minutes and dried under vacuum in a Biorad gel drier for 1 hour at 80°C and exposed to hyperfilm. The amount of radiolabelled protein was quantitated using the Biorad Multianalyst.

### **2.5.2. GCV Kinase Assay (*in vitro*)**

The recombinant baculovirus expressed UL97 was purified by immuno affinity chromatography and incubated in a GCV kinase assay buffer with radiolabelled GCV ([<sup>3</sup>H] GCV, Moravek) as the substrate. A time course of GCV phosphorylation was performed from 0 – 1 hour at 10 minute intervals then every hour up to 4 hours at 37°C. At each time point, 50 $\mu$ l aliquots were removed and spotted onto 20mm diameter DE81 chromatographic paper discs. These are discs coated in DEAE which selectively binds negatively charged molecules such as the monophosphorylated GCV. The discs were then washed twice in 3 ml of 10mM ammonium acetate for 10 minutes, followed by two washes in 95% ethanol for 10 minutes each. The discs were allowed to dry and placed in a scintillation vial with 5 ml of scintillant (Sigmafluor<sup>TM</sup>). The radioactivity was measured in counts per minute using a rackbeta liquid scintillation counter. The kinase assay buffer comprised of 50mM HEPES (pH 7.5), 5 $\mu$ M ATP, 5 $\mu$ M MgCl<sub>2</sub>, 7mM NaF, 10mM DTT, 2 $\mu$ l [<sup>3</sup>H] GCV and made up to 75 $\mu$ l with SDW.

**2.5.3. GCV kinase assay (*in vitro* / *in vivo*)**

Sf21 cells were infected with BVMB-UL97 wild type and mutant viruses at an MOI 10 and incubated at 28°C. After 48 hours post infection the TC100 tissue culture medium was removed and replaced with fresh TC100 supplemented with 1.0mM GCV and 5µCi [<sup>3</sup>H] GCV at 100mCi/mmol. After 72 hours post infection, the cells were harvested, washed three times in PBS and the nucleotides extracted by acid hydrolysis of the cells with 0.5M perchloric acid. This was neutralised with 2.5M KOH, 1.5M KH<sub>2</sub>PO<sub>4</sub> to pH 6.8 and centrifuged at 13000 x g for 5 minutes to remove cell debris and precipitated proteins. The supernatant was spotted onto DE81 chromatographic paper discs and the detection step performed as in section 2.5.2.

**2.5.4. Plaque Reduction Assay**

To determine the sensitivity to GCV of the WT UL97-recombinant baculovirus (AcMNVP) and the level of GCV resistance conferred by each of the UL97 mutations, a plaque reduction assay was performed. SF21 cells were seeded in a 35mm<sup>2</sup> dish at a density of 1.5 x 10<sup>6</sup> and infected at an MOI of 0.3 for 1 hour. Following the infection, the inoculum was removed and replaced with 2ml of TC100 supplemented with 0.0, 0.2, 0.4, 0.6, 1.0 and 1.4mM GCV. The cells were incubated for 72 hours at 28°C, the culture media was harvested and subjected to plaque assay at 10<sup>-4</sup>, 10<sup>-5</sup> and 10<sup>-6</sup> dilutions. As a set of controls, uninfected cells were incubated with the supplemented TC100 to ensure GCV was not toxic to the cells, and a baculovirus containing the lac Z gene alone was subjected to the same analysis to ensure it was not sensitive to the GCV. The number of plaques were determined and plotted as % reduction in plaques from the total at a GCV concentration of 0.0mM.



**CHAPTER 3**  
**Tissue Distribution of Drug Resistant UL97 Mutants**  
**of HCMV**

### **3.1. Introduction**

Since the initial isolation of ganciclovir resistant HCMV strains from immunocompromised patients receiving long term ganciclovir therapy, an increasing number of studies have demonstrated the development of systemic phenotypic resistant virus (Erice et al., 1989, Stanat et al., 1991, Lurain et al., 1992). The clinical significance of these resistant viruses is now well documented in AIDS patients (Boivin et al., 1996, Chou et al., 1997, Erice et al., 1997, Liu et al., 1998, Bowen et al., 1997, 1999). Before the advent of highly active antiretroviral therapy, HCMV retinitis was the major disease manifestation, with up to 40% of patients developing this disease. Despite the availability of both licensed and investigational antivirals, maintenance therapy was continued indefinitely and HCMV retinitis (disease) progression invariably occurred, regardless of the initial choice of drug regimen. Disease progression may be due to a number of factors, predominantly the emergence of antiviral drug resistance, but including poor patient compliance, progressive loss of the host immune function and poor ocular bioavailability of drug. The UL97 and UL54 genes have been examined in the blood and vitreous fluid of these patients for point mutations shown by marker transfer experiments to confer ganciclovir resistance. The most common point mutations in the UL97 gene occur at codons 460, 520, 594 and 595, although mutations at codon 592 are increasing in frequency (Chou et al., 1995, Lurain et al., 1994, Wolf et al., 1995, Baldanti et al., 1996, Boivin et al., 1996).

The presence of point mutations in the UL97 gene can be detected rapidly by utilising a method initially designed for mapping AZT resistance mutations in the reverse transcriptase gene of HIV. The microtitre point mutation assay (Kaye et al., 1992) was originally developed to detect single point mutations in a microtitre format so allowing the rapid detection of resistance in a large number of clinical samples to produce 'real time' results. A further advantage to the assay is the quantitative discrimination between wild type and mutant virus present in the same clinical sample without having to clone and sequence the individual virus strains. The UL97 microtitre point mutation assay was adapted from the assay designed by Kaye et al to detect the six most common point mutations in the HCMV UL97 (Bowen et al., 1997), namely M460I, M460V, H520Q, A594V, L595S and L595F. Figure 3.1 illustrates the principles of the point mutation assay, which is based upon the initial amplification of the UL97 with the

### *3.0 Analysis of UL97 point mutations*

---

relevant primers, one of which is biotinylated, which enables the immobilisation of the PCR amplicons to the streptavidin coated microtitre plate. Following denaturation of the amplicon by NaOH, oligonucleotide probes to detect the point mutations are annealed to the biotinylated strand. These probes terminate one base prior to the point mutation to be detected, thus the addition of each of the four <sup>35</sup>S labelled dNTP's to four individual wells identifies the nucleotide annealed to the complementary wild type or mutant base. The probe with the labelled nucleotide is denatured from the target DNA, scintillated and radioactivity determined, thus revealing the percentage of wild type and/or mutant virus present in the population.

This chapter describes the detection and quantification of HCMV genomes in multiple post mortem tissues using a quantitative competitive PCR (Fox et al., 1992). The UL97 gene was analysed in these tissues using the microtitre point mutation assay to determine the presence and relative proportion of the UL97 mutations. This analysis was used to investigate the relationships between HCMV load and the presence of UL97 mutations in different post mortem tissues of AIDS patients treated with ganciclovir.

## **3.2. Results**

### **3.2.1. HCMV gB quantitative competitive polymerase chain reaction**

A total of 61 post mortem tissues from 5 patients were examined by qualitative and quantitative competitive PCR. HCMV was detected in 83% (53/61) of the tissues by qualitative gB (UL55) PCR. One microgram of total DNA extracted from each tissue was subjected to a co-amplification PCR with varying concentrations of control plasmid. The pUC18 plasmid contained the fragment of HCMV gB amplified by the primers as in section 2.3.2. The PCR amplicons were digested for 1 hour with Hpa 1 and the DNA fragments separated by 12% acrylamide gel electrophoresis (figure 3.2). Densitometric analysis of the electronically scanned images of the ethidium bromide stained gels was performed by the NIH image software [available by anonymous FTP from [zippy.nimh.nih.gov\(128.231.98.32\)](http://zippy.nimh.nih.gov(128.231.98.32))]. The viral load was determined as in section 2.3.2. and plotted for each tissue from each patient (figure 3.3). The highest median viral load was found in the adrenal gland ( $3.4 \times 10^5$  genome equivalents per  $\mu\text{g}$  total DNA), whilst the kidney, duodenum and heart had the lowest median viral loads

### 3.0 Analysis of UL97 point mutations

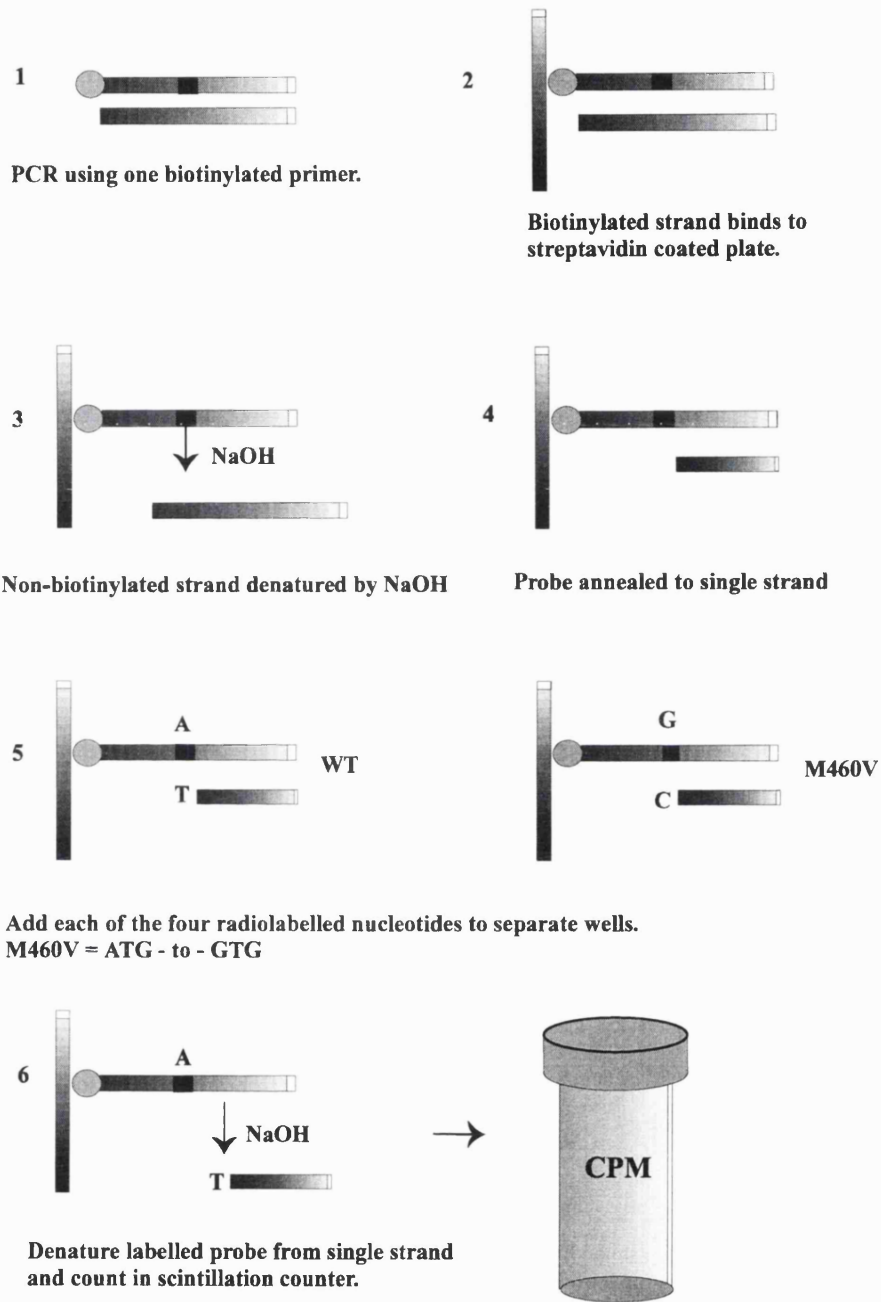


Figure 3.1. Principle of the Microtitre Point Mutation Assay

### *3.0 Analysis of UL97 point mutations*

---

( $3.0 \times 10^3$  and  $8.2 \times 10^2$  and 41 genomes per  $\mu\text{g}$  DNA respectively).

#### **3.2.2. Analysis of the distribution of mutant to wild type alleles of HCMV UL97**

One microgram of total DNA extracted from the 53 post mortem tissues in which HCMV DNA was detected were subjected to a UL97 PCR as in section 2.3.3. This PCR was designed to amplify a region of the UL97 catalytic domain in which the most common point mutations associated with clinical ganciclovir resistance occur. UL97 was only amplified in 34 of the 53 tissues (64%) in which HCMV was detected by a gB specific PCR. The amplified UL97 was subjected to a point mutation assay (section 2.3.4) and the ratio of mutant to wild type UL97 was plotted as a function of viral load. The results of this distribution are shown in figures 3.4 – 3.8. Each of the five patients exhibited differences in the mutant/wild type ratios at each codon. Patient 1 (figure 3.4) was treated intermittently with GCV over a 5 month period, had a median tissue viral load of  $1.4 \times 10^5$  genome equivalents per  $\mu\text{g}$  total DNA and point mutations in codons 595 and 594 of the UL97 gene were found in the salivary gland and in the stomach. Patient 2 (figure 3.5) was treated with GCV for 3 months, had a median HCMV tissue load of  $1.4 \times 10^5$  genomes per  $\mu\text{g}$  DNA, and showed resistance mutations in codon 595 only. Patient 3 (figure 3.6) was treated with GCV for 6 months, had a median HCMV tissue load of  $4.9 \times 10^6$  genomes per  $\mu\text{g}$  DNA, and had resistance mutations in codons 595, 594 and 460, particularly in the spleen and the adrenal gland where the viral loads were  $1.8 \times 10^5$  and  $9.8 \times 10^6$  genomes per  $\mu\text{g}$  DNA respectively. The L595F mutation was detected in 7/10 of these tissues, of which the average composition was 74% mutant virus (median 74.5%, range 67-79%). Patient 4 (figure 3.7) was treated with GCV for 17 months, had a median HCMV tissue load of  $1.4 \times 10^4$  genomes/ $\mu\text{g}$  DNA, and had resistance mutations in codons 595, 594, 520 and 460 all of which were present in the lymph nodes, salivary gland and the pancreas. Patient 5 (figure 3.8) had the highest median HCMV tissue load of  $1.8 \times 10^7$  genomes/ $\mu\text{g}$  DNA and had resistance genotypes predominantly in the salivary and adrenal glands and spleen. To determine if a relationship between higher viral load and presence of mutations existed, a graph was plotted of presence or absence of mutations against increasing viral load. There was no statistically significant difference in viral load

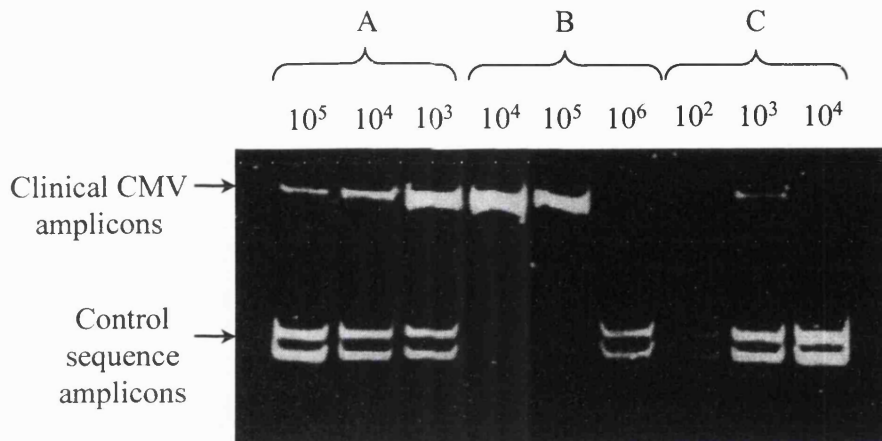


**Figure 3.2. Quantitative Competitive Polymerase Chain Reaction.**

One microgram of total DNA extracted from the individual tissues of post mortem patients was co-amplified in a gB PCR with varying concentrations of control sequence DNA. The amplicons were digested with Hpa 1 and separated by electrophoresis on a 12% acrylamide gel. The three lanes under A show an ideal 50:50 ratio between the wild type and control sequence DNA against the numbers which indicate the genome copies of control sequence used in each experiment. The lanes under B show an excess of wild type DNA and the lanes under C show an excess of control sequence.

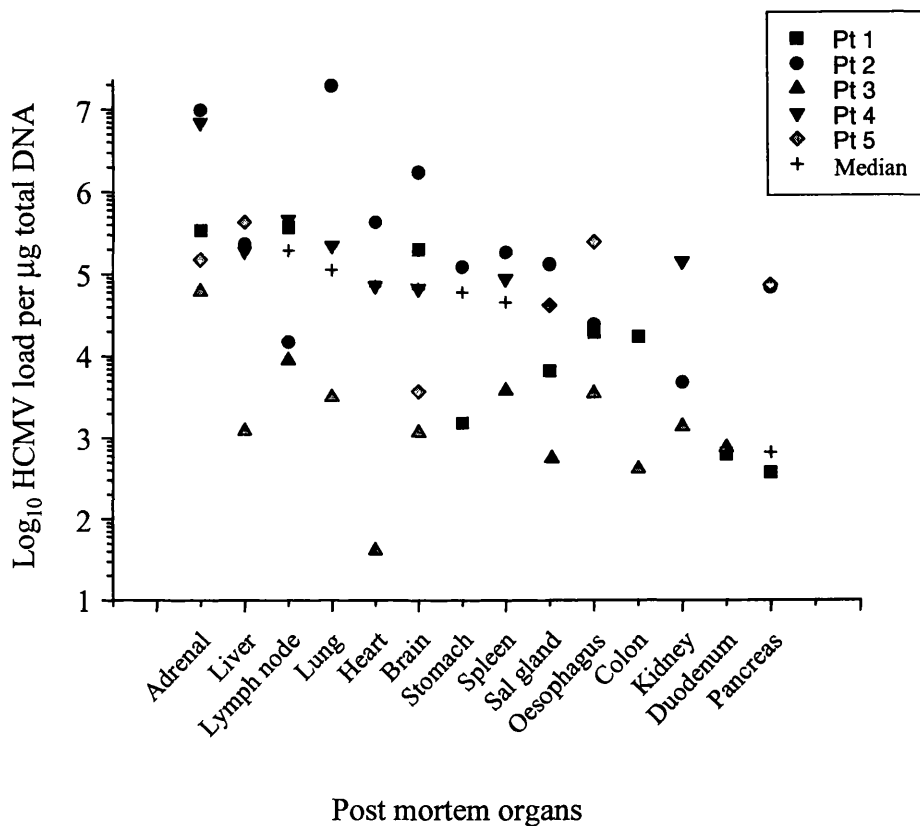


**Figure 3.3. Analysis of the Median HCMV Loads in Multiple Post Mortem Tissues.**

The HCMV viral load was determined by quantitative competitive PCR. The PCR amplicons were analysed using the NIH image. The viral load determined by comparison of the density of the wild type DNA with the control sequence DNA. The HCMV loads were plotted for each patient in order of decreasing median viral load for each tissue (+). The adrenal gland, lymph nodes and liver had the highest median loads, and the kidney, duodenum and pancreas had the lowest HCMV loads.

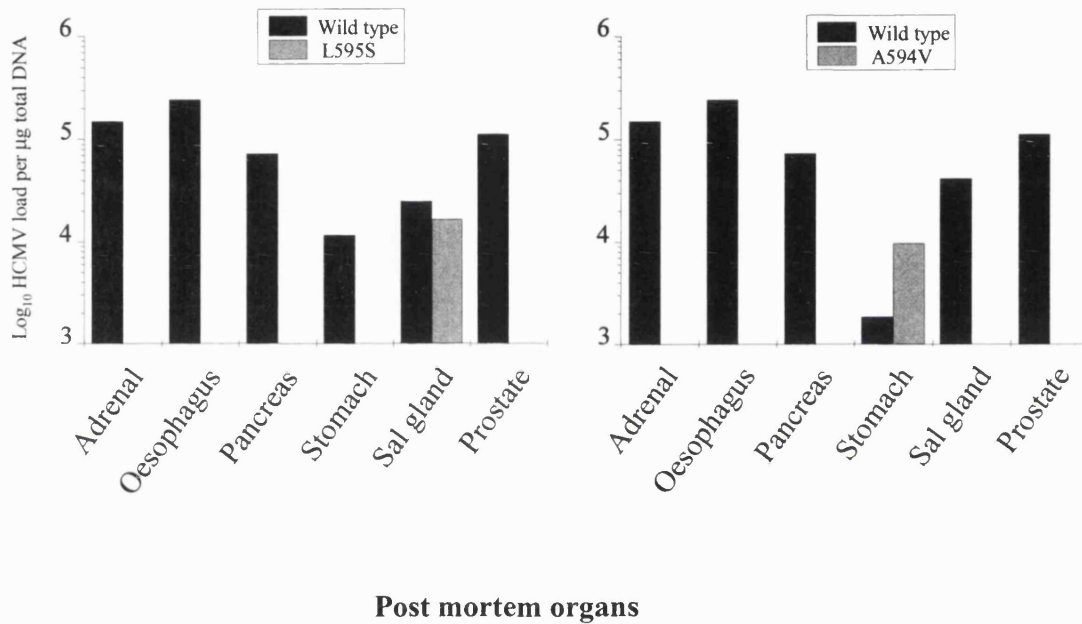


**Figure 3.4. Distribution of Wild Type and Mutant UL97 Genotypes in Multiple Post Mortem Organs of AIDS Patient 1.**

Distribution of genotypes at codons 594 and 595 in the HCMV UL97 gene in multiple post mortem organ samples from AIDS patient 1 following GCV therapy. The histograms represent the viral load of the wild type virus and each point mutation. Histograms for mutations 520 or 460 are not shown as the viral population was exclusively wild type in all organs.



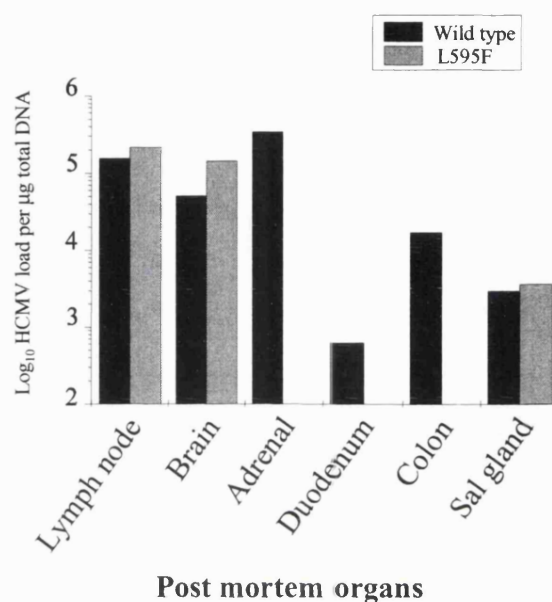


**Figure 3.5. Distribution of Wild Type and Mutant UL97 Genotypes in Multiple Post Mortem Organs of AIDS Patient 2.**

Distribution of genotypes at codon 595 in the HCMV UL97 gene in multiple post mortem organ samples from AIDS patient 2 following GCV therapy. The histograms represent the viral load of the wild type virus and each point mutation. Histograms for mutations 460, 520 and 594 are not shown as only wild type sequences were present in all organs.

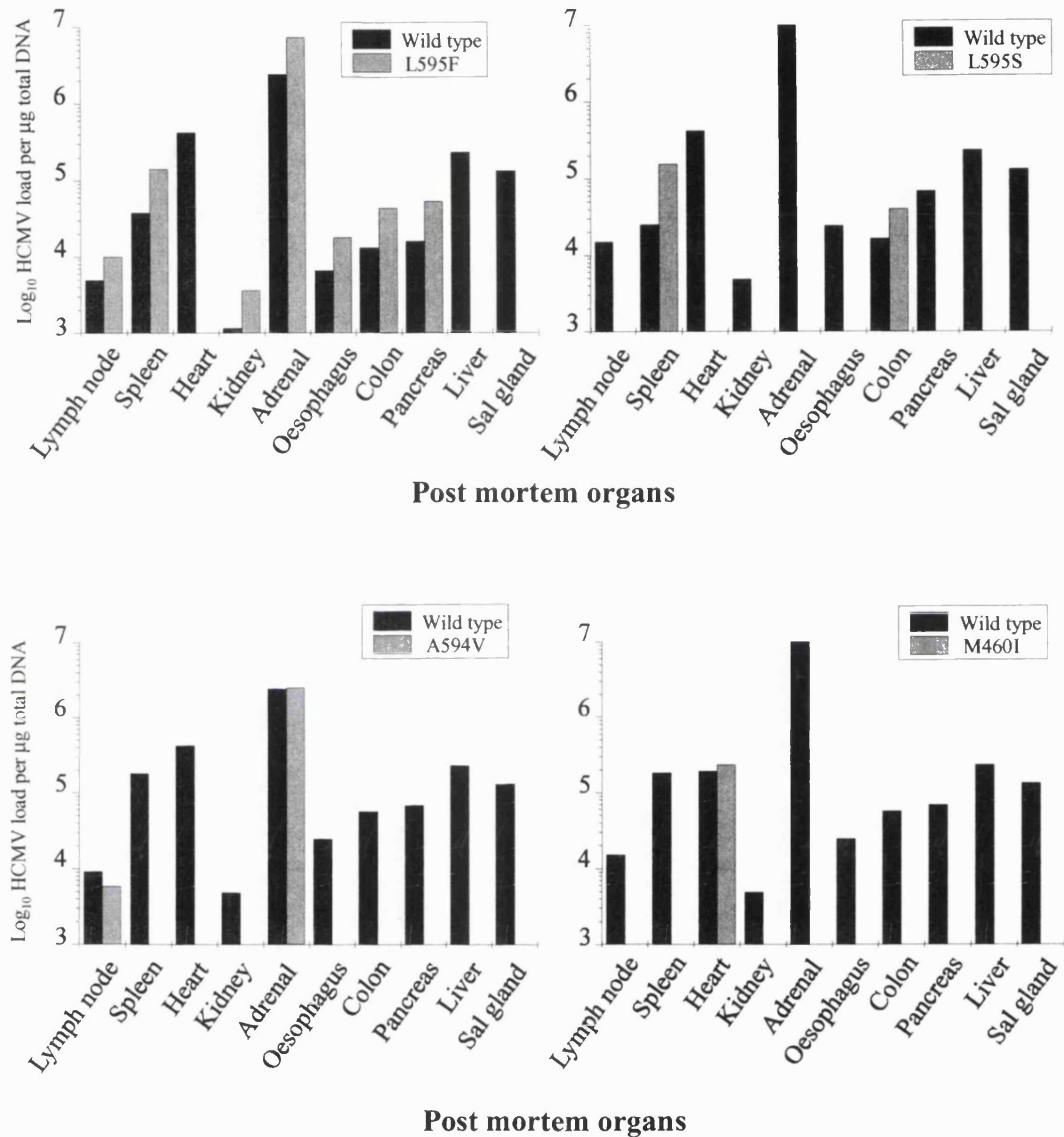


**Figure 3.6. Distribution of Wild Type and Mutant UL97 Genotypes in Multiple Post Mortem Organs of AIDS Patient 3.**

Distribution of genotypes at codons 460, 594 and 595 in the HCMV UL97 gene in multiple post mortem organ samples from AIDS patient 3 following GCV therapy. The histograms represent the viral load of the wild type virus and each point mutation. Histograms for mutations at codon 520 are not shown as only wild type sequences were found in all organs.

### 3.0 Analysis of UL97 point mutations

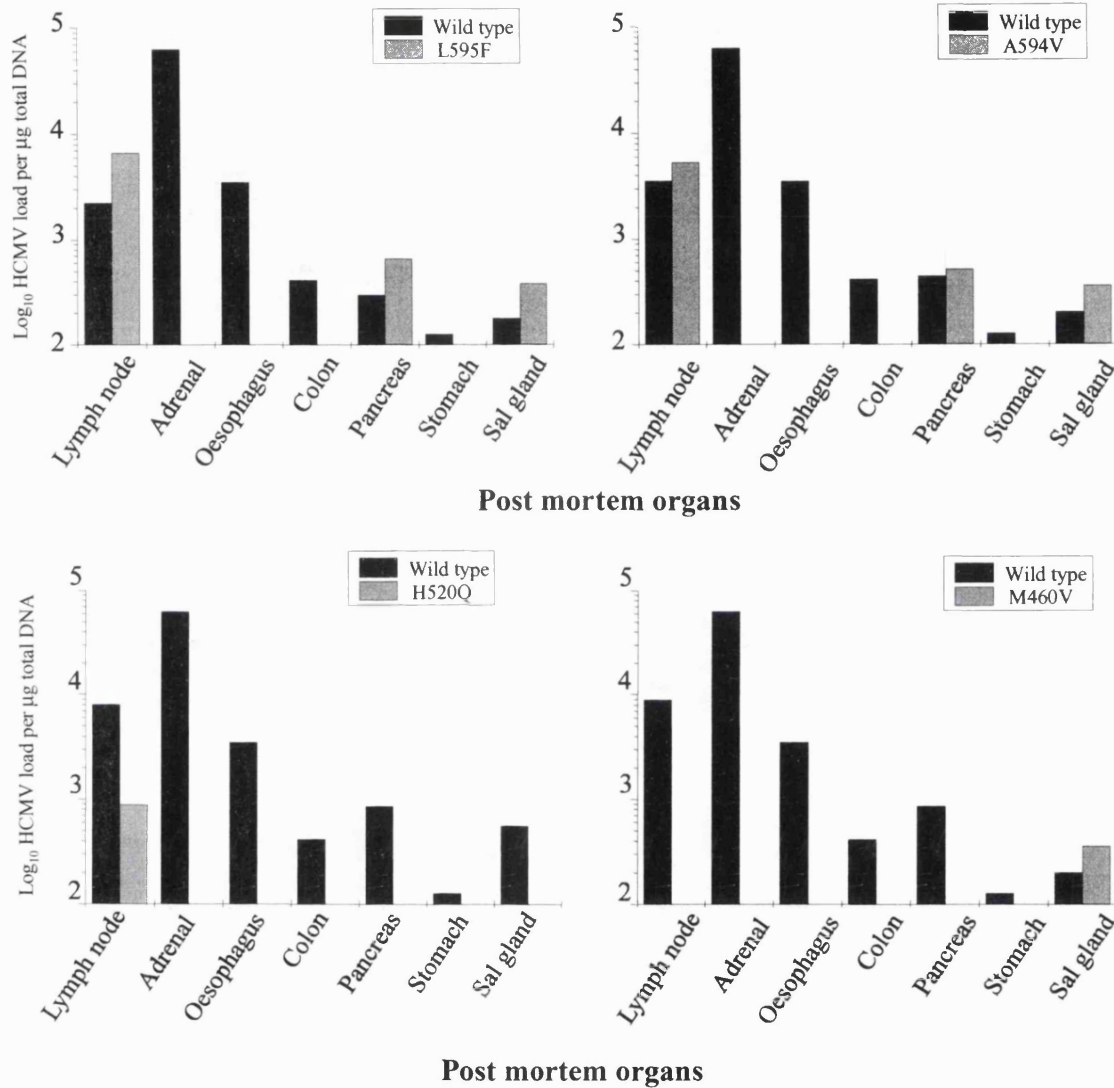


**Figure 3.7. Distribution of Wild Type and Mutant UL97 Genotypes in Multiple Post Mortem Organs of Patient 4.**

Distribution of genotypes at codons 460, 520, 594 and 595 in the HCMV UL97 gene in multiple post mortem organ samples from AIDS patient 4 following GCV therapy. The histograms represent the viral load of the wild type virus and each point mutation.

### 3.0 Analysis of UL97 point mutations

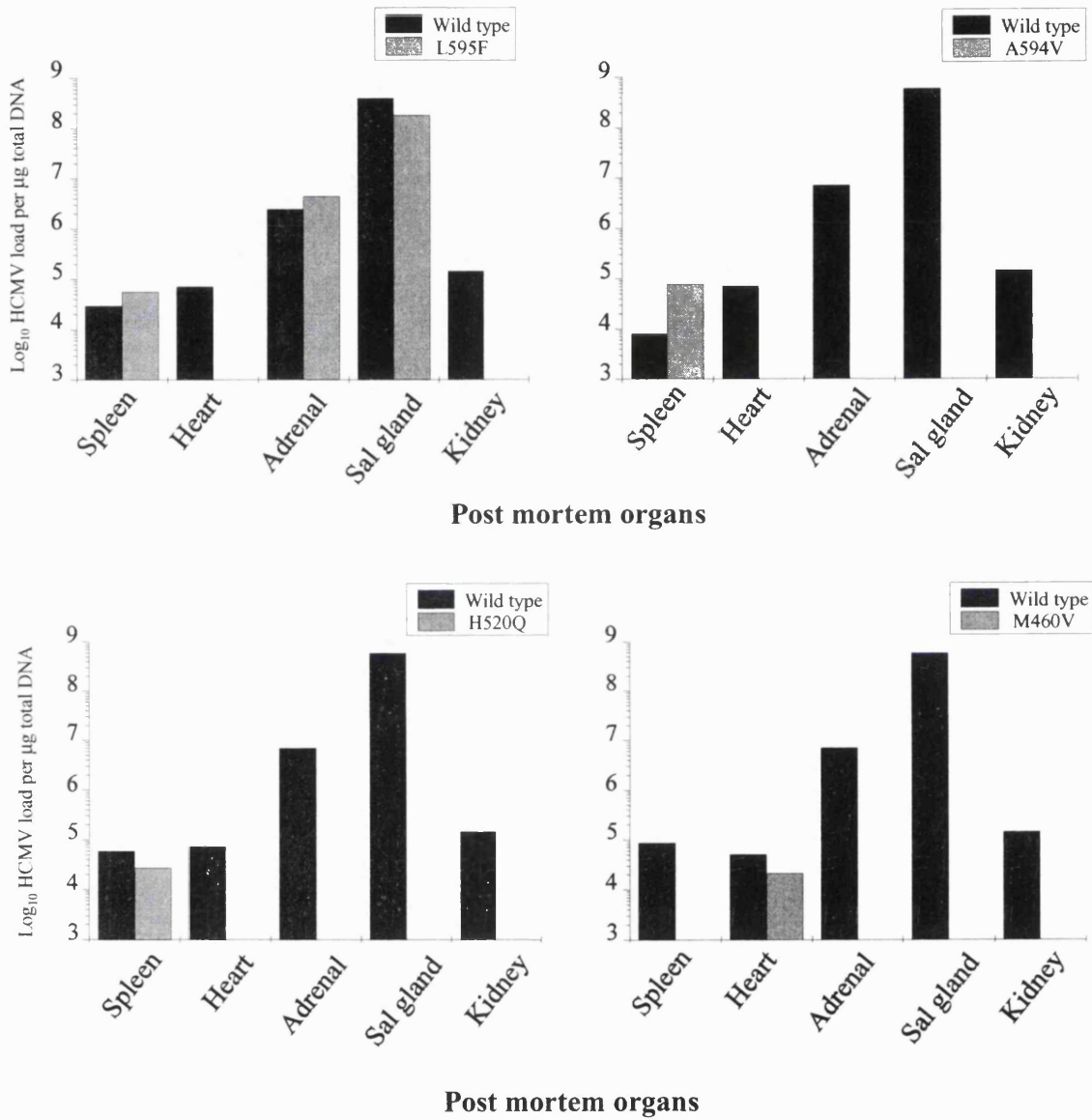


**Figure 3.8. Distribution of Wild Type and Mutant UL97 Genotypes in Multiple Post Mortem Organs of AIDS Patient 5.**

Distribution of genotypes at codons 460, 520, 594 and 595 in the HCMV UL97 gene in multiple post mortem organ samples from AIDS patient 5 following GCV therapy. The histograms represent the viral load of the wild type virus and each point mutation.

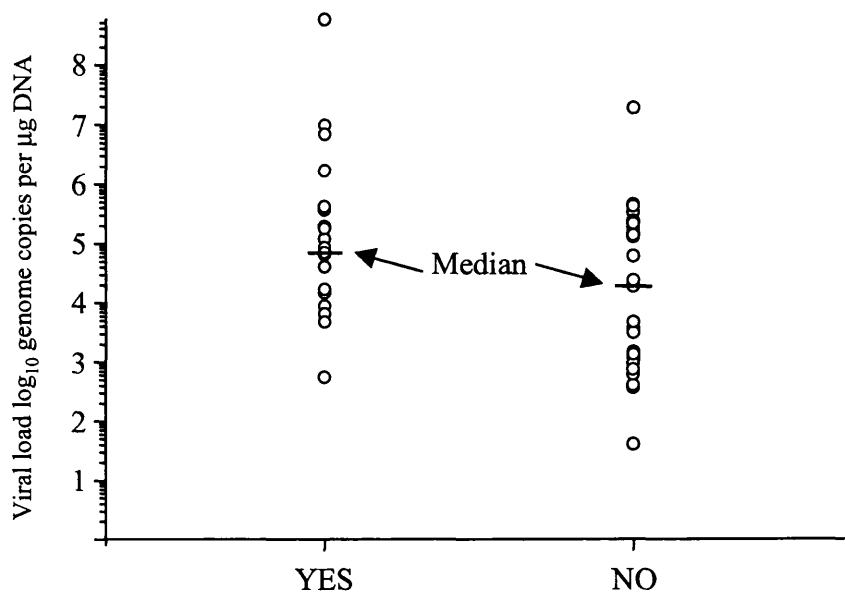


**Figure 3.9. Correlation between Presence of UL97 Mutations and Viral Load.**

The viral load of each organ in which a UL97 point mutation occurred was plotted against each organ without a mutation. The mean (-) and median(-) viral load for each set is shown, suggesting there is no relationship between the occurrence of mutations and viral load.

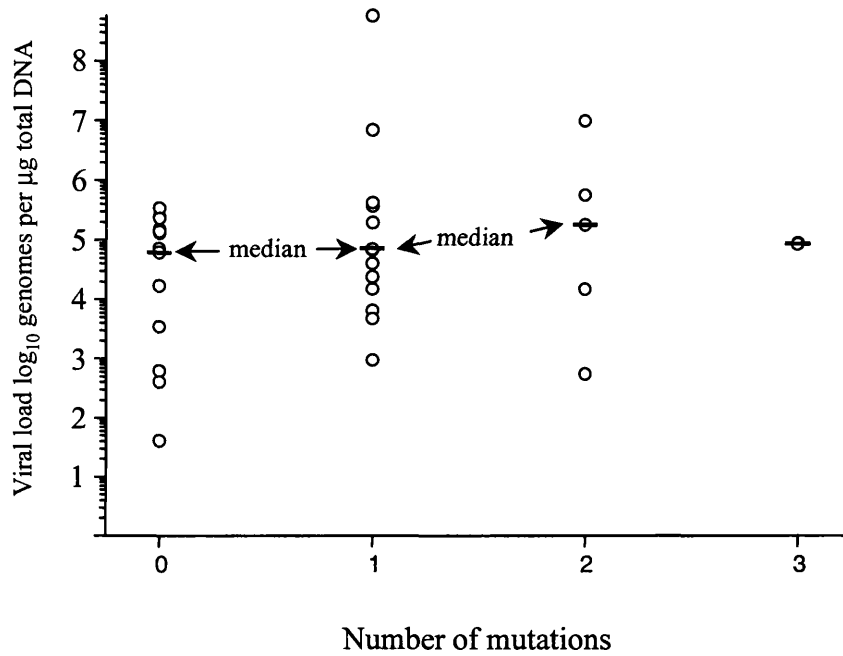


**Figure 3.10. Correlation Between the Number of UL97 Mutations and Viral Load.**

The number of point mutations, which occurred in each organ, was plotted against the viral load. The mean (-) and median (-) values for each set is shown, suggesting there is no relationship between viral load and number of point mutations in each organ.

between organs with or without evidence of UL97 drug resistance mutations. In order to determine if a correlation exists between the presence of point mutations with an increasing viral load, the presence or absence of point mutations within the UL97 gene was plotted against viral load (figure 3.9). The Mann Whitney U test demonstrated a significant statistical difference between the presence or absence of mutations with the log median viral load,  $p=0.04$  and  $p=0.02$  respectively. Therefore the higher the median viral load, the higher the probability of generating a point mutation within the UL97 gene. A similar analysis was performed to determine if the number of mutations within the UL97 gene increases with a higher median viral load (figure 3.10). A significant P value ( $p=0.02$ ) was observed for the presence of a single mutation, but not for  $>1$  mutations, thus an increasing median viral load significantly correlated with the occurrence of 1 mutation.

### **3.3. Discussion**

The nested PCR originally developed by Bowen et al, (1997) was redesigned with a new primer set in an attempt to increase the sensitivity of the assay. The optimised conditions enabled the detection of 500 copies of the UL97 using a plasmid containing a truncated UL97, however this sensitivity was not reflected in the amplification of UL97 from clinical samples. An explanation for this difference lies in the purity of the plasmid DNA, compared with the total DNA extracted from the post mortem tissues or the presence of inhibitory substances in the extracted DNA. However, attempts to counteract this by initial dilution of input DNA did not result in an increase in sensitivity. Finally, UL97 has a high degree of secondary structure due to its G:C composition, which may result in the decreased efficiency of primer annealing, so leading to a decrease in the overall sensitivity of the PCR.

Investigation of the multiple organs from the AIDS patients treated with ganciclovir has revealed quantitative differences in resistant genotypes between organs of the same individual. These data imply that different physiological compartments provide different niches for the evolution of resistance. This observation is reminiscent of data regarding the non-uniform distribution of HIV drug resistant genotypes on multiple organs of the same individual reported by others (Atkins et al.,1998, Wu et al.,1997). The differences between genotypic resistance in organs may reflect multiple factors.

### *3.0 Analysis of UL97 point mutations*

---

For example, if the viral load is lower or the replication of HCMV in particular cell types slower, then the evolution of resistance may be reduced. Alternatively, the tissue penetration and metabolism of ganciclovir to the active triphosphate form may differ between tissues due to the variable levels of virus encoded or host enzymes required for drug anabolism. For example, since the UL97 protein of HCMV is required for monophosphorylation of ganciclovir it is possible that organs with high levels of replication may be more likely to provide a high selective pressure for the evolution of genotypic resistance to GCV. However, since UL97 also facilitates inhibition of replication by activating GCV, high loads might be associated with imminent control of HCMV load and so a low risk of resistance. In this study a significant relationship between viral load in the organ and the quantitative presence of genotypic resistance was detected. Figure 3.9 shows a plot of the organs with and without mutations against viral load. A significant correlation was observed between median viral load and presence of mutations. This is also the case for the correlation of the number of mutations against the mean viral load for the occurrence of a single mutation. Strains of HCMV resistant to GCV through changes in UL97 usually appear within the first few months of therapy giving rise to low level resistance (Smith et al.,1997). This may be followed by the appearance of UL54 mutations selected by more extended periods of GCV therapy. The combination of UL97 and UL54 sequence variations occurs predominantly during extended periods of GCV therapy and such virus strains exhibit a high level of GCV resistance plus cross-resistance to cidofovir. Since UL54 mutations in the absence of UL97 mutations are rare, I concentrated on assessing the presence of UL97 mutations. A higher frequency of genotypic resistance was observed in patients who had been prescribed ganciclovir for longer periods of time but due to the small numbers of patients analysed, this relationship did not achieve statistical significance.

There are increasing data suggesting that drug resistant strains of virus are frequently debilitated in their replication capacity. This phenomenon has been described extensively for HIV drug resistant strains but has only recently been investigated for GCV resistant strains of HCMV (Bowen et al.,1998, Emery et al.,1999). Bowen et al. (1998) showed the repopulation of wild type HCMV strains versus UL97 resistant virus following replacement of ganciclovir therapy with cidofovir therapy consistent with cidofovir not requiring UL97 for activation. In addition, Baldanti et al. (1996) showed that mutations in UL54 (V715M and T700A) resulted in a virus with a slow growth



### *3.0 Analysis of UL97 point mutations*

---

phenotype. Interestingly, the viral loads detected in the tissues harbouring resistant virus was not always the highest load observed in all organs from the same individual. However, in all organs where genotypic resistance was identified a mixed population of species still existed indicating the persistence of wild type virus together with genotypic resistant virus under the influence of ganciclovir selection.

In summary, in patients exposed to continuous GCV therapy, resistance is common at autopsy and does not occur uniformly in different tissue types such that high level resistance in one organ is not always reflected in other organs of the same patient. Previous studies reported HCMV isolation from urine in only 8% of AIDS patients receiving GCV monotherapy (Yuen et al.,1995). It follows that merely assessing the appearance of resistant virus in one body compartment may provide misleading data as to the true prevalence of resistant virus in other target organs; information which should be considered in the design of future trials with other antiviral compounds active against HCMV.

**CHAPTER 4**

**Construction of a Recombinant Baculovirus Expressing  
the HCMV UL97 Phosphotransferase**

### 4.1. Introduction

The majority of enzymes encoded by the herpesviruses are involved in DNA replication and nucleotide metabolism, however very few herpesvirus protein kinase genes have been identified. This is notable since herpesvirus phosphoproteins in infected cells contribute a significant class of gene products ranging from immediate early trans-activators (Pereira et al., 1977) to structural components (Jahn et al., 1987). Several phosphoproteins have been found to be associated with herpesvirus virions (Lemaster and Roizman., 1980, Roby and Gibson., 1986) and it has been suggested that these may be of cellular origin (Stevley et al., 1985). Indeed, the functional role of cellular protein kinases in the phosphorylation of herpesvirus proteins may be important but their role has not been defined in detail. In an attempt to clarify the role of viral protein kinases, Chee et al., (1989) identified protein kinases in each of the alphaherpesviruses (HSV-1 and VZV), betaherpesviruses (HCMV and HHV-6) and the gammaherpesviruses (EBV) by sequence homology. The HCMV UL97 and the HHV-6 U69 were identified by sequencing the *Hind*III fragment of the HCMV AD169 and the *Sal*I fragment of HHV-6. Various computer based library searches were performed upon these genes and further herpesvirus proteins, and led to the identification of five herpesvirus protein kinase homologues based upon cellular protein kinase catalytic domains originally identified by Hanks et al., (1988, described in section 1.8). These included UL13 of HSV-1 (McGeoch et al., 1988), ORF47 of VZV (Davison and Scott., 1986) and BGLF4 of EBV (Baer et al., 1984), although homologies between BGLF4, ORF47 and UL13 had previously been identified (Davison and Taylor., 1987, McGeogh et al., 1988). The homology between these protein kinases however is very low, so identification of highly conserved residues found in protein kinases enabled the classification of the five herpesvirus proteins into the protein kinase superfamily. It was also found that all five genes reside in equivalent positions in their respective genomes. More recently further members of this protein class have been identified in HHV-7 (U69) and HHV-8 (ORF 36). This chapter describes the cloning and expression of the entire HCMV UL97 ORF using recombinant baculovirus systems.

## 4.2 Results

### 4.2.1. PCR amplification of the HCMV UL97 ORF

A series of PCR reactions designed to amplify the complete UL97 gene were performed as described in section 2.1.2. Each reaction contained from 100ng to 1µg of template HCMV DNA and suitable control reactions were included. The PCR amplification products were separated by 1% agarose gel electrophoresis (figure 4.1) and a single product of approximately 2.2 kbp was observed, corresponding to the predicted size of the UL97 ORF. No products were observed after amplification of the DNA extracted from uninfected cells.

### 4.2.2. Cloning of the UL97 into pGEM-T Easy

The PCR products were subjected to low melting point agarose gel electrophoresis (figure 4.2). The band corresponding to the size of UL97 (2.2kbp) was excised from the gel and purified as described in section 2.1.3. The UL97 DNA was ligated into pGEM-T Easy (1:1 molar ratio) as described in section 2.1.4. Each ligation was transformed into competent *E.coli* JM109 cells as described in section 2.1.5.

### 4.2.3. Restriction enzyme analysis of the putative recombinant clones

The putative recombinant clones were selected, plasmid DNA extracted (section 2.1.6) and analysed by restriction enzyme digestion with *EcoR*I as described in section 2.1.7. The digests shown in figure 4.3 revealed that all the clones picked contained the UL97 gene cloned into pGEM-T. The presence of UL97 in these clones was further confirmed by performing a PCR with UL97 specific primers (section 2.1.1.) as shown in figure 4.4.

### 4.2.4. Sequencing of the UL97 ORF

DNA sequencing of the entire cloned UL97 ORF revealed a number of differences from the database sequence available on Genbank, however these mutations were non-coding point mutations. These DNA mutations are listed in table 4.1 and include the sequence differences between Towne and AD169.

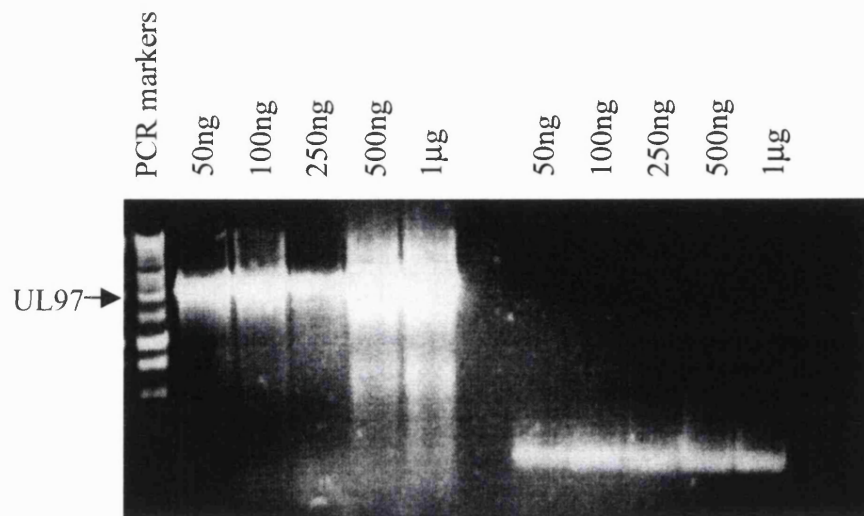


**Figure 4.1. Polymerase Chain Reaction Amplification of the UL97 ORF.**

The HCMV UL97 ORF was amplified using the DyNAzyme proof-reading enzyme from different DNA concentrations extracted from HCMV-infected HEL cells. The PCR amplicons were analysed by 1% gel electrophoresis. Negative controls were included in the PCR amplification.

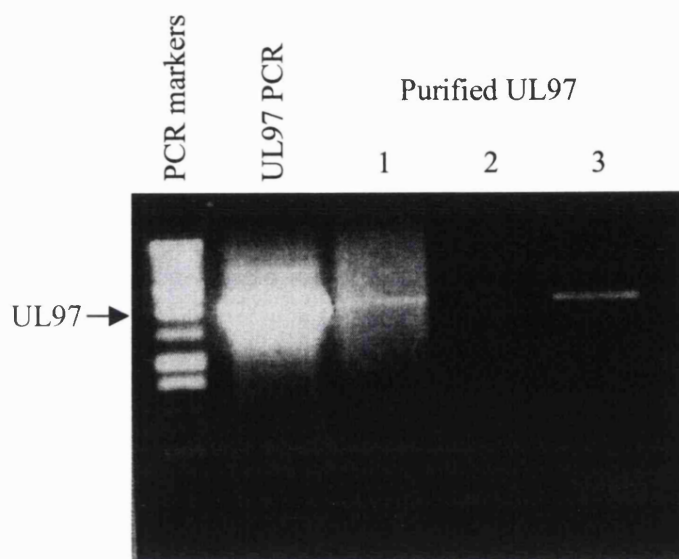


**Figure 4.2. Purification of the PCR-Amplified UL97.**

The PCR-amplified UL97 was excised and purified from a 1% low melting point gel. The purified UL97 was analysed by 1% gel electrophoresis to determine the purity and concentration of the UL97 DNA required to give a 1:1 molar ratio for cloning into pGEM T-easy. Lanes 1, 2 and 3 show individual DNA purifications.

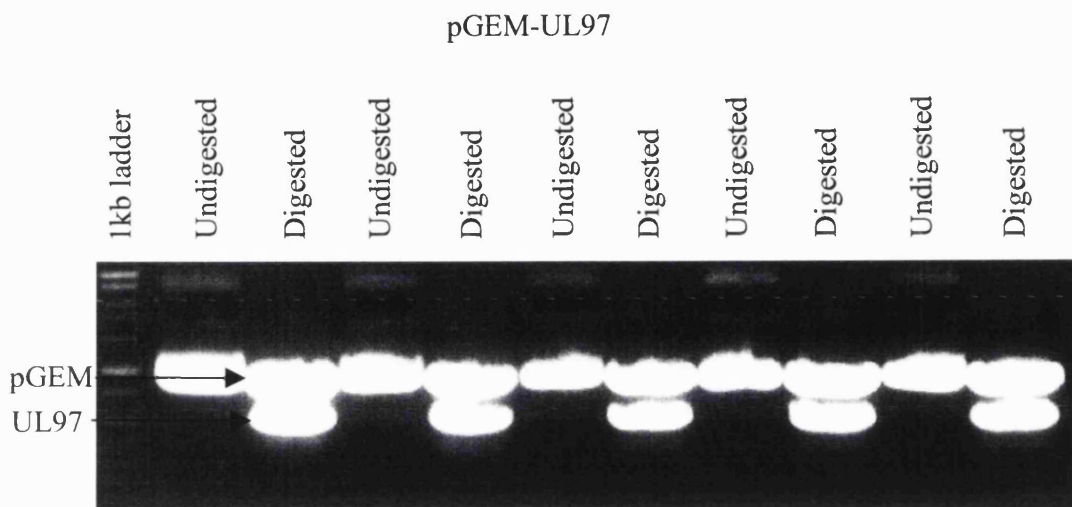


**Figure 4.3. Restriction Enzyme Digestion of pGEM-UL97.**

Five pGEM-UL97 clones were digested with the restriction enzyme *EcoR*I. The digests were analysed by 1% gel electrophoresis. The pGEM-UL97 contains 2 *EcoR*I restriction sites in the pGEM multiple cloning region but none in the UL97, thus the UL97 was cleaved from the vector.

### 4.2.5. Restriction enzyme digestion of pGem-T-UL97, pBlueBacHis and pMelBac

The plasmid pGEM-T-UL97 and the baculovirus transfer vectors pBlueBacHis and pMelBac were digested with *Hind*III and *Kpn*I (figures 4.5 and 4.6 respectively). The digests were electrophoresed in a low melting point agarose gel and the band corresponding to the UL97 ORF was excised from the gel and purified by the method described in section 2.1.3. The digested, purified UL97 was analysed by 1% agarose gel electrophoresis (figure 4.7).

### 4.2.6. Subcloning of the UL97 into the baculovirus transfer vectors pBlueBacHis and pMelBac

Ligations between UL97 and pBlueBacHis and pMelBac were performed at a 1:1 molar ratio and each ligation was transformed into the JM109 strain of *E.coli* using the method in section 2.1.5. Plasmid DNA was extracted from 5 overnight cultures of *E.coli* and subjected to a double restriction enzyme analysis with *Xho*I and *Sal*I as shown in figure 4.8. All the plasmid digests gave bands of the expected molecular size and plasmids from cultures 1 (pBlueBacHis-UL97) and 4 (pMelBac-UL97), designated BBH-WT and MB-WT respectively, were selected for cotransfection. All plasmids obtained from the *E.coli* cultures were subjected to PCR with the UL97 specific primers described in section 2.1.1. The agarose gel analysis is shown in figure 4.9, illustrating that all the plasmids gave a band corresponding to the molecular size of UL97 (approx 2.2kbp).

### 4.2.7. Co-transfection of BBH-WT, MB-WT and Bac-N-Blue linearized DNA to produce recombinant baculoviruses

The baculovirus transfer vectors BBH-WT and MB-WT and the linearized Bac-N-Blue DNA were cotransfected into Sf21 cells with the aid of insectin liposomes using the method described in section 2.1.20. The cotransfection supernatant was harvested and subjected to plaque assay as described in section 2.1.21. Following the staining of the assay (figure 4.10), the putative plaques were selected, expanded and analysed as in section 2.1.23. The supernatant was harvested and the DNA extracted from the infected cells of the P1 stock and subjected to a PCR with both UL97 specific and baculovirus specific primers as described in section 2.1.1 and 2.1.23. The PCR products were analysed by 1% agarose



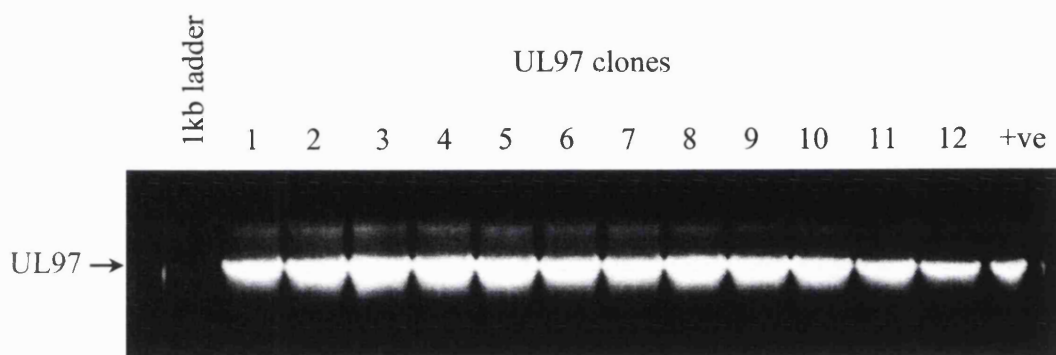


**Figure 4.4. Polymerase Chain Reaction Analysis of pGEM-UL97.**

Twelve individual pGEM-UL97 clones were subjected to a PCR using UL97-specific primers to ensure the UL97 had been cloned into the pGEM-T vector. The PCR amplicons were analysed by 1% gel electrophoresis.

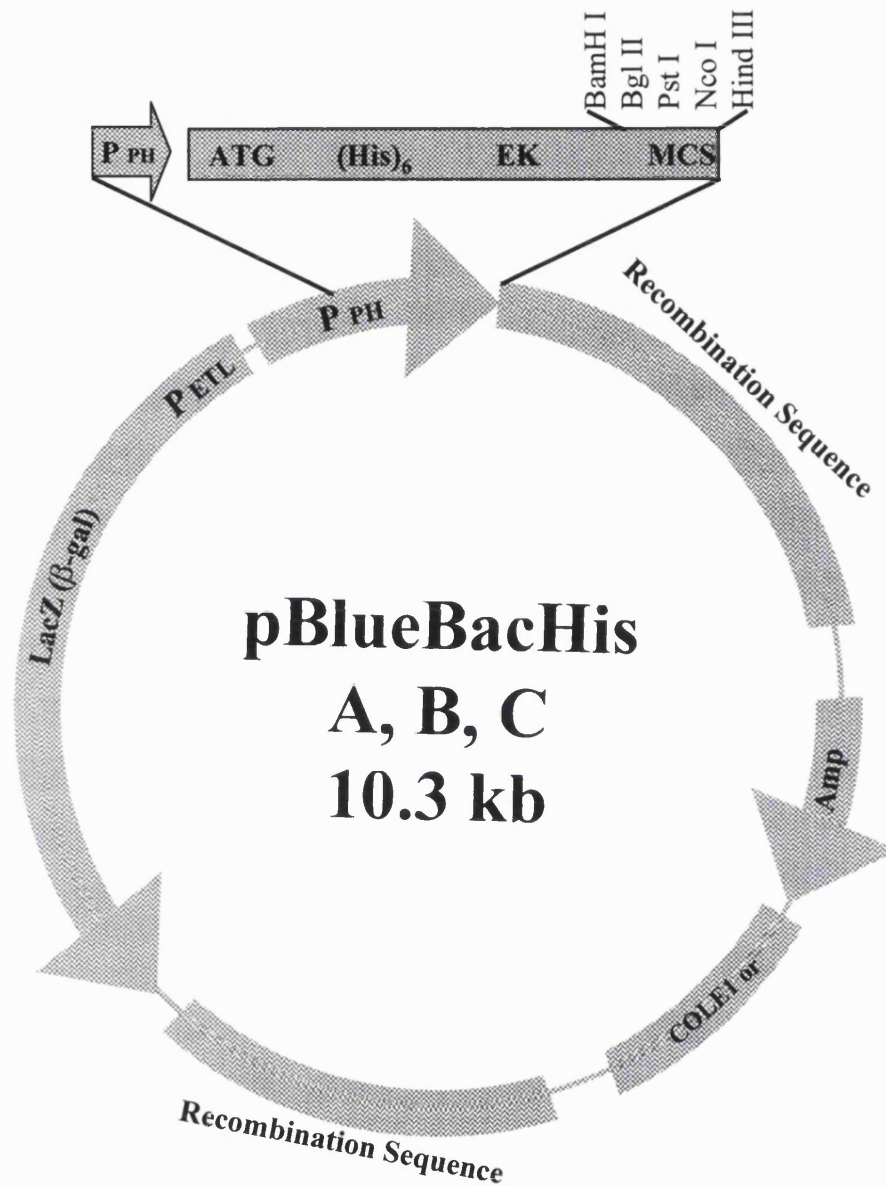


**Figure 4.5. Baculovirus Transfer Vector pBlueBacHis C (Invitrogen).**

P<sub>PH</sub> = polyhedrin promoter; ATG = start codon; (His)<sub>6</sub> = hexahistidine tag; EK = enterokinase cleavage site; MCS = multiple cloning site; recombination sequences allow the transfer vector to align with the appropriate baculovirus DNA; ColE1 = allows the transfer vector to be maintained in *E.coli*; Amp = selectable marker; LacZ = gene encoding β-galactosidase; P<sub>ETL</sub> = baculovirus promoter driving expression of LacZ gene.

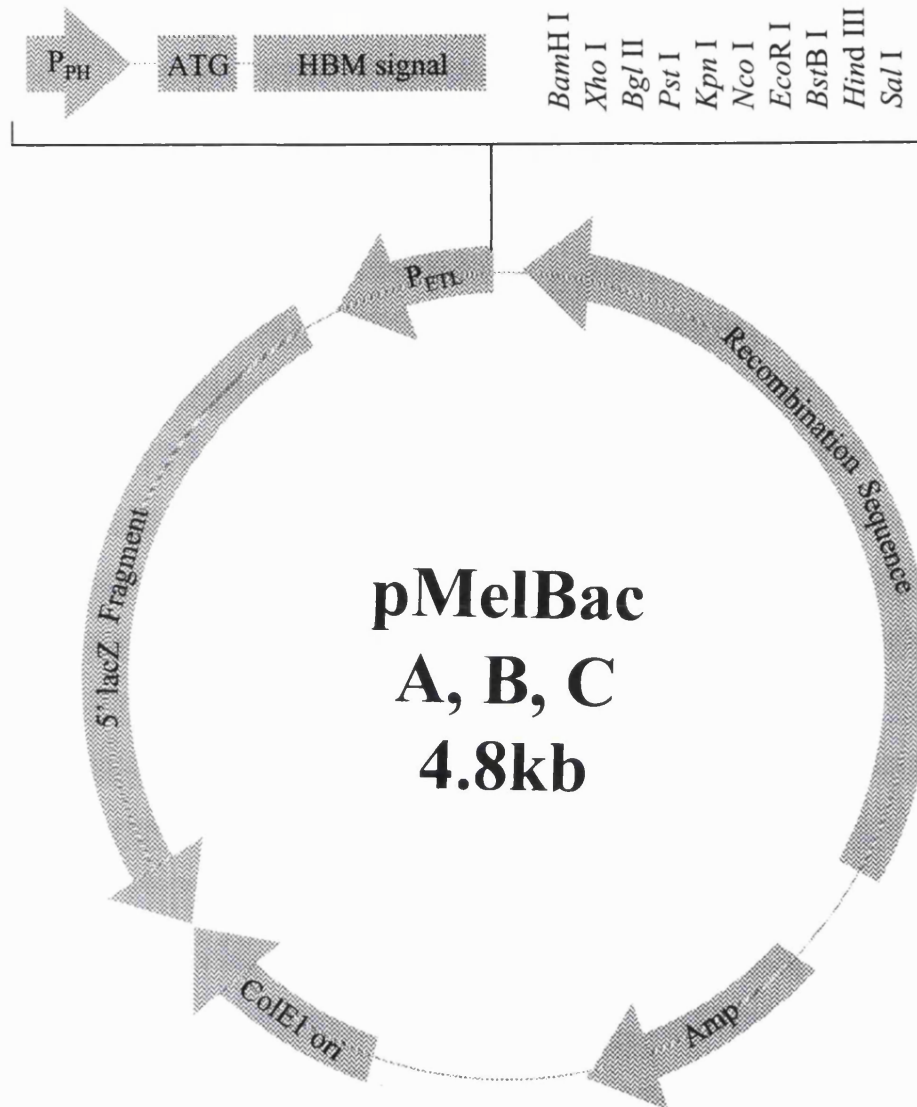


**Figure 4.6. Baculovirus Transfer Vector pMelBac C (Invitrogen).**

$P_{PH}$  = polyhedrin promoter; ATG = start codon; HBM = honey bee melittin signal sequence; recombination sequence allows the transfer vector to align with the appropriate baculovirus DNA; ColE1 = allows the transfer vector to be maintained in *E.coli*; Amp = selectable marker; LacZ = gene encoding  $\beta$ -galactosidase;  $P_{ETL}$  = baculovirus promoter driving expression of the lacZ gene.

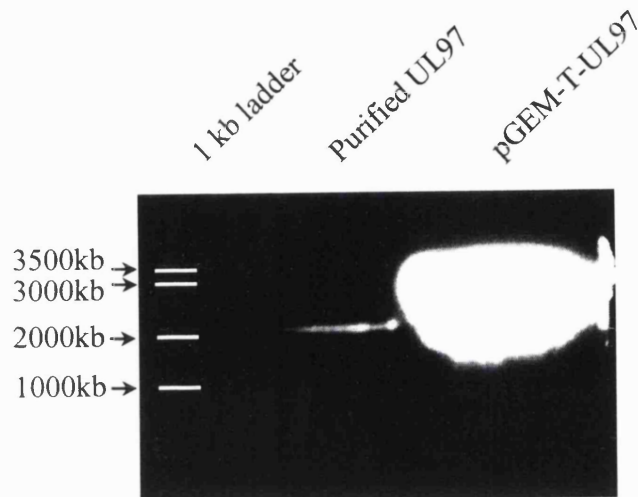


**Figure 4.7. Purification of the Digested UL97.**

A single pGEM-UL97 clone was digested with *Hind*III and *Kpn*I and subjected to low melting point 1% agarose gel electrophoresis. The band was excised, purified and subjected to 1% gel electrophoresis to determine the approximate concentration of the digested DNA.

assay (figure 4.10), the putative plaques were selected, expanded and analysed as in section 2.1.23. The supernatant was harvested and the DNA extracted from the infected cells of the P1 stock and subjected to a PCR with both UL97 specific and baculovirus specific primers as described in section 2.1.1 and 2.1.23. The PCR products were analysed by 1% agarose gel electrophoresis, as shown in figure 4.11. and revealed a single DNA band corresponding to the approximate size of the UL97 without contamination by wild type baculovirus DNA. The UL97-specific primers generated a product of 2142bp, the baculovirus primers for BVMB-UL97 generated a product of 2466bp and for BVBBH-UL97 generated a product of 2478bp.

#### **4.2.8. Analysis of protein expression of BVBBH-WT and BVMB-WT**

The recombinant UL97 containing baculovirus stocks were expanded into high titre stocks as described in section 2.1.24. The expression of UL97 by the viruses were analysed by SDS-PAGE followed by Coomassie brilliant blue staining and Western blot as described in sections 2.4.4. to 2.4.6. Negative controls (BVLacZ and mock infected) were included in each experiment and similarly analysed. Sf21 cells were infected with the p-3 stock of the viruses at an MOI of 1, 5 and 10 and harvested at 24, 48 and 72 hours post infection. Crude lysates of the proteins were prepared and subjected to SDS-PAGE. The proteins were stained with Coomassie brilliant blue and electrophoretically transferred onto PVDF membrane. The membrane was then probed with an anti-UL97 monoclonal antibody as described in section 2.4.6. The Coomassie blue stained gel (figure 4.12) showed the accumulation of the  $\beta$ -galactosidase protein expressed by the polyhedrin promoter over time and the down regulation of the cellular proteins characteristic of baculovirus infection. A protein band was detected which corresponded to the molecular weight of the UL97 (BVBBH 96 kDa and BVMB 90 kDa) which accumulated from 48 hours post infection and was maximal at 72 hours post infection. This accumulation was confirmed by the Western blot (figure 4.13.), which also indicated that an MOI 10 and 72 hours post infection was optimal for expression of the UL97.

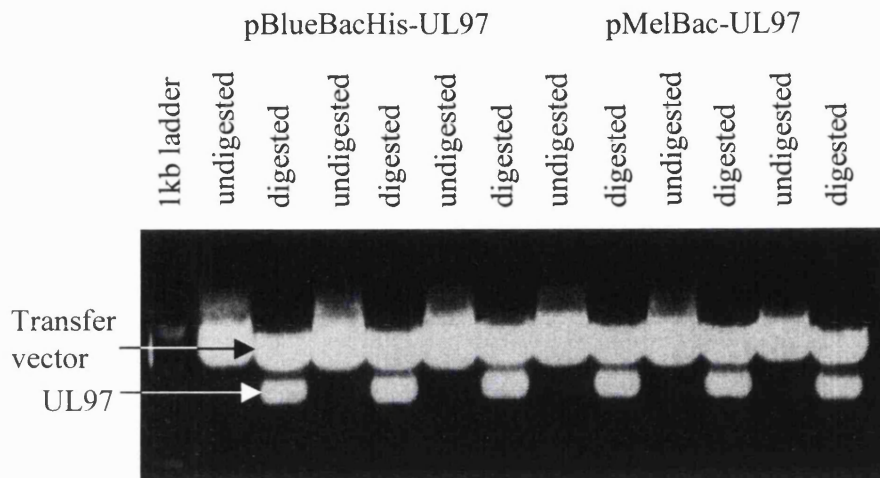


**Figure 4.8. Restriction Enzyme Digestion of pBlueBacHis-UL97 and pMelBac-UL97.** Individual clones of the pBlueBacHis-UL97 and pMelBac-UL97 baculovirus transfer vectors were digested with the restriction enzymes *XhoI* and *SalI*. The digests were analysed by 1% agarose gel electrophoresis. The transfer vectors contain one restriction site in the multiple cloning site for each of the enzymes enabling the UL97 to be digested from the transfer vectors as a single band.

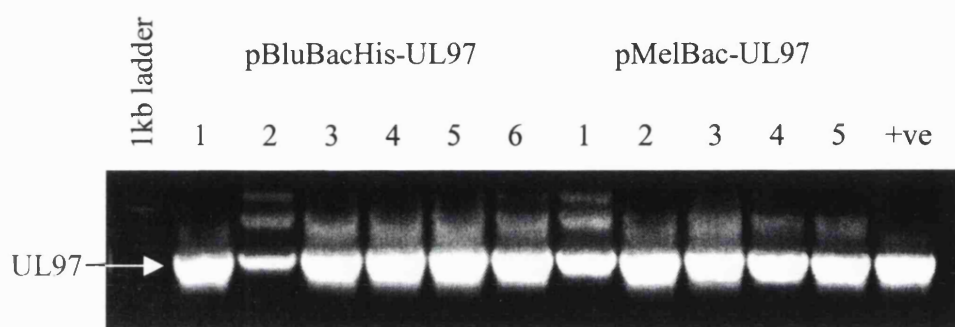


**Figure 4.9. PCR analysis of the pBlueBacHis-UL97 and the pMelBac-UL97.**

Individual clones of the pBlueBacHis-UL97 and pMelBac-UL97 were subjected to a PCR using UL97-specific primers to ensure the UL97 had been incorporated into the baculovirus transfer vectors. The PCR amplicons were analysed by 1% agarose gel electrophoresis.

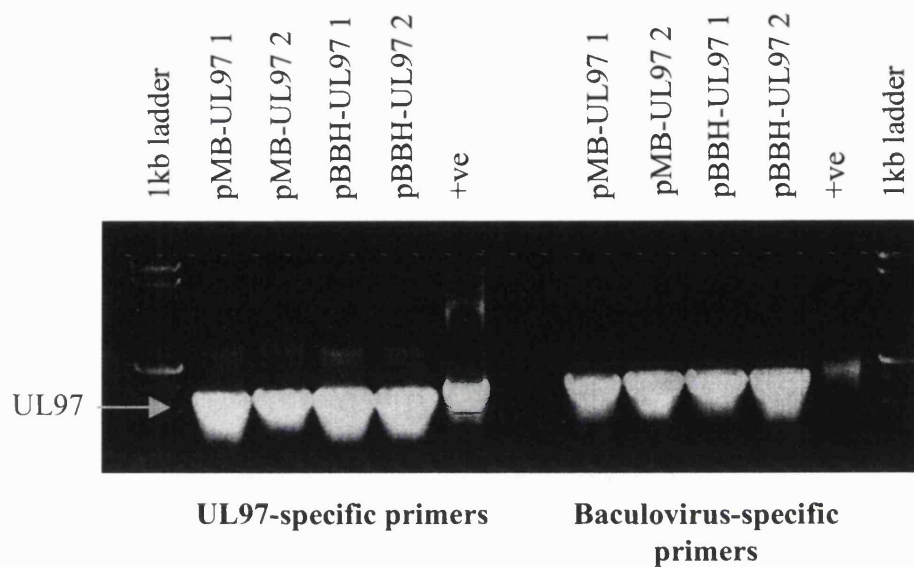


**Figure 4.10. Plaque Purification of the Putative Recombinant Baculoviruses BVBBH-WT and BVMB-WT.**

The cotransfection culture media was serially diluted and subjected to plaque assay at neat, 10<sup>-1</sup> and 10<sup>-2</sup> dilutions in duplicate. The plaque assays were stained with X-Gal and the individually blue stained plaques were picked and analysed for the presence of recombinant UL97-expressing baculovirus.



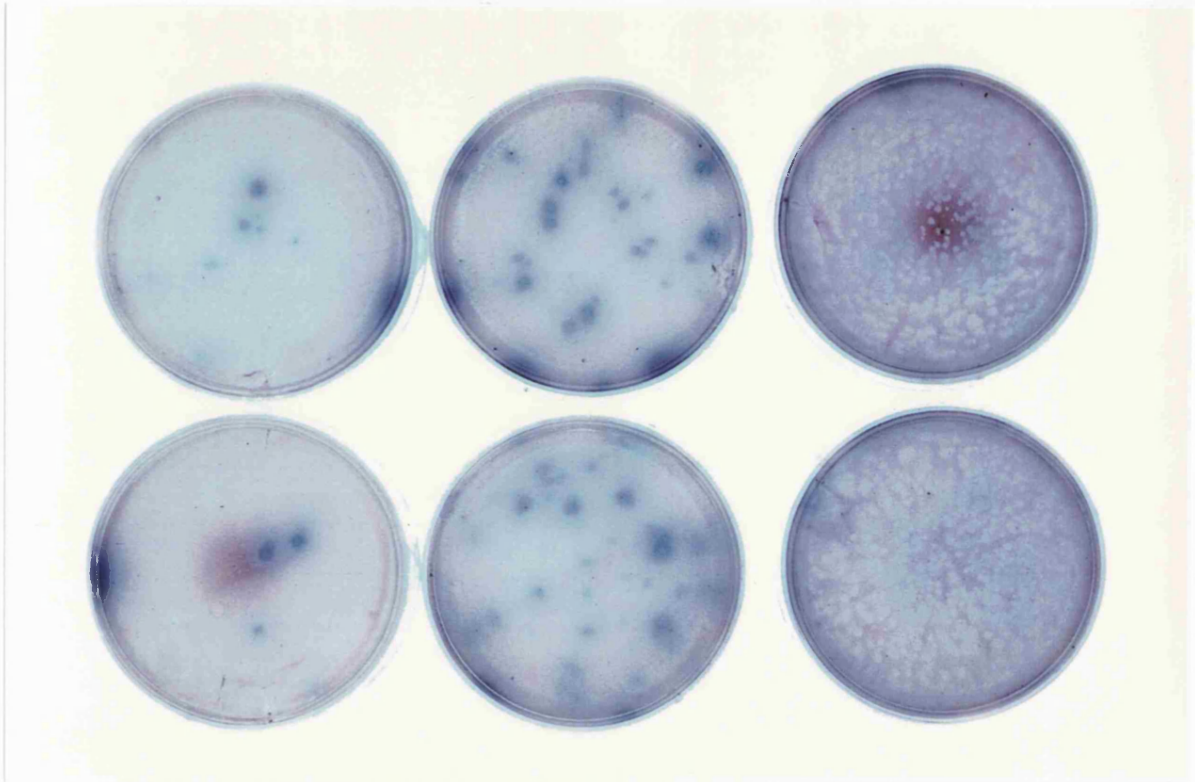


**Figure 4.11. PCR Analysis of Plaque Purified Recombinant Baculoviruses.**

The culture media was harvested from the cotransfection of the baculovirus transfer vectors pMelBac-UL97 and pBlueBacHis with Bac'N' Blue linearized baculovirus DNA into Sf21 insect cells. The media was subjected to plaque assay and putative plaques were picked. Sf21 insect cells were infected with each of the putative recombinant viruses for 4 days, the DNA was harvested from the cells and was subjected to PCR with both UL97-specific and baculovirus-specific primers. The amplicons were analysed by 1% agarose gel electrophoresis.

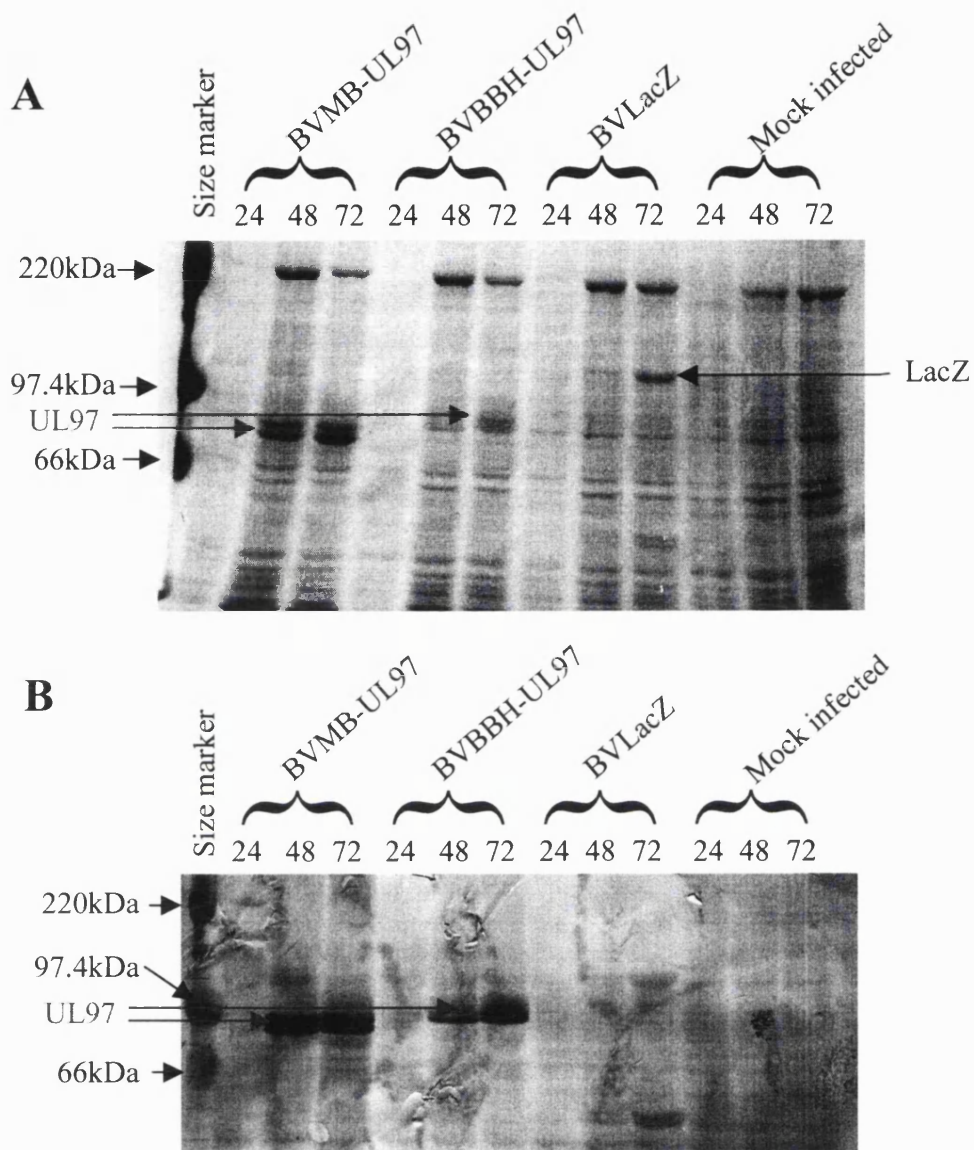


**Figure 4.12. Time Course of UL97 Expression in BVMB-UL97 and BVBBH-UL97 Infected Insect Cells.**

Crude lysates of the Sf21 insect cells infected with the recombinant UL97 baculoviruses BVMB-UL97 and BVBBH-UL97, plus the BVLacZ control and mock infected cells were subjected to SDS-PAGE. Duplicate gels were either stained with Coomassie brilliant blue (A) or electrophoretically transferred to PVDF membrane and analysed by Western blotting (B). Both methods identified a protein product which accumulated from 48 hours post infection of approximately 80-85kDa.

### **4.3. Discussion**

Recombinant baculovirus expression systems are now one of the most common ways for the production of recombinant proteins in a eukaryotic environment. They have the distinct advantage over *E.coli* expression systems whereby eukaryotic post translational modifications are performed and the proteins are largely soluble. Transfer vectors are now widely available which enable the easy purification of the recombinant proteins. These code for N- and C- terminal fusion tags such as GST, hexahistidine and thioredoxin, which are generally supplied with monoclonal antibodies specific to the tags and the honey bee melitin secretion signal to enable secretion of the recombinant protein and purification from tissue culture fluid. Furthermore, technologies have progressed such that the gene of interest can be amplified by PCR and directly cloned into transfer vectors so reducing the time to generate a recombinant baculovirus from a number of weeks to a number of days.

The UL97 sequence was analysed to enable identification of restriction enzymes which do not perform internal digestions on the UL97, and primers were designed to incorporate the restriction sites. The cloning and transfer vectors used to generate the baculovirus contained only one restriction site for the enzymes identified, thus enabling identification of recombinant clones without having to perform complex restriction fragment length polymorphism analysis. The entire UL97 was amplified and cloned into the pGEM-T-easy vector which enables blunt ended PCR products to be cloned by utilising the T overhang generated by every PCR reaction. These vectors dramatically ease the cloning of a PCR product and reduce the time to perform the cloning procedure. The recombinant clones were identified and restricted with the appropriate enzymes to allow the subcloning of the UL97 ORF into the baculovirus transfer vectors. This step can now be performed directly from the PCR product without the need for incorporation of restriction sites in the primers. The TA technology originating in the cloning vectors such as pGEM-T-Easy has been adapted for the directional cloning of PCR products into transfer vectors using topoisomerase I rather than DNA ligase. The 5' primer is designed with CACC at the 5' end to enable the directional cloning and the topoisomerase is covalently bound to the transfer vector to increase the efficiency of ligation. At this point, the gene can be sequenced to ensure both the correct orientation of the gene and the correct DNA sequence.

#### *4.0 Construction of recombinant baculoviruses*

---

The entire UL97 was cloned because expression of recombinant proteins from the transfer vectors pBluBacHis and pMelBac require the cloned gene to provide a start codon (ATG) downstream of the polyhedrin promoter. The recombinant transfer vectors were cotransfected with Bac-n-Blue™ DNA into insect cells using Insectin™ liposomes which are positively charged insect cell specific liposomes. The recombinant plaques were identified by virtue of the blue staining of the plaques due to expression of  $\beta$ -galactosidase upon the addition of X-gal.

The efficiency of the cotransfection procedure greatly depends upon the quality of the transfer vector DNA. For this reason, the large scale preparation of transfer vector plasmid (section 2.1.6) was performed using an endotoxin removal step and anion exchange which efficiently removes contaminating substances. Another important factor which affects the efficiency of cotransfection is the choice of liposome. Insectin was used due to its charged properties, and proved to be efficient. The recombinant plaques were analysed by PCR using baculovirus specific primers, which showed recombination had occurred at the correct loci. The recombinant baculoviruses were expanded into high titre stocks and analysed for protein expression. UL97 was detected by Coomassie brilliant blue staining from 48 hours post infection, typical of the very late polyhedrin promoter kinetics. The expression of MB-UL97 was particularly high, compared with the BBH-UL97 which was somewhat unexpected as historically baculovirus expression of UL97 and the related HHV-6 U69 protein kinase usually occurs at low levels. Secondly, the MB-UL97 has a honey bee melitin secretion signal sequence, designed to enable secretion of UL97 for large scale purification. It has been reported that some proteins are less well expressed in insect cells than others (King and Possee, 1992). For instance it was generally found that glycoproteins, secreted proteins and membrane bound proteins were expressed at lower levels than structural proteins. This may suggest that the melitin secretion signal sequence could lower the expression of the UL97 in insect cells. The expression of the UL97 was good however, especially compared to that of the BBH-UL97 which contained a 4kDa hexahistidine N-terminal fusion. Other reports of protein kinases expressed in insect cells encoding this N-terminal fusion also showed relatively poor expression, suggesting this fusion limits the expression of the protein in such expression systems (Ansari and Emery, 2000, He et al., 1997). The MB-UL97 had to be purified using conventional biochemical

#### *4.0 Construction of recombinant baculoviruses*

---

techniques as it did not contain a purification tag such as the hexahistidine tag of the BBH-U97.

One problem with expression of recombinant proteins from baculovirus-infected insect cells is the constant necessity to infect cells in order to generate the protein of interest. This can now be overcome by the stable transfection of a plasmid fusion containing the gene of interest into insect cell lines, where expression is driven by the baculovirus *Orgyia pseudotsugata* multicapsid nuclear polyhedrosis virus (OpMNPV) promoter, Opie-2. The PCR generated gene of interest is cloned into a donor vector using the topoisomerase method described above. An acceptor vector, containing the appropriate transcription regulatory sequences and the translation initiation sequences, is mixed with the donor vector and recombination occurs via the cre-lox site-specific recombination system using Cre recombinase. The plasmids are transformed into TOP10 E.coli and the recombinants selected by antibiotic resistance markers. The recombinant plasmid is then transfected into insect cells such as Sf9, High Five or Sf21 and stable cell lines expressing the protein of interest are created by blasticidin selection. These cell lines can be used to express the protein either in adherent cell culture or in a suspension culture. The advantages of this system include the stable production of recombinant proteins in a eukaryotic environment, so negating the need for performing continuous infections to produce proteins. A major disadvantage to this technique however was that even under optimal conditions, only 10 – 20% of cells are transformed and the selection of a clonal stable cell line requires careful manipulation. Stable cell lines are created by multiple copy integration of the vector. This can be overcome by generating a polyclonal cell line where the transfected cells are allowed to grow under blasticidin selection while the untransfected cells are killed. Some groups have found relatively high levels of constitutive expression (Hegedus et al., 1999), but others have found protein expression was not as high as might be expected from baculovirus late promoters such as polyhedrin (Jarvis et al., 1996). However, once transformed, the transfected cell lines are maintained in the same manner as uninfected cells but under continuous blasticidin selection.

## **CHAPTER 5**

# **Expression, purification and biochemical analysis of the HCMV UL97**

### 5.1. Introduction

The Baculovirus expression system generally produces large amounts of soluble recombinant protein. Thus the aim of the present study was to express large amounts of the recombinant UL97 protein using the Baculovirus expression system for purification and biochemical analysis of the impact of GCV resistance mutations on the function of UL97. In order to facilitate purification, two recombinant UL97 protein species were made, both designed to use different purification strategies. The first was expressed as a fusion protein with an N-terminal hexahistidine tag. The hexahistidine tag is designed to be used in immobilised metal chelate affinity chromatography (IMCAC) using nickel ions covalently attached to agarose beads. The six histidine residues bind the immobilised Ni<sup>2+</sup>-NTA and elution is performed by competition for the Ni<sup>2+</sup> by providing high concentrations of imidazole or EDTA, which have a higher affinity for the Ni<sup>2+</sup> ions than histidine. The second encoded the honey bee melitin secretion signal to induce the secretion of the UL97 into the tissue culture medium. Serum free suspension cell culture is used for protein secretion experiments as firstly, the protein can be secreted from every surface of the cell in suspension, so increasing the yield of protein. Secondly, purification of a recombinant protein from tissue culture medium, which contains relatively few proteins and no serum, is considerably easier than purification away from total cell proteins.

Mutations were introduced into the UL97-transfer vector by site directed mutagenesis. These mutations included a combination of GCV resistance mutations, a 1263W94 resistance mutation and structural mutations to examine the relative importance of specific amino acid residues within catalytic domains of the UL97 kinase. The most frequently described GCV resistance mutations occur in codons 460, 520, 594 and 595 as discussed in chapter 3. The 520, 594 and 595 mutations occur in the region of the UL97 kinase proposed to be responsible for substrate recognition. Although GCV is a nucleoside analogue and its mode of action depends upon the initial phosphorylation by UL97, UL97 is not a nucleoside kinase so it is somewhat surprising that UL97 uses GCV as a substrate. This begs the question, how exactly do the mutations affect the function of the kinase with respect to GCV phosphorylation and indeed, do they affect the natural function of the protein since they reside in the substrate recognition domain. Mutations occurring at codon 460 are more surprising since this codon occurs within the conserved kinase domain HRDLKXXN,

although the codon corresponds to a non-conserved amino acid, as described in chapter 1. This motif forms the catalytic loop responsible for phosphotransfer, so it is reasonable to assume mutations at codon 460 may impair phosphotransfer.

The data presented in this chapter describes the optimisation of the expression of recombinant UL97 as both a hexahistidine tagged protein and as a secreted protein. Optimisation of the secretion of UL97 into tissue culture medium was performed. The proteins were purified to near homogeneity using conventional biochemical purification techniques including ammonium sulphate precipitation and anion exchange chromatography. The purified UL97 was used to analyse the enzyme kinetics of autophosphorylation of each of the wild type and mutant UL97 proteins.

## 5.2. Results

### 5.2.1. Preparation of soluble protein extracts from insect cells

Sf21 insect cells were infected at an MOI of 10 with the baculoviruses BVMB-UL97, BVBBH-UL97, BVLacZ or were mock infected. The cells were harvested at 24, 48 or 72 hours post infection and the crude cell lysates were prepared as in section 2.4.1. The insoluble proteins and cell debris were removed by centrifugation and the soluble fraction was subjected to SDS-PAGE. The proteins were analysed by staining with Coomassie brilliant blue or were electrophoretically transferred onto PVDF membrane (section 2.4.6) and probed with either anti-RGS His antibody or anti-UL97 monoclonal antibody. Figure 5.1. shows the MB-UL97 can be identified on the Coomassie brilliant blue stained gel and the Western blot. The BBH-UL97 was not identified on the Coomassie blue gel but was readily detectable on the Western blot, (figure 5.1 is identical to figure 4.10).

### 5.2.2. Protein kinase assay of the soluble crude lysate of Baculovirus infected cells

To determine if the UL97 expressed by insect cells was functional, crude lysates from BVMB-UL97, BVBBH-UL97, BVLacZ and mock infected insect cells were subjected to a protein kinase assay (section 2.5.1) for 30 minutes at 37°C. The reactions were terminated by the addition of sample buffer, subjected to SDS-PAGE and exposed to autoradiography. The assay analyses the catalysis of transfer of the  $\gamma$ -radiolabelled phosphates from ATP to UL97 itself (autophosphorylation). The autoradiograph showed a major radiolabelled



protein species, which co-migrated with UL97 as shown in the Western blot (figure 5.1), accumulated from 48 hours to 72 hours (figure 5.2). This protein species was not present in the crude lysates from mock infected and BVLacZ infected insect cells, indicating UL97 was becoming phosphorylated.

### 5.2.3. Secretion of UL97 from infected insect cells

The Baculovirus BVMB-UL97 encodes the Honey bee melitin secretion signal sequence fused to the recombinant UL97 to enable the secretion of UL97 following expression. To determine if the UL97 is secreted from Sf9 serum free insect cells in suspension culture,  $10^7$  Sf9 cells in 10ml Sf900 serum free medium were infected with BVMB-UL97, BVBBH-UL97, BVLacZ or mock infected at an MOI 5 for 1 hour. The cells were centrifuged and the medium was replaced with 50ml fresh medium. The cells and culture medium was harvested at 24, 48, 72 and 96 hours post infection. The tissue culture fluid was concentrated using a Centricon 50 concentration tube and the crude cell lysate was prepared as in section 2.4.1. The crude lysate and concentrated culture medium were subjected to SDS-PAGE and the proteins were either stained with Coomassie brilliant blue or electrophoretically transferred to PVDF membrane. The MB-UL97 was detected in the crude lysates of the insect cells by Western blot accumulating from 48 hours (figure 5.3), but no such species was detected in the BVLacZ or mock infected cells. MB-UL97 was not detected in the concentrated culture medium in either the Western blot (figure 5.4) or the Coomassie brilliant blue stained gel (figure 5.5).

### 5.2.4. Optimisation of secretion of UL97 from infected insect cells

Sf9 insect cells were infected or mock infected with BVMB-UL97 and BVLacZ at an MOI of 10, 15 and 20. The viruses had previously been passaged through Sf9 serum free insect cells and titred by plaque assay. The cells and culture medium were harvested at 24, 48, 72 and 96 hours post infection. The crude lysate and the concentrated culture medium were subjected to SDS-PAGE and the proteins stained with Coomassie brilliant blue or electrophoretically transferred to PVDF membrane and probed with anti-UL97 monoclonal antibody. UL97 was detected by Western blot (figure 5.6) in the crude lysate of the infected cells, accumulating from 48 hours post infection. UL97 was not detected in the

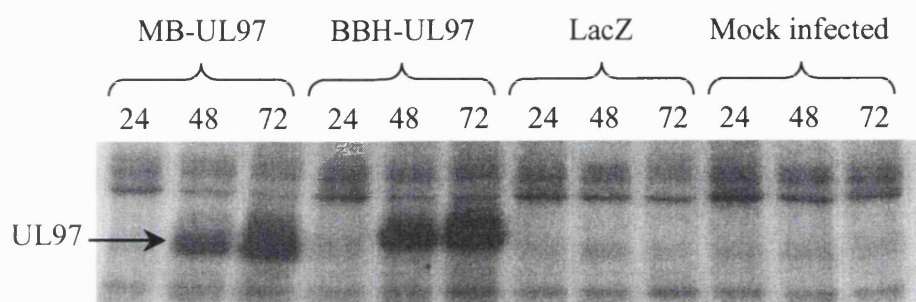


**Figure 5.1. Phosphorylation of Baculovirus expressed UL97.**

Insect cells were infected with BVMB-UL97, BVBBH-UL97, BVLacZ or mock infected and harvested at 24, 48 or 72 hours post infection. The protein extracts were subjected to a protein kinase assay, separated by SDS-PAGE and exposed to autoradiography. A major phosphorylated species was identified from 48 hours post infection and was optimal at 72 hours post infection. The phosphorylated species comigrated with the recombinant UL97 identified by Western blot. The histidine-tagged (BBH) UL97 migrated slower than the melitin-tagged (MB) UL97.

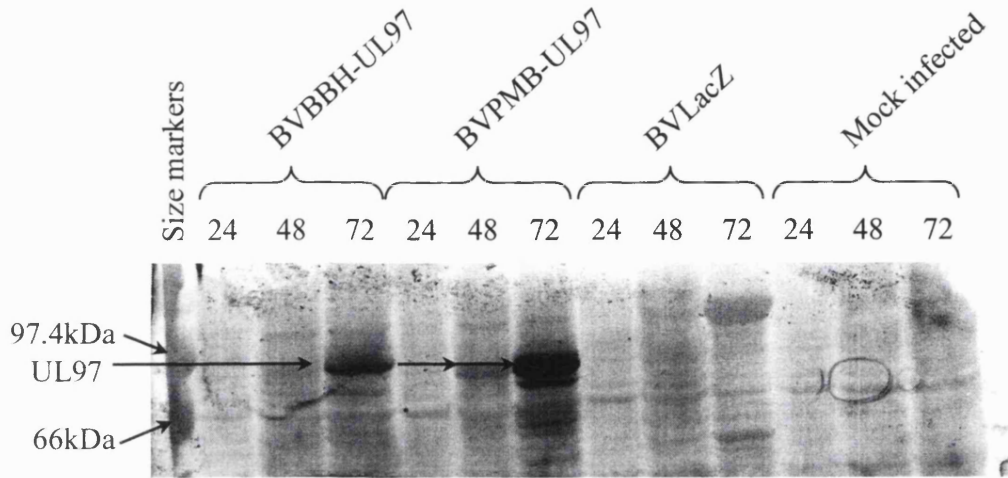


**Figure 5.2. Time Course of Expression of UL97 in Recombinant Baculovirus Infected Serum Free Insect Cells.**

Crude lysates of Sf9 serum free insect cells infected with BVBBH-UL97, BVMB-UL97, and BVLacZ at an MOI 5 and mock-infected cells were subjected to SDS-PAGE and Western blot. Maximal UL97 expression was observed at 72 hours post infection, as in Sf21 cells. No signal was detected in the BVLacZ or the mock infected cells.

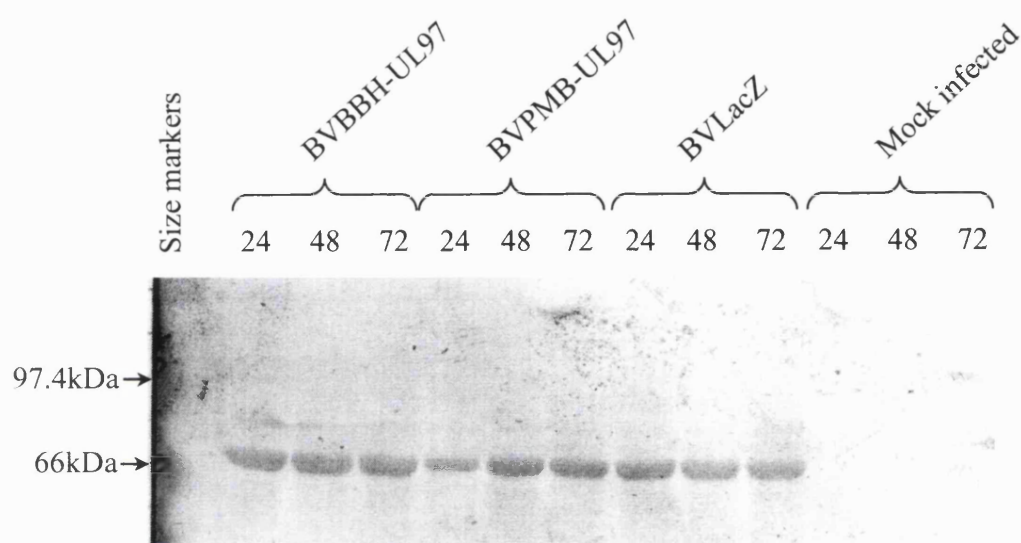


**Figure 5.3. Time Course of UL97 Expression and Secretion from Sf9 Serum Free Insect Cells.**

The tissue culture medium from Sf9 serum free insect cells infected with BVMB-UL97, BVBBH-UL97, BVLacZ and mock infected cells was harvested at 24, 48 and 72 hours post infection. The medium was subjected to SDS-PAGE and Western blot. UL97 was not detected in the medium at any stage during the time course, or when maximal UL97 expression was observed in the crude cell lysate.

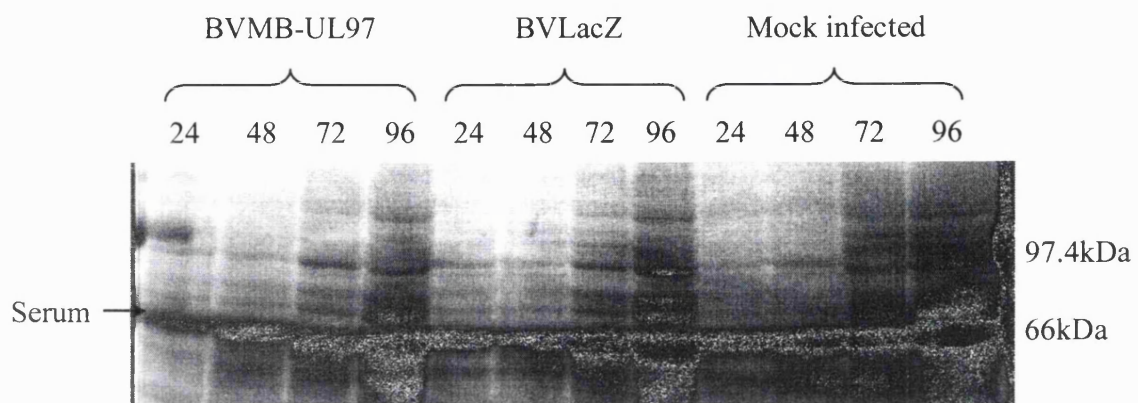


**Figure 5.4. Expression and Secretion of Recombinant UL97 from Serum Free Insect Cells Following Protein Concentration.**

Sf9 serum free insect cells were infected at an MOI 5 for 24, 48, 72 and 96 hours. The culture medium was harvested at each time point, concentrated using a Centricon 50 concentration tube, subjected to SDS-PAGE and stained with Coomassie brilliant blue. UL97 was not detected in the concentrated culture medium at any time point. Serum was detected suggesting the virus should be passaged through serum free cells to ensure its removal.

corresponding concentrated culture medium at any time point or MOI by either Western blot (figure 5.7) or the Coomassie brilliant blue stained gel (figure 5.8).

### 5.2.5. Optimisation of the ammonium sulphate precipitation

The crude lysate of the BVMB-UL97 infected insect cells was made up to 100ml with 50mM Tris HCl, pH 7.6, 100mM NaCl. Ammonium sulphate was added to give a 10%, 20%, 30%, 40%, 50% and 60% saturation of the protein solution as in section 2.4.2. Following each cut, the precipitated proteins were removed by centrifugation at 4°C, dissolved in 1ml 50mM Tris HCl, pH 7.6, 100mM NaCl and dialysed in this buffer overnight at 4°C. The insoluble protein pellets were removed by centrifugation and both the soluble and insoluble fractions were subjected to SDS-PAGE, stained with Coomassie brilliant blue or electrophoretically transferred to PVDF membrane and probed with anti-UL97 monoclonal antibody. The UL97 was not detected when stained with Coomassie brilliant blue (figure 5.9). The majority of UL97 detected by Western blot (figure 5.10) was precipitated between 20% to 40% ammonium sulphate and all the UL97 detected was insoluble.

### 5.2.6. Optimisation of the solubility of UL97

The crude lysate of BVMB-UL97 infected cells was subjected to a 20% to 40% ammonium sulphate precipitation, re-dissolved in 50mM Tris HCl at pH 7.0, 7.5, 8.0 and 8.5, 100mM NaCl. The precipitated proteins were dialysed to 1/10 000 dilution of ammonium sulphate in 50mM Tris HCl, 100mM NaCl, at the same pH in which the proteins were dissolved. The insoluble proteins were pelleted by centrifugation and both the soluble and insoluble fractions were subjected to SDS-PAGE, stained with Coomassie brilliant blue or electrophoretically transferred to PVDF membrane for Western blot (figure 5.11). The optimal solubility of UL97 occurred when the proteins were re-dissolved in 50mM Tris HCl, pH 8.5, 100mM NaCl (figure 5.11). To increase the solubility of the proteins following precipitation, 1% Triton-X-100 or 0.5% Sarkosyl was added to the buffer. This did not result in an increase in solubility of the UL97.

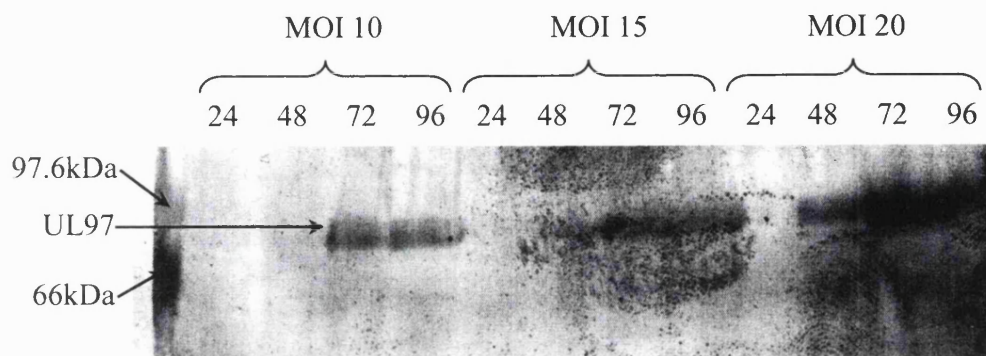


**Figure 5.5. Western Blot of MOI Optimisation for UL97 Expression and Secretion.**

Crude lysates of serum free Sf9 insect cells infected with BVMB-UL97 at an MOI 10, 15 or 20 were subjected to SDS-PAGE and Western blot. The recombinant UL97 was expressed from 48 hours post infection and was optimal by 72 hours post infection.

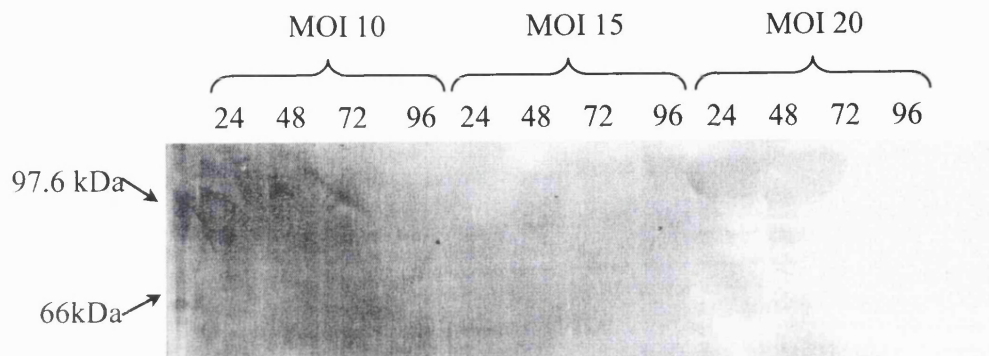


**Figure 5.6. Western Blot of concentrated secreted proteins from BVMB-UL97 infected insect cells.**

The tissue culture medium was harvested from Sf9 insect cells infected with BVMB-UL97 at an MOI of 10, 15 or 20. The medium was concentrated using Centricon 50 concentration tubes, subjected to SDS-PAGE and Western blot. UL97 was not detected in the concentrated protein supernatant at any time point post infection, or at any MOI.



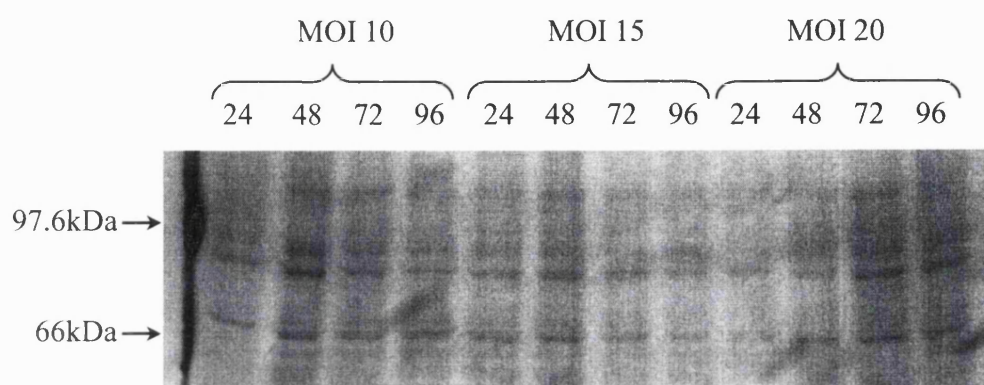


**Figure 5.7. Optimisation of Secretion of UL97 from BVMB-UL97 Infected Insect Cells.** The culture medium from Sf9 insect cells infected at an MOI 10, 15 or 20 by BVMB-UL97 was harvested from 24 to 96 hours post infection, concentrated and subjected to SDS-PAGE. The gel was stained with Coomassie brilliant blue, but UL97 was not detected in the concentrated culture supernatant at any MOI or for up to 96 hours post infection.

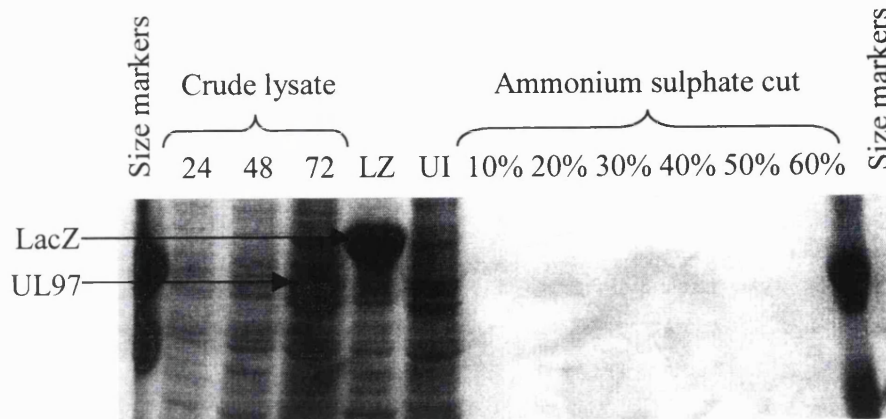


**Figure 5.8. Optimisation of the Ammonium Sulphate Precipitation.**

The crude lysate of insect cells infected with BVMB-UL97, expressing UL97 was subjected to a 10% to 60% ammonium sulphate precipitation. The proteins precipitated out at each cut were pelleted, resuspended in 50mM Tris HCl, pH 7.6, 100mM NaCl, dialysed overnight at 4°C and subjected to SDS-PAGE. The gel was stained with Coomassie brilliant blue and UL97 was observed at 72 hours post infection in the crude lysate, but not observed following precipitation.

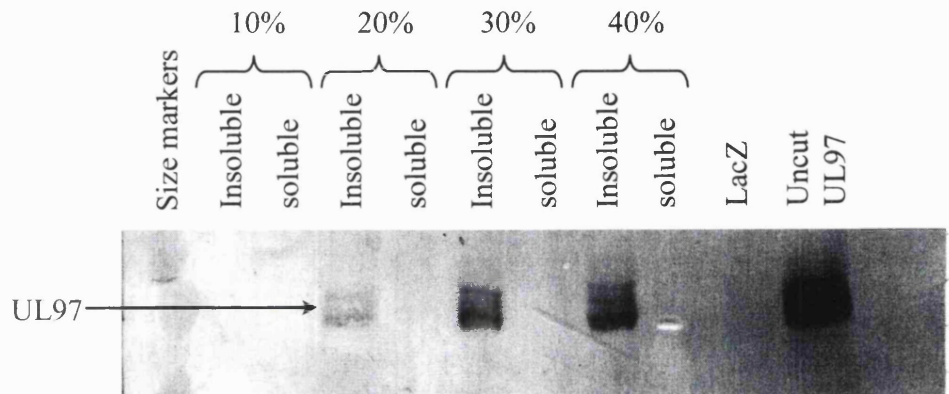


**Figure 5.9. Optimisation of the Ammonium Sulphate Precipitation.**

The crude lysate of the BVMB-UL97 infected cells was subjected to a 10% to 60% ammonium sulphate precipitation. The precipitated proteins were resuspended in 50mM Tris HCl, pH 7.6, 100mM NaCl, dialysed overnight at 4°C and the insoluble proteins were pelleted. The soluble and insoluble fractions were subjected to SDS-PAGE and Western blot. The majority of UL97 was precipitated between 20% to 40%, but the majority of the UL97 was insoluble.

### 5.2.7. Anion exchange chromatography

The crude lysate of BVMB-UL97 infected cells was subjected to a 20% to 40% ammonium sulphate precipitation. The precipitated proteins were dialysed in 50mM Tris HCl, pH 8.5, 100mM NaCl at 4°C to give a total dilution of 1/10 000 of the ammonium sulphate. The insoluble proteins were removed by centrifugation and the soluble fraction was applied to DEAE cellulose. The anion exchange chromatography was optimised by binding the UL97 to the DEAE cellulose in either 20mM Piperazine which has optimal buffering capacity of pH 5.0 to 6.0, 20mM bis-Tris propane (pH 6.5 to 7.0), 20mM Tris HCl (pH 7.5 to 8.5) and 20mM Ethanolamine (pH 9.0). The binding was performed at 4°C for 1 hour and the proteins were eluted in 1M NaCl in their respective buffers. The eluted proteins were initially concentrated with a Centricon-50 concentration tube then subjected to SDS-PAGE and either stained with Coomassie brilliant blue (data not shown) or electrophoretically transferred to PVDF membrane and probed with anti-UL97 monoclonal antibody (figure 5.12). The majority of UL97 was eluted from the DEAE cellulose at pH 8.0 and 8.5, although a large proportion of the UL97 was eluted at pH 6.0. Thus the optimal conditions for binding UL97 to DEAE cellulose occurred in 20mM Tris HCl, pH 8.0, 20mM NaCl. An optimal salt concentration for elution of the UL97 occurred at 0.5M NaCl with a prior wash in 20mM Tris HCl, pH 8.5, 50mM NaCl to remove contaminating proteins.

### 5.2.8. Immunoprecipitation of UL97

The UL97 purified to near homogeneity by ammonium sulphate precipitation and anion exchange chromatography was subjected to immunoprecipitation using a mouse anti-UL97 monoclonal antibody as described in section 2.4.4. The antigen-antibody complex was disassociated in by centrifugation in disassociation buffer at either pH 2.5 or pH 9.0 and immediately neutralised in 0.2 volumes of Tris HCl, pH 9.0. Aliquots of the protein were subjected to SDS-PAGE and exposed to autoradiography (figure 5.14).

### 5.2.9. Purification of the recombinant wild type and mutant UL97 proteins.

The wild type and mutant UL97 proteins were subjected to ammonium sulphate precipitation followed by anion exchange chromatography, concentration and subjected to SDS-PAGE and either stained with Coomassie brilliant blue (figure 5.13 A and B) or electrophoretically transferred to PVDF membrane and probed with an anti-UL97

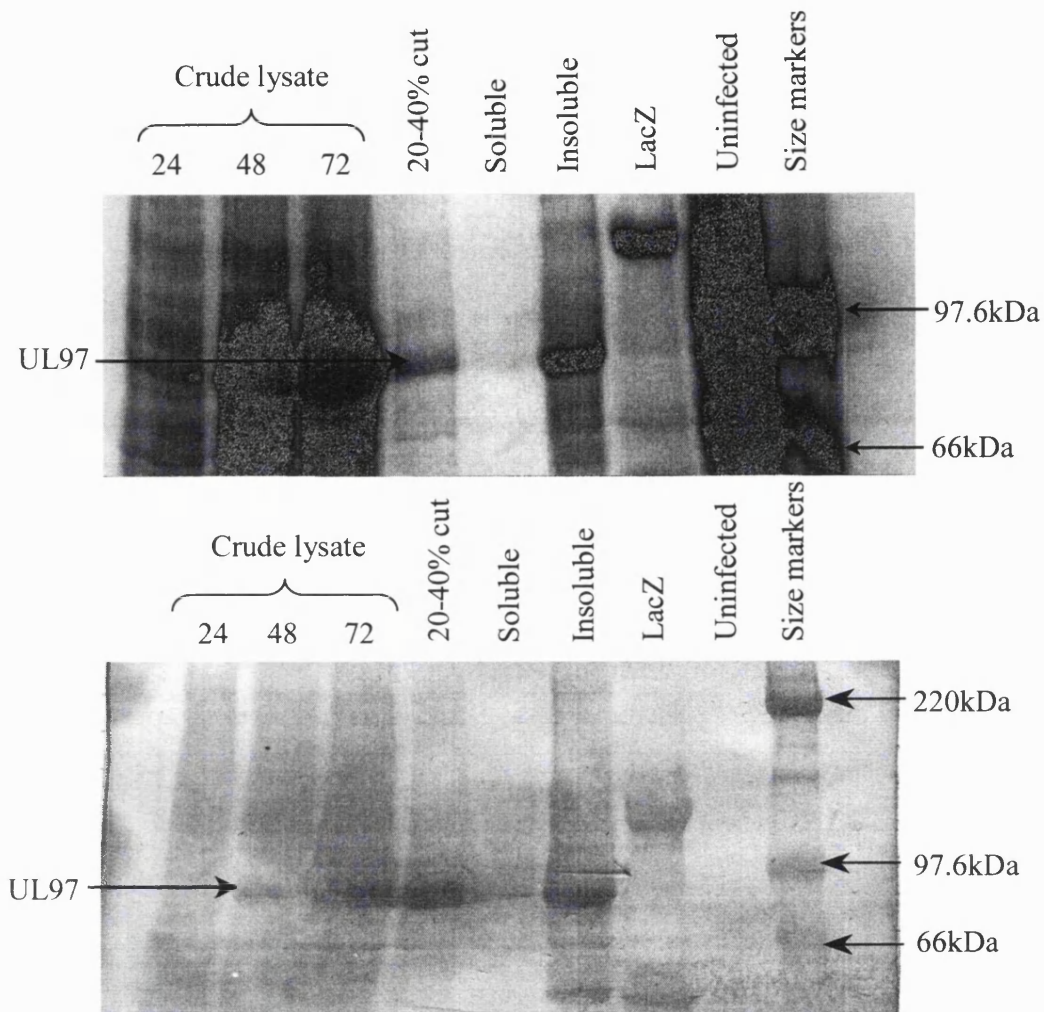


**Figure 5.10. Ammonium Sulphate Precipitation of UL97.**

The crude lysate of BVMB-UL97 infected insect cells was subjected to a 20% to 40% ammonium sulphate precipitation. The precipitated proteins were dialysed overnight at 4°C in 50mM Tris HCl, pH 8.5, 100mM NaCl and centrifuged to remove the insoluble proteins. SDS-PAGE was performed on the soluble and insoluble proteins and the gel was stained with Coomassie brilliant blue. The majority of the UL97 remained insoluble, but a very small proportion of the UL97 was soluble.

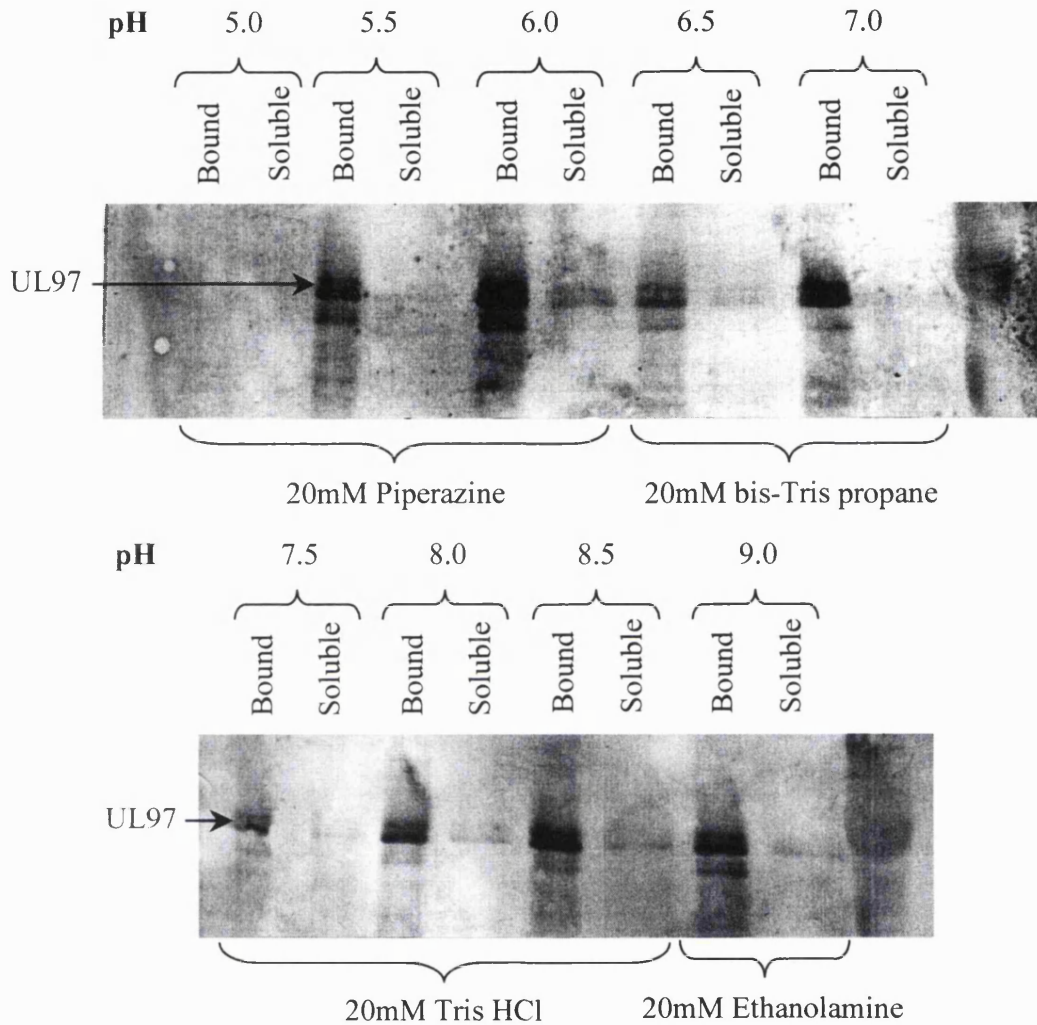


**Figure 5.11. Optimisation of Anion Exchange Chromatography.**

The crude lysate of BVMB-UL97 infected cells was subjected to a 20% to 40% ammonium sulphate precipitation and the precipitated proteins dialysed O/N to give a total of 1/10 000 ammonium sulphate. The soluble proteins were subjected to anion exchange (DEAE cellulose) chromatography to optimise the pH for protein binding to the DEAE. The proteins were eluted in 1M NaCl in their respective buffers. Following SDS-PAGE and Western blot, the majority of UL97 was found to be eluted in 20mM Tris HCl, pH 8.0 to 8.5 and was soluble, although protein was also eluted in pH 6.0.



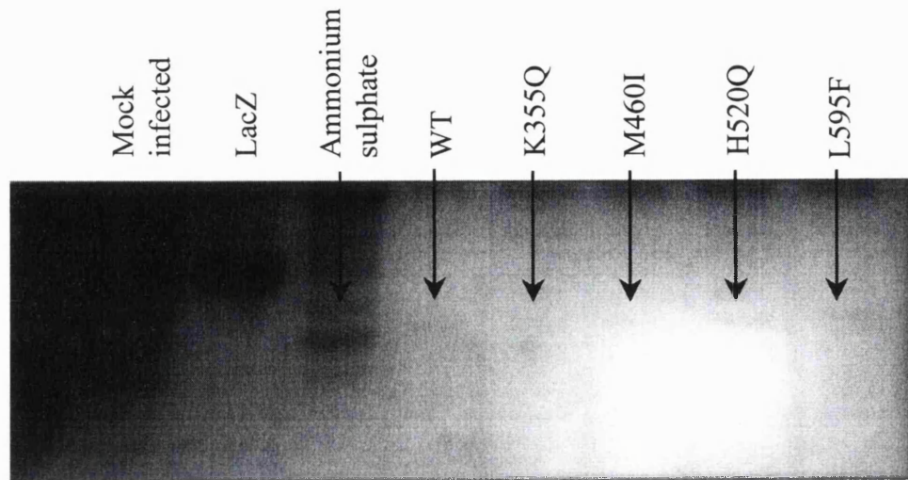


**Figure 5.12 A. Purification of the Wild Type and Mutant UL97 proteins.**

The wild type and mutant UL97 proteins were purified to near homogeneity using a combination of ammonium sulphate precipitation followed by anion exchange chromatography. The proteins were concentrated to approximately 50 $\mu$ l and subjected to SDS-PAGE followed by Coomassie brilliant blue stain (upper panel) or Western blot using an anti-UL97 monoclonal antibody. One band is visible on the Coomassie stained gel, which comigrated with the UL97 detected by Western blot.

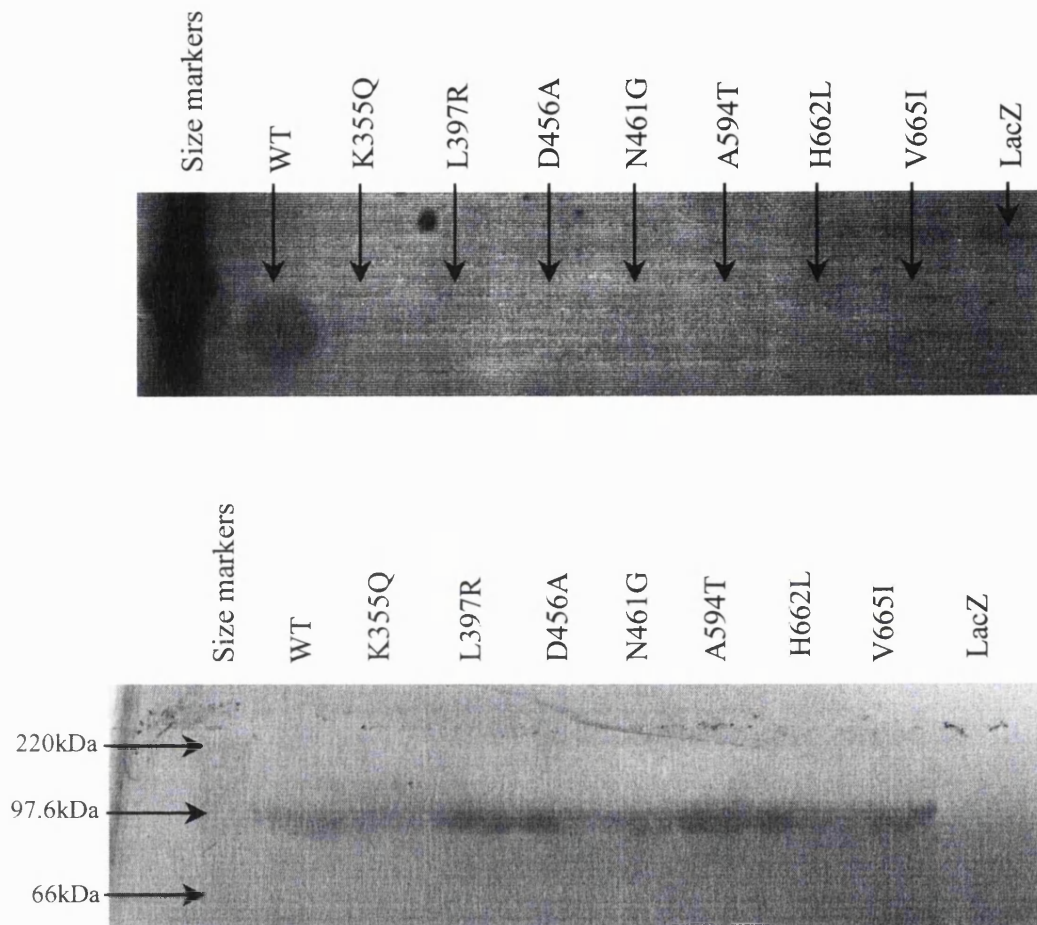


**Figure 5.12 B. Purification of the wild type and mutant UL97 proteins.**

The wild type and mutant UL97 proteins were purified to near homogeneity. The single bands detected in the Coomassie blue stained gel (upper panel) comigrated with the UL97 detected by Western blot (lower panel).



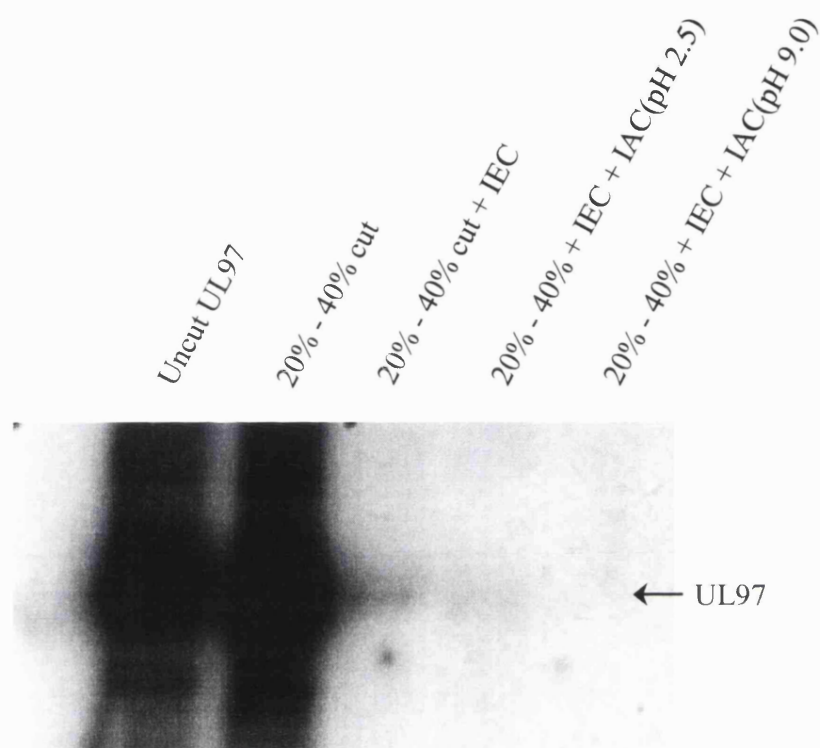


**Figure 5.13. Immunoprecipitation of UL97**

UL97 was initially subjected to ammonium sulphate precipitation, concentrated, ion exchange chromatography then immuno-affinity chromatography using an anti-UL97 monoclonal antibody. The antibody-antigen complex was dissociated in buffer at pH 2.5 or 9.0 and the purified UL97 subjected to a protein kinase assay. Following SDS-PAGE, the gel was exposed to film and the autoradiograph is shown. Only a small portion of the UL97, which was eluted at pH 2.5 with immediate neutralisation, was active.

monoclonal antibody (figure 5.13 A and B). One major single band was observed on the Coomassie blue stained gel, which comigrated with the UL97 probed on the Western blot. This suggested the proteins were purified to near homogeneity.

### 5.2.10. Analysis of UL97 autophosphorylation.

The autophosphorylation reaction of UL97 was investigated with respect to time using ATP as the phosphate donor. The protein kinase reactions were performed from 2 to 60 minutes and analysed by SDS-PAGE and autoradiography. The amount of radiolabel incorporated at each time point was determined using the BioRad Multianalyst and the density of each band determined against the incubation time. The maximum rate of phosphate incorporation occurred during the first 20 minutes of the reaction and reached equilibrium after 40 minutes.

### 5.2.11. Enzyme kinetic analysis of autophosphorylation.

In order to analyse the enzyme kinetics of autophosphorylation, the Michaelis constant ( $K_m$ ) for ATP was determined. UL97 was subjected to a protein kinase assay for 5 minutes, at which time the rate of phosphate incorporation was maximal as shown in section 5.2.8. The protein kinase assay reaction conditions were constant, but each assay was performed with increasing concentrations (2 to 20 $\mu$ M) of ATP. The reactions were examined by autoradiography (figure 5.15A) and the amount of phosphate incorporation was determined using the BioRad Multianalyst. The phosphate incorporation was plotted against ATP concentration ( $\mu$ M, figure 5.15B) and Lineweaver Burke plots were generated (figure 5.17).

The best fit straight lines were determined and extrapolated to the x-axis, enabling the calculation of the  $K_m$  value for ATP.

Straight line equation;

$$y = 14.85x + 0.55$$

$$\text{If } y = 0$$

$$\text{Then } (-1/K_m) x = -0.036$$

$$\text{Therefore } K_m = 27\mu\text{M}$$

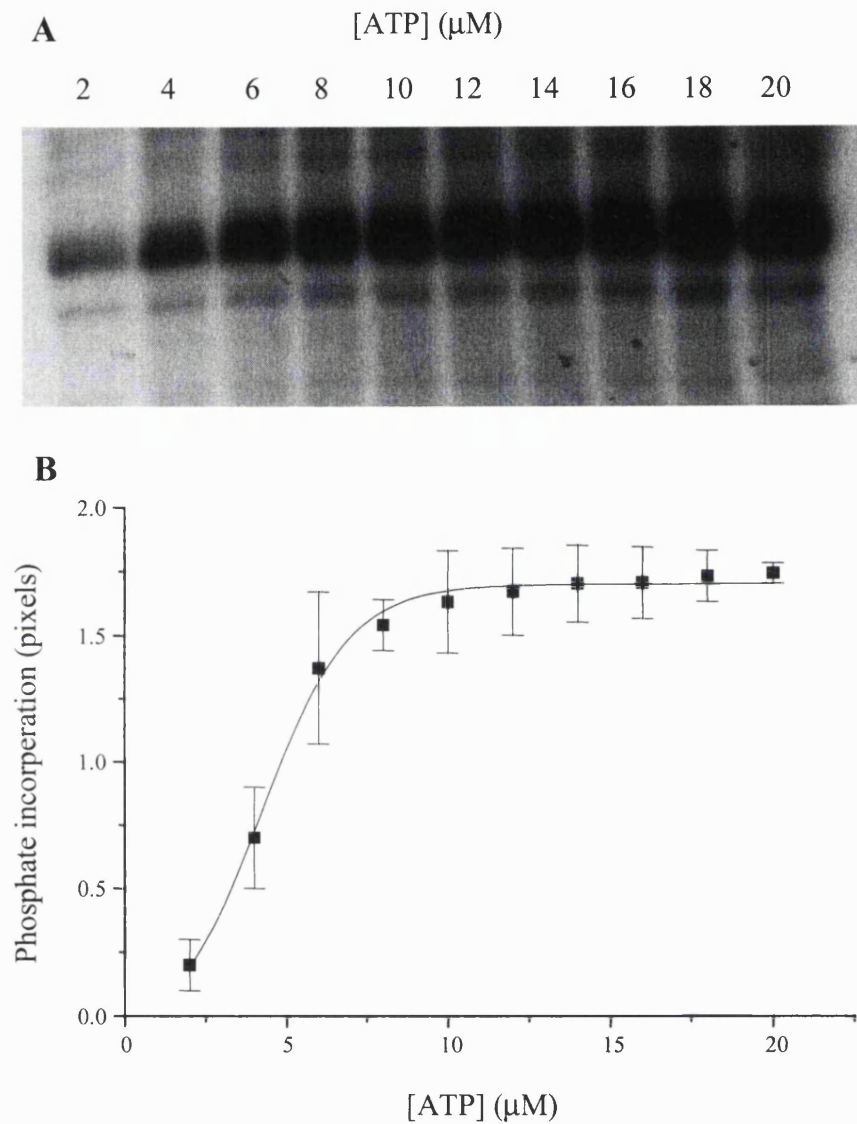


**Figure 5.14. Analysis of UL97 Autophosphorylation.**

The autophosphorylation of UL97 (panel A) was analysed by the BioRad Multianalyst and the density of each band was plotted against the corresponding ATP concentration (panel B).

### 5.2.12. Analysis of mutant UL97 autophosphorylation

MB-UL97 was purified to near homogeneity using ammonium sulphate precipitation followed by anion exchange chromatography. The resulting proteins were subjected to protein kinase assays in order to examine the effect of single point mutations in the UL97 gene upon the autophosphorylation of the protein. The kinase assays were performed on the same concentrations of UL97 proteins at 37°C for 30 minutes, terminated and analysed by SDS-PAGE and autoradiography. The densities of each phosphorylated UL97 species were determined using the BioRad Multianalyst and the densities of the mutant phosphorylated UL97 species were plotted against the phosphorylated wild type UL97 (figure 5.17). Autophosphorylation of the UL97 species containing the point mutations, which confer clinical GCV resistance H520Q, A594T and L595F exhibit phosphorylation to levels equivalent to the wild type UL97. The M460I mutant exhibited approximately 85% of the phosphorylation levels of the wild type UL97. The mutation of the invariant lysine K355Q completely inhibited the phosphorylation of the protein as did the mutation N461G. The mutation conferring 1263W94 resistance L397R resulted in a reduction in phosphorylation of approximately 92%. The remaining mutations occurring within the UL97 gene (D456A, H662L and V665I) did not result in any change in autophosphorylation compared to the wild type UL97.

### 5.2.13. Enzyme kinetic analysis of mutant UL97 autophosphorylation

Enzyme kinetic analyses were performed upon the wild type and mutant UL97 proteins to calculate the Michaelis constants ( $K_m$ ) for ATP. The near purified UL97 proteins were incubated in a protein kinase assay for 5 minutes (to avoid the reaction reaching equilibrium) in constant reaction conditions, but with increasing ATP concentrations (2 $\mu$ M to 20 $\mu$ M). The amount of phosphate incorporated was determined by measuring the density of the UL97 bands following autoradiography. The phosphate incorporation was plotted against the corresponding ATP concentrations and Lineweaver Burke plots were generated by plotting the reciprocal of the phosphate incorporation against the reciprocal of ATP concentration (figures 5.18). The best fit lines were determined with extrapolation to the x-axis, from which the  $K_m$  values for ATP were calculated. The  $K_m$  of ATP for the wild type UL97 was 27 $\mu$ M (SD: 2.2 $\mu$ M) and for the mutants, the  $K_m$  values were as follows: 460 was

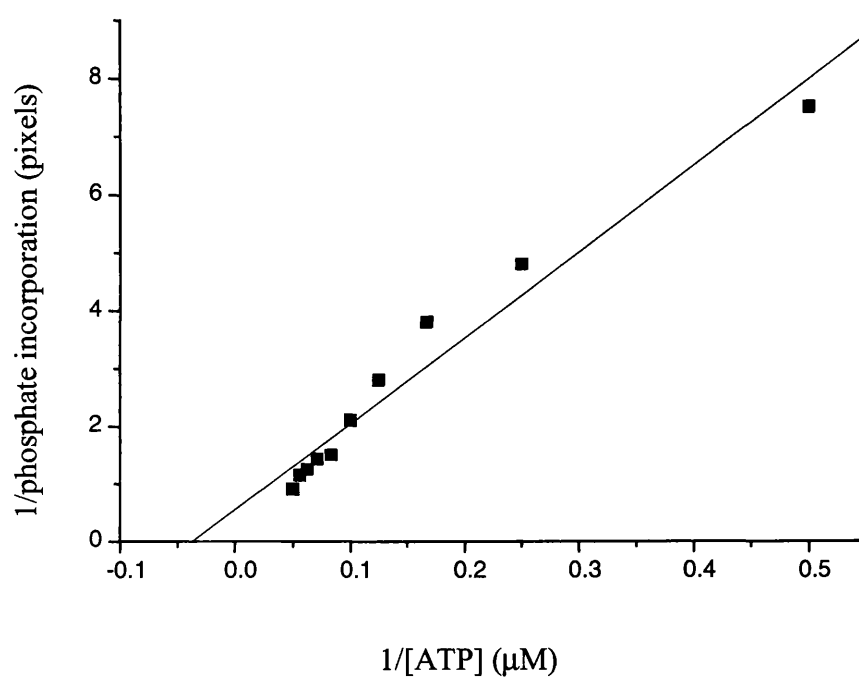


**Figure 5.15. Lineweaver Burke Analysis of UL97 Autophosphorylation.**

The inverse of the velocity of autophosphorylation was plotted against the corresponding inverse of the ATP concentration. The straight line equation was determined and the  $K_m$  value deduced.

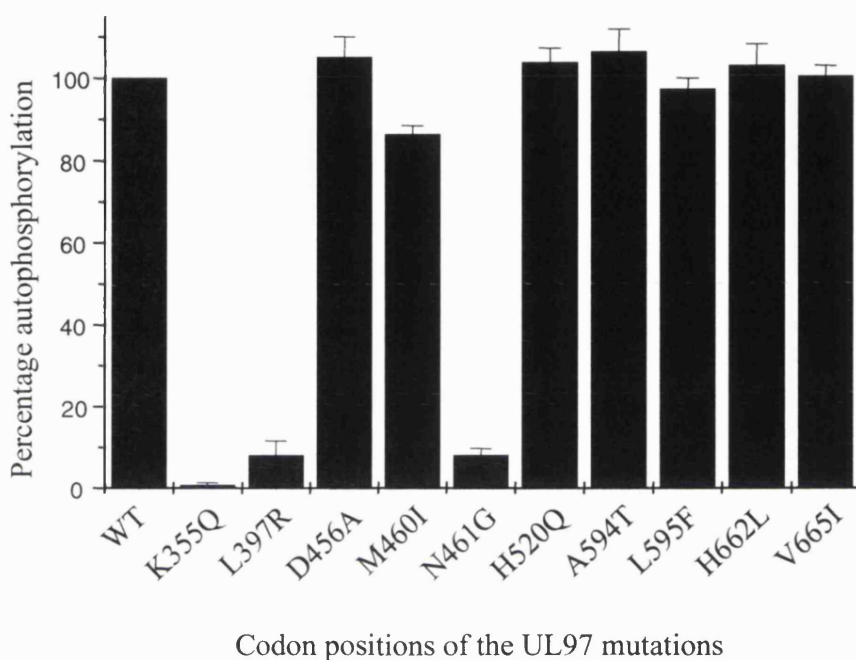


**Figure 5.16. Autophosphorylation of the Recombinant Mutant and Wild Type UL97.**

Insect cells were infected with the wild type and mutant recombinant UL97 baculoviruses at an MOI 10 and harvested 72 hours post infection. The wild type and mutant UL97 proteins were purified to near homogeneity and subjected to a protein kinase assay, separated by SDS-PAGE and exposed to film. The autoradiograph was analysed by the BioRad Multianalyst and the phosphorylation of each mutant UL97 species was compared to that of the wild type UL97.

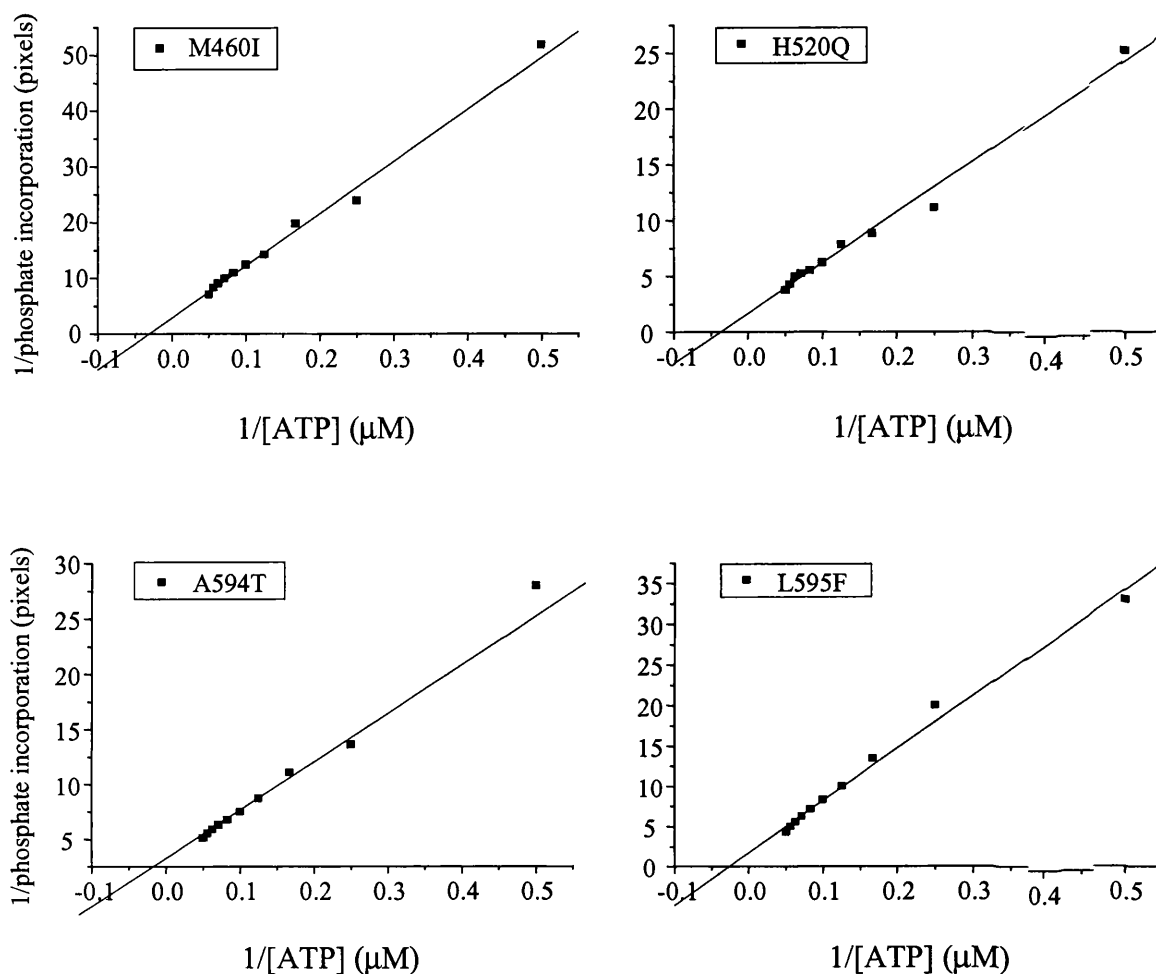


**Figure 5.17. Lineweaver Burke Analysis of UL97 Autophosphorylation of the Mutant UL97 Species.**

UL97 species encoding the mutations observed in clinical resistance were purified to near homogeneity. Protein kinase assays containing increasing concentrations of ATP (2 μM to 20 μM) were performed and the inverse of the velocity of autophosphorylation was plotted against the corresponding inverse of the ATP concentration. The  $K_m$  and  $V_{max}$  values were determined for each of the UL97 species.

28 $\mu$ M (SD: 2 $\mu$ M), 520 was 25 $\mu$ M (SD: 2.4 $\mu$ M) , 594 was 40 $\mu$ M (SD: 4.2 $\mu$ M) and 595 was 31 $\mu$ M (SD: 4.5 $\mu$ M).

Calculation of Km values for UL97 mutants:

**M460I**

Straight line equation;

$$y = 93.0 x + 2.93$$

If  $y = 0$

$$\text{Then } (-1/K_m) x = -0.035$$

Therefore  $K_m = 28\mu\text{M}$

**A594T**

Straight line equation;

$$y = 51.3 x + 1.94$$

If  $y = 0$

$$\text{Then } (-1/K_m) x = -0.025$$

Therefore  $K_m = 40\mu\text{M}$

**H520Q**

Straight line equation;

$$y = 45.1 x + 1.71$$

If  $y = 0$

$$\text{Then } (-1/K_m) x = -0.04$$

Therefore  $K_m = 25\mu\text{M}$

**L595F**

Straight line equation;

$$y = 64.98 x + 1.72$$

If  $y = 0$

$$\text{Then } (-1/K_m) x = -0.032$$

Therefore  $K_m = 31\mu\text{M}$

### **5.3. Discussion**

In order to perform the functional analysis of recombinant UL97, soluble protein was required. Soluble protein was obtained by harvesting the Baculovirus infected insect cells at specific time points and sonication in buffer previously described by He et al., (1997) to maintain UL97 in a soluble form. The insoluble cellular material was removed by centrifugation and the soluble fraction was analysed by Coomassie brilliant blue and Western blot using an anti-UL97 Mab. The UL97 could be detected by both Coomassie brilliant blue staining and by Western analysis, confirming the solubility of UL97 when expressed in insect cells.

In order to ensure the soluble protein retained its functionality, in the form of autophosphorylation, BV-UL97, BV-lacZ and mock infected cellular extracts were subjected to protein kinase assays. These revealed the accumulation of a major radiolabelled protein species, which appeared from 48 hours post infection, consistent with polyhedrin promoter kinetics. The radiolabelled protein co-migrated with the UL97 as detected by



## 5.0 UL97 Expression, purification and biochemistry

---

Western analysis, so confirming the catalysis of the transfer of the  $\gamma$ -phosphate from [ $\gamma^{32}\text{P}$ ] ATP. The radiolabelled protein band was not present in either the BVLacZ or mock infected cells. This is consistent with previous reports that UL97 can autophosphorylate, as demonstrated by the presence of a major phosphorylated species following purification of UL97 (He et al., 1997).

Analysis of the UL97 protein biochemistry was performed with purified UL97 to ensure the enzyme activity was not affected by either cellular or Baculovirus encoded proteins. During Baculovirus infection of insect cells, only proteins under the control of the polyhedrin promoter are expressed after 48 hours infection. If Baculovirus or cellular proteins were to interfere with UL97 autophosphorylation, it would occur maximally at 48 hours, but it is unlikely that either interfere as UL97 phosphorylation accumulates from 48 hours. The MB-UL97 did not encode an N-terminal tag for purification, such as the hexahistidine tag which is utilised in immobilised metal chelate affinity chromatography, so the success of these traditional techniques with regard to UL97 depended upon the high level of expression which was achieved with the MB-UL97. Previous reports suggest maximal secretion of proteins using the melitin secretion signal sequence occurred at 72 hours post infection at an MOI 5. The UL97 was detected in the crude cellular extracts from 48 hours in the serum free Sf9 cells used for secretion, however it was not observed in either the neat or concentrated tissue culture supernatant at an MOI of either 1, 5 or 10. The baculoviruses were passaged through the Sf9 cells twice as this appeared to enhance the infection in Sf9 cells, and the cells infected at an MOI 10, 15 and 20 for up to 120 hours. The UL97 was not detected in the supernatant even when 5 ml of supernatant was concentrated to 50 $\mu\text{l}$ , while it was detectable in crude cellular lysates. This is in contrast with a control virus encoding human MEPE, where expression was detected from 48 hours post infection in the tissue culture supernatant. This suggests the UL97 was not released from the cells. The nature of the melitin secretion signal and indeed many signal sequences, means the signal sequence is cleaved upon secretion into the culture medium. In non-polarized cells, such as Sf9 cells in suspension, proteins are carried through the ER and the Golgi apparatus to the cell surface by the constitutive secretory pathway, as opposed to regulated secretion which occurs upon signal-mediated stimulation such as hormone or neurotransmitter (Lodish., 1988, Rothman., 1987). Usually when genes encoding secretory proteins are transferred to cells in which they

are not normally expressed, the foreign protein is packaged into secretory vesicles for the final transport from the Golgi to the cell surface (Griffiths and Simon, 1986, Orci et al., 1987). A protein band which comigrated with UL97 from the crude cell lysate was not detected by Coomassie brilliant blue staining in the culture supernatant, even when highly concentrated, implying UL97 was not secreted. Different amino terminal signal sequences can be transferred between proteins to redirect that protein to a different destination. For example, an ER signal at the beginning of a cytosolic protein can redirect the protein to the ER (Garoff., 1985). This suggests the recombinant UL97 should be re-targeted through the secretory pathway of the insect cells, but the results suggest that this process is inhibited for the UL97. The nuclear targeting signal sequence of UL97 was still present within the cloned gene, so implying the inhibition of secretion of UL97 may be caused by interference between the two signal sequences. Immunofluorescence staining of the insect cells infected with BVMB-UL97 using the anti-UL97 Mab identified punctate staining throughout the cytoplasm of the cell compared to the nuclear staining of the BVBBH-UL97 infected cells (data not shown). To overcome this problem, point mutations could have been introduced into the nuclear targeting signal, such that it no longer functions, allowing the new secretory signal to function.

Attempts were made to purify the Baculovirus expressed MB-UL97 proteins by employing traditional biochemical purification techniques. Considerable loss of protein occurred during purification, either by loss in solubility of the protein, or inefficiency of binding of the protein to immobilised substrates. Initially, the ammonium sulphate precipitation was optimised to precipitate most of the UL97 between 20% and 40% salt saturation, so sacrificing small amounts of UL97 to remove greater concentrations of contaminating proteins. Ammonium sulphate precipitation has the advantage of protein stabilisation in non-denaturing conditions, but resolubilisation of the protein precipitates posed a particular problem, as demonstrated by the high concentration of insoluble UL97 compared to the soluble concentrations. The ammonium sulphate was removed and the protein resolubilised during the clarification/buffer exchange in 50mM Tris HCl, pH 8.0, 100mM NaCl, however 2% Triton X-100 or 1.5% sarkosyl detergents were added to the buffers and the salt concentrations varied in an attempt to increase the solubility of the UL97. The triton X-100 slightly increased the solubility of the UL97 and did not have to be removed following

## *5.0 UL97 Expression, purification and biochemistry*

---

solubilisation before ion exchange as it is removed during ion exchange. The starting conditions for ion exchange chromatography were initially optimised to determine the pH and salt concentration required for binding the UL97, and the change in salt concentration required for elution. The target protein binds to an anion exchanger when the pH of the buffer is above the isoelectric point (pI) of the protein, thus the pI of UL97 was determined by computer modelling of the amino acid sequence, based upon the number of charged amino acid groups. Net charge was plotted against pH and gave an isoelectric point of 7.65 for UL97 and an anion exchange using DEAE cellulose was chosen (pH range 5 – 9). The UL97 was dialysed into the respective buffers so the starting pH and ionic strength of the UL97 was the same as that of the starting buffer and optimal binding occurred between a pH range of 8.0 to 9.0. A pH of 8.5 was chosen and the optimal salt concentration for binding was performed at this pH. The optimal NaCl concentration for binding was 50mM and the optimal concentration for elution was 250mM, thus a binding buffer consisting of 20mM Tris HCl and 50mM NaCl was used for all further purification experiments. Immunoprecipitation experiments also resulted in considerable loss of the protein, largely due to the conditions necessary for dissociation of the antibody-antigen complex. The low pH required to perform the dissociation inactivated the majority of the UL97, which was observed in the protein kinase assay and compared to dissociation at a pH of 9.0 where very little UL97 was harvested.

These purification techniques enabled biochemical analysis to be performed on UL97 purified to near homogeneity. In order to assess the autophosphorylation of UL97, the initial phosphorylation of GCV and to determine the function of 1263W94, it was essential that the UL97 was purified away from all other cellular proteins. The effect of each individual mutant UL97 species on each of these activities could also be differentiated.

## **CHAPTER 6**

### **Analysis of UL97 function using the antivirals GCV and 1263W94**

## **6.1 Introduction**

The antiviral drugs GCV, cidofovir (HPMPC) and foscarnet (PFA) are the currently used and approved antiviral chemotherapeutics in the treatment of cytomegalovirus infections. GCV remains the first-line drug for the treatment of cytomegalovirus disease in the immunocompromised patient groups, but the emergence of GCV-resistant strains of the virus has become an increasing problem. In addition, each of these drugs has several limitations to their use, which include poor oral bioavailability, dose-limiting toxicity and the potential to generate resistance. The potential for cross-resistance between these drugs is possible as each interacts with the virally encoded DNA polymerase (UL54). The incidence of HCMV disease and other opportunistic infections in AIDS patients has significantly declined since the introduction of HAART. Before the introduction of HAART, HCMV retinitis occurred in up to 40% of these patients, maintenance therapy was continued indefinitely and disease progression occurred eventually, regardless of the initial choice of regimen. This was predominantly due to the development of point mutations in the UL97 and the UL54 genes resulting in resistance to GCV and cross-resistance to cidofovir. Following HAART, HCMV disease was controlled by the resulting immune reconstitution and restoration of HCMV-specific CD4<sup>+</sup> T-lymphocyte responses, which accompanied HAART (Komanduri et al., 1998). Furthermore, patients could be taken off their maintenance therapy completely without disease progression (Tural et al., 1998, Macdonald et al., 1998, Deayton et al., 2000). However, evidence is emerging concerning the breakthrough of HCMV disease due to the immunological and virological failure of HAART (Torriani et al., 2000, Macdonald et al., 2000). This has highlighted the need for the development of new anti-HCMV drugs with unique mechanisms of action.

In 1995 a new and potent inhibitor of HCMV replication was described (Townsend et al., 1995). BDCRB (2-bromo-5,6-dichloro-1-( $\beta$ -D-ribofuranosyl benzimidazole) was found by marker transfer experiments to map to the UL89 and the UL56 open reading frames of the HCMV (Underwood et al., 1998, Krosky et al., 1998). Both genes are known to be essential for viral DNA cleavage and packaging into preformed capsids. Unfortunately, BDCRB showed poor pharmacokinetic properties and was rapidly metabolised when administered to animals. 1263W94 was identified from a panel of benzimidazole analogues. It has exhibited potent antiviral activity specific against HCMV (Chulay et al., 1999) and EBV

(Zacny et al.,1999), with an  $IC_{50}$  of approximately 4- to 10-fold lower than GCV for HCMV. However, the mechanism of action of 1263W94 is distinct from that of BDCRB; it does not inhibit the processing of HCMV DNA and is active against the BDCRB resistant virus. The target of 1263W94 was identified as UL97 following gene transfer experiments, although the precise mechanism of inhibition of the UL97 is presently unknown.

The aims of this study were firstly to quantify the level of GCV monophosphorylation by the wild type and mutant UL97 proteins, including those with mutations identified in genotypic GCV resistant strains of HCMV and mutations in different putative UL97 protein kinase domains, and secondly, to identify the mechanism by which 1263W94 inhibits the HCMV encoded UL97 and thirdly, to determine the effect of 1263W94 upon the genotypic resistance mutants and the 1263W94-resistant mutant identified by marker transfer experiments.

## **6.2. Results**

### **6.2.1. Cytotoxicity of GCV for Sf21 insect cells**

In order to insure the growth of Sf21 insect cells was maintained at the concentrations of used in the plaque reduction assay, growth media was supplemented with GCV at concentrations of 0.0, 0.2, 0.4, 0.6, 1.0 and 1.2 mM. The cells were harvested at 24, 48, 72 and 96 hours, subjected to the trypan blue exclusion test and counted. The cell counts are graphically represented in figure 6.1, which shows the cell numbers increase over 48 hours. The cell replication slows from 72 to 96 hours and none of the GCV concentrations appear to be inhibitory to replication, indicating is not cytotoxic at the concentrations used.

### **6.2.2. Plaque reduction assay of the wild type and mutant UL97-expressing baculoviruses**

Sf21 insect cells were infected with baculoviruses encoding the wild type and mutant HCMV UL97 genes as described in section 2.5.4. The media was supplemented with GCV at concentrations from 0.0, 0.2, 0.4, 0.6, 1.0 and 1.2mM. Following a 72-hour incubation, the culture media was harvested and the virus titre was determined by plaque assay.

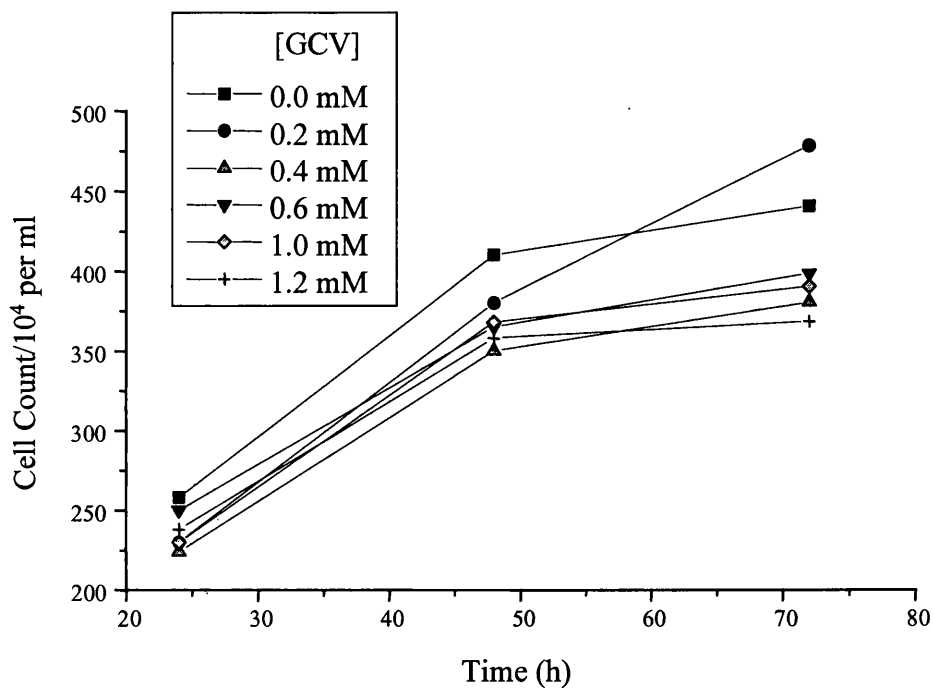


**Figure 6.1. Cytotoxicity of GCV for Sf21 insect cells.**

Sf21 insect cells were cultured in medium supplemented with GCV of concentrations from 0.0mM to 2.0mM. The cells were incubated for 24, 48 and 72 hours, following which they were counted by the trypan blue exclusion test. The number of cells at each concentration were counted and plotted against time.

Each set of infections were performed in triplicate and each plaque assay was performed in duplicate. The plaque reduction assays of each of the baculoviruses are graphically represented in figures 6.2 and 6.3. Figure 6.2 shows the results of the plaque assays of the baculoviruses expressing the mutant UL97 species encoding genotypic GCV-resistance point mutations. The replication of the baculovirus expressing the wild type UL97 was significantly reduced compared to that of the mutant UL97 species. The IC<sub>50</sub> for the wild type UL97 was calculated to be 0.13mM. The IC<sub>50</sub> values calculated for each of the mutant UL97 species were calculated to be 0.75mM for A594T and 0.95mM for L595F. The IC<sub>50</sub> for the remaining viruses were determined by extrapolation to be 1.8mM for M460I and 2.84mM for H520Q. The replication of the baculovirus expressing the K355Q mutation (invariant lysine) was not reduced upon culture with any of the GCV concentrations tested. The replication of the virus expressing the L397R mutation was reduced by a mean of 12.5%. All the viruses were compared with the control virus BVLacZ which was not reduced upon culture with GCV.

### **6.2.3. Plaque reduction assay of the baculoviruses expressing structural mutations in the UL97 gene**

Plaque reduction assays were performed as in section 6.2.2 and the replication rates of the baculoviruses were graphically represented as percentage reduction in number of plaques over the range of GCV concentrations (figure 6.3).

### **6.2.4. GCV phosphorylation by recombinant UL97**

SF21 insect cells were infected with the wild type or mutant UL97-expressing baculoviruses at an MOI 10 and incubated at 28°C for 48 hours. After 48 hours incubation, the medium was supplemented with tritiated GCV. The nucleotides were harvested following 72 hours incubation by acid hydrolysis of the cells and bound to DE81 filter paper. The phosphorylated tritiated GCV was detected in scintillant by measurement of DPM by the Rackbeta beta counter. All assays were performed in triplicate and a negative control was included of uninfected SF21 cells with media supplemented with GCV. The GCV phosphorylation was plotted as a percentage phosphorylation compared to the wild type UL97 as shown in figure 6.4.



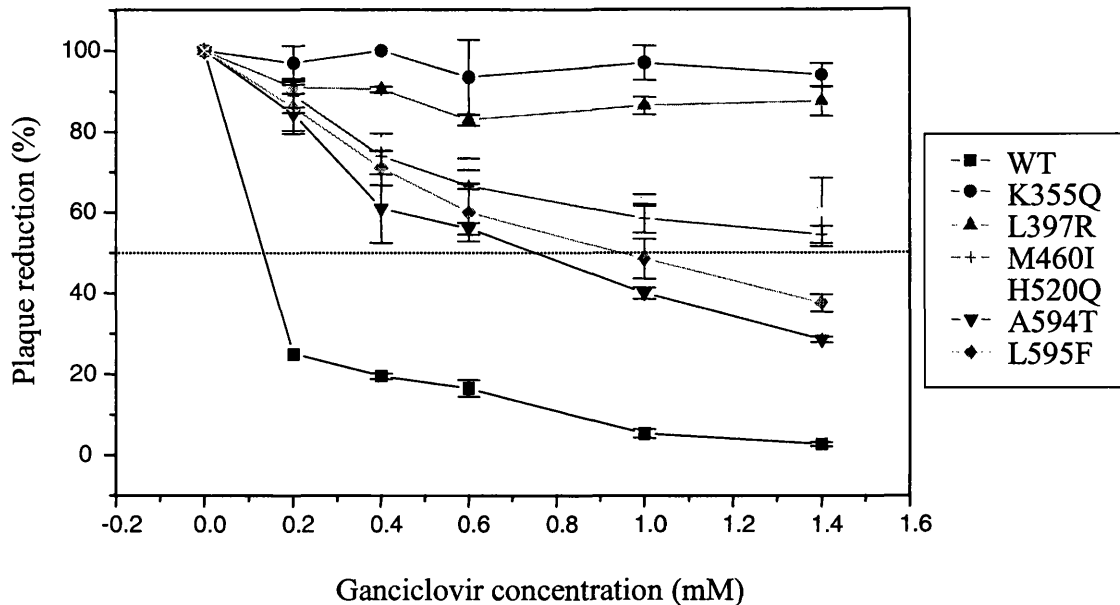


**Figure 6.2. Graphical Representation of the Plaque Reduction Assays of the Drug Resistant Baculoviruses.**

Baculoviruses expressing the UL97 of HCMV were individually cultured in increasing concentrations of GCV (0.0 mM to 1.4 mM) and the effect of the drug on the virus replication was measured by plaque assay. The replication of the baculovirus expressing wild type UL97 was significantly reduced compared to that of the baculoviruses expressing UL97 carrying mutations associated with clinical GCV resistance. Replication of the baculovirus expressing UL97 with the K355Q mutation (invariant lysine) was not reduced by any concentration of GCV, compared to that of the negative control. The replication of the baculovirus carrying the L397R mutation was reduced by a mean of 12.5%.

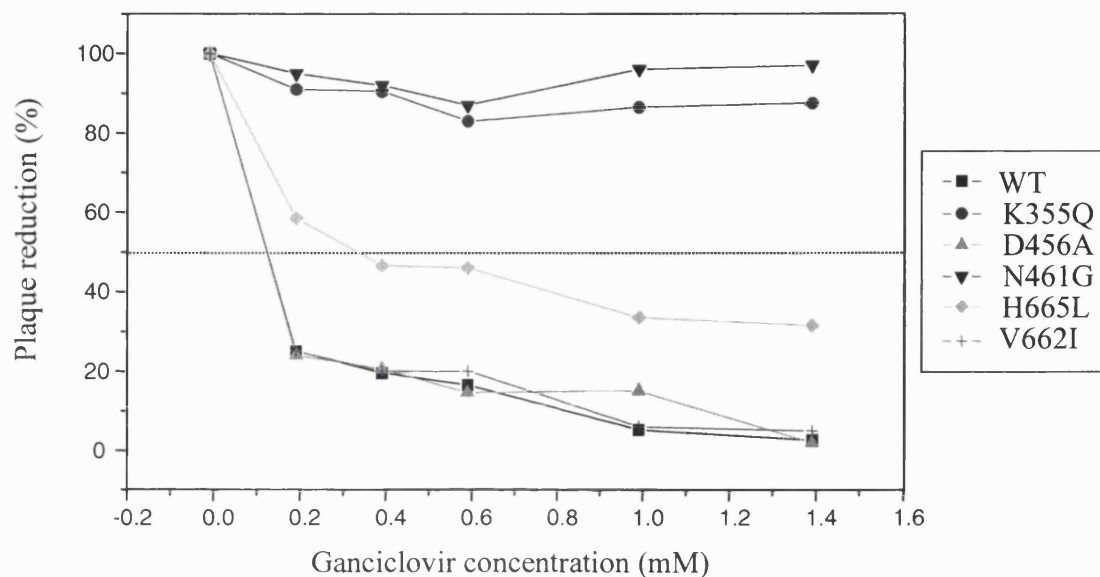


**Figure 6.3. Graphical Representation of the Plaque Assays of the Structurally Mutated UL97-Expressing Baculoviruses.**

Baculoviruses expressing the UL97 of HCMV were individually cultured in increasing concentrations of GCV (0.0 mM to 1.4 mM) and the effect of the drug on the virus replication was measured by plaque assay. The replication of the baculoviruses expressing UL97 carrying mutations within specific catalytic domains of the protein kinase was reduced to between 15% and 92% of the control virus (BVLacZ) or the K355Q mutant (invariant lysine).

The GCV phosphorylation by the genotypic GCV-resistance mutants (M460I, H520Q, A594T and L595F) were reduced to between 20% and 10% of that of the wild type UL97. The mutated invariant lysine (K355Q) did not exhibit any GCV phosphorylation, and the 1263W93-resistant (L397R) mutant exhibit an average of 8% of GCV phosphorylation as compared to the wild type UL97. The mutations generated in the region of the UL97 surrounding the M460 showed a total loss of GCV phosphorylation at the 461 codon, but no reduction in phosphorylation at the 456 codon. The mutations around a His-X-aromatic-hydrophobic motif at codons H662L and V665I showed a reduction in GCV phosphorylation of between 12% and 72%.

#### **6.2.5. Phosphorylation of recombinant UL97 in the presence of 1263W94**

Crude lysates of the UL97 recombinant baculovirus infected cells were subjected to protein kinase assays either with or without 0.05 $\mu$ M 1263W94. The proteins were separated by SDS-PAGE and exposed to film. The autoradiographs, as shown in figure 6.5, were examined for the effect of the 1263W94 upon the autophosphorylation of UL97. The autophosphorylation of every species (mutant and wild type) of UL97 was inhibited upon addition of the 1263W94, as demonstrated by the disappearance of the phosphorylated UL97 species. The phosphorylated protein species of the uninfected cells used as the negative control all remained phosphorylated following addition of the drug.

#### **6.2.6. Comparison of the wild type and mutant UL97 autophosphorylation in the presence of 1263W94**

The autoradiographs of the protein kinase assays from section 6.2.5 were analysed by the BioRad Multianalyst and plotted as a percentage of the total phosphorylation of the wild type UL97 phosphorylation in the absence of 1263W94, as shown in figure 6.6. In the presence of 1263W94, the autophosphorylation of every species of UL97 was reduced to below 10% of the total phosphorylation of the wild type UL97. The autophosphorylation of the L397R mutant, which is the 1263W94 resistant UL97 mutant, was not reduced in the presence of 1263W94.

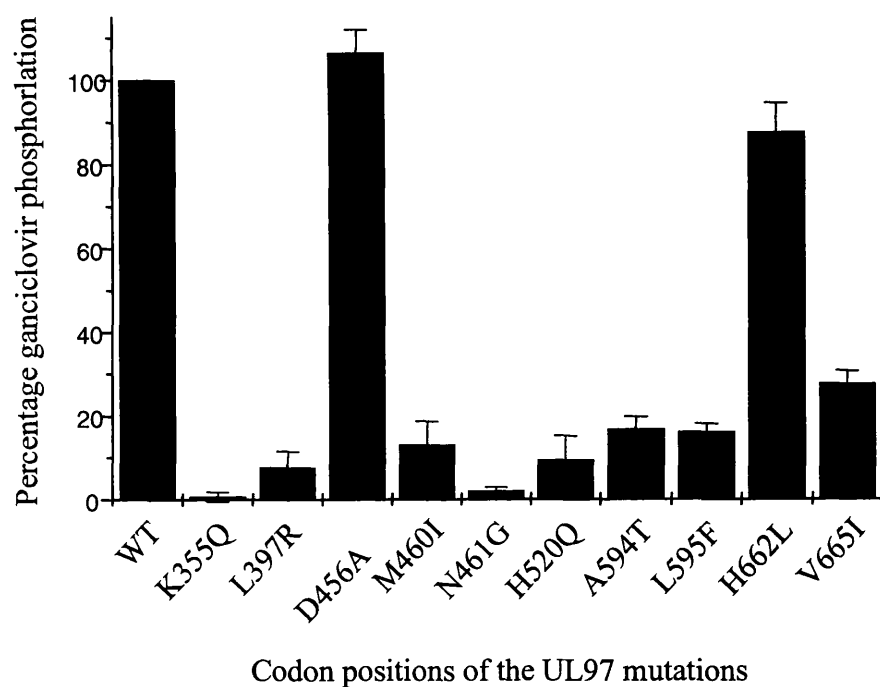


**Figure 6.4. GCV phosphorylation by recombinant UL97.**

Insect cells were infected with the wild type or mutant UL97 baculoviruses at an MOI 10. The medium was supplemented with both cold and tritiated GCV at 48 hours. The nucleotides were harvested at 72 hours and bound to DE81 filter paper. The phosphorylated GCV was detected in scintillant and plotted as % phosphorylation compared to the wild type UL97.

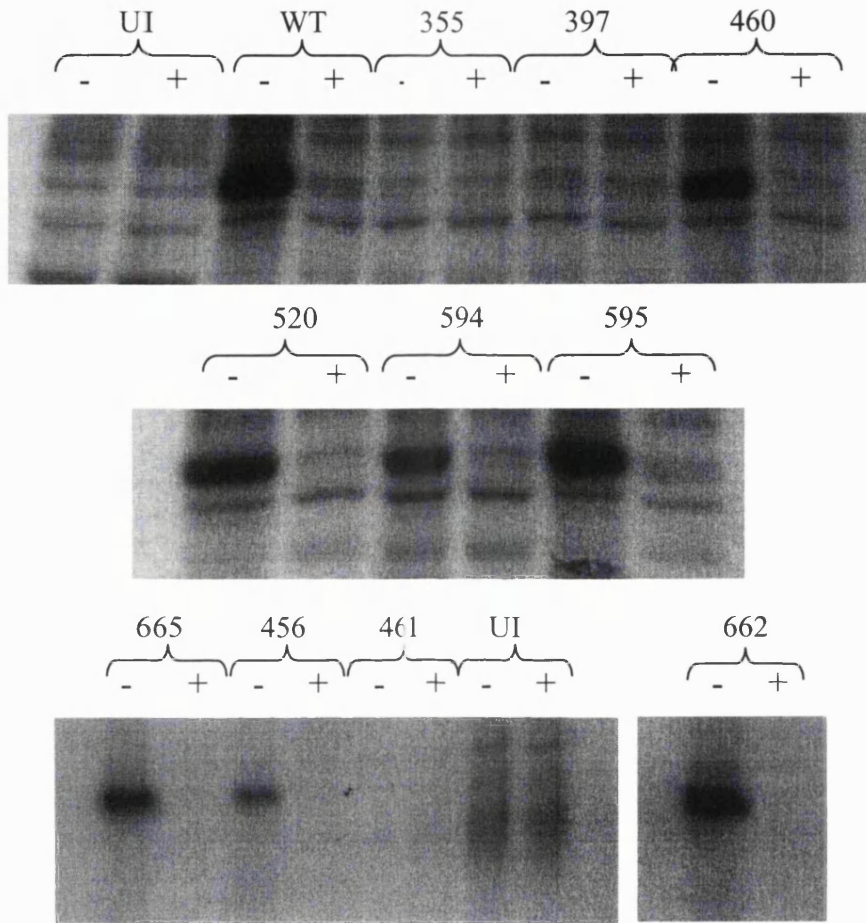


**Figure 6.5. Autoradiographs of the Protein Kinase Assays of UL97 in the presence of 1263W94.**

Crude lysates of cells infected with the recombinant wild type and mutant UL97 expressing baculoviruses were subjected to protein kinase assays with (+) or without (-) 0.05 $\mu$ M of 1263W94. The proteins were subjected to SDS-PAGE, exposed to film and the autoradiographs examined for the effect of the drug upon the autophosphorylation of UL97. The autophosphorylation of UL97 was inhibited upon the addition of 1263W94 to the assays for both the mutants and the wild type UL97 species.

### **6.2.7. Titration of 1263W94 against the wild type and mutant UL97**

In order to assess the effect of increasing 1263W94 concentration on the individual UL97 mutants, protein kinase assays were performed on UL97 purified to near homogeneity including 0.0 $\mu$ M to 5.0 $\mu$ M 1263W94. Figure 6.7 shows the autophosphorylation of the wild type and the genotypic GCV resistant UL97 species. The UL97 species containing mutations in conserved amino acids are not shown.

### **6.2.8. Determination of the IC<sub>50</sub> of 1263W94 against the wild type and mutant UL97 species**

The autoradiographs generated from the protein kinase assays in section 6.2.7 were analysed by the BioRad Multianalyst and the percentage reduction in UL97 autophosphorylation of the UL97 species were plotted against the 1263W94 concentration, as shown in figure 6.8. An exponential decay curve was fitted and the IC<sub>50</sub> of 1263W94 was determined for each of the UL97 species. The IC<sub>50</sub> for wild type UL97 was 0.034 $\mu$ M, 0.033 $\mu$ M for H520Q, 0.031 $\mu$ M for A594T and 0.028 $\mu$ M for L595F. With no autophosphorylation evident for the K355Q and N461G, the proteins were not examined in the presence of 1263W94. The 1263W94-resistant mutant (L397R) did not exhibit a reduction in autophosphorylation with concentrations of the drug of up to 100 $\mu$ M. The IC<sub>50</sub> values for the D456A, H662L and V665I mutant UL97 species were determined at 0.034 $\mu$ M, 0.04 $\mu$ M and 0.03 $\mu$ M respectively, (graphs not shown).

### **6.2.9. IC<sub>50</sub> of 1263W94 against the UL97 encoding the M460I mutation.**

The UL97 containing the M460I mutation was subjected to a protein kinase assay as in section 6.2.7 and the percentage reduction in autophosphorylation plotted against 1263W94 concentration as shown in figure 6.9. An exponential decay curve was fitted and the IC<sub>50</sub> of 1263W94 was determined at 0.0048M. This indicates a four-fold increase in sensitivity of the M460I mutant of UL97 to 1263W94.

### **6.2.10. Inhibition of UL97 autophosphorylation by 1263W94**

In order to determine the mechanism of action of the 1263W94, a protein kinase assay was performed upon the wild type UL97 in increasing concentrations of ATP (2 $\mu$ M to 20 $\mu$ M) and consecutively with increasing concentrations of ATP with the addition of 0.02 $\mu$ M 1263W94.

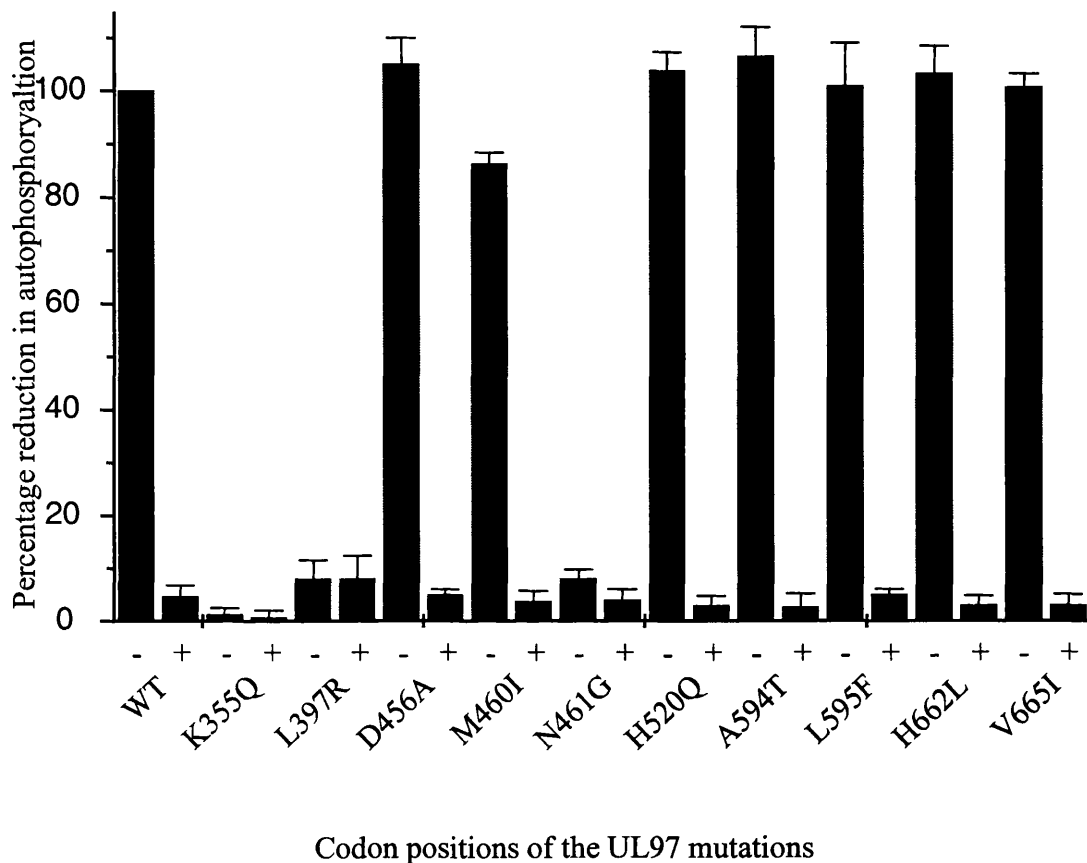


**Figure 6.6. Graphical Representation of the Autophosphorylation of UL97 in the presence of 1263W94.**

Protein kinase assays were performed upon the wild type and mutant UL97 proteins. The phosphorylated proteins were subjected to SDS-PAGE and autoradiography and analysed by the BioRad Multianalyst. The autophosphorylation of each UL97 species was plotted as a percentage of the phosphorylation of the wild type UL97. In the presence of the drug, autophosphorylation of the wild type and mutant UL97 proteins were reduced to below 10% of that of the wild type UL97. The autophosphorylation of the L397R mutant-UL97 was unaffected upon the addition of the drug to the assay.

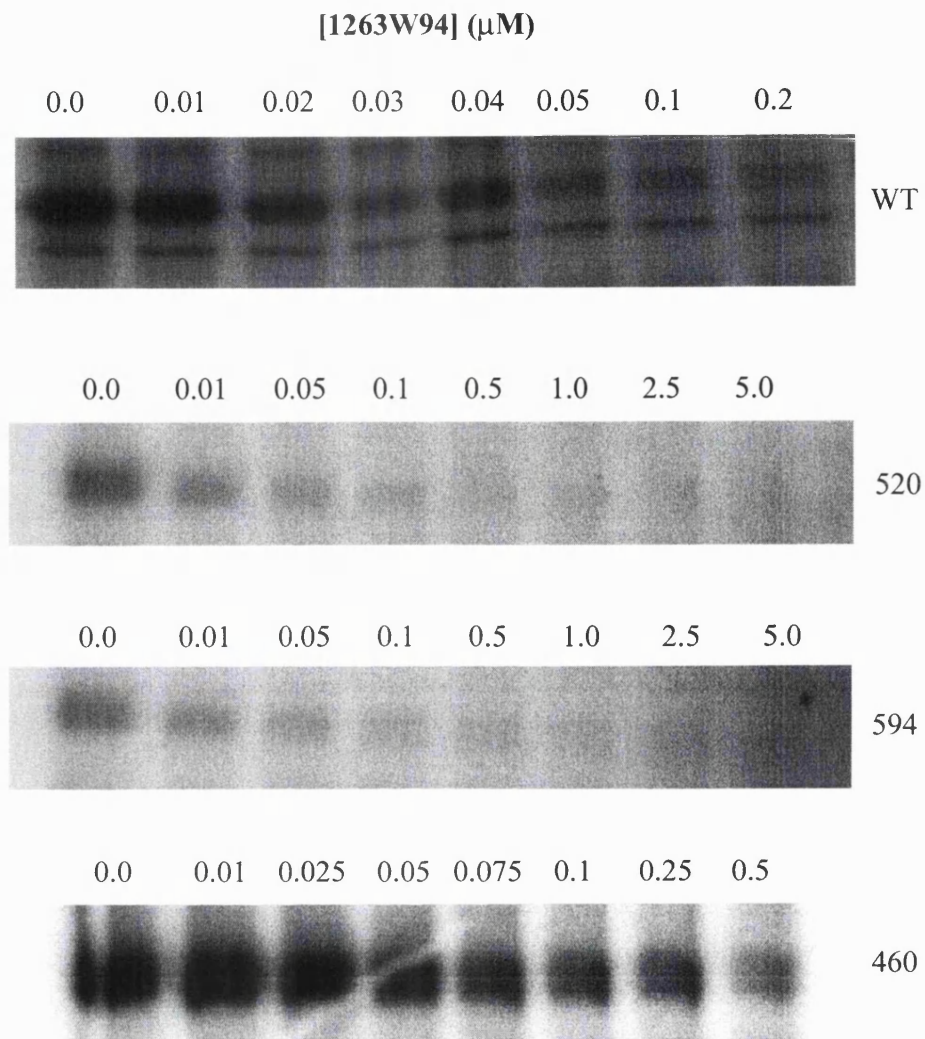


**Figure 6.7. 1263W94 Titration against UL97.**

Protein kinase assays were performed on the wild type and mutant UL97 proteins using increasing concentrations of 1263W94. The assays were subjected to SDS-PAGE, exposed to film and the autoradiographs were analysed by the BioRad Multianalyst. The autoradiographs for the wild type, H520Q, A594T and the M460I mutants are shown. Increasing concentrations of 1263W94 reduced the UL97 autophosphorylation.



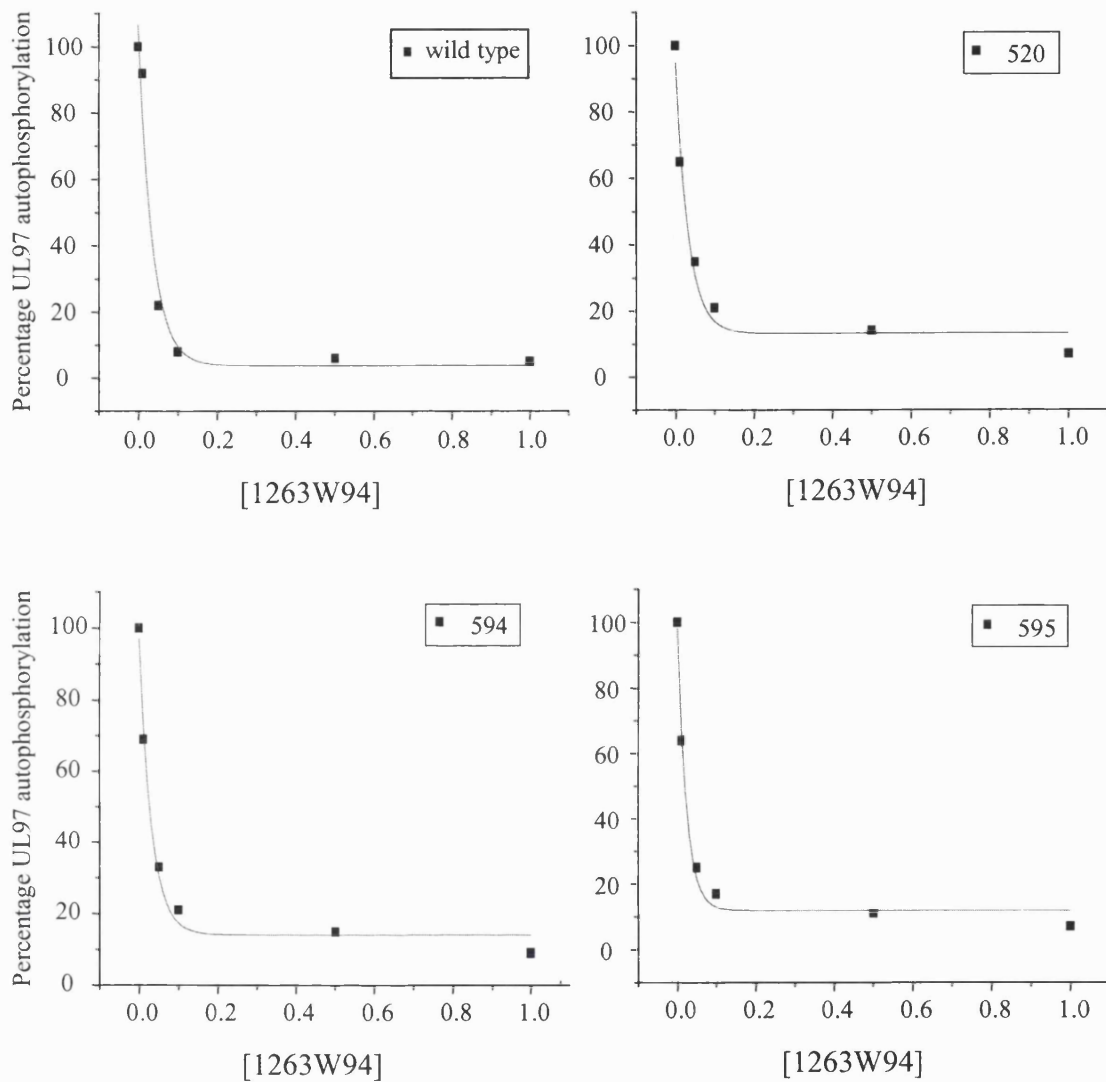


**Figure 6.8. IC<sub>50</sub> of 1263W94 for the Wild Type and Mutant UL97 Protein Species.**

The wild type and mutant UL97 proteins were subjected to protein kinase assays with varying concentrations of 1263W94 (0.01 – 1.0 $\mu$ M). The autoradiographs were analysed using the BioRad Multianalyst and the UL97 phosphorylation was plotted as a percentage of the total phosphorylation without 1263W94. An exponential decay curve was fitted and the IC<sub>50</sub> of 1263W94 was determined for each of the proteins.

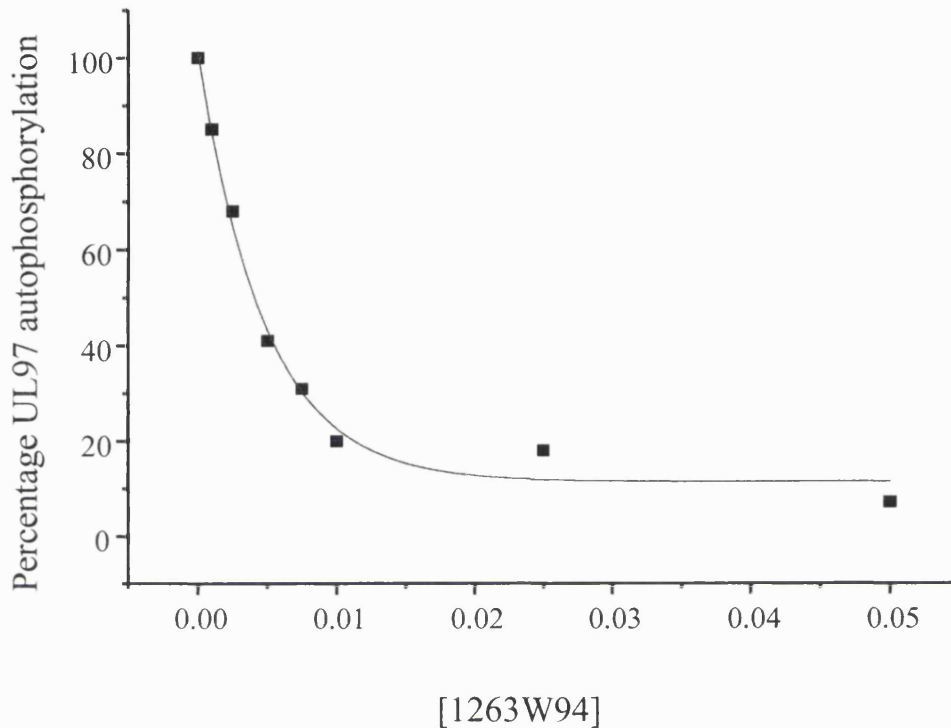


**Figure 6.9. IC<sub>50</sub> of 1263W94 for the M460I Encoded UL97.**

The M460I mutant UL97 protein was subjected to a protein kinase assay with varying concentrations of 1263W94 (0.01 – 1.0 $\mu$ M). The autoradiograph was analysed using the BioRad Multianalyst and plotted as a percentage of the total UL97 phosphorylation without 1263W94. An exponential decay curve was fitted and the IC<sub>50</sub> of 1263W94 was determined. The autoradiographs are shown in figure 6.10. The addition of the 1263W94 reduced the level of autophosphorylation, as observed by a decrease in autophosphorylation intensity at all the concentrations of ATP used in the assay.

### 6.2.11. Analysis of 1263W94 inhibition of UL97 autophosphorylation

Protein kinase assays were performed upon the wild type UL97 with increasing concentrations of ATP as in section 6.2.10. Each assay set included increasing concentrations of 1263W94 from 0.01 $\mu$ M to 0.025 $\mu$ M. The autoradiographs are shown in figure 6.11. The level of UL97 autophosphorylation decreased upon addition of 1263W94 for each ATP concentration and for each increase in 1263W94 concentration, thus a greater inhibition of UL97 autophosphorylation with increasing concentrations of 1263W94, irrespective of the ATP concentration in the kinase assay.

### 6.2.12. Lineweaver Burke analysis of 1263W94 mediated phosphorylation inhibition

The autoradiographs from sections 6.2.11 and 6.2.12 were analysed by the BioRad Multianalyst and Lineweaver Burke plots generated by plotting the reciprocal of the phosphate incorporation against the reciprocal of the ATP concentration, as shown in figure 6.12. The best-fit lines were determined with the extrapolation to the x-axis, from which the  $K_m$  and  $K_i$  values were determined for ATP in the presence of 1263W94. The plots from figure 6.12 were merged to generate figure 6.13. This shows a convergence of the lines around the Y-axis and at approximately  $1/V_{max}$ . The affinity of the inhibitor for the enzyme is expressed quantitatively through the inhibition constant  $K_i$ , which is the dissociation constant of the enzyme inhibitor complex. This can be determined by the equation:-

$$K_m' = K_m(1+[I]/K_i).$$

Thus the  $K_i$  for 1263W94 at 0.01 $\mu$ M is determined by:-

$$K_i = \frac{[I] K_m}{K_m' - K_m} = 0.01\mu\text{M} \quad \left\{ K_i = \frac{0.01 \times 27}{53-27} \right\}$$

The  $K_m$  and  $K_i$  values for each of the concentrations of 1263W94 are shown in table 6.1.

**Table 6.1. Analysis of 1263W94 inhibition of UL97 autophosphorylation.**

<b>Inhibitor concentration [I]</b>	<b><math>K_m</math></b>	<b><math>K_i</math></b>
0.00 $\mu\text{M}$	27 $\mu\text{M}$	
0.01 $\mu\text{M}$	53 $\mu\text{M}$	0.01 $\mu\text{M}$
0.015 $\mu\text{M}$	66 $\mu\text{M}$	0.01 $\mu\text{M}$
0.02 $\mu\text{M}$	74 $\mu\text{M}$	0.01 $\mu\text{M}$

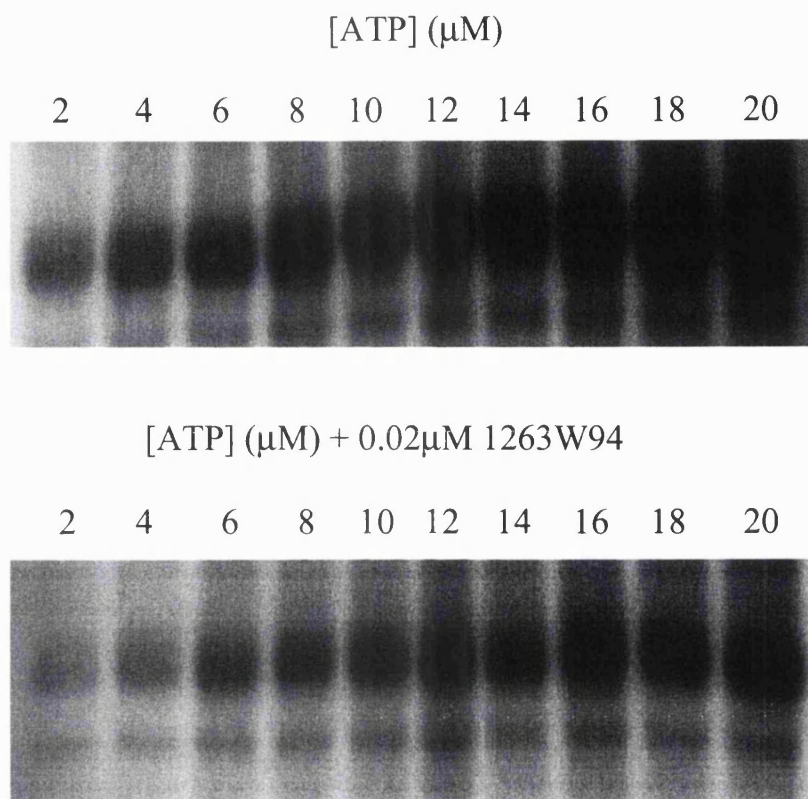


**Figure 6.10. Inhibition of UL97 Autophosphorylation by 1263W94.**

Protein kinase assays were performed upon the UL97 in increasing concentrations of ATP. 1263W94 was added to one assay at a concentration of 0.02 $\mu\text{M}$ . The assays were subjected to SDS-PAGE, exposed to film and the autoradiographs analysed by the BioRad Multianalyst. Increasing ATP concentrations resulted in an increase in UL97 autophosphorylation. Addition of 1263W94 to the assays resulted in a decrease in the level of UL97 autophosphorylation, as observed by intensity of signal.

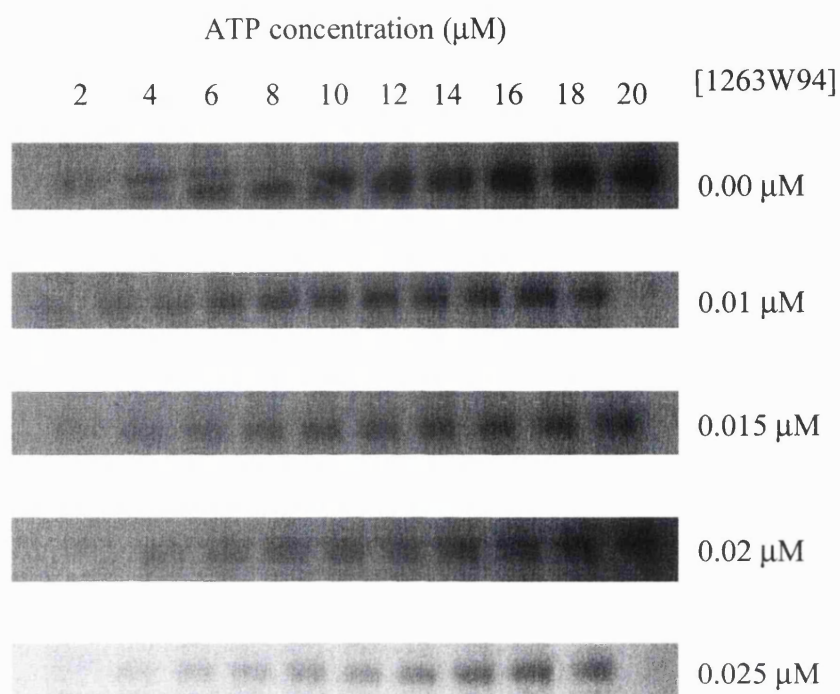


**Figure 6.11. Analysis of 1263W94 Inhibition of UL97 Autophosphorylation.**

Protein kinase assays were performed using increasing concentrations of ATP in the presence of constant concentrations of 1263W94. The assays were subjected to SDS-PAGE, exposed to film and analysed using the BioRad Multianalyst. The autoradiographs show an increase in UL97 autophosphorylation with increasing concentration of ATP. Addition of increasing concentrations of 1263W94 resulted a progressively greater inhibition of UL97 autophosphorylation, as observed by the decrease in intensity of the signal.

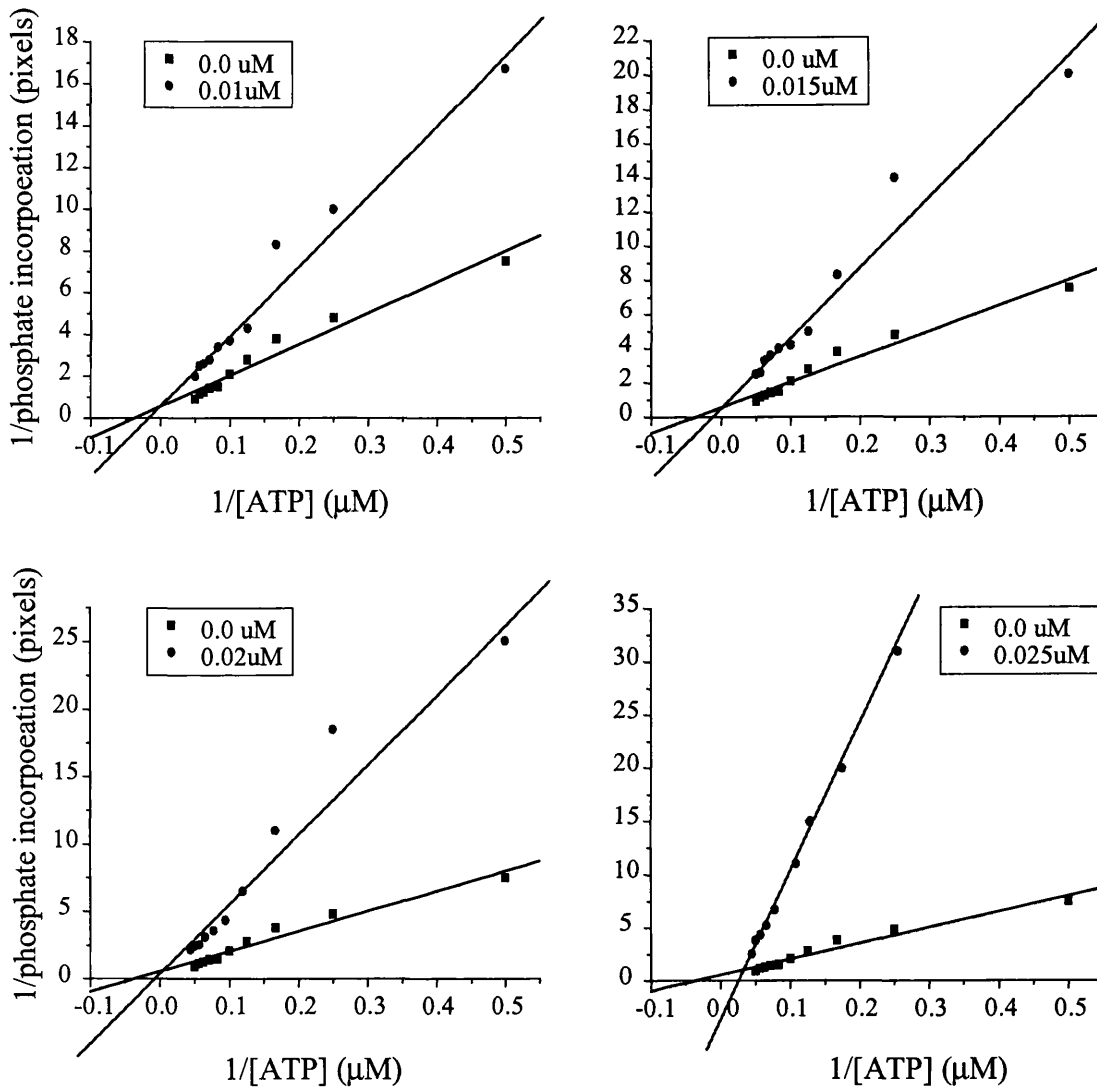


**Figure 6.12. Lineweaver Burke Analysis of 1263W94 Mediated Phosphorylation inhibition.**

UL97 purified to near homogeneity was subjected to protein kinase assays containing increasing concentrations of ATP (2μM - 20μM). 1263W94 was added to each assay at a concentration of 0.0μM, 0.01μM, 0.015μM, 0.2μM or 0.025μM. The inverse of the velocity of autophosphorylation was plotted against the corresponding inverse of the [ATP]. The  $K_m$  and  $K_i$  values were determined for UL97 in the presence of 1263W94.

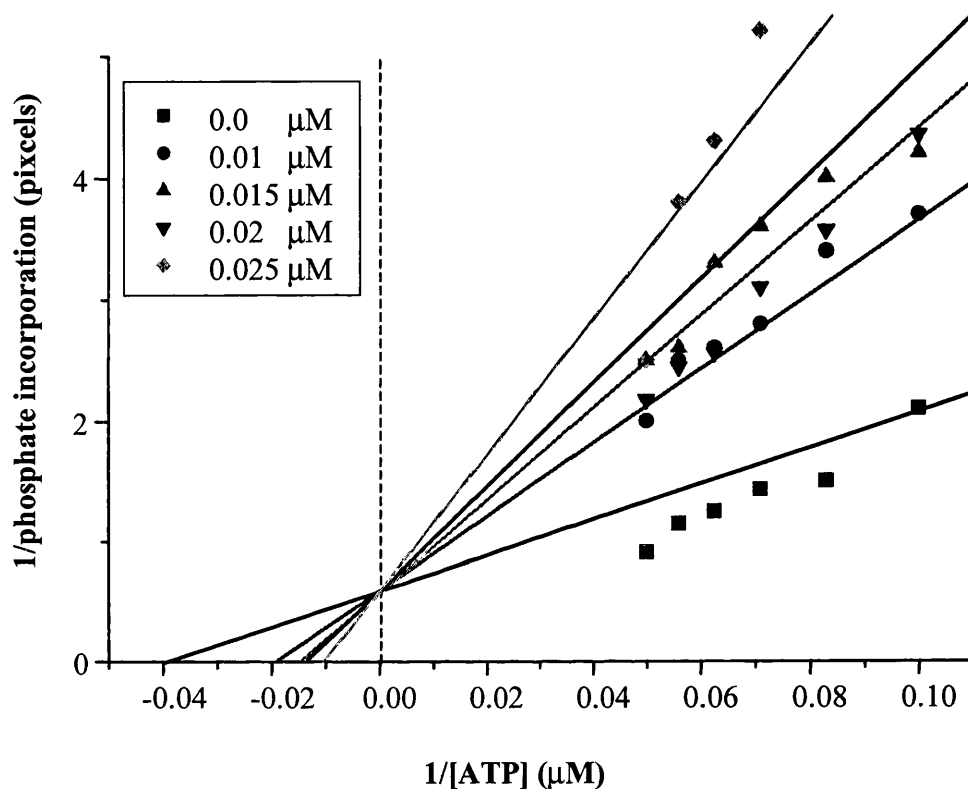


**Figure 6.13. Analysis of the Lineweaver Burke Plots of 1263W94 Mediated UL97 Autophosphorylation Inhibition.**

The individual Lineweaver Burke plots from Figure 6.12 were plotted together to determine the pattern of autophosphorylation inhibition which indicates the nature of 1263W94 inhibition of the enzyme. The plot indicates the UL97 autophosphorylation is inhibited by the competitive inhibition of ATP.



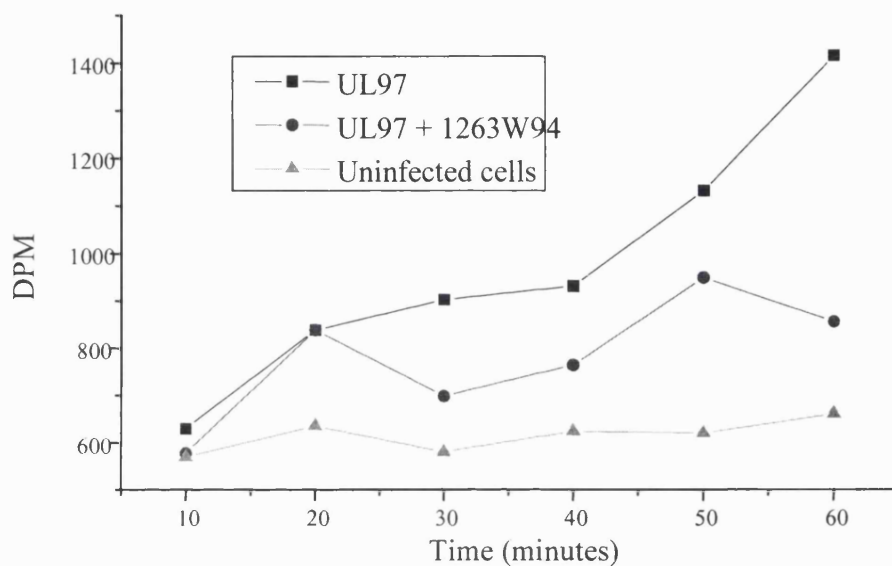


**Figure 6.14. 1263W94 mediated inhibition of GCV phosphorylation.**

Purified UL97 was subjected to a GCV kinase assay in the presence or absence of 1263W94 over a 60-minute time course. GCV phosphorylation was determined every 10 minutes by binding the phosphorylated GCV to DE81 filter paper, scintillation and DPM counting in the RackBeta scintillation counter. DPM was plotted against time (minutes) to determine the effect of 1263W94 upon the phosphorylation of GCV.

### **6.2.13. Inhibition of phosphorylation by 1263W94.**

Purified wild type UL97 was subjected to a GCV kinase assay using the conditions originally described by He et al., 1997. The kinase assay was performed either in the presence or absence of 1263W94 for varying times from 10 minutes to 60 minutes. GCV phosphorylation was determined by binding of the phosphorylated GCV to DE81 filter paper, scintillation and DPM counting in the RackBeta scintillation counter. As a control, uninfected cell lysate was used following the same purification performed upon the UL97. The DPM was plotted for each time point for the control and the UL97 in the presence or absence of 1263W94. The control exhibited what appeared to be background GCV phosphorylation and the UL97 exhibited increased GCV phosphorylation over the 60 minutes of the assay. UL97 in the presence of 1263W94 exhibited a reduced level of GCV phosphorylation over this time period.

### **6.3. Discussion**

This chapter describes the investigations performed to determine the catalysis of phosphate transfer from  $\gamma$ -radiolabelled ATP onto GCV via the kinase activity of the HCMV encoded UL97. The enzymes used to perform this analysis include the wild type UL97 protein kinase, mutants identified as phenotypically resistant to GCV and mutants carrying mutations in structurally important domains of the kinase enzyme. This chapter also goes on to describe the function and mechanism of antiviral action of the novel benzimidazole L-riboside, 1263W94.

Chapter 5 showed that the baculovirus-infected insect cells were efficiently expressing the recombinant wild type and mutant UL97 species. The proteins were purified by a combination of ammonium sulphate precipitation, ion exchange chromatography and immuno-affinity chromatography. Following purification, a small amount of the UL97 remained soluble, which was sufficient to perform various biochemical analyses, including the catalysis of transfer of  $\gamma$  radiolabelled phosphate from ATP onto themselves (autophosphorylation). This chapter also uses the purified wild type and mutant UL97 species in an attempt to show a direct interaction between GCV and the UL97 species. Previously published data show UL97 controls the phosphorylation of GCV (Sullivan et al., 1992; Littler et al., 1992; Metzger et al., 1994; He et al., 1997; Zimmerman et al., 1997),

however these data do not show a direct interaction between GCV and UL97. In order to demonstrate that the recombinant UL97 controls the phosphorylation of GCV, and to assess the effect of the point mutations introduced into the UL97 upon the GCV phosphorylation, the wild type and mutant UL97-expressing recombinant baculoviruses plus the control LacZ baculovirus were cultured in increasing concentrations of GCV. The reduction in the replication of the viruses was determined by plaque reduction assay. Initially, the trypan blue exclusion test was employed to ensure the increasing concentrations of were not cytotoxic for the insect cells in which the baculoviruses were cultured. This revealed the cell viability remained near 100% during the 72-hour culture. The LacZ baculovirus was used as the second control to ensure the effect of GCV was specific to the UL97-expressing baculoviruses. As expected, the number of plaques generated by the LacZ-expressing baculovirus was not significantly reduced upon culture in increasing concentrations of GCV. The plaque reduction assay showed that the baculovirus expressing the wild type UL97 was sensitive to all concentrations of GCV used in the assay, with an  $IC_{50}$  of 0.13mM. This indicates that the presence of the UL97 is required for the activation of the GCV, thereby inducing GCV sensitivity upon the otherwise resistant baculovirus, including the wild type and LacZ baculoviruses, as observed in a recent publication (He et al., 1997). The plaque reduction assay was performed upon all the baculoviruses encoding the mutant UL97 species. The most commonly detected mutations occurring in clinical isolates within the UL97 gene, conferring GCV resistance, are those in codons 460, 594, 595 and 520 (Chou et al., 1995; Jabs et al., 2001). The mutation occurring at codon 520 is less frequently however. The effect of these mutations upon the baculovirus-expressed UL97 was examined to determine if the phosphorylation of GCV was impaired to varying degrees, depending upon which mutation was present. The initial virus concentration added to each assay was equal as determined by plaque assay, to ensure comparative results when analysing the effect of each mutant upon the GCV-induced reduction in plaque number. The genotypic GCV-resistance mutants, M460I, H520Q, A594T and L595F consistently showed a reduction in sensitivity to GCV, indicating impairment of GCV phosphorylation. M460I and H520Q appeared to exhibit greater resistance to GCV than the mutants A594T and L595F, as observed by their failure to reach an  $IC_{50}$  by 1.4mM GCV. This suggests the positions of these mutations within the protein kinase conserved domains have a greater functional importance with respect to GCV phosphorylation, than the 594/595 region. M460I is positioned within the conserved domain VI of the UL97 protein kinase and the H520Q is

part of the sequence YHPAF 519-523. This putative domain is highly conserved exclusively among cytomegaloviruses and is located between domains VII and VIII (Michael et al., 1999). The A594T and L595F mutations reside in a region between codons 590 and 607, homologous to domains IX and X. In order to further clarify these differences, the GCV kinase assay was employed to determine if indeed the mutations at codons 460 and 520 induced a greater resistance to GCV than those observed in codons 594 and 595. The results showed that the mean reduction in GCV phosphorylation by the M460I mutant UL97 was slightly less than the phosphorylation by the 594 and 595 mutants. The 520 mutant UL97 induced a further 2 fold reduction in GCV phosphorylation. The results however, showed that the mutations observed in clinical isolates exhibiting GCV resistance did not completely inhibit the phosphorylation of GCV. This has previously been observed within a vaccinia-based system (Michel et al., 1999).

The conserved kinase domain encompassing the 460 codon was further examined to determine the importance of the region in the function of the UL97 for autophosphorylation and GCV phosphorylation. The D456A mutant exhibited autophosphorylation comparable to that of the wild type UL97, and indeed a similar GCV phosphorylation, suggesting this amino acid does not play a direct role in the function of the kinase. However, the N461G mutant exhibited a complete loss of both autophosphorylation and GCV phosphorylation. The D456 and N461 both correspond to the protein kinase consensus sequence HRDLKXXN, and are both highly conserved. This motif forms the catalytic loop responsible for the phosphotransfer, suggesting the N461 codon is directly involved in this process, but the 460 codon impairs the phosphotransfer, probably by sterically altering the catalytic loop. By impairing the phosphotransfer and not inhibiting it, the 460 mutant may impair the natural function of the enzyme, so leading to a less fit virus in terms of replication dynamics. This would explain why a virus with a fully functional UL97 would be more fit than the phenotypic GCV-resistant mutants, especially since the UL97 function is essential for virus replication (Emery and Griffiths, 2000).

UL97 autophosphorylation has been identified as a prerequisite for the phosphorylation of GCV (Michel et al., 1999). This has been verified by the examination of three mutant UL97 species, whereby a loss in UL97 autophosphorylation resulted in a loss of GCV phosphorylation. The mutations of the invariant lysine at codon 355 and the conserved asparagine at codon 461 resulted in a complete loss of UL97 and GCV phosphorylation.

Interestingly, the mutation of the leucine at codon 397 also resulted in a near total loss of UL97 phosphorylation and a complete loss in GCV phosphorylation. This amino acid does not appear to be conserved among the herpesviruses, yet it was identified following treatment of HCMV with increasing concentrations of 1263W94, as the mutation conferring 1263W94 resistance. This shall be discussed later in this chapter. The fact that no phenotypic GCV-resistance mutants resulted in a complete loss of GCV phosphorylation suggested autophosphorylation may be associated with the biological function of UL97. This is particularly significant, considering the mutant UL97 species expressed were the most common mutants isolated from GCV resistant isolates.

The advantage of the plaque reduction assay in the baculovirus system over culturing HCMV in fibroblasts is the rapidity of the assay, by virtue of the speed of replication of the baculovirus (48 hr). HCMV is a slow growing virus in culture and this rate of replication is reduced upon development of mutations within the UL97 ORF (Emery et al., 2000). Inconsistencies have been observed in attempts to determine IC<sub>50</sub> values for GCV against the wild type and the phenotypic GCV-resistant HCMV isolates. This has led to various attempts to standardise the methodologies to determine the IC<sub>50</sub> for each individual mutation (Erice et al., 1999). The situation with HCMV isolates becomes complicated upon addition of further UL97 point mutations, and further complications arise from mutations occurring within the UL54 ORF. Further, upon culture of the GCV-resistant HCMV isolates, the potential of the virus is to repopulate with wild type virus due to the growth advantage of the wild type virus over the mutant virus. This means the GCV selective pressure should be maintained in cell culture. Perhaps the greatest complicating factor arises due to mixed virus populations within clinical isolates from immunocompromised patients treated with GCV (Gerna et al., 1992; Baldanti et al., 1998a, 1998b; Erice et al., 1999). The advantage of the baculovirus system in this situation arises from the fact that UL97 is not essential for baculovirus replication. Thus the presence of a mutation within the UL97 ORF will not adversely affect the rate of baculovirus replication, as occurs in the GCV-resistant HCMV isolate. This effectively means that the reduction in the number of plaques induced by increasing concentrations of GCV accurately reflects the effect of the individual UL97 mutation upon the initial phosphorylation of GCV. A further advantage of the baculovirus system to determine antiviral resistance profiles is that HCMV grown in cell culture over a relatively short period of time genotypically adapt to the cell culture system, thus potentially

altering the replication of the virus in culture and so the accuracy of the antiviral testing. Although the  $IC_{50}$  values for GCV determined for the wild type and mutant UL97 species in the baculovirus system appear higher than those observed with the clinical isolates, this can be explained by the fact that the drug is being used in an insect cell culture system as opposed to human cells, where the enzymes are different. Given the potential accuracy of the plaque reduction assay in the baculovirus system, it would be interesting to determine the effect on GCV sensitivity of mixed virus populations, including wild type and mutant UL97 species. Also, determination of the potential additive effect of increasing numbers of individual mutations in resistance of the virus to GCV.

Although the plaque reduction assay gives an accurate reflection of the impact of each mutation upon GCV sensitivity, it does not show a direct interaction between the UL97 and GCV. In order to clarify this interaction, an assay was designed to demonstrate the phosphorylation of the GCV itself. Controls used in this assay included uninfected insect cells and LacZ baculovirus-infected cells. GCV phosphorylation was not demonstrated in either control indicating the LacZ and the innate protein kinases of the insect cells were not capable of performing the initial phosphorylation of GCV. This activity appeared to be specific to the UL97 baculovirus-infected cells, suggesting UL97 was responsible for the phosphorylation. However another explanation can be found for this phosphorylation. Accessory proteins from the insect cells could be activated by phosphorylation induced by the UL97, which in turn perform the phosphorylation of the GCV. This is why it is essential to demonstrate GCV phosphorylation in the absence of contaminating accessory proteins. This assay can provide quantitative information regarding the reduction in GCV phosphorylation by the mutant UL97 species compared to the wild type virus, but it can not provide further information regarding the kinetics of phosphorylation of because it does not demonstrate a direct interaction between the UL97 and the GCV. This elusive goal can only be demonstrated with purified UL97, without the interference of accessory proteins.

Direct phosphorylation of GCV by recombinant UL97 was previously demonstrated by He and colleagues (He et al., 1998, unpublished data), using an *in vitro* GCV kinase assay designed to measure the phosphorylation of GCV by highly purified baculovirus expressed UL97. The *in vitro* GCV kinase assay should theoretically show the extent of GCV phosphorylation by the wild type UL97 protein kinase and indicate the effect of each point

mutation upon the protein kinase activity of the UL97. Unfortunately the *in vitro* kinase assay did not produce reliable kinetic data despite multiple repetitions using different conditions to try to optimise the UL97 kinase activity.

The method described by He et al., 1997 yielded the best results, in that the scintillation counts were higher than those of the negative controls, but these results were not always repeatable. Further to this, upon performing a time course of GCV phosphorylation by the purified UL97, the phosphorylation of GCV did not follow the kinetics expected of a first order reaction, as demonstrated with the kinetics of UL97 autophosphorylation, although the scintillation counts were greater than those of the negative controls. The method was modified to that originally described by Littler et al., (1992), but yielded scintillation counts no greater than those achieved by the He et al (1997) method, with little difference between the negative controls (LacZ and uninfected cell lysates) and the recombinant UL97.

1263W94 has not yet been defined in terms of antiviral function. UL97 was identified following the development of the point mutation L397R after multiple passage of AD169 through increasing concentrations of 1263W94, as the gene upon which the drug acts. As the drug is not a nucleoside analogue, it does not need initial activation by phosphorylation; therefore its antiviral activity would not be due to inhibition of this process, unlike GCV. In order to determine the mechanism of action of 1263W94, the drug was added to purified UL97 and subjected to a protein kinase assay. 1263W94 was initially tested against a crude cellular lysate containing the UL97 species and the negative controls, uninfected cells and LacZ-infected cells, to ensure the drug specifically inhibited the UL97. Phosphorylation of the protein species in the crude cell lysates, which are also phosphorylated in the kinase assay, remained unaffected in the presence of 1263W94. The 1263W94 specifically abolished the UL97 autophosphorylation in the wild type and all GCV-resistant mutants of UL97, to <10% of that of the uninhibited wild type UL97 phosphorylation. The autophosphorylation of the 1263W94-resistant UL97 (L397R) remained unaffected, at about 10% of that of the wild type UL97. The IC<sub>50</sub> of 1263W94 for the wild type and mutant UL97 species were determined to investigate if the presence of the point mutations within the UL97 affected the efficacy of 1263W94. The IC<sub>50</sub> for 1263W94 of all the UL97 species were within 0.012µM of each other, with a mean value of 0.033µM. The significant point is

that each of the phenotypic GCV-resistant mutants exhibited the equivalent sensitivity to 1263W94 as the wild type UL97. This means that in the clinical setting, 1263W94 can be used as a real alternative to the current second line drugs, foscarnet and cidofovir as treatment for GCV-resistant HCMV disease. The  $IC_{50}$  of 1263W94 for the M460I mutant however, indicated a four times increase in the sensitivity to the drug, at  $0.0048\mu\text{M}$ . Again, this may be due to the position of the 460 codon within the conserved protein kinase consensus sequence HRDLKXXN within the catalytic loop. Since the N461G mutation exhibited a total loss in autophosphorylation, this theory could not be tested using 1263W94.

The presence of the L397R mutation in the subdomain III of the protein kinase, involved in the stabilisation of the interaction between the invariant lysine and the  $\alpha$ - and  $\beta$ - phosphates of the ATP, suggests the 1263W94 affected this interaction. To determine how the 1263W94 inhibited the autophosphorylation of UL97, protein kinase assays were performed in which the drug concentration was kept constant in an assay with increasing concentrations of ATP. This assay would indicate whether 1263W94 was interacting with ATP binding. Generation of Lineweaver-Burke plots at each inhibitor concentration for the reciprocal of phosphate incorporation against the reciprocal of ATP concentration, showed inhibition by 1263W94 was alleviated at high concentrations of the substrate (ATP) and increasing concentrations of 1263W94 reduced the phosphate incorporation, as determined by UL97 autophosphorylation. When the plots were merged, the resulting family of lines converged around the Y-axis at approximately  $1/V_{\text{max}}$ . These observations are consistent with the 1263W94 acting as a competitive inhibitor of ATP. The 1263W94 is not an exact analogue of ATP, but observation of the structure of 1263W94 indicates many similarities between ATP and the drug. The inhibition constant ( $K_i$ ) for each of the 1263W94 concentrations were  $0.01\mu\text{M}$ , suggesting the drug is a potent inhibitor of ATP.

Finally, if UL97 autophosphorylation is a prerequisite for the activation of GCV, it would follow that inhibition of this phosphorylation would result in an inactivation of GCV. In order to test this theory and to determine the effect of 1263W94-mediated UL97 autophosphorylation inhibition upon GCV phosphorylation, a GCV kinase assay was performed either in the presence or absence of 1263W94. The initial observation suggests that upon inhibition of UL97 autophosphorylation, there is a reduction in GCV



phosphorylation. Upon closer inspection however, the enzyme is not behaving in the manner expected in a first order rate of reaction, as observed for UL97 autophosphorylation in chapter 5. The preliminary results are therefore inconclusive, and are primarily prone to the same problems encountered when trying to perform the GCV kinase kinetic experiments discussed earlier. Perhaps a better experiment to perform in the light of the results indicating 1263W94 does not affect any of the proteins from the crude cell lysate, would be a plaque reduction assay with GCV either in the presence or absence of 1263W94. Additionally, this would show the activity of both drugs and their interaction in a more physiological environment.

The concentration of UL97 added to each assay was approximately equal, as determined by the measurement of the optimal density of the protein solutions at an absorbance of 670nm, and comparative measurement of the protein expression levels by western blot using the anti-UL97 monoclonal antibody. The concentrations of the protein used in each assay were extremely low. To improve the reproducibility of the assays, higher concentrations of the recombinant protein, or indeed by more sensitive measuring devices such as HPLC would be preferable. When conventional methods such as autoradiography are utilised, background levels of radioactivity will always be present to fog the film, and so the resulting autoradiography bands have to be normalised in order to reduce the background. Analysis of the incorporation of radio-labelled ATP would be more accurately performed by the phosphorimager for the BioRad multianalyst. This would measure the exact amount of incorporated radioactivity and the result digitised. A combination of better purification techniques yielding a greater concentration of protein, together with the phosphorimager would increase the accuracy and reproducibility of the results.

Since DNA microarrays were pioneered for the study of genes within the cell cycles of various organisms, kinase chips have been developed in which kinases are tested for their ability to phosphorylate immobilised substrates. The investigators were able to successfully immobilise the substrate proteins on a surface using a specialised linking chemistry involving epoxy-silane, conduct the kinase reactions in volumes  $\leq 0.5\mu\text{l}$  and quantify the phosphoryl transfer using a high resolution phosphorimager (Snyder et al., 2001). This technology can be used to identify potent and selective inhibitors of kinases, so can be

adapted for performing assays to determine IC<sub>50</sub> values and the enzyme analysis involved in enzyme inhibition. The protein chips do however require highly purified protein preferably with a tag such as GST for immobilisation purposes, but the concentration of protein used is considerably less than that of conventional assays of protein kinase activity involving transfer of the  $\gamma$ -phosphoryl group from radioactive  $\gamma$ -<sup>32</sup>P-ATP to individual proteins, followed by polyacrylamide gel electrophoresis to separate the ATP from the phosphorylated product.

**CHAPTER 7**  
**General Discussion**

In the clinical setting, HCMV is controlled with GCV, ACV, foscarnet and cidofovir. The *in vivo* efficacy of these compounds have been extensively studied, as indeed has the emergence of phenotypic and genotypic ganciclovir resistance mutants following long term therapy. An important consideration in both the pathogenesis of antiviral-resistant virus and the clinical options is the contribution of resistant virus to the disease process. Does the resistant virus actually cause disease or indeed potentiate existing disease? This question has been answered by molecular methodologies, applied to detect mutant virus in mixed populations of both mutant and wild type virus. During and following antiviral therapy, viral load can be monitored and the proportion of mutant virus determined within that population. Pathologists have used these data in conjunction with clinical observations to indicate the potential of the resistant virus to exacerbate clinical disease. Evidence for the pathogenic potential of resistant virus has been observed in the AIDS population. Disease progression often occurred in HCMV retinitis patients following prolonged GCV therapy (Bowen et al., 1996). The eye is a good model to study the pathogenicity of resistant virus, as the eye is an immunologically privileged site (Koevary., 2000). The bioavailability of antiviral drugs to the eye is low (Gane et al., 1997), so suboptimal, and development of antiviral resistance can potentially occur independently of the situation occurring in the blood (Bowen et al., 1996). Thus, ophthalmic observations confirming retinal lesion enlargement, an increase in viral load and virtually 100% of the virus analysed from such lesions comprising of mutant virus, strongly correlates with the mutant virus causing disease progression.

Data on the HCMV load and distribution of GCV-resistant mutations within different organs have not previously been described. This thesis showed that in patients exposed to continuous GCV therapy, resistance to GCV is common at autopsy and does not occur uniformly in different tissue types, such that high level resistance in one organ is not always reflected in other organs of the same patient. Also a significant correlation between increasing viral load and the presence of GCV-resistance mutations was identified. These data suggest that merely assessing the appearance of resistant virus in one body compartment may provide misleading data on the true prevalence of resistant virus in other target organs. Additionally, it is increasingly important to control viral replication the data suggests that mutant virus can replicate to high levels, and as previously stated, this will

result in disease progression. Most importantly, these facts should be carefully considered in the design of future trials with other antiviral compounds active against HCMV.

Mathematical models have been employed to examine the dynamics of HCMV replication *in vivo* and to determine the relative fitness, in terms of repopulation of wild type and mutant viruses under the selective pressure of ganciclovir (Emery et al., 1999, Emery and Griffiths, 2000). The replication of wild type virus is inhibited by the presence of the antiviral drug, GCV. Selective pressure exerted upon the wild type virus by the continued presence of the drug results in the generation of GCV-resistance mutants. These mutants have a distinct replication advantage over the wild type virus in the presence of GCV, which is exemplified by the presence of near total mutant virus populations in the blood and vitreous fluid of AIDS patients following long term ganciclovir therapy. The increase in fitness of HCMV with one mutation in the UL97 gene was shown to range from 3.7% to 9% (L595F, H520Q and M460V/I), and with 2 mutations from 2.6% to 7.5% (A594V + M460I and L595F + M460I). Conversely, when therapy was changed from GCV to cidofovir the selective pressure was against the mutants resulting in a relative fitness gain for wild type virus of 3.5% to 5.6% for single mutations and 12.8% for double mutations. Expanding upon these results, the time to appearance of GCV resistance mutants and relative proportion of the mutant within the virus population following short- and long-term GCV therapy was determined.

A detailed characterisation of the impact of each point mutation upon the function of the HCMV UL97 kinase activity, in terms of UL97 phosphorylation and ganciclovir phosphorylation, may highlight how the reduction in viral fitness is achieved following GCV therapy. The study of UL97 kinase activity has previously been problematic as the molar quantity of the protein is very low, so isolation of the protein from other cellular proteins has been difficult. Heterologous protein expression systems designed to express large quantities of the desired protein for efficient purification and characterisation of the protein would be useful. However, as discussed in section 1.9, it is essential to study the protein which has been correctly post translationally modified and purified from the host

proteins as a soluble, functionally active protein. This is especially important when identifying the impact of single point mutations upon the function of the protein.

In order to overexpress the HCMV UL97, in a correctly post translationally modified form, the baculovirus expression system was chosen. Initially the recombinant baculoviruses, BVMelBac-UL97 and BVBluBacHis-UL97, were constructed with the expression of the UL97 ORF under the control of the polyhedrin promoter. This resulted in the expression of large quantities of the pMelBac-UL97 and pBluBacHis-UL97 as detected by coomassie brilliant blue staining and western blot, although the expression of the latter was considerably less than that of the former. The reasons for this remain unclear, but may be a result of the N-terminal fusions or possibly due to codon usage.

The BVMelBac-UL97 was chosen for further work, not only due to the higher level of UL97 expression, but for the potential of the protein in this expression system to be secreted into the tissue culture medium. Secretion should make purification of the protein considerably easier, resulting in greater concentrations than have previously been observed. Following a failure to detect the recombinant UL97 in the culture medium, even at a high MOI and despite consistent detection of the protein in the insect cells themselves, it was postulated that competition may be occurring between the signal sequences for nuclear localisation (UL97), and secretion (N-terminal honey bee melitin) signal. To determine the location of the expressed UL97, the insect cells were stained with an anti-UL97 monoclonal antibody. This resulted in the identification of the UL97 throughout the cell and not specifically within the nucleus or at the plasma membrane.

Following construction of the recombinant baculoviruses expressing the wild type UL97, point mutations were engineered into the UL97 ORF by site directed mutagenesis. The specific mutations were chosen due to the frequency in which the mutations were detected in GCV-resistant clinical strains of HCMV following GCV therapy. Additionally, previous work upon these isolates highlighted a reduction in replicative fitness of the mutant viruses compared to the wild type virus. The biochemical analysis of the recombinant wild type and mutant UL97 species was performed by two approaches. Initially autophosphorylation of the

wild type and mutant species of UL97 was examined to quantitatively determine the effect of each point mutation upon the autophosphorylation of the UL97 itself, and to equate the differences with reduction in relative fitness of the clinical isolates. Secondly, phosphorylation of GCV was performed to determine the effect of each point mutation upon this activity. To perform any of the biochemical analysis, highly purified UL97 was required to eliminate the interference of any co-purified protein kinase. With the honey bee secretion signal being inactive in this system, the proteins had to be purified by conventional biochemical means. These methods are time consuming and inefficient, but highly purified UL97 was obtained following ion exchange chromatography and ammonium sulphate precipitation. This purification was essential for the study of GCV phosphorylation and to determine the antiviral activity of the novel antiviral, 1263W94. Interestingly, the only genotypic GCV-resistant mutant exhibiting a reduction in UL97 autophosphorylation, compared to the wild type UL97, was the M460I mutant. This suggests that the reduction in viral fitness may not be associated with UL97 autophosphorylation. Autophosphorylation however, appears to be a prerequisite for GCV phosphorylation. This has been shown here and has previously been described for UL97 mutants engineered with point mutations in conserved amino acids. The fact that no genotypic GCV-resistant mutants have been shown to be completely impaired in UL97 autophosphorylation suggests the contrary however.

Comparison of the results of UL97 autophosphorylation, GCV phosphorylation and the lower level of viral fitness of the mutant viruses compared to the wild type virus presents somewhat of a conundrum. The majority of GCV-resistant clinical isolates exhibit the same level of autophosphorylation as the wild type virus but the level of GCV phosphorylation is reduced to below 20% of that of the wild type. Additionally, the relative fitness difference of the mutant and wild type viruses is 5.6%, as demonstrated by mathematical modelling (Emery and Griffiths., 2000). Why would the mutant viruses have the same level of UL97 autophosphorylation but have a reduced fitness. This suggests that autophosphorylation is necessary for ganciclovir monophosphorylation but unnecessary for the phosphorylation of the natural substrate of UL97. The reduction in viral fitness may be the result of inefficient binding of the natural substrate to UL97 with resistance mutations. Additionally, clinical isolates with 2 mutations in the UL97 are relatively uncommon and isolates in which 3 or

more mutations have been detected in the UL97 is previously undescribed. A distinct problem with this hypothesis is the lack of clinical isolates detected in which UL97 is not phosphorylated, although it may be assumed that autophosphorylation is coincidental to the function of the kinase thus you would not expect to see such isolates. In order to examine the combined effects of these mutations, as opposed to the single mutation introduced into the UL97 gene, it would be useful to generate mutants with 2 or more of the GCV resistance mutations. This would indicate if the presence of 2 or mutations causes a reduction in the autophosphorylation of the UL97, and if not, would further suggest the redundancy of autophosphorylation.

Three experimental routes could be taken to determine the necessity of autophosphorylation in the natural function of the kinase, which shall be discussed individually. Firstly, the natural substrate of UL97 is currently unknown, however UL97 is a protein kinase, which phosphorylates on serines and threonines. One substrate for such kinases is histones and it has been demonstrated that UL97 can phosphorylate the H2b histone. Using the wild type and mutant UL97 species, the H2b could be used in a protein kinase assay and the resulting histone phosphorylation quantified for each mutant. This would identify the relative inefficiency of histone phosphorylation as a function of the point mutations, and not as a result of autophosphorylation. The level of autophosphorylation of the mutant identified to be resistant to 1263W94 (L397R) was decreased to below 15% of that of the wild type virus. This mutant could be used for the negative control to determine if the histone was still phosphorylated in the absence of UL97 autophosphorylation.

This mutant leads the way to the second set of experiments, whereby the point mutation can be transferred to a GCV-sensitive HCMV strain such as AD169 by homologous recombination. If autophosphorylation is essential for the natural function of the kinase, it would be expected that in a time course experiment to follow the replication of the virus by detection of DNA or RNA, using wild type AD169 in parallel experiment, the mutant virus would be severely debilitated in its replication, given the essential nature of UL97 in the replication of HCMV. This could be taken further by co-culturing the mutant virus with wild type virus in a similar assay, either in the presence or absence of 1263W94. If a 1:1



ratio of wild type to mutant virus were used in the absence of 1263W94, it would be expected that the wild type virus would out-compete the resistant mutant virus and could be easily demonstrable with such technologies such as Taqman real time PCR. The real time PCR could determine the proportion of wild type virus to mutant virus in the mixed population by probe annealing and melting point differentiation and indicate the extent to which the mutant virus has been outcompeted. In a similar assay with a 1:1 ratio of viruses in the presence of 1263W94, the mutant virus may only marginally outcompete the wild type virus if autophosphorylation were essential, since it retains approximately 15% of its autophosphorylation activity. If autophosphorylation were unnecessary for the natural function of the protein, it would be expected that the mutant virus would outcompete the wild type virus in the presence of drug. Of course this would depend upon the mutation not inhibiting the natural function of the kinase. The extent of this competition could be examined by altering the input ratios of the wild type and mutant viruses, whereby up to 90% of one virus could be tested in the system in the presence of absence of drug. The third line of experiments to determine the essential nature of autophosphorylation would involve identification of the serine or threonine residues upon which the UL97 autophosphorylates. The serine residues identified lie predominantly towards the N-terminal section of the protein and outside of the kinase catalytic domains. This was observed by transphosphorylation experiments, whereby a truncated UL97 expressing from aa 300 was not phosphorylated by co-incubation with wild type UL97 in a protein kinase assay (data not shown). By performing site directed mutagenesis upon these serine residues and replacing them with a similarly basic amino acid, it would be possible to locate the residues involved in the autophosphorylation and determine if their involvement is essential.

There may however be a further, simpler explanation. The reduction in viral fitness is as small as 5%, therefore the assay to determine the degree of autophosphorylation of UL97 may not be sensitive enough to detect such a small reduction. Indeed, the concentration of UL97 used for each assay was sufficiently small that the standard deviation between each assay may be +/- 5%.

The plaque assay, essential for the isolation of the recombinant baculovirus clones, the generation of high titre stocks and the titration of the virus stocks was optimised. The titration of the virus stocks was reliable and highly reproducible, so ensuring the optimisation of the MOI for protein expression was reproducible. It also ensured the difference in expression of the two protein species, pMelBac-UL97 and pBluBacHis-UL97, was not merely due to differences in initial virus titre. Analysis of the UL97 activity was achieved by virtue of the  $\beta$ -galactosidase expression by the recombinant baculoviruses. A titration of the baculoviruses by plaque assay resulted in blue plaques following staining with X-gal, allowing a clear identification of the infected cells. Using this marker, co-cultivation of the mutant and wild type UL97-expressing viruses with increasing concentrations of GCV resulted in a large reduction in the number of plaques of the wild type UL97 virus. Culture of the mutant UL97 baculoviruses in increasing concentrations of GCV resulted in GCV-induced inhibition of baculovirus replication, which differed according to which mutations were present. The GCV-resistant mutants in which the inhibition was greatest were those occurring within domains conserved throughout the protein kinase superfamily, although the amino acids themselves were not conserved. The mutations in the UL97, which confer GCV resistance, also induced a reduction in the number of plaques upon co-cultivation with GCV. Thus the plaque reduction assay was a good screening assay to identify the effect of the mutations with regard to the resistance of the virus to the antiviral action of GCV induced by the mutations and may reflect the *in vivo* situation of the effect of the mutants upon GCV phosphorylation.

Novel antivirals with novel mechanisms of action are increasingly in demand in the HCMV setting. This is due to the poor bioavailability of the currently used drugs, the risk of serious side effects following long term treatment and the fact that the current drugs all ultimately have the same target, the HCMV DNA polymerase. This means selection of cross-resistant mutants is more likely to occur. The novel antiviral 1263W94 and its precursor BDCRB were selected as potent inhibitors of HCMV replication from a panel of benzimidazole ribosides. BDCRB was shown to inhibit the viral replication at the stage of viral DNA maturation, when the viral DNA concatamers are processed to form unit length DNA for packaging into the viral capsids. 1263W94 has a completely different mechanism of action

from the BDCRB, as was demonstrated by the development of a point mutation within the UL97 following culture of the HCMV lab strain AD169 in increasing concentrations of 1263W94. GCV activity relies on the initial monophosphorylation performed by the UL97 protein kinase, incorporation of the triphosphorylated GCV into the growing DNA chain and inhibition of the DNA polymerase. 1263W94 however does not require an initial phosphorylation catalysed by UL97 and it does not interact with the DNA polymerase, so not inhibiting its activity. Thus, the mechanisms of action of the GCV and 1263W94 are completely different. This is confirmed by the lack of cross resistance of the GCV-resistant isolates to 1263W94.

Data in this thesis has shown 1263W94 is a competitive inhibitor of ATP binding, resulting in an inhibition of UL97 autophosphorylation. This observation has important implications with respect to treatment of patients with HCMV disease. Firstly, 1263W94 is effective against all genotypic GCV-resistance mutations. This means that HCMV disease can be controlled following development of mutations inducing GCV resistance following long term therapy. Two obvious problems are however indicated. The fact that autophosphorylation may be required for GCV phosphorylation means that dual treatment with GCV and 1263W94 will not be possible. Also, if following long term treatment of HCMV disease with 1263W94 induces mutations resulting in mutants lacking autophosphorylation, such as the L397R mutation, a change of treatment back to GCV would not be possible. It would therefore be necessary to treat the resistant virus with the second line antivirals foscarnet and cidofovir. These two drugs do not require the action of UL97, so cross resistance due to the requirement of the same gene for the activity of the drug will not be a problem. Conclusive data to show the elimination of UL97 autophosphorylation does not inhibit GCV phosphorylation had been very difficult to demonstrate.

The observation that the autophosphorylation of UL97 is essential for the activation of GCV has been based upon the fact that in the absence of UL97 autophosphorylation, GCV is not monophosphorylated. This may not be entirely correct, as the observation was made using UL97 species generated with mutants engineered into amino acids conserved among protein

kinases. Autophosphorylation may therefore not occur as these conserved domains are essential for the natural activity of the UL97 kinase, which includes autophosphorylation. It would be expected that if the natural function of UL97 has been disrupted, the phosphorylation of GCV would also be affected. This is backed up by the fact that no mutants have been isolated from clinical samples, which completely lack autophosphorylation. It would therefore be interesting to determine the effect of the 1263W94 mutation upon the activity of the virus in an *in vivo* situation, given that the L397R mutant exhibits a greatly reduced autophosphorylation and GCV phosphorylation activity. The autophosphorylation of the L397R mutant was reduced to below 15% of that of the wild type virus, suggesting a significant reduction in viral fitness so probably a gross effect upon the natural activity of the UL97, impairing the viability of the 1263W94-resistant virus. This means the L397R mutation would not be advantageous to the virus even in the presence of 1263W94. This situation is not that unusual among viruses. Mutations occurring within the DNA polymerase gene of Hepatitis B following treatment with lamivudine have been shown to render these viruses less fit in terms of replication (Gaillard et al., 2002). These mutations have been mapped to the highly conserved YMDD motif and an upstream motif FLLAQ, so resulting in a lowered affinity of the mutant polymerase for the natural dNTP substrates, and a decreased affinity to the activated lamivudine triphosphate. Mutations in the reverse transcriptase of HIV following treatment with HAART also induces a reduction in the replicative fitness of the virus. Devereaux et al., (2001) observed a reduction in the viral fitness of between 11.6% and 21% for mutant viruses, which were rapidly displaced by wild type virus following the cessation of therapy. Generally in HIV, primary drug resistance, mutations occur in the reverse transcriptase and protease, which reduce the fitness of the virus relative to the wild type virus. Further acquisition of secondary mutations however, appears to restore the replicative fitness of these drug resistant strains.

With prolonged GCV therapy necessary for the transplant populations and more especially the AIDS populations, particularly now that HAART failures have been identified, novel antivirals are becoming increasingly necessary as alternatives to GCV. Prolonged GCV therapy can result in leukopenia, thrombocytopenia, leukoplasia, anaemia and bone marrow

toxicity (Crumpacker, 1996). In comparison, BDCRB and 1263W94 exhibit reduced cytotoxicity to bone marrow cells (Townsend et al., 1995, Chulay et al., 2000), which is particularly important when considering the bone marrow transplant populations. This reduction in cytotoxicity and good bioavailability, combined with the extremely high potency of 1263W94 against HCMV suggests 1263W94 would be preferable as a first line antiviral in the treatment of HCMV, especially in the transplant populations. It would be interesting to determine the concentration of the drug within different organs and tissues, when considering high viral loads were found in the liver, lymph nodes and adrenal glands and GCV-resistance mutations were also found in these tissues. This need for novel antivirals with activity against HCMV using different mechanisms of action has been highlighted in recent years with the failure of HAART and the emergence once again of GCV-resistant virus. With 1263W94 potentially unable to be used in combination therapy with GCV, other antivirals with the ability to be used in combination with either 1263W94 and/or GCV, such as fomiversen, the non-nucleoside inhibitors and potential inhibitors of the HCMV protease, should be sought.

## **REFERENCES**

## REFERENCES

Ahn JH, Jang WJ, Hayward GS. The human cytomegalovirus IE2 and UL112-113 proteins accumulate in viral DNA replication compartments that initiate from the periphery of promyelocytic leukemia protein-associated nuclear bodies (PODs or ND10). *J Virol* 1999;73:10458-71.

Ahn K, Angulo A, Ghazal P, Peterson PA, Yang Y, Fruh K. Human cytomegalovirus inhibits antigen presentation by a sequential multistep process. *Proc Natl Acad Sci U S A* 1996;93:10990-10995.

Ahn K, Gruhler A, Galocha B et al. The ER-luminal domain of the HCMV glycoprotein US6 inhibits peptide translocation by TAP. *Immunity* 1997;6:613-21.

Alain S, Honderlick P, Grenet D et al. Failure of ganciclovir treatment associated with selection of a ganciclovir-resistant cytomegalovirus strain in a lung transplant recipient. *Transplantation* 1997;63:1533-36.

Alford CA, Stagno S, Pass RF, Britt WJ. Congenital and perinatal cytomegalovirus infections. *Rev Infect Dis* 1990;12 Suppl 7:S745-S753.

Anderson KP, Fox MC, Brown-Driver V, Martin MJ, Azad RF. Inhibition of human cytomegalovirus immediate-early gene expression by an antisense oligonucleotide complementary to immediate-early RNA. *Antimicrob Agents Chemother* 1996;40:2004-11.

Ansari A, Emery VC. The U69 gene of human herpesvirus 6 encodes a protein kinase which can confer ganciclovir sensitivity to baculoviruses. *J Virol* 1999;73:3284-91.

Asano Y, Yoshikawa T, Suga S, Yazaki T, Kondo K, Yamanishi K. Fatal fulminant hepatitis in an infant with human herpesvirus-6 infection [letter]. *Lancet* 1990;335:862-63.

Asano Y, Yoshikawa T, Kajita Y et al. Fatal encephalitis/encephalopathy in primary human

herpesvirus-6 infection. *Arch Dis Child* 1992;67:1484-85.

Atkins M, Strappe P, Kaye S et al. Quantitative differences in the distribution of zidovudine resistance mutations in multiple post-mortem tissues from AIDS patients. *J Med Virol* 1998;55:138-46.

Autran B, Carcelain G, Li TS et al. Positive effects of combined antiretroviral therapy on CD4+ T cell homeostasis and function in advanced HIV disease. *Science* 1997;277:112-16.

Bacigalupo A, van Lint MT, Tedone E et al. Early treatment of CMV infections in allogeneic bone marrow transplant recipients with foscarnet or ganciclovir. *Bone Marrow Transplant* 1994;13(6):753-8.

Badley AD, Patel R, Portela DF et al. Prognostic significance and risk factors of untreated cytomegalovirus viremia in liver transplant recipients. *J Infect Dis* 1996;173:446-49.

Badley AD, Seaberg EC, Porayko MK et al. Prophylaxis of cytomegalovirus infection in liver transplantation: a randomized trial comparing a combination of ganciclovir and acyclovir to acyclovir. NIDDK Liver Transplantation Database. *Transplantation* 1997;64:66-73.

Baer R, Bankier AT, Biggin MD et al. DNA sequence and expression of the B95-8 Epstein-Barr virus genome. *Nature* 1984;310:207-11.

Baldanti F, Underwood MR, Stanat SC et al. Single amino acid changes in the DNA polymerase confer foscarnet resistance and slow-growth phenotype, while mutations in the UL97- encoded phosphotransferase confer ganciclovir resistance in three double-resistant human cytomegalovirus strains recovered from patients with AIDS. *J Virol* 1996;70:1390-1395.

(A)Baldanti F, Simoncini L, Sarasini A et al. Ganciclovir resistance as a result of oral



ganciclovir in a heart transplant recipient with multiple human cytomegalovirus strains in blood. *Transplantation* 1998;66:324-29.

(B)Baldanti F, Underwood MR, Talarico CL et al. The Cys607-->Tyr change in the UL97 phosphotransferase confers ganciclovir resistance to two human cytomegalovirus strains recovered from two immunocompromised patients. *Antimicrob Agents Chemother* 1998;42:444-46.

Balfour HH, Jr., Chace BA, Stapleton JT, Simmons RL, Fryd DS. A randomized, placebo-controlled trial of oral acyclovir for the prevention of cytomegalovirus disease in recipients of renal allografts. *N Engl J Med* 1989;320:1381-87.

Bancroft GJ, Shellam GR, Chalmer JE. Genetic influences on the augmentation of natural killer (NK) cells during murine cytomegalovirus infection: correlation with patterns of resistance. *J Immunol* 1981;126:988-94.

Barkholt LM, Ehrnst A, Veress B, Johansson B, Andersson J, Groth GC. New criteria for diagnosing cytomegalovirus hepatitis in liver transplant patients. *Transplant Proc* 1995;27:1224-5.

Barkholt L, Lewensohn-Fuchs U, Ericzon BG, Tyden G, Andersson J. High dose acyclovir prophylaxis reduces cytomegalovirus disease in liver transplant patients. *Transpl Infect Dis* 1999; 1(2):89-97.

Barnes PD, Grundy JE. Down-regulation of the class I HLA heterodimer and beta 2-microglobulin on the surface of cells infected with cytomegalovirus. *J Gen Virol* 1992;73 (Pt 9):2395-403.

Batra R, Khayat R, Tong L. Molecular mechanism for dimerization to regulate the catalytic activity of human cytomegalovirus protease. *Nat Struct Biol* 2001;8:810-817.

Beaudet-Miller M, Zhang R, Durkin J, Gibson W, Kwong AD, Hong Z. Virus-specific interaction between the human cytomegalovirus major capsid protein and the C terminus of the assembly protein precursor. *J Virol* 1996;70:8081-88.

Beck S, Barrell BG. Human cytomegalovirus encodes a glycoprotein homologous to MHC class-I antigens. *Nature* 1988;331:269-72.

Beersma MF, Bijlmakers ML, Ploegh HL. Human cytomegalovirus down-regulates HLA class I expression by reducing the stability of class I H chains 1993;151(9):4455-64.

Belyaev AS, Roy P. Development of baculovirus triple and quadruple expression vectors: co-expression of three or four bluetongue virus proteins and the synthesis of bluetongue virus-like particles in insect cells. *Nucleic Acids Res* 1993;21:1219-23.

Belyaev AS, Hails RS, Roy P. High-level expression of five foreign genes by a single recombinant baculovirus. *Gene* 1995;156:229-33.

Benedict CA, Butrovich KD, Lurain NS et al. Cutting edge: a novel viral TNF receptor superfamily member in virulent strains of human cytomegalovirus. *J Immunol* 1999;162:6967-70.

Berenguer J, Gonzalez J, Pulido F et al. Discontinuation of secondary prophylaxis in patients with cytomegalovirus retinitis who have responded to highly active antiretroviral therapy. *Clin Infect Dis* 2002;34:394-97.

Bernad A, Blanco L, Lazaro JM, Martin G, Salas M. A conserved 3'----5' exonuclease active site in prokaryotic and eukaryotic DNA polymerases. *Cell* 1989;59:219-28.

Berneman ZN, Ablashi DV, Li G et al. Human herpesvirus 7 is a T-lymphotropic virus and is related to, but significantly different from, human herpesvirus 6 and human cytomegalovirus. *Proc Natl Acad Sci U S A* 1992;89:10552-56.

Billstrom MA, Johnson GL, Avdi NJ, Worthen GS. Intracellular signaling by the chemokine receptor US28 during human cytomegalovirus infection. *J Virol* 1998;72:5535-44.

Biron CA, Byron KS, Sullivan JL. Severe herpesvirus infections in an adolescent without natural killer cells. *N Engl J Med* 1989;320:1731-35.

Biron KK. Cytomegalovirus: genetics of drug resistance. *Adv Exp Med Biol* 1996;394:135-43.

Bodaghi B, Jones TR, Zipeto D et al. Chemokine sequestration by viral chemoreceptors as a novel viral escape strategy: withdrawal of chemokines from the environment of cytomegalovirus-infected cells. *J Exp Med* 1998;188:855-66.

Boeckh M, Gooley TA, Myerson D, Cunningham T, Schoch G, Bowden RA. Cytomegalovirus pp65 antigenemia-guided early treatment with ganciclovir versus ganciclovir at engraftment after allogeneic marrow transplantation: a randomized double-blind study. *Blood* 1996;88:4063-71.

Boeckh M, Gooley TA, Bowden RA. Effect of high-dose acyclovir on survival in allogeneic marrow transplant recipients who received ganciclovir at engraftment or for cytomegalovirus pp65 antigenemia. *J Infect Dis* 1998;178:1153-57.

Bogner E, Radsak K, Stinski MF. The gene product of human cytomegalovirus open reading frame UL56 binds the pac motif and has specific nuclease activity. *J Virol* 1998;72:2259-64.

Boivin G, Erice A, Crane DD, Dunn DL, Balfour HH, Jr. Ganciclovir susceptibilities of cytomegalovirus (CMV) isolates from solid organ transplant recipients with CMV viremia after antiviral prophylaxis. *J Infect Dis* 1993;168:332-35.

Boivin G, Chou S, Quirk MR, Erice A, Jordan MC. Detection of ganciclovir resistance mutations quantitation of cytomegalovirus (CMV) DNA in leukocytes of patients with fatal disseminated CMV disease. *J Infect Dis* 1996;173:523-28.

Bolovan-Fritts CA, Mocarski ES, Wiedeman JA. Peripheral blood CD14(+) cells from healthy subjects carry a circular conformation of latent cytomegalovirus genome. *Blood* 1999;93:394-98.

Bonavida B, Katz J, Gottlieb M. Mechanism of defective NK cell activity in patients with acquired immunodeficiency syndrome (AIDS) and AIDS-related complex. I. Defective trigger on NK cells for NKCF production by target cells, and partial restoration by IL 2. *J Immunol* 1986;137:1157-63.

Bossemeyer D. Protein kinases--structure and function. *FEBS Lett* 1995;369:57-61.

Bowen EF, Wilson P, Atkins M et al. Natural history of untreated cytomegalovirus retinitis. *Lancet* 1995;346:1671-73.

Bowen EF, Wilson P, Cope A et al. Cytomegalovirus retinitis in AIDS patients: influence of cytomegaloviral load on response to ganciclovir, time to recurrence and survival. *AIDS* 1996;10:1515-20.

Bowen EF, Sabin CA, Wilson P et al. Cytomegalovirus (CMV) viraemia detected by polymerase chain reaction identifies a group of HIV-positive patients at high risk of CMV disease. *AIDS* 1997;11:889-93.

Bowen EF, Emery VC, Wilson P et al. Cytomegalovirus polymerase chain reaction viraemia in patients receiving ganciclovir maintenance therapy for retinitis. *AIDS* 1998;12:605-11.

Bowen EF, Cherrington JM, Lamy PD, Griffiths PD, Johnson MA, Emery VC. Quantitative

changes in cytomegalovirus DNAemia and genetic analysis of the UL97 and UL54 genes in AIDS patients receiving cidofovir following ganciclovir therapy. *J Med Virol* 1999;58:402-7.

Boyle KA, Compton T. Receptor-binding properties of a soluble form of human cytomegalovirus glycoprotein B. *J Virol* 1998;72:1826-33.

(A)Braud VM, Allan DS, Wilson D, McMichael AJ. TAP- and tapasin-dependent HLA-E surface expression correlates with the binding of an MHC class I leader peptide. *Curr Biol* 1998;8:1-10.

(B)Braud VM, Allan DS, O'Callaghan CA et al. HLA-E binds to natural killer cell receptors CD94/NKG2A, B and C. *Nature* 1998;391:795-99.

Brechtbuehl K, Whalley SA, Dusheiko GM, Saunders NA. A rapid real-time quantitative polymerase chain reaction for hepatitis B virus. *J Virol Methods* 2001;93:105-13.

Browne H, Churcher M, Minson T. Construction and characterization of a human cytomegalovirus mutant with the UL18 (class I homolog) gene deleted. *J Virol* 1992;66:6784-87.

Buchbinder S, Elmaagacli AH, Schaefer UW, Roggendorf M. Human herpesvirus 6 is an important pathogen in infectious lung disease after allogeneic bone marrow transplantation [In Process Citation]. *Bone Marrow Transplant* 2000;26:639-44.

Buhles WC, Jr., Mastre BJ, Tinker AJ, Strand V, Koretz SH. Ganciclovir treatment of. *Rev Infect Dis* 1988;10 Suppl 3:S495-S506.

Cane PA, Cook P, Ratcliffe D, Mutimer D, Pillay D. Use of real-time PCR and fluorimetry to detect lamivudine resistance-associated mutations in hepatitis B virus. *Antimicrob Agents Chemother* 1999;43:1600-1608.

Carrigan DR, Knox KK. Human herpesvirus 6 (HHV-6) isolation from bone marrow: HHV-6 associated bone marrow suppression in bone marrow transplant patients. *Blood* 1994;84(10):3307-10.

Casado JL, Arrizabalaga J, Montes M et al. Incidence and risk factors for developing cytomegalovirus retinitis in HIV-infected patients receiving protease inhibitor therapy. Spanish CMV- AIDS Study Group. *AIDS* 1999;13:1497-502.

Cesarman E, Chang Y, Moore PS, Said JW, Knowles DM. Kaposi's sarcoma-associated herpesvirus-like DNA sequences in AIDS-related body-cavity-based lymphomas. *N Engl J Med* 1995;332:1186-91.

Cha TA, Tom E, Kemble GW, Duke GM, Mocarski ES, Spaete RR. Human cytomegalovirus clinical isolates carry at least 19 genes not found in laboratory strains. *J Virol* 1996;70:78-83.

Chan JH, Chamberlain SD, Biron KK et al. Synthesis and evaluation of a series of 2'-deoxy analogues of the antiviral agent 5,6-dichloro-2-isopropylamino-1-(beta-L-ribofuranosyl)-1H-benzimidazole (1263W94). *Nucleosides Nucleotides Nucleic Acids* 2000;19:101-23.

Chang Y, Cesarman E, Pessin MS et al. Identification of herpesvirus-like DNA sequences in AIDS-associated Kaposi's sarcoma. *Science* 1994;266:1865-69.

Chee M, Barrell B. Herpesviruses: a study of parts. *Trends Genet* 1990;6:86-91.

Chee MS, Lawrence GL, Barrell BG. Alpha-, beta- and gammaherpesviruses encode a putative phosphotransferase. *J Gen Virol* 1989;70 ( Pt 5):1151-60.

Chee MS, Satchwell SC, Preddie E, Weston KM, Barrell BG. Human cytomegalovirus encodes three G protein-coupled receptor homologues. *Nature* 1990;344:774-77.

Cheng YC, Huang ES, Lin JC et al. Unique spectrum of activity of 9-[(1,3-dihydroxy-2-propoxy)methyl]-guanine against herpesviruses in vitro and its mode of action against herpes simplex virus type 1. *Proc Natl Acad Sci USA* 1983;80:2767-70.

Cheng YC, Grill SP, Dutschman GE et al. Effects of 9-(1,3-dihydroxy-2-propoxymethyl)guanine, a new antiherpesvirus compound, on synthesis of macromolecules in herpes simplex virus-infected cells.

(A)Chou S, Guentzel S, Michels KR, Miner RC, Drew WL. Frequency of UL97 phosphotransferase mutations related to ganciclovir resistance in clinical cytomegalovirus isolates. *J Infect Dis* 1995;172:239-42.

(B)Chou S, Erice A, Jordan MC et al. Analysis of the UL97 phosphotransferase coding sequence in clinical cytomegalovirus isolates and identification of mutations conferring ganciclovir resistance. *J Infect Dis* 1995;171:576-83.

Chou S, Marousek G, Guentzel S et al. Evolution of mutations conferring multidrug resistance during prophylaxis and therapy for cytomegalovirus disease. *J Infect Dis* 1997;176:786-89.

Chou S, Marousek G, Parenti DM et al. Mutation in region III of the DNA polymerase gene conferring foscarnet resistance in cytomegalovirus isolates from 3 subjects receiving prolonged antiviral therapy. *J Infect Dis* 1998;178:526-30.

(A)Chou S. Antiviral drug resistance in human cytomegalovirus. *Transpl Infect Dis* 1999;1:105-14.

(B)Chou S, Lurain NS, Weinberg A, Cai GY, Sharma PL, Crumpacker CS. Interstrain variation in the human cytomegalovirus DNA polymerase sequence and its effect on genotypic diagnosis of antiviral drug resistance. Adult AIDS Clinical Trials Group CMV Laboratories. *Antimicrob Agents Chemother* 1999;43:1500-1502.

(A)Chou S, Meichsner CL. A nine-codon deletion mutation in the cytomegalovirus UL97 phosphotransferase gene confers resistance to ganciclovir. *Antimicrob Agents Chemother* 2000;44:183-85.

(B)Chou S, Miner RC, Drew WL. A deletion mutation in region V of the cytomegalovirus DNA polymerase sequence confers multidrug resistance. *J Infect Dis* 2000;182:1765-68.

Chulay J, Biron K, Wang L et al. Development of novel benzimidazole riboside compounds for treatment of cytomegalovirus disease. *Adv Exp Med Biol* 1999;458:129-34.

Cihlar T, Chen MS. Identification of enzymes catalyzing two-step phosphorylation of cidofovir and the effect of cytomegalovirus infection on their activities in host cells. *Mol Pharmacol* 1996;50:1502-10.

Cihlar T, Fuller MD, Cherrington JM. Expression of the catalytic subunit (UL54) and the accessory protein (UL44) of human cytomegalovirus DNA polymerase in a coupled in vitro transcription/translation system. *Protein Expr Purif* 1997;11:209-18.

(A)Cihlar T, Fuller MD, Mulato AS, Cherrington JM. A point mutation in the human cytomegalovirus DNA polymerase gene selected in vitro by cidofovir confers a slow replication phenotype in cell culture. *Virology* 1998;248:382-93.

(B)Cihlar T, Fuller MD, Cherrington JM. Characterization of drug resistance-associated mutations in the human cytomegalovirus DNA polymerase gene by using recombinant mutant viruses generated from overlapping DNA fragments. *J Virol* 1998;72:5927-36.

Cohen GH, Ponce dL, Diggelmann H, Lawrence WC, Vernon SK, Eisenberg RJ. Structural analysis of the capsid polypeptides of herpes simplex virus types 1 and 2. *J Virol* 1980;34:521-31.



Compton T, Nowlin DM, Cooper NR. Initiation of human cytomegalovirus infection requires initial interaction with cell surface heparan sulfate. *Virology* 1993;193:834-41.

(A)Cope AV, Sabin C, Burroughs A, Rolles K, Griffiths PD, Emery VC. Interrelationships among quantity of human cytomegalovirus (HCMV) DNA in blood, donor-recipient serostatus, and administration of methylprednisolone as risk factors for HCMV disease following liver transplantation. *J Infect Dis* 1997;176:1484-90.

(B)Cope AV, Sweny P, Sabin C, Rees L, Griffiths PD, Emery VC. Quantity of cytomegalovirus viruria is a major risk factor for cytomegalovirus disease after renal transplantation. *J Med Virol* 1997;52:200-205.

Couchoud C, Cucherat M, Haugh M, Pouteil-Noble C. Cytomegalovirus prophylaxis with antiviral agents in solid organ transplantation: a meta-analysis. *Transplantation* 1998;65:641-47.

Cranage MP, Smith GL, Bell SE et al. Identification and expression of a human cytomegalovirus glycoprotein with homology to the Epstein-Barr virus BXLF2 product, varicella-zoster virus gpIII, and herpes simplex virus type 1 glycoprotein H. *J Virol* 1988;62:1416-22.

Cresswell P. Invariant chain structure and MHC class II function. *Cell* 1996;84:505-7.

Crumpacker CS. Ganciclovir. *N Engl J Med* 1996;335:721-29.

Danner SA, Matheron S. Cytomegalovirus retinitis in AIDS patients: a comparative study of intravenous and oral ganciclovir as maintenance therapy. *AIDS* 1996;10 Suppl 4:S7-11.

Davison AJ, Scott JE. The complete DNA sequence of varicella-zoster virus. *J Gen Virol* 1986;67 ( Pt 9):1759-816.

Davison AJ, Taylor P. Genetic relations between varicella-zoster virus and Epstein-Barr

virus. *J Gen Virol* 1987;68 ( Pt 4):1067-79.

De Clercq E. Antivirals for the treatment of herpesvirus infections. *J Antimicrob Chemother* 1993;32 Suppl A:121-32.

Deayton J, Mocroft A, Wilson P, Emery VC, Johnson MA, Griffiths PD. Loss of cytomegalovirus (CMV) viraemia following highly active antiretroviral therapy in the absence of specific anti-CMV therapy. *AIDS* 1999;13:1203-6.

Deayton JR, Griffiths PD. When can cytomegalovirus prophylaxis and maintenance therapy be stopped in HIV disease? *Curr Opin Infect Dis* 2000;13:637-41.

del Val M, Munch K, Reddehase MJ, Koszinowski UH. Presentation of CMV immediate-early antigen to cytolytic T lymphocytes is selectively prevented by viral genes expressed in the early phase. *Cell* 1989;58:305-15.

del Val M, Hengel H, Hacker H et al. Cytomegalovirus prevents antigen presentation by blocking the transport of peptide-loaded major histocompatibility complex class I molecules into the medial-Golgi compartment. *J Exp Med* 1992;176:729-38.

Devereux HL, Emery VC, Johnson MA, Loveday C. Replicative fitness in vivo of HIV-1 variants with multiple drug resistance-associated mutations. *J Med Virol* 2001;65:218-24.

Dieterich DT, Poles MA, Lew EA et al. Concurrent use of ganciclovir and foscarnet to treat cytomegalovirus infection in AIDS patients. *J Infect Dis* 1993;167:1184-8.

Di Perri G, Vento S, Mazzi R et al. Recovery of long-term natural protection against reactivation of CMV retinitis in AIDS patients responding to highly active antiretroviral therapy. *J Infect* 1999;39:193-97.

Dodt KK, Jacobsen PH, Hofmann B et al. Development of cytomegalovirus (CMV) disease

may be predicted in HIV- infected patients by CMV polymerase chain reaction and the antigenemia test. *AIDS* 1997;11:F21-F28.

(A) Drew WL, Miner RC, Busch DF et al. Prevalence of resistance in patients receiving ganciclovir for serious cytomegalovirus infection. *J Infect Dis* 1991;163:716-19.

(B) Drew WL. Clinical use of ganciclovir for cytomegalovirus infection and the development of drug resistance. *J Acquir Immune Defic Syndr* 1991;4 Suppl 1:S42-S46.

Drew WL, Ives D, Lalezari JP et al. Oral ganciclovir as maintenance treatment for cytomegalovirus retinitis in patients with AIDS. Syntex Cooperative Oral Ganciclovir Study Group. *N Engl J Med* 1995;333:615-20.

Drobyski WR, Dunne WM, Burd EM et al. Human herpesvirus-6 (HHV-6) infection in allogeneic bone marrow transplant recipients: evidence of a marrow-suppressive role for HHV-6 in vivo. *J Infect Dis* 1993;167:735-9.

Dummer JS. Cytomegalovirus infection after liver transplantation: clinical manifestations and strategies for prevention. *Rev Infect Dis* 1990;12 Suppl 7:S767-S775.

Duncan SR, Grgurich WF, Iacono AT et al. A comparison of ganciclovir and acyclovir to prevent cytomegalovirus after lung transplantation. *Am J Respir Crit Care Med* 1994;150:146-52.

Dunn W, Trang P, Khan U, Zhu J, Liu F. RNase P-mediated inhibition of cytomegalovirus protease expression and viral DNA encapsidation by oligonucleotide external guide sequences. *Proc Natl Acad Sci U S A* 2001;98:14831-36.

Egan JJ, Lomax J, Barber L et al. Preemptive treatment for the prevention of cytomegalovirus disease: in lung and heart transplant recipients. *Transplantation* 1998;65:747-52.

Emery VC, Bishop DH. The development of multiple expression vectors for high level synthesis of eukaryotic proteins: expression of LCMV-N and AcNPV polyhedrin protein by a recombinant baculovirus. *Protein Eng* 1987;1:359-66.

(A)Emery VC. Viral dynamics during active cytomegalovirus infection and pathology. *Intervirology* 1999;42:405-11.

(B)Emery VC, Atkins MC, Bowen EF et al. Interactions between beta-herpesviruses and human immunodeficiency virus in vivo: evidence for increased human immunodeficiency viral load in the presence of human herpesvirus 6. *J Med Virol* 1999;57:278-82.

(C)Emery VC, Cope AV, Bowen EF, Gor D, Griffiths PD. The dynamics of human cytomegalovirus replication in vivo. *J Exp Med* 1999;190:177-82.

(A)Emery VC, Sabin CA, Cope AV, Gor D, Hassan-Walker AF, Griffiths PD. Application of viral-load kinetics to identify patients who develop cytomegalovirus disease after transplantation. *Lancet* 2000;355:2032-36.

(B)Emery VC, Cope AV, Sabin CA et al. Relationship between IgM antibody to human cytomegalovirus, virus load, donor and recipient serostatus, and administration of methylprednisolone as risk factors for cytomegalovirus disease after liver transplantation. *J Infect Dis* 2000;182:1610-1615.

Emery VC, Griffiths PD. Prediction of cytomegalovirus load and resistance patterns after antiviral chemotherapy. *Proc Natl Acad Sci* 2000;97:8039.

Emery VC. Prophylaxis for CMV should not now replace pre-emptive therapy in solid organ transplantation. *Rev Med Virol* 2001;11:83-86.

Engstrand M, Tournay C, Peyrat MA et al. Characterization of CMVpp65-specific CD8+ T

lymphocytes using MHC tetramers in kidney transplant patients and healthy participants. *Transplantation* 2000;69:2243-50.

Erice A, Jordan MC, Chace BA, Fletcher C, Chinnock BJ, Balfour HH, Jr. Ganciclovir treatment of cytomegalovirus disease in transplant recipients and other immunocompromised hosts. *JAMA* 1987;257:3082-87.

Erice A, Chou S, Biron KK, Stanat SC, Balfour HH, Jr., Jordan MC. Progressive disease due to ganciclovir-resistant cytomegalovirus in immunocompromised patients. *N Engl J Med* 1989;320:289-93.

Erice A, Holm MA, Gill PC et al. Cytomegalovirus (CMV) antigenemia assay is more sensitive than shell vial cultures for rapid detection of CMV in polymorphonuclear blood leukocytes. *J Clin Microbiol* 1992;30:2822-25.

Erice A, Gil-Roda C, Perez JL et al. Antiviral susceptibilities and analysis of UL97 and DNA polymerase sequences of clinical cytomegalovirus isolates from immunocompromised patients [see comments]. *J Infect Dis* 1997;175:1087-92.

Erice A, Borrell N, Li W, Miller WJ, Balfour HH, Jr. Ganciclovir susceptibilities and analysis of UL97 region in cytomegalovirus (CMV) isolates from bone marrow recipients with CMV disease after antiviral prophylaxis. *J Infect Dis* 1998;178:531-34.

Erice A. Resistance of human cytomegalovirus to antiviral drugs. *Clin Microbiol Rev* 1999;12:286-97.

Everett RD, Dunlop M. Trans activation of plasmid-borne promoters by adenovirus and several herpes group viruses. *Nucleic Acids Res* 1984;12:5969-78.

Fox JC, Griffiths PD, Emery VC. Quantification of human cytomegalovirus DNA using the polymerase chain reaction. *J Gen Virol* 1992;73 ( Pt 9):2405-8.

Fox JC, Kidd IM, Griffiths PD, Sweny P, Emery VC. Longitudinal analysis of cytomegalovirus load in renal transplant recipients using a quantitative polymerase chain reaction: correlation with disease. *J Gen Virol* 1995;76 ( Pt 2):309-19.

Gaillard RK, Barnard J, Lopez V et al. Kinetic analysis of wild type and YMDD mutant hepatitis B virus polymerases and effects of deoxyribonucleotide concentrations on polymerase activity. *Antimicrob Agents Chemother* 2002;46:1005-13.

Gallant JE, Moore RD, Richman DD, Keruly J, Chaisson RE. Incidence and natural history of cytomegalovirus disease in patients with advanced human immunodeficiency virus disease treated with zidovudine. The Zidovudine Epidemiology Study Group. *J Infect Dis* 1992;166:1223-27.

Gane E, Saliba F, Valdecasas GJ et al. Randomised trial of efficacy and safety of oral ganciclovir in the prevention of cytomegalovirus disease in liver-transplant recipients. The Oral Ganciclovir International Transplantation Study Group [corrected]. *Lancet* 1997;350:1729-33.

Gao M, Matusick-Kumar L, Hurlburt W et al. The protease of herpes simplex virus type 1 is essential for functional capsid formation and viral growth. *J Virol* 1994;68:3702-12.

Garoff H. Using recombinant DNA techniques to study protein targeting in the eucaryotic cell. *Annu Rev Cell Biol* 1985;1:403-45.

Gerna G, Baldanti F, Sarasini A et al. Effect of foscarnet induction treatment on quantitation of human cytomegalovirus (HCMV) DNA in peripheral blood polymorphonuclear leukocytes and aqueous humor of AIDS patients with HCMV retinitis. The Italian Foscarnet Study Group. *Antimicrob Agents Chemother* 1994;38:38-44.

Gerna G, Piccinini G, Genini E et al. Declining levels of rescued lymphoproliferative

response to human cytomegalovirus (HCMV) in AIDS patients with or without HCMV disease following long-term HAART. *J Acquir Immune Defic Syndr* 2001;28:320-331.

Gibbs JS, Chiou HC, Bastow KF, Cheng YC, Coen DM. Identification of amino acids in herpes simplex virus DNA polymerase involved in substrate and drug recognition. *Proc Natl Acad Sci U S A* 1988;85:6672-76.

Gilbert MJ, Riddell SR, Plachter B, Greenberg PD. Cytomegalovirus selectively blocks antigen processing and presentation of its immediate-early gene product. *Nature* 1996;383:720-722.

Gillespie GM, Wills MR, Appay V et al. Functional heterogeneity and high frequencies of cytomegalovirus-specific CD8(+) T lymphocytes in healthy seropositive donors. *J Virol* 2000;74:8140-8150.

Gilquin J, Piketty C, Thomas V, Gonzales-Canali G, Belec L, Kazatchkine MD. Acute cytomegalovirus infection in AIDS patients with CD4 counts above 100 x 10<sup>6</sup> cells/l following combination antiretroviral therapy including protease inhibitors. *AIDS* 1997;11:1659-60.

Gor D, Sabin C, Prentice HG et al. Longitudinal fluctuations in cytomegalovirus load in bone marrow transplant patients: relationship between peak virus load, donor/recipient serostatus, acute GVHD and CMV disease. *Bone Marrow Transplant* 1998;21:597-605.

Greaves RF, Mocarski ES. Defective growth correlates with reduced accumulation of a viral DNA replication protein after low-multiplicity infection by a human cytomegalovirus *ie1* mutant. *J Virol* 1998;72:366-79.

Gretch DR, Kari B, Rasmussen L, Gehrz RC, Stinski MF. Identification and characterization of three distinct families of glycoprotein complexes in the envelopes of

human cytomegalovirus. *J Virol* 1988;62:875-81.

Griffiths G, Simons K. The trans Golgi network: sorting at the exit site of the Golgi complex. *Science* 1986;234:438-43.

Griffiths PD, Baboonian C. Intra-uterine transmission of cytomegalovirus in women known to be immune before conception. *J Hyg (Lond)* 1984;92:89-95.

Griffiths PD. Studies to define viral cofactors for human immunodeficiency virus. *Infect Agents Dis* 1992;1:237-44.

Griffiths PD. Studies of viral co-factors for human immunodeficiency virus in vitro and in vivo. *J Gen Virol* 1998;79 ( Pt 2):213-20.

Griffiths PD, Ait-Khaled M, Bearcroft CP et al. Human herpesvirus 6 and 7 as potential pathogens after liver transplant: prospective comparison with the effect of cytomegalovirus. *J Med Virol* 1999;59:496-501.

Griffiths PD, Clark DA, Emery VC. Betaherpesviruses in transplant recipients. *J Antimicrob Chemother* 2000;45 Suppl T3:29-34.

Grundy JE, Lui SF, Super M et al. Symptomatic cytomegalovirus infection in seropositive kidney recipients: reinfection with donor virus rather than reactivation of recipient virus. *Lancet* 1988;2:132-35.

Gyulai Z, Endresz V, Burian K et al. Cytotoxic T lymphocyte (CTL) responses to human cytomegalovirus pp65, IE1-Exon4, gB, pp150, and pp28 in healthy individuals: reevaluation of prevalence of IE1-specific CTLs. *J Infect Dis* 2000;181:1537-46.

Hahn G, Jores R, Mocarski ES. Cytomegalovirus remains latent in a common precursor of dendritic and myeloid cells. *Proc Natl Acad Sci U S A* 1998;95:3937-42.



Hanks SK, Quinn AM, Hunter T. The protein kinase family: conserved features and deduced phylogeny of the catalytic domains. *Science* 1988;241:42-52.

Hanson MN, Preheim LC, Chou S, Talarico CL, Biron KK, Erice A. Novel mutation in the UL97 gene of a clinical cytomegalovirus strain conferring resistance to ganciclovir. *Antimicrob Agents Chemother* 1995;39:1204-5.

Hardens M. Ganciclovir evaluation in AIDS patients with cytomegalovirus retinitis: a European study of treatment patterns and resource utilization. *AIDS* 1996;10 Suppl 4:S25-S30.

Hardie G, Hanks S. *The protein kinase facts book*. Academic Press limited, London 1995.  
Hassan-Walker AF, Cope AV, Griffiths PD, Emery VC. Transcription of the human cytomegalovirus natural killer decoy gene, UL18, in vitro and in vivo. *J Gen Virol* 1998;79 ( Pt 9):2113-16.

Hassan-Walker AF, Kidd IM, Sabin C, Sweny P, Griffiths PD, Emery VC. Quantity of human cytomegalovirus (CMV) DNAemia as a risk factor for CMV disease in renal allograft recipients: relationship with donor/recipient CMV serostatus, receipt of augmented methylprednisolone and antithymocyte globulin (ATG). *J Med Virol* 1999;58:182-87.

He Z, He YS, Kim Y et al. The human cytomegalovirus UL97 protein is a protein kinase that autophosphorylates on serines and threonines. *J Virol* 1997;71:405-11.

Heemels MT, Ploegh H. Generation, translocation, and presentation of MHC class I-restricted peptides. *Annu Rev Biochem* 1995;64:463-91.

Hegedus DD, Pfeifer TA, Theilmann DA et al. Differences in the expression and localization of human melanotransferrin in lepidopteran and dipteran insect cell lines. *Protein Expr Purif* 1999;15:296-307.

Hengel H, Esslinger C, Pool J, Goulmy E, Koszinowski UH. Cytokines restore MHC class I complex formation and control antigen presentation in human cytomegalovirus-infected cells. *J Gen Virol* 1995;76 ( Pt 12):2987-97.

Hengel H, Flohr T, Hammerling GJ, Koszinowski UH, Momburg F. Human cytomegalovirus inhibits peptide translocation into the endoplasmic reticulum for MHC class I assembly. *J Gen Virol* 1996;77 ( Pt 9):2287-96.

Hengel H, Koopmann JO, Flohr T et al. A viral ER-resident glycoprotein inactivates the MHC-encoded peptide transporter. *Immunity* 1997;6:623-32.

Hengel H, Brune W, Koszinowski UH. Immune evasion by cytomegalovirus--survival strategies of a highly adapted opportunist. *Trends Microbiol* 1998;6:190-197.

Hewitt EW, Gupta SS, Lehner PJ. The human cytomegalovirus gene product US6 inhibits ATP binding by TAP. *EMBO J* 2001;20:387-96.

Holwerda BC, Wittwer AJ, Duffin KL et al. Activity of two-chain recombinant human cytomegalovirus protease. *J Biol Chem* 1994;269:25911-15.

Honess RW, Roizman B. Regulation of herpesvirus macromolecular synthesis. I. Cascade regulation of the synthesis of three groups of viral proteins. *J Virol* 1974;14:8-19.

Huber MT, Compton T. Characterization of a novel third member of the human cytomegalovirus glycoprotein H-glycoprotein L complex. *J Virol* 1997;71:5391-98.

Huber MT, Compton T. The human cytomegalovirus UL74 gene encodes the third component of the glycoprotein H-glycoprotein L-containing envelope complex. *J Virol* 1998;72:8191-97.

Huber MT, Compton T. Intracellular formation and processing of the heterotrimeric gH-gL-gO (gCIII) glycoprotein envelope complex of human cytomegalovirus. *J Virol* 1999;73:3886-92.

Humar A, Kumar D, Caliendo AM et al. Clinical impact of human herpesvirus 6 infection after liver transplantation. *Transplantation* 2002;73:599-604.

Imbert-Marcille BM, Tang XW, Lepelletier D et al. Human Herpesvirus 6 Infection after Autologous or Allogeneic Stem Cell Transplantation: A Single-Center Prospective Longitudinal Study of 92 Patients. *Clin Infect Dis* 2000;31:881-86.

Jabs DA, Martin BK, Forman MS et al. Longitudinal observations on mutations conferring ganciclovir resistance in patients with acquired immunodeficiency syndrome and cytomegalovirus retinitis: The Cytomegalovirus and Viral Resistance Study Group Report Number 8. *Am J Ophthalmol* 2001;132:700-10.

Jacobson MA, Kramer F, Bassiakos Y et al. Randomized phase I trial of two different combination foscarnet and ganciclovir chronic maintenance therapy regimens for AIDS patients with cytomegalovirus retinitis: AIDS clinical Trials Group Protocol 151. *J Infect Dis* 1994;170:189-93.

(A)Jacobson MA. Cytomegalovirus retinitis: new developments in prophylaxis and therapy. *AIDS Clin Rev* 1997;249-69.

(B)Jacobson MA. Treatment of cytomegalovirus retinitis in patients with the acquired immunodeficiency syndrome. *N Engl J Med* 1997;337:105-14.

Jahn G, Scholl BC, Traupe B, Fleckenstein B. The two major structural phosphoproteins (pp65 and pp150) of human cytomegalovirus and their antigenic properties. *J Gen Virol* 1987;68 ( Pt 5):1327-37.

Jarvis DL, Weinkauff C, Guarino LA. Immediate-early baculovirus vectors for foreign gene expression in transformed or infected insect cells. *Protein Expr Purif* 1996;8:191-203.

Jones TR, Hanson LK, Sun L, Slater JS, Stenberg RM, Campbell AE. Multiple independent loci within the human cytomegalovirus unique short region down-regulate expression of major histocompatibility complex class I heavy chains. *J Virol* 1995;69:4830-4841.

Jones TR, Wiertz EJ, Sun L, Fish KN, Nelson JA, Ploegh HL. Human cytomegalovirus US3 impairs transport and maturation of major histocompatibility complex class I heavy chains. *Proc Natl Acad Sci U S A* 1996;93:11327-33.

Jouan M, Saves M, Tubiana R et al. Discontinuation of maintenance therapy for cytomegalovirus retinitis in HIV-infected patients receiving highly active antiretroviral therapy. *AIDS* 2001;15:23-31.

Kari B, Gehrz R. A human cytomegalovirus glycoprotein complex designated gC-II is a major heparin-binding component of the envelope. *J Virol* 1992;66:1761-64.

Kari B, Li W, Cooper J, Goertz R, Radeke B. The human cytomegalovirus UL100 gene encodes the gC-II glycoproteins recognized by group 2 monoclonal antibodies. *J Gen Virol* 1994;75 ( Pt 11):3081-86.

Karre K. NK cells, MHC class I molecules and the missing self. *Scand J Immunol* 2002;55:221-28.

Kaye S, Loveday C, Tedder RS. A microtitre format point mutation assay: application to the detection of drug resistance in human immunodeficiency virus type-1 infected patients treated with zidovudine. *J Med Virol* 1992;37:241-46.

Kearns AM, Draper B, Wipat W et al. LightCycler-based quantitative PCR for detection of cytomegalovirus in blood, urine, and respiratory samples. *J Clin Microbiol* 2001;39:2364-

65.

Keay S, Merigan TC, Rasmussen L. Identification of cell surface receptors for the 86-kilodalton glycoprotein of human cytomegalovirus. *Proc Natl Acad Sci U S A* 1989;86:10100-10103.

Keay S, Baldwin B. The human fibroblast receptor for gp86 of human cytomegalovirus is a phosphorylated glycoprotein. *J Virol* 1992;66:4834-38.

Kidd IM, Fox JC, Pillay D, Charman H, Griffiths PD, Emery VC. Provision of prognostic information in immunocompromised patients by routine application of the polymerase chain reaction for cytomegalovirus. *Transplantation* 1993;56:867-71.

Kidd IM, Clark DA, Sabin CA et al. Prospective study of human betaherpesviruses after renal transplantation: association of human herpesvirus 7 and cytomegalovirus co-infection with cytomegalovirus disease and increased rejection. *Transplantation* 2000;69:2400-2404.

Kirk O, Lundgren JD, Pedersen C, Nielsen H, Gerstoft J. Can chemoprophylaxis against opportunistic infections be discontinued after an increase in CD4 cells induced by highly active antiretroviral therapy? *AIDS* 1999;13:1647-51.

Koevary SB. Cytomegalovirus retinitis: pathogenesis and treatment options. *Optometry* 2000;71:146-7.

Komanduri KV, Viswanathan MN, Wieder ED et al. Restoration of cytomegalovirus-specific CD4+ T-lymphocyte responses after ganciclovir and highly active antiretroviral therapy in individuals infected with HIV-1. *Nat Med* 1998;4:953-56.

Kondo K, Xu J, Mocarski ES. Human cytomegalovirus latent gene expression in granulocyte-macrophage progenitors in culture and in seropositive individuals. *Proc Natl Acad Sci U S A* 1996;93:11137-42.

Krosky PM, Underwood MR, Turk SR et al. Resistance of human cytomegalovirus to benzimidazole ribonucleosides maps to two open reading frames: UL89 and UL56. *J Virol* 1998;72:4721-28.

Kruger RM, Shannon WD, Arens MQ, Lynch JP, Storch GA, Trulock EP. The impact of ganciclovir-resistant cytomegalovirus infection after lung transplantation. *Transplantation* 1999;68:1272-79.

Kusne S, Grossi P, Irish W et al. Cytomegalovirus PP65 antigenemia monitoring as a guide for preemptive therapy: a cost effective strategy for prevention of cytomegalovirus disease in adult liver transplant recipients. *Transplantation* 1999;68:1125-31.

LaFemina RL, Hayward GS. Replicative forms of human cytomegalovirus DNA with joined termini are found in permissively infected human cells but not in non-permissive Balb/c-3T3 mouse cells. *J Gen Virol* 1983;64 (Pt 2):373-89.

Larder BA, Kemp SD, Darby G. Related functional domains in virus DNA polymerases. *EMBO J* 1987;6:169-75.

Leach CT. Human herpesvirus-6 and -7 infections in children: agents of roseola and other syndromes. *Curr Opin Pediatr* 2000;12:269-74.

Leatham MP, Witte PR, Stinski MF. Alternate promoter selection within a human cytomegalovirus immediate-early and early transcription unit (UL119-115) defines true late transcripts containing open reading frames for putative viral glycoproteins. *J Virol* 1991;65:6144-53.

Lee N, Goodlett DR, Ishitani A, Marquardt H, Geraghty DE. HLA-E surface expression depends on binding of TAP-dependent peptides derived from certain HLA class I signal sequences. *J Immunol* 1998;160:4951-60.

Lee S, Yoon J, Park B et al. Structural and functional dissection of human cytomegalovirus US3 in binding major histocompatibility complex class I molecules. *J Virol* 2000;74:11262-69.

Leeds JM, Henry SP, Bistner S, Scherrill S, Williams K, Levin AA. Pharmacokinetics of an antisense oligonucleotide injected intravitreally in monkeys. *Drug Metab Dispos* 1998;26:670-675.

Lehner PJ, Karttunen JT, Wilkinson GW, Cresswell P. The human cytomegalovirus US6 glycoprotein inhibits transporter associated with antigen processing-dependent peptide translocation. *Proc Natl Acad Sci U S A* 1997;94:6904-9.

Lemaster S, Roizman B. Herpes simplex virus phosphoproteins. II. Characterization of the virion protein kinase and of the polypeptides phosphorylated in the virion. *J Virol* 1980;35:798-811.

Leong CC, Chapman TL, Bjorkman PJ et al. Modulation of natural killer cell cytotoxicity in human cytomegalovirus infection: the role of endogenous class I major histocompatibility complex and a viral class I homolog. *J Exp Med* 1998;187:1681-87.

Li L, Nelson JA, Britt WJ. Glycoprotein H-related complexes of human cytomegalovirus: identification of a third protein in the gCIII complex. *J Virol* 1997;71:3090-3097.

Limaye AP, Corey L, Koelle DM, Davis CL, Boeckh M. Emergence of ganciclovir-resistant cytomegalovirus disease among recipients of solid-organ transplants. *Lancet* 2000;356:645-49.

Littler E, Arrand JR. Characterisation of the Epstein-Barr virus-encoded thymidine kinase expressed in heterologous eucaryotic and procaryotic systems. *J Virol* 1988;62:3892-5.

Littler E, Stuart AD, Chee MS. Human cytomegalovirus UL97 open reading frame encodes

a protein that phosphorylates the antiviral nucleoside analogue ganciclovir. *Nature* 1992;358:160-162.

Liu W, Kuppermann BD, Martin DF, Wolitz RA, Margolis TP. Mutations in the cytomegalovirus UL97 gene associated with ganciclovir-resistant retinitis. *J Infect Dis* 1998;177:1176-81.

Ljunggren HG, Karre K. In search of the 'missing self': MHC molecules and NK cell recognition. *Immunol Today* 1990;11:237-44.

Ljungman P, Deliliers GL, Platzbecker U et al. Cidofovir for cytomegalovirus infection and disease in allogeneic stem cell transplant recipients. The Infectious Diseases Working Party of the European Group for Blood and Marrow Transplantation. *Blood* 2001;97:388-92.

Ljungman P, Griffiths P, Paya C. Definitions of cytomegalovirus infection and disease in transplant recipients. *Clin Infect Dis* 2002;34:1094-97.

Lodish HF. Transport of secretory and membrane glycoproteins from the rough endoplasmic reticulum to the Golgi. A rate-limiting step in protein maturation and secretion. *J Biol Chem* 1988;263:2107-10.

Lowance D, Neumayer HH, Legendre CM et al. Valacyclovir for the prevention of cytomegalovirus disease after renal transplantation. International Valacyclovir Cytomegalovirus Prophylaxis Transplantation Study Group. *N Engl J Med* 1999;340:1462-70.

Lurain NS, Thompson KD, Holmes EW, Read GS. Point mutations in the DNA polymerase gene of human cytomegalovirus that result in resistance to antiviral agents. *J Virol* 1992;66:7146-52.

Lurain NS, Spafford LE, Thompson KD. Mutation in the UL97 open reading frame of



- human cytomegalovirus strains resistant to ganciclovir. *J Virol* 1994;68:4427-31.
- Lusso P, Malnati MS, Garzino-Demo A, Crowley RW, Long EO, Gallo RC. Infection of natural killer cells by human herpesvirus 6. *Nature* 1993;362:458-62.
- Macdonald JC, Torriani FJ, Morse LS, Karavellas MP, Reed JB, Freeman WR. Lack of reactivation of cytomegalovirus (CMV) retinitis after stopping CMV maintenance therapy in AIDS patients with sustained elevations in CD4 T cells in response to highly active antiretroviral therapy. *J Infect Dis* 1998;177:1182-87.
- Macdonald JC, Karavellas MP, Torriani FJ et al. Highly active antiretroviral therapy-related immune recovery in AIDS patients with cytomegalovirus retinitis. *Ophthalmology* 2000;107:877-81.
- Maine GT, Stricker R, Schuler M et al. Development and clinical evaluation of a recombinant-antigen-based cytomegalovirus immunoglobulin M automated immunoassay using the Abbott AxSYM analyzer. *J Clin Microbiol* 2000;38:1476-81.
- Mallolas J, Arrizabalaga J, Lonca M et al. Cytomegalovirus disease in HIV-1-infected patients treated with protease inhibitors. *AIDS* 1997;11:1785-87.
- Marchini A, Liu H, Zhu H. Human cytomegalovirus with IE-2 (UL122) deleted fails to express early lytic genes. *J Virol* 2001;75:1870-1878.
- (A)Martinez A, Gil C, Perez C et al. Nonnucleoside human cytomegalovirus inhibitors: synthesis and antiviral evaluation of (chlorophenylmethyl)benzothiadiazine dioxide derivatives. *J Med Chem* 2000;43:3267-73.
- (B)Martinez A, Gil C, Abasolo MI et al. Benzothiadiazine dioxide dibenzyl derivatives as potent human cytomegalovirus inhibitors: synthesis and comparative molecular field analysis. *J Med Chem* 2000;43:3218-25.

McGeoch DJ, Dalrymple MA, Davison AJ et al. The complete DNA sequence of the long unique region in the genome of herpes simplex virus type 1. *J Gen Virol* 1988;69 ( Pt 7):1531-74.

McGuffin RW, Shiota FM, Meyers JD. Lack of toxicity of acyclovir to granulocyte progenitor cells in vitro. *Antimicrob Agents Chemother* 1980;18:471-73.

McGuirt PV, Furman PA. Acyclovir inhibition of viral DNA chain elongation in herpes simplex virus-infected cells. *Am J Med* 1982;73:67-71.

McSharry JJ, McDonough A, Olson B et al. Susceptibilities of human cytomegalovirus clinical isolates to BAY38- 4766, BAY43-9695, and ganciclovir. *Antimicrob Agents Chemother* 2001;45:2925-27.

McVoy MA, Adler SP. Human cytomegalovirus DNA replicates after early circularization by concatemer formation, and inversion occurs within the concatemer. *J Virol* 1994;68:1040-1051.

McVoy MA, Nixon DE, Adler SP, Mocarski ES. Sequences within the herpesvirus-conserved *pac1* and *pac2* motifs are required for cleavage and packaging of the murine cytomegalovirus genome. *J Virol* 1998;72:48-56.

Meier JL, Stinski MF. Regulation of human cytomegalovirus immediate-early gene expression. *Intervirology* 1996;39:331-42.

Mendez JC, Sia IG, Tau KR et al. Novel mutation in the CMV UL97 gene associated with resistance to ganciclovir therapy. *Transplantation* 1999;67:755-57.

Meyers JD, Flournoy N, Thomas ED. Risk factors for cytomegalovirus infection after human marrow transplantation. *J Infect Dis* 1986;153:478-88.

Michel D, Pavic I, Zimmermann A et al. The UL97 gene product of human cytomegalovirus is an early-late protein with a nuclear localization but is not a nucleoside kinase. *J Virol* 1996;70:6340-6346.

Michel D, Schaarschmidt P, Wunderlich K et al. Functional regions of the human cytomegalovirus protein pUL97 involved in nuclear localization and phosphorylation of ganciclovir and pUL97 itself. *J Gen Virol* 1998;79 ( Pt 9):2105-12.

Michel D, Kramer S, Hohn S, Schaarschmidt P, Wunderlich K, Mertens T. Amino acids of conserved kinase motifs of cytomegalovirus protein UL97 are essential for autophosphorylation. *J Virol* 1999;73:8898-901.

Milne RS, Paterson DA, Booth JC. Human cytomegalovirus glycoprotein H/glycoprotein L complex modulates fusion-from-without. *J Gen Virol* 1998;79 ( Pt 4):855-65.

Mocarski ES, Liu AC, Spaete RR. Structure and variability of the a sequence in the genome of human cytomegalovirus (Towne strain). *J Gen Virol* 1987;68 ( Pt 8):2223-30.

Mocarski ES. The herpesviruses. In Fields BN, Knipe MK, Howley PM (eds), *Fields Virology*. Lippencott-Raven, Philadelphia. 1996.

Mocarski ES, Kemble GW, Lyle JM, Greaves RF. A deletion mutant in the human cytomegalovirus gene encoding IE1(491aa) is replication defective due to a failure in autoregulation. *Proc Natl Acad Sci U S A* 1996;93:11321-26.

Mocarski ES. The herpesviruses. In Fields BN, Knipe MK, Howley PM (eds), *Fields Virology*. Lippencott-Raven, Philadelphia. 2001.

Mocroft A, Vella S, Benfield TL et al. Changing patterns of mortality across Europe in patients infected with HIV-1. EuroSIDA Study Group. *Lancet* 1998;352:1725-30.

Monick MM, Geist LJ, Stinski MF, Hunninghake GW. The immediate early genes of human cytomegalovirus upregulate expression of the cellular genes *myc* and *fos*. *Am J Respir Cell Mol Biol* 1992;7:251-56.

Moyle G, Harman C, Mitchell S, Mathalone B, Gazzard BG. Foscarnet and Ganciclovir in the treatment of CMV retinitis in AIDS patients: a randomised comparison. *J Infect* 1992;25:21-27.

Navarro D, Paz P, Tugizov S, Topp K, La Vail J, Pereira L. Glycoprotein B of human cytomegalovirus promotes virion penetration into cells, transmission of infection from cell to cell, and fusion of infected cells. *Virology* 1993;197:143-58.

Nelson JA, Reynolds-Kohler C, Oldstone MB, Wiley CA. HIV and HCMV coinfect brain cells in patients with AIDS. *Virology* 1988;165:286-90.

Neote K, DiGregorio D, Mak JY, Horuk R, Schall TJ. Molecular cloning, functional expression, and signaling characteristics of a C-C chemokine receptor. *Cell* 1993;72:415-25.

Newcomb WW, Homa FL, Thomsen DR et al. Assembly of the herpes simplex virus capsid: characterization of intermediates observed during cell-free capsid formation. *J Mol Biol* 1996;263:432-46.

Ng TI, Talarico C, Burnette TC, Biron K, Roizman B. Partial substitution of the functions of the herpes simplex virus 1 U(L)13 gene by the human cytomegalovirus U(L)97 gene. *Virology* 1996;225:347-58.

Nitsche A, Steuer N, Schmidt CA, Landt O, Siebert W. Different real-time PCR formats compared for the quantitative detection of human cytomegalovirus DNA. *Clin Chem* 1999;45:1932-37.

Odeberg J, Cerboni C, Browne H et al. Human cytomegalovirus (HCMV)-infected endothelial cells and macrophages are less susceptible to natural killer lysis independent of the downregulation of classical HLA class I molecules or expression of the HCMV class I homologue, UL18. *Scand J Immunol* 2002;55:149-61.

Orci L, Ravazzola M, Amherdt M et al. The trans-most cisternae of the Golgi complex: a compartment for sorting of secretory and plasma membrane proteins. *Cell* 1987;51:1039-51.

Palella FJ, Jr., Delaney KM, Moorman AC et al. Declining morbidity and mortality among patients with advanced human immunodeficiency virus infection. HIV Outpatient Study Investigators. *N Engl J Med* 1998;338:853-60.

Pari GS, Anders DG. Eleven loci encoding trans-acting factors are required for transient complementation of human cytomegalovirus oriLyt-dependent DNA replication. *J Virol* 1993;67:6979-88.

Pari GS, Kacica MA, Anders DG. Open reading frames UL44, IRS1/TRS1, and UL36-38 are required for transient complementation of human cytomegalovirus oriLyt-dependent DNA synthesis. *J Virol* 1993;67:2575-82.

Pass RF, Hutto C, Ricks R, Cloud GA. Increased rate of cytomegalovirus infection among parents of children attending day-care centers. *N Engl J Med* 1986;314:1414-18.

Pass RF, Little EA, Stagno S, Britt WJ, Alford CA. Young children as a probable source of maternal and congenital cytomegalovirus infection. *N Engl J Med* 1987;316:1366-70.

Pass RF. Immunization strategy for prevention of congenital cytomegalovirus infection. *Infect Agents Dis* 1996;5:240-244.

Paya CV, Hermans PE, Wiesner RH et al. Cytomegalovirus hepatitis in liver

transplantation: prospective analysis of 93 consecutive orthotopic liver transplantations. *J Infect Dis* 1989;160:752-58.

Paya CV, Marin E, Keating M, Dickson R, Porayko M, Wiesner R. Solid organ transplantation: results and implications of acyclovir use in liver transplants. *J Med Virol* 1993;Suppl 1:123-27.

Penfold ME, Mocarski ES. Formation of cytomegalovirus DNA replication compartments defined by localization of viral proteins and DNA synthesis. *Virology* 1997;239:46-61.

Penfold ME, Dairaghi DJ, Duke GM et al. Cytomegalovirus encodes a potent alpha chemokine. *Proc Natl Acad Sci U S A* 1999;96:9839-44.

Pereira L, Wolff MH, Fenwick M, Roizman B. Regulation of herpesvirus macromolecular synthesis. V. Properties of alpha polypeptides made in HSV-1 and HSV-2 infected cells. *Virology* 1977;77:733-49.

Pescovitz MD, Rabkin J, Merion RM et al. Valganciclovir results in improved oral absorption of ganciclovir in liver transplant recipients. *Antimicrob Agents Chemother* 2000;44:2811-5.

Piasecki P. Fomiverson sodium approved to treat CMV retinitis. *J Am Pharm Assoc (Wash)* 1999;39:84-85.

Pietropaolo R, Compton T. Interference with annexin II has no effect on entry of human cytomegalovirus into fibroblast cells. *J Gen Virol* 1999;80 ( Pt 7):1807-16.

Pietropaolo RL, Compton T. Direct interaction between human cytomegalovirus glycoprotein B and cellular annexin II. *J Virol* 1997;71:9803-7.

Pillay D, Charman H, Burroughs AK, Smith M, Rolles K, Griffiths PD. Surveillance for CMV infection in orthotopic liver transplant recipients. *Transplantation* 1992;53:1261-65.

Pillay D, Ali AA, Liu SF, Kops E, Sweny P, Griffiths PD. The prognostic significance of positive CMV cultures during surveillance of renal transplant recipients. *Transplantation* 1993;56:103-8.

Portela D, Patel R, Larson-Keller JJ et al. OKT3 treatment for allograft rejection is a risk factor for cytomegalovirus disease in liver transplantation. *J Infect Dis* 1995;171:1014-18.

Prichard MN, Gao N, Jairath S et al. A recombinant human cytomegalovirus with a large deletion in UL97 has a severe replication deficiency. *J Virol* 1999;73:5663-70.

Pruksananonda P, Hall CB, Insel RA et al. Primary human herpesvirus 6 infection in young children [see comments]. *N Engl J Med* 1992;326:1445-50.

Qiu X, Culp JS, DiLella AG et al. Unique fold and active site in cytomegalovirus protease. *Nature* 1996;383:275-79.

Ranjan D, Burke G, Esquenazi V et al. Factors affecting the ten-year outcome of human renal allografts. The effect of viral infections. *Transplantation* 1991;51:113-17.

Rasmussen LE, Nelson RM, Kelsall DC, Merigan TC. Murine monoclonal antibody to a single protein neutralizes the infectivity of human cytomegalovirus. *Proc Natl Acad Sci U S A* 1984;81:876-80.

Raulet DH, Liao NS, Correa I, Bix M. Lymphocyte development in mice deficient for MHC class I expression. *Adv Exp Med Biol* 1992;323:67-72.

Remberger M, Kumlien G, Aschan J et al. Risk factors for moderate-to-severe chronic graft-versus-host disease after allogeneic hematopoietic stem cell transplantation. *Biol Blood Marrow Transplant* 2002;8:674-82.

Reusser P. Oral valganciclovir: a new option for treatment of cytomegalovirus infection and disease in immunocompromised hosts. *Expert Opin Investig Drugs* 2001;10:1745-53.

Reyburn HT, Mandelboim O, Vales-Gomez M, Davis DM, Pazmany L, Strominger JL. The class I MHC homologue of human cytomegalovirus inhibits attack by natural killer cells. *Nature* 1997;386:514-17.

Roby C, Gibson W. Characterization of phosphoproteins and protein kinase activity of virions, noninfectious enveloped particles, and dense bodies of human cytomegalovirus. *J Virol* 1986;59:714-27.

Roizman B. The herpesviruses. In Fields BN, Knipe MK, Howley PM (eds), *Fields Virology*. Lippencott-Raven, Philadelphia. 1996.

Romanowski MJ, Shenk T. Characterization of the human cytomegalovirus *irsl* and *trsl* genes: a second immediate-early transcription unit within *irsl* whose product antagonizes transcriptional activation. *J Virol* 1997;71:1485-96.

Rosen HR, Benner KG, Flora KD et al. Development of ganciclovir resistance during treatment of primary cytomegalovirus infection after liver transplantation. *Transplantation* 1997;63:476-78.

Rothman JE. Protein sorting by selective retention in the endoplasmic reticulum and Golgi stack. *Cell* 1987;50:521-22.

Rubin RH, Cosimi AB, Hirsch MS, Herrin JT, Russell PS, Tolkoff-Rubin NE. Effects of antithymocyte globulin on cytomegalovirus infection in renal transplant recipients. *Transplantation* 1981;31:143-45.

Sabin CA, Phillips AN, Lee CA, Janossy G, Emery V, Griffiths PD. The effect of CMV infection on progression of human immunodeficiency virus disease in a cohort of



haemophilic men followed for up to 13 years from seroconversion. *Epidemiol Infect* 1995;114:361-72.

Scalzo AA, Fitzgerald NA, Wallace CR et al. The effect of the Cmv-1 resistance gene, which is linked to the natural killer cell gene complex, is mediated by natural killer cells. *J Immunol* 1992;149:581-89.

Scheffczik H, Savva CG, Holzenburg A, Kolesnikova L, Bogner E. The terminase subunits pUL56 and pUL89 of human cytomegalovirus are DNA- metabolizing proteins with toroidal structure. *Nucleic Acids Res* 2002;30:1695-703.

Shieh HS, Kurumbail RG, Stevens AM et al. Three-dimensional structure of human cytomegalovirus protease. *Nature* 1996;383:279-82.

Shinkai M, Bozzette SA, Powderly W, Frame P, Spector SA. Utility of urine and leukocyte cultures and plasma DNA polymerase chain reaction for identification of AIDS patients at risk for developing human cytomegalovirus disease. *J Infect Dis* 1997;175:302-8.

Shiraki K, Ogino T, Yamanishi K, Takahashi M. Immunochemical characterization of pyrimidine kinase induced by varicella-zoster virus. *J Gen Virol* 1985;66 ( Pt 2):221-29.

Sinclair J, Sissons P. Latent and persistent infections of monocytes and macrophages. *Intervirology* 1996;39:293-301.

Singh N, Carrigan DR. Human herpesvirus-6 in transplantation: an emerging pathogen. *Ann Intern Med* 1996;124:1065-71.

(A)Singh N, Paterson DL. Encephalitis caused by human herpesvirus-6 in transplant recipients: relevance of a novel neurotropic virus. *Transplantation* 2000;69:2474-79.

(B)Singh N, Paterson DL, Gayowski T, Wagener MM, Marino IR. Cytomegalovirus

## *References*

---

antigenemia directed pre-emptive prophylaxis with oral versus I.V. ganciclovir for the prevention of cytomegalovirus disease in liver transplant recipients: a randomized, controlled trial. *Transplantation* 2000;70:717-22.

Singhal S, Shaw JC, Ainsworth J et al. Direct visualization and quantitation of cytomegalovirus-specific CD8<sup>+</sup> cytotoxic T-lymphocytes in liver transplant patients. *Transplantation* 2000;69:2251-59.

Sinzger C, Jahn G. Human cytomegalovirus cell tropism and pathogenesis. *Intervirology* 1996;39:302-19.

Slobedman B, Mocarski ES. Quantitative analysis of latent human cytomegalovirus. *J Virol* 1999;73:4806-12.

Smith GE, Summers MD, Fraser MJ. Production of human beta interferon in insect cells infected with a baculovirus expression vector. 1983. *Biotechnology* 1992;24:434-43.

Smith IL, Shinkai M, Freeman WR, Spector SA. Polyradiculopathy associated with ganciclovir-resistant cytomegalovirus in an AIDS patient: phenotypic and genotypic characterization of sequential virus isolates. *J Infect Dis* 1996;173:1481-84.

Smith IL, Cherrington JM, Jiles RE, Fuller MD, Freeman WR, Spector SA. High-level resistance of cytomegalovirus to ganciclovir is associated with alterations in both the UL97 and DNA polymerase genes. *J Infect Dis* 1997;176:69-77.

Smith IL, Taskintuna I, Rahhal FM et al. Clinical failure of CMV retinitis with intravitreal cidofovir is associated with antiviral resistance. *Arch Ophthalmol* 1998;116:178-85.

Soderberg-Naucler C, Nelson JY. Human cytomegalovirus latency and reactivation - a delicate balance between the virus and its host's immune system. *Intervirology* 1999;42:314-21.

Soldan SS, Berti R, Salem N et al. Association of human herpes virus 6 (HHV-6) with multiple sclerosis: increased IgM response to HHV-6 early antigen and detection of serum HHV-6 DNA. *Nat Med* 1997;3(12):1394-7.

Soriano V, Dona C, Rodriguez-Rosado R, Barreiro P, Gonzalez-Lahoz J. Discontinuation of secondary prophylaxis for opportunistic infections in HIV-infected patients receiving highly active antiretroviral therapy. *AIDS* 2000;14:383-86.

Soulier J, Grollet L, Oksenhendler E et al. Kaposi's sarcoma-associated herpesvirus-like DNA sequences in multicentric Castleman's disease. *Blood* 1995;86:1276-80.

Spector SA, McKinley GF, Lalezari JP et al. Oral ganciclovir for the prevention of cytomegalovirus disease in persons with AIDS. Roche Cooperative Oral Ganciclovir Study Group. *N Engl J Med* 1996;334:1491-97.

Spector SA, Hsia K, Crager M, Pilcher M, Cabral S, Stempien MJ. Cytomegalovirus (CMV) DNA load is an independent predictor of CMV disease and survival in advanced AIDS. *J Virol* 1999;73:7027-30.

Squires KE. Oral ganciclovir for cytomegalovirus retinitis in patients with AIDS: results of two randomized studies. *AIDS* 1996;10 Suppl 4:S13-S18.

Stagno S, Pass RF, Dworsky ME, Alford CA. Congenital and perinatal cytomegalovirus infections. *Semin Perinatol* 1983;7:31-42.

Stanat SC, Reardon JE, Erice A, Jordan MC, Drew WL, Biron KK. Ganciclovir-resistant cytomegalovirus clinical isolates: mode of resistance to ganciclovir. *Antimicrob Agents Chemother* 1991;35:2191-97.

Steele RW, Marmer DJ, Keeney RE. Comparative in vitro immunotoxicology of acyclovir

and other antiviral agents. *Infect Immun* 1980;28:957-62.

Stevely WS, Katan M, Stirling V, Smith G, Leader DP. Protein kinase activities associated with the virions of pseudorabies and herpes simplex virus. *J Gen Virol* 1985;66 ( Pt 4):661-73.

Stevens JT, Mapelli C, Tsao J et al. In vitro proteolytic activity and active-site identification of the human cytomegalovirus protease. *Eur J Biochem* 1994;226:361-67.

Sullivan V, Talarico CL, Stanat SC, Davis M, Coen DM, Biron KK. A protein kinase homologue controls phosphorylation of ganciclovir in human cytomegalovirus-infected cells. *Nature* 1992;358:162-64.

Sullivan V, Biron KK, Talarico C et al. A point mutation in the human cytomegalovirus DNA polymerase gene confers resistance to ganciclovir and phosphonylmethoxyalkyl derivatives. *Antimicrob Agents Chemother* 1993;37:19-25.

Sutherland S, Bracken P, Wreghitt TG, O'Grady J, Calne RY, Williams R. Donated organ as a source of cytomegalovirus in orthotopic liver transplantation. *J Med Virol* 1992;37:170-173.

Takemoto Y, Takatsuka H, Wada H et al. Evaluation of CMV/human herpes virus-6 positivity in bronchoalveolar lavage fluids as early detection of acute GVHD following BMT: evidence of a significant relationship. *Bone Marrow Transplant* 2000;26:77-81.

Talarico CL, Burnette TC, Miller WH et al. Acyclovir is phosphorylated by the human cytomegalovirus UL97 protein. *Antimicrob Agents Chemother* 1999;43:1941-6.

Tanaka-Taya K, Kondo T, Nakagawa N et al. Reactivation of human herpesvirus 6 by infection of human herpesvirus 7. *J Med Virol* 2000;60:284-89.

## *References*

---

Tanaka N, Kimura H, Iida K et al. Quantitative analysis of cytomegalovirus load using a real-time PCR assay. *J Med Virol* 2000;60:455-62.

Tatarowicz WA, Lurain NS, Thompson KD. A ganciclovir-resistant clinical isolate of human cytomegalovirus exhibiting cross-resistance to other DNA polymerase inhibitors. *J Infect Dis* 1992;166:904-7.

Taylor-Wiedeman J, Sissons JG, Borysiewicz LK, Sinclair JH. Monocytes are a major site of persistence of human cytomegalovirus in peripheral blood mononuclear cells. *J Gen Virol* 1991;72 ( Pt 9):2059-64.

Tomazin R, Boname J, Hegde NR et al. Cytomegalovirus US2 destroys two components of the MHC class II pathway, preventing recognition by CD4+ T cells. *Nat Med* 1999;5:1039-43.

Tong L, Qian C, Massariol MJ, Bonneau PR, Cordingley MG, Lagace L. A new serine-protease fold revealed by the crystal structure of human cytomegalovirus protease. *Nature* 1996;383:272-75.

Torriani FJ, Freeman WR, Macdonald JC et al. CMV retinitis recurs after stopping treatment in virological and immunological failures of potent antiretroviral therapy. *AIDS* 2000;14:173-80.

Townsend LB, Devivar RV, Turk SR, Nassiri MR, Drach JC. Design, synthesis, and antiviral activity of certain 2,5,6-trihalo-1- (beta-D-ribofuranosyl)benzimidazoles. *J Med Chem* 1995;38:4098-105.

Tung PP, Summers WC. Substrate specificity of Epstein-Barr virus thymidine kinase. *Antimicrob Agents Chemother* 1994;38:2175-9.

Tural C, Romeu J, Sirera G et al. Long-lasting remission of cytomegalovirus retinitis

without maintenance therapy in human immunodeficiency virus-infected patients. *J Infect Dis* 1998;177:1080-1083.

Ulbrecht M, Martinozzi S, Grzeschik M et al. Cutting edge: the human cytomegalovirus UL40 gene product contains a ligand for HLA-E and prevents NK cell-mediated lysis. *J Immunol* 2000;164:5019-22.

Underwood MR, Harvey RJ, Stanat SC et al. Inhibition of human cytomegalovirus DNA maturation by a benzimidazole ribonucleoside is mediated through the UL89 gene product. *J Virol* 1998;72:717-25.

Valiante NM, Uhrberg M, Shilling HG et al. Functionally and structurally distinct NK cell receptor repertoires in the peripheral blood of two human donors. *Immunity* 1997;7:739-51.

van Zeijl M, Fairhurst J, Baum EZ, Sun L, Jones TR. The human cytomegalovirus UL97 protein is phosphorylated and a component of virions. *Virology* 1997;231:72-80.

Wagstaff AJ, Faulds D, Goa KL. Aciclovir. A reappraisal of its antiviral activity, pharmacokinetic properties and therapeutic efficacy. *Drugs* 1994;47:153-205.

Wagstaff AJ, Bryson HM. Foscarnet. A reappraisal of its antiviral activity, pharmacokinetic properties and therapeutic use in immunocompromised patients with viral infections. *Drugs* 1994;48:199-226.

Wang XZ, Ooi BG, Miller LK. Baculovirus vectors for multiple gene expression and for occluded virus production. *Gene* 1991;100:131-37.

Ward PL, Ogle WO, Roizman B. Assemblons: nuclear structures defined by aggregation of immature capsids and some tegument proteins of herpes simplex virus 1. *J Virol* 1996;70:4623-31.

Warren AP, Ducroq DH, Lehner PJ, Borysiewicz LK. Human cytomegalovirus-infected

cells have unstable assembly of major histocompatibility complex class I complexes and are resistant to lysis by cytotoxic T lymphocytes. *J Virol* 1994;68:2822-29.

Webster A, Lee CA, Cook DG et al. Cytomegalovirus infection and progression towards AIDS in haemophiliacs with human immunodeficiency virus infection. *Lancet* 1989;2:63-66.

Webster A, McLaughlin JE, Johnson MA, Emery VC, Griffiths PD. Use of the polymerase chain reaction to detect genomes of human immunodeficiency virus and cytomegalovirus in post-mortem tissues. *J Med Virol* 1995;47:23-28.

Weir MR, Henry ML, Blackmore M et al. Incidence and morbidity of cytomegalovirus disease associated with a seronegative recipient receiving seropositive donor-specific transfusion and living-related donor transplantation. A multicenter evaluation. *Transplantation* 1988;45:111-16.

Welch AR, Woods AS, McNally LM, Cotter RJ, Gibson W. A herpesvirus maturational proteinase, assemblin: identification of its gene, putative active site domain, and cleavage site. *Proc Natl Acad Sci U S A* 1991;88:10792-96.

Welsh RM, Brubaker JO, Vargas-Cortes M, O'Donnell CL. Natural killer (NK) cell response to virus infections in mice with severe combined immunodeficiency. The stimulation of NK cells and the NK cell-dependent control of virus infections occur independently of T and B cell function. *J Exp Med* 1991;173:1053-63.

Welsh RM, O'Donnell CL, Shultz LD. Antiviral activity of NK 1.1+ natural killer cells in C57BL/6 scid mice infected with murine cytomegalovirus. *Nat Immun* 1994;13:239-45.

Whitcup SM, Fortin E, Lindblad AS et al. Discontinuation of anticytomegalovirus therapy in patients with HIV infection and cytomegalovirus retinitis. *JAMA* 1999;282:1633-37.

Wiertz EJ, Tortorella D, Bogoy M et al. Sec61-mediated transfer of a membrane protein from the endoplasmic reticulum to the proteasome for destruction. *Nature* 1996;384:432-38.

Wiertz EJ, Jones TR, Sun L, Bogoy M, Geuze HJ, Ploegh HL. The human cytomegalovirus US11 gene product dislocates MHC class I heavy chains from the endoplasmic reticulum to the cytosol. *Cell* 1996;84:769-79.

Winston DJ, Wirin D, Shaked A, Busuttill RW. Randomised comparison of ganciclovir and high-dose acyclovir for long- term cytomegalovirus prophylaxis in liver-transplant recipients. *Lancet* 1995;346:69-74.

Wolf DG, Spector SA. Diagnosis of human cytomegalovirus central nervous system disease in AIDS patients by DNA amplification from cerebrospinal fluid. *J Infect Dis* 1992;166:1412-15.

(A)Wolf DG, Smith IL, Lee DJ, Freeman WR, Flores-Aguilar M, Spector SA. Mutations in human cytomegalovirus UL97 gene confer clinical resistance to ganciclovir and can be detected directly in patient plasma. *J Clin Invest* 1995;95:257-63.

(B)Wolf DG, Lee DJ, Spector SA. Detection of human cytomegalovirus mutations associated with ganciclovir resistance in cerebrospinal fluid of AIDS patients with central nervous system disease. *Antimicrob Agents Chemother* 1995;39:2552-54.

(A)Wolf DG, Yaniv I, Honigman A, Kassis I, Schonfeld T, Ashkenazi S. Early emergence of ganciclovir-resistant human cytomegalovirus strains in children with primary combined immunodeficiency. *J Infect Dis* 1998;178:535-38.

(B)Wolf DG, Honigman A, Lazarovits J, Tavor E, Panet A. Characterization of the human cytomegalovirus UL97 gene product as a virion-associated protein kinase. *Arch Virol* 1998;143:1223-32.



(A)Wolf DG, Yaniv I, Ashkenazi S, Honigman A. Emergence of multiple human cytomegalovirus ganciclovir-resistant mutants with deletions and substitutions within the UL97 gene in a patient with severe combined immunodeficiency. *Antimicrob Agents Chemother* 2001;45:593-95.

(B)Wolf DG, Courcelle CT, Prichard MN, Mocarski ES. Distinct and separate roles for herpesvirus-conserved UL97 kinase in cytomegalovirus DNA synthesis and encapsidation. *Proc Natl Acad Sci U S A* 2001;98:1895-900.

Wong JK, Ignacio CC, Torriani F, Havlir D, Fitch NJ, Richman DD. In vivo compartmentalization of human immunodeficiency virus: evidence from the examination of pol sequences from autopsy tissues. *J Virol* 1997;71:2059-71.

Wright JF, Kurosky A, Pryzdial EL. Host cellular annexin II is associated with cytomegalovirus particles isolated from cultured human fibroblasts. *J. Virol* 1995;69:4784-91.

Xiong X, Smith JL, Chen MS. Effect of incorporation of cidofovir into DNA by human cytomegalovirus DNA polymerase on DNA elongation. *Antimicrob Agents Chemother* 1997;41:594-99.

Ye LB, Huang ES. In vitro expression of the human cytomegalovirus DNA polymerase gene: effects of sequence alterations on enzyme activity. *J Virol* 1993;67:6339-47.

Yuen GJ, Drusano GL, Fletcher C et al. Population differences in ganciclovir clearance as determined by nonlinear mixed-effects modelling. *Antimicrob Agents Chemother* 1995;39:2350-2352.

Zacny VL, Gershburg E, Davis MG, Biron KK, Pagano JS. Inhibition of Epstein-Barr virus replication by a benzimidazole L- riboside: novel antiviral mechanism of 5, 6-dichloro-2-(isopropylamino)- 1-beta-L-ribofuranosyl-1H-benzimidazole. *J Virol* 1999;73:7271-77.

Zhang F, Robbins DJ, Cobb MH, Goldsmith EJ. Crystallization and preliminary X-ray studies of extracellular signal- regulated kinase-2/MAP kinase with an incorporated His-tag. *J Mol Biol* 1993;233:550-552.

Zimmermann A, Michel D, Pavic I et al. Phosphorylation of aciclovir, ganciclovir, penciclovir and S2242 by the cytomegalovirus UL97 protein: a quantitative analysis using recombinant vaccinia viruses. *Antiviral Res* 1997;36:35-42.